Investigating the roles of the alternative Isoforms of the preTCR alpha (pTα) chain in T cell development

Juliet L Mahtani-Patching

Research Thesis submitted for
the Degree of Doctor of Philosophy of
the University of London
August 2010

Laboratory of T Cell Immunology,
Centre for Immunology and Infectious Diseases,
Blizard Institute of Cell and Molecular Science,
Barts and The London Medical School,
Queen Mary College, London University,
4 Newark Street, London E1 2AT.

Abstract

The pre-T cell receptor (preTCR) is required for αβ T cell development and hence efficient adaptive immunity. Composed of a rearranged TCRβ chain paired with the invariant preTCR α chain (pTα), it drives immature thymocytes through the "β-selection" checkpoint, promoting differentiation, proliferation and survival. Although two functional splice isoforms of pTα exist, non-redundant roles for $pT\alpha^a$ and $pT\alpha^b$ have yet to be ascribed.

This thesis demonstrates that $pT\alpha^a$ and $pT\alpha^b$ display non-identical expression patterns in immature thymocyte subsets. Moreover, it demonstrates that $preTCR^a$ and $preTCR^b$ promote divergent T cell development; $preTCR^a$ drives prolonged expansion of post-β-selection thymocytes, while $preTCR^b$ drives rapid maturation of $TCR\alpha\beta^{(+)}$ cells. Importantly, by mutating charged residues in the extracellular domain of pTα, it is shown that pTα oligomerization is not required for preTCR signalling *per se*, as had previously been proposed. Instead, the capacity for oligomerization regulates surface preTCR levels, which in turn dictates subsequent developmental potential.

This thesis also presents preliminary evidence for a novel role for the preTCR; that preTCR signalling sensitises the extracellular signal-regulated kinase (ERK) mitogen-activated protein (MAP) kinase pathway that in turn regulates the signalling thresholds for positive and negative selection in $CD4^{(+)}CD8^{(+)}$ double positive (DP) cells. Indeed, it is suggested that this process may be critical for central tolerance in the thymus.

Finally, this thesis describes the generation and initial characterisation of $pT\alpha^a$ and $pT\alpha^b$ BAC transgenic mice that will facilitate the separate investigation of $pT\alpha^a$ and $pT\alpha^b$ in a pTα-deficient background *in vivo*.

Collectively, the results presented in this thesis ascribe non-redundant roles for the two isoforms of pTα and necessitate a fresh examination of the mechanism by which the preTCR initiates signalling. The implications of these results for αβ T cell development and the immune system as a whole are discussed.

Acknowledgements

First and foremost I would like to thank my supervisor Dr Daniel J Pennington, for this wonderful opportunity, for his excellent supervision, mentorship and guidance and for reviewing my thesis. I would like to thank the members of the DJP lab; Ana, John, Gavin and Joana for all their expert help, input and advice over the years. My thanks to Dr Marta Monteiro for her help setting-up single cell multiplex PCR, to Dr Patrick Costello and Dr Diane Maurice for their help with intracellular ERK-phosphorylation analysis and reagents and to Dr Hilde Cheroutre for providing the TL-tetramer. Also thank you, to Dr Garry Warnes, Dr Guglielmo Rosignoli and Sandra Martins for help with flow cytometry, to Vladimir Grigoriev for generating the transgenic mice, to Anthony Price and the members of the BSU for their help with animal work. I would like to thank Evelyn for opening her home to me, for her generosity and support while writing-up. Finally, I would like to thank my parents, my sisters, as well as Vassia, Linia and Richard for their love, friendship and encouragement and for always believing in me. I am grateful to you all for making this possible, thank you.

Contributions

In the following results sections the named individuals contributed to the indicated experiments or figures:

Results chapter 1.3: Semi-quantitative PCR for $pT\alpha^a$ and $pT\alpha^b$ of $TL^{(+)}$ and $TL^{(-)}$ DP cells from E16-17 C57BL/6 mice (Figure 1.5) was performed by Dr Dick John Pang.

Results chapter 2.2: Cloning $pT\alpha^a$ into pLZ (Figure 2.5) was done with the help of Tasneem Najwa.

Results chapters 2.2 and 4.3: Illustration of Foetal thymic organ cultures in a six-well plate (Figure 2.2 and Figure 4.6) was kindly provided by Kosta Stoenchev.

List of contents

Abbreviations

7-AAD	7-Amino-Actinomycin-D
ABC	ATP-Binding Cassette
AIRE	Autoimmune Regulator
APC	Antigen Presenting Cell
APC	Allophycocyanin
APECED	Autoimmune Polyendocrinopathy-Candidiasis-Ectodermal Dystrophy
ATP	Adenosine triphosphate
BAC	Bacterial Artificial Chromosome
BAX	Bcl-2 associated X protein
Bcl	B cell lymphoma
Bcl-X_L	B cell lymphoma-extra large
BHLH	Basic-Helix-Loop-Helix
BM	Bone Marrow
bp	Base pairs
BSA	Bovine Serum Albumin
CBF1	C repeat/dehydration-responsive element binding factor 1
CCL-21	Chemokine (C-C motif) Ligand-21
CCL-25	Chemokine (C-C motif) Ligand-25
CCR-7	C-C Chemokine Receptor Type 7
CCR-9	C-C Chemokine Receptor Type 9
CD	Cluster of Differentiation
cdc2	cell division control protein 2
CDK2	Cyclin Dependent Kinase 2
cDNA	complimentary DNA
CP	Cryptopatch
Cre	Cre-recombinase
CSA	Cyclosporin A
CSL	CBF1/RBP-Jκ/Suppressor of Hairless/LAG-1
cTEC	cortical Thymic Epithelial Cells
CTL	Cytotoxic T Lymphocyte
CXCL12	Chemokine (C-X-C motif) Ligand-12
CXCR4	Chemokine (C-X-C motif) Receptor-4
DAG	Diacylglycerol
DL-1	Delta like-1
DMEM	Dulbecco's Modified Eagle's Medium
DN	Double negative

DNA	Deoxyribonucleic acid
dNTP	Deoxyribonucleotide triphosphate
DP	Double Positive
E. coli	*Escherichia coli*
EDTA	Ethylenediaminetetraacetic acid
eGFP	enhanced Green Fluorescent Protein
Egr	Early growth response
EMSA	Electrophoretic Mobility Shift Assay
EPOR	Erythropoietin Receptor
ER	Endoplasmic Reticulum
ERK	Extracellular-signal-regulated kinases
ES-cells	Embryonic Stem cells
FACS	Fluorescence Activated Cell Sorting
FCS	Foetal Calf Serum
FITC	Fluorescein Isothiocyanate
Foxp3	Forkhead box P3
FSC	Forward scatter
FTOC	Foetal Thymic Organ Culture
GAD65	Glutamic Acid Decarboxylase of 65kDa
galK	Galactokinase gene
GFP	Green Fluorescent Protein
GPCR	G-protein Coupled Receptor
HEB	HeLa E-box binding protein
HES-1	Hairy and Enhancer of Split 1
HI FCS	Heat-Inactivated Foetal Calf Serum
HIV	Human Immunodeficiency Virus
HLA	Human Leukocyte Antigen
HSA	Heat Stable Antigen
Id3	Inhibitor of DNA binding 3
IEL	Intraepithelial Lymphocyte
IkB	Inhibitor of kappa B
IKK	IκB kinase
IL-7	Interleukin-7
IL-7Rα	Interleukin-7 receptor alpha
IP_3	Inositol trisphosphate
IP_3R	Inositol trisphosphate-Receptor
IRES	Internal Ribosomal Entry Site
ISP	Immature Single Positive
ITAM	Immunoreceptor Tyrosine-based Activation Motifs
JAK	Janus Kinase

JNK	c-Jun N-terminal kinases
kb	Kilobases
KO	Knock-Out
LAT	Linker for Activation of T cells
LB	Luria Bertani
Lck	Leukocyte-specific protein tyrosine kinase
LEF-1	Lymphoid Enhancer-Binding Factor-1
Ig	Immunoglobulin
LP	Leader Peptide
LTR	Long Terminal Repeat
MAPK	Mitogen Activated Protein Kinase
MEK	Mitogen-activated protein kinase kinase
MFI	Mean Fluorescence Intensity
MHC	Major Histocompatibility Complex
MMLV	Moloney Murine Leukaemia Virus
MMTV	Mouse Mammary Tumour Virus
mTEC	medullary Thymic Epithelial Cell
NFκB	Nuclear-factor-kappa-B
NFAT	Nuclear factor of activated T-cells
NGFR	Nerve growth factor receptor
NK	Natural Killer
ns	not significant
Oligo	Oligonucleotide
PBS	Phosphate buffered saline
PCR	Polymerase chain reaction
PE	Phycoerythrin
Pen/Strep	Penicillin/ Streptomysin
PI_3K	Phosphatidylinositol 3-kinases
PIP_2	Phosphatidylinositol bisphosphate
PKC	Protein Kinase-C
PLC-γ	Phospholipase C-γ
pLZ	pLZRS-IRES-eGFP plasmid
PMA	Phorbol Myristate Acetate
PSGL1	P-selectin Glycoprotein Ligand -1
pTα	pre T cell receptor alpha
RAG	Recombination Activating Genes
RBPj	Recombination site binding protein J
RN	Retronectin
RNA	Ribonucleic acid
RORγt	Thymus specific isoform of Retinoid related orphan receptor-γ

rpm	rounds per minute
RT	Reverse Transcription
RUNX-3	Runt-related transcription factor-3
S1P	Sphingosine-1-phosphate
SCID	Severe Combine Immune Deficiency
SCZ	Subcapsular Zone
SDM	Site directed mutagenesis
SH2	Src-Homology 2 domain
SLP-76	SH2 domain containing leukocyte protein of 76kDa
SOCS-1	Suppressor of cytokine signalling-1
SP	Single positive
SCPCR	Single Cell PCR
STAT-5	Signal transducer and activator of transcription-5
TALL	T cell Acute Lymphoblastic leukaemia
TAP	Transporter associated with antigen processing
TB	Tuberculosis
TCF-1	T cell Factor-1
TCR	T Cell Receptor
TEA-promoter	T early alpha promoter
TEC	Thymic Epithelial Cell
TL	Thymic Leukaemia Antigen
TM	Transmembrane
TP	Triple Positive
T-regs	Regulatory T cells
WT	Wild-Type
ZAP-70	Zeta-chain-associated protein kinase-70
ZBP-89	Zinc-finger DNA binding protein-89

Introduction

Chapter 1

T cells occupy a central position in adaptive immune responses.

The purpose of adaptive immunity is to protect. The body is under constant threat from invading pathogens such as bacteria, viruses and parasites. As part of the adaptive immune response, T cells function to recognise invaders and eliminate them.

1.1 T cells.

T cells originate from pluripotent hematopoietic stem cells from the bone marrow or foetal liver, which migrate to the thymus, the sole function of which is to initiate and support the T lineage developmental programme (Rothenberg et al., 2008). Indeed, the “T” in T cell stands for thymus in recognition of the fact that the vast majority of T cells differentiate in this organ.

T cells are distinguished from other lymphocyte populations by their expression of T cell receptors (TCRs). TCRs are heterodimeric surface protein complexes that possess immunoglobulin extracellular domains that serve to recognise antigen. Antigen recognition by the TCR initiates intracellular signalling cascades that result in activation of T cell effector function. Two major subtypes of T cell exist; those that express the $\alpha\beta$ TCR and those that express the $\gamma\delta$ TCR. $\alpha\beta$ T cells are further characterised by their expression of co-receptor molecules CD4 and CD8.

1.2 T cells recognise antigen presented by MHC.

T cells recognise pathogens through their TCRs, which bind antigens presented on the surface of cells (Germain, 1994). Antigens are defined as parts of molecules that can be recognised by antigen receptors, i.e. the TCR or antibodies. In the context of disease, antigens are derived from viruses or intracellular bacteria that replicate within cells or from pathogens and their products that have been endocytosed. Antigen presentation is mediated by peptide-binding glycoproteins encoded in a large gene cluster called the major histocompatibility complex (MHC). Recognition of antigen peptide presented by MHC molecules is one of the distinctive features of T cells. MHC molecules exist as two major types; MHC class I and MHC class II, which differ in their structure, antigen processing function and expression pattern on cells and tissues of the body. The MHC loci contain several different class I and class II genes equipping an individual with the capacity to present a broad range of antigens to T cells. Importantly the MHC is also polymorphic; meaning there are multiple variants of each gene within a population. This contributes to the ability of T cells to respond to the vast array of pathogens that may be encountered throughout one's life.

1.2.1 MHC-I.

MHC class I molecules are expressed on all nucleated cells. Their function is to process and present intracellular antigens to T cells expressing the CD8 co-receptor, i.e. cytotoxic T cells, whose principle function is to kill infected cells (Germain, 1994; Williams et al., 2002). Peptide loading of MHC-I molecules occurs in the lumen of the endoplasmic reticulum (Figure 1.1). The proteosome is part of the ubiquitin-dependent degradation pathway for cytosolic proteins and is involved in processing antigenic

peptides for presentation by MHC-I molecules. Two ATP-dependent ABC transporters, TAP-1 and TAP-2, are responsible for transporting peptides from the cytosol into the lumen of the endoplasmic reticulum. The appropriate folding and formation of MHC-I bound to β_2m is regulated by chaperones in the ER, such as calnexin and Erp57, and is dependent on peptide loading facilitated by TAP and Tapasin. Once the peptide is bound the stabilised peptide-MHC-I complexes are transported to the surface of the cell (Williams et al., 2002).

Figure 1.1

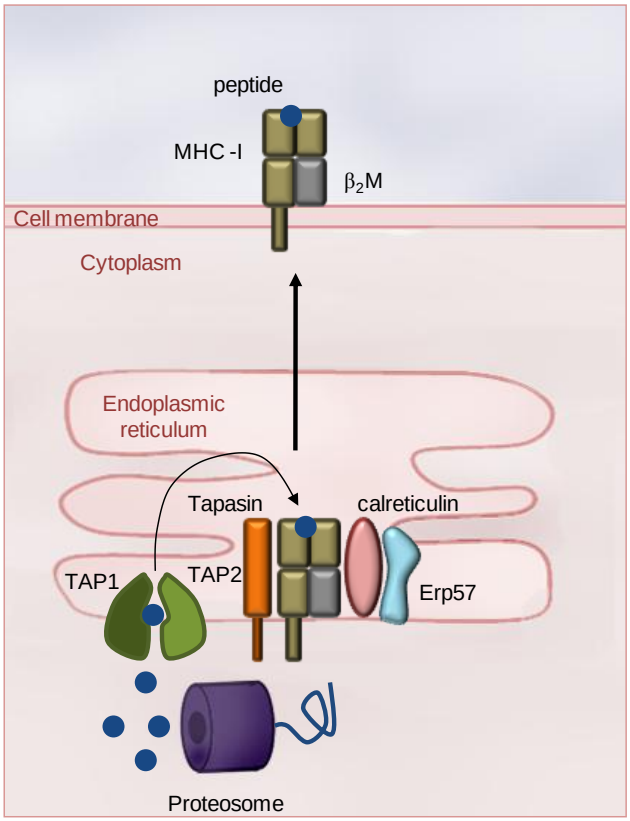

Figure 1.1 Antigen processing for presentation by MHC-I. Endogenous polypeptides are degraded by the proteosome in the cytoplasm producing peptide fragments that are transported into the lumen of the endoplasmic reticulum by TAP1 and TAP2. MHC-I molecules are formed in the endoplasmic reticulum where they bind chaperones (Erp57 and calreticulin) and TAP via tapasin. MHC-1 molecules are then loaded with peptide and subsequently traffic to the surface of the cell.

1.2.2 MHC-II.

Peptides presented by MHC-II are recognised by $CD4^{(+)}$ helper T cells which function to activate other effector cells of the immune system. Consequently MHC-II molecules are expressed only on “professional” antigen presenting cells such as dendritic cells, B cells, macrophages and thymic epithelial cells. MHC-II presents antigens from pathogens that reside in intracellular vesicles such as tuberculosis which infect macrophages, or those from extracellular pathogens and their products that have been endocytosed (Villadangos, 2001) (Figure 1.2).

Figure 1.2

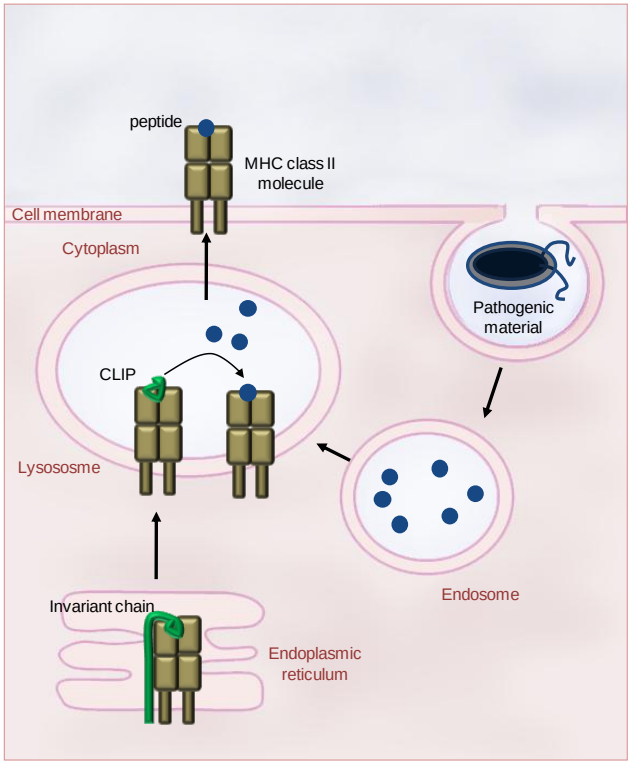

Figure 1.2 Antigen processing for presentation by MHC-II. Exogenous material is internalised by the endocytic pathway. Degradation of endosomal cargo occurs after fusion with lysosomes. MHC-II molecules formed in the ER are prevented from binding antigen by association with the invariant chain. After targeting to the endosomal compartments the invariant chain is cleaved and CLIP is removed and replaced with antigen before trafficking to the cell surface.

The endosomes containing antigen become increasingly acidic and after fusing with lysosomes allow acid proteases to become active and degrade the polypeptides to presentable peptides. MHC-II is formed in the endoplasmic reticulum bound to invariant chain. The invariant chain blocks the peptide binding groove, thus preventing peptide loading within the endoplasmic reticulum. The invariant chain targets class II molecules to acidic endosomes where it is cleaved by acidic proteases leaving a peptide fragment, CLIP, still bound to the peptide groove. Removal of CLIP and subsequent loading of antigen is catalysed by HLA-DM and the loaded class II molecule is subsequently trafficked to the cell surface (Villadangos, 2001; Watts, 1997).

1.3 T cell receptor rearrangement creates the diversity required for comprehensive immune protection.

In a perfect world one would produce a different T cell with a TCR that recognised each pathogen that exists on the face of the planet. Of course this is not possible; bacteria and viruses rapidly and continually evolve and therefore the pool of pathogens is ever expanding. Furthermore, the number of genes required would be unfeasible to incorporate into the genome. The solution, therefore is to make a limitless supply of different T cells by rearrangement of the immunoglobulin receptor genes that code for the TCR (Davis and Bjorkman, 1988; Tonegawa, 1983). TCR chains consist of two main regions; the variable domain (V-region) that encodes the extracellular Ig-loop that interacts with antigen-MHC, and the constant domain (or C-region) that encodes a further Ig-loop, as well as the transmembrane and short intracellular regions of the chain (Figure 1.3). Diverse antigen specificities of TCRs are determined by variation in the amino acid sequences of the V-regions.

Figure 1.3

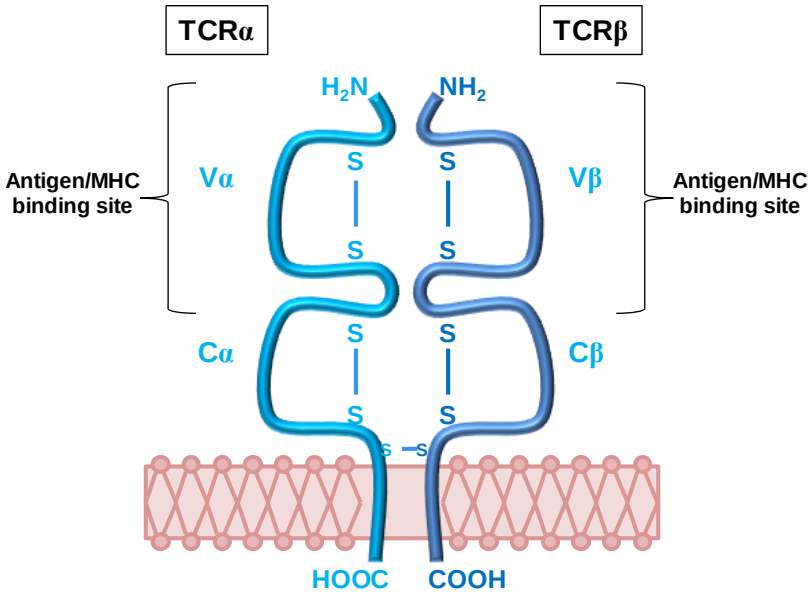

Figure 1.3 The αβ T cell receptor. A schematic of TCRαβ showing the Ig-loops that represent the variable (V) and constant (C) regions. Ig-loops are held together by disulphide bonds (s-s). The two TCR chains are also connected by a disulphide bond. The variable regions constitute the antigen/MHC binding sites of the TCR chains.

TCR chains are encoded by several gene segments that need to be brought together to form a functional gene. The TCRα chain is encoded by V (variable), J (joining) and C (constant) segments, while TCRβ is encoded by V, D (diversity), J and C regions. The V(D)J segments are joined to form a complete T cell receptor by a process known as gene rearrangement, which happens in T cells during their development in the thymus (Figure 1.4).

The mouse TCRβ locus consists of 20-30 Vβ segments that lie upstream of two gene clusters consisting of a single Dβ gene segment, 6 Jβ segments and a single Cβ segment and rearrange by looping out and deletion of the intervening DNA. One Vβ segment lies downstream of the DβJβCβ elements and rearranges by inversion. In mice the TCRα locus consists of

~75-100 Vα segments followed by 50 Jα segments and a single Cα gene (Figure 1.5) (Davis and Bjorkman, 1988).

Figure 1.4

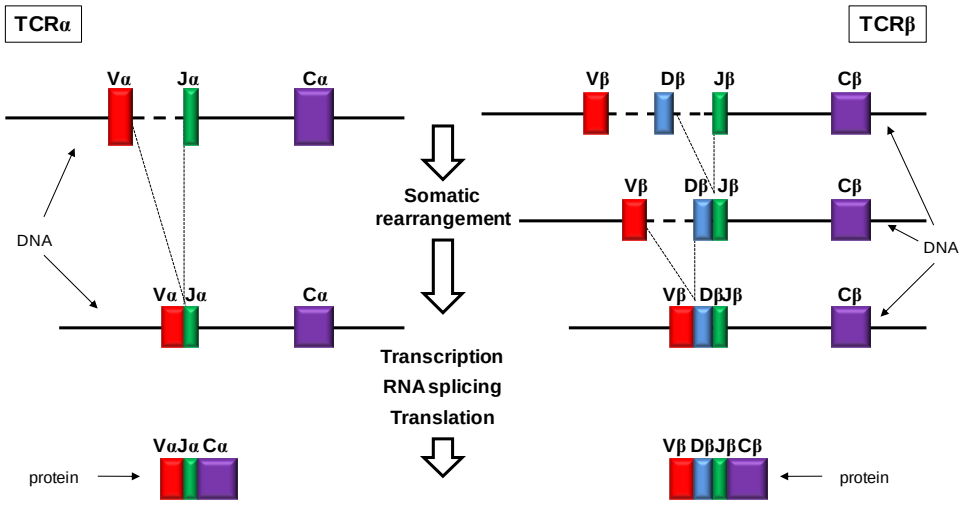

Figure 1.4 T cell receptor gene rearrangements. Schematic representation of TCRα and TCRβ gene rearrangement. Different V regions of TCR chains are generated by different combinations of V(D) and J segments being used by a single T cell. For TCRα genes rearrangement occurs in a single step to bring together Vα and Jα segments by removal of the intervening sequences. For TCRβ genes two rearrangement steps are required; the first unites D and J segments the second joins the DJ segment to the V segments on the gene.

Figure 1.5

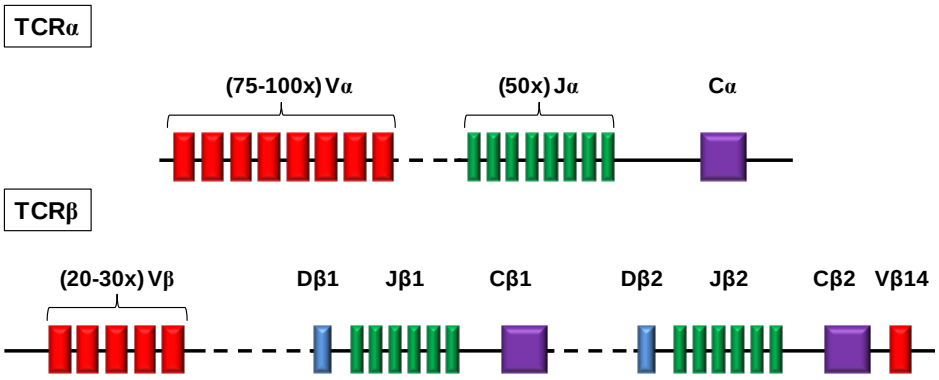

Figure 1.5 Organisation of TCR genes in mice. Schematic representation of the TCRα and TCRβ genes in mice. Expression of multiple V and J segments increases TCR diversity for antigen recognition.

An elegant mechanism exists to ensure the site specific rearrangement and joining of V D and J segments (Tonegawa, 1983). Conserved heptamer (5'CACAGTG-3') and nonamer (5'-ACAAAAACC-3') sequences exist adjacent to the sites at which recombination takes place. The heptamer and nonamers are separated by either 12bp or 23bp "spacers". Gene segments carrying a 12bp spacer can only be joined to a gene segment carrying a 23bp spacer. Thus in TCRβ Vβ segments can only be joined with Dβ segments and not Jβ segments (Figure 1.6). The products of two lymphocyte specific recombination-activating genes; RAG-1 and RAG-2 are the key enzymes that mediate V(D)J recombination through recognition and binding of the heptamer-spacer-nonamer recognition sequences (Mombaerts et al., 1992b; Shinkai et al., 1992).

Figure 1.6

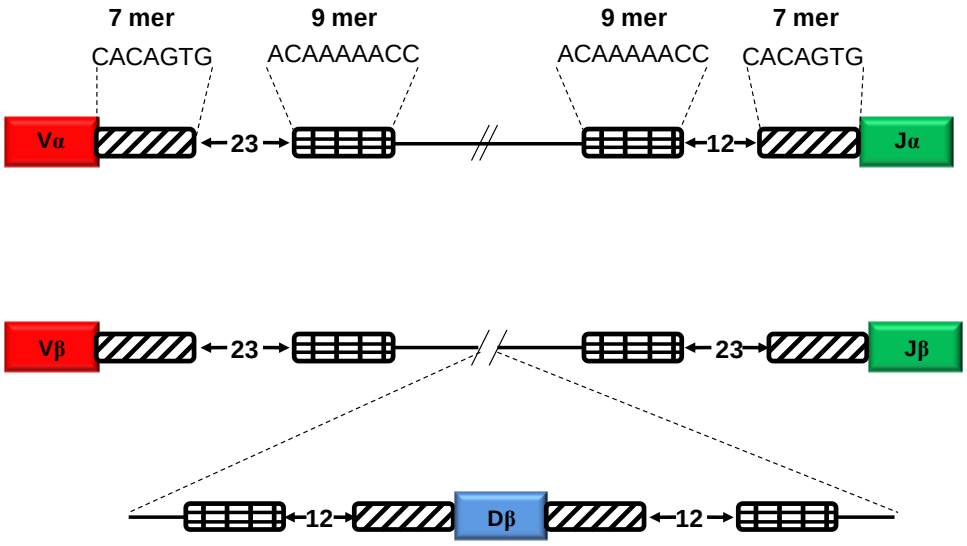

Figure 1.6 The 12/23 rearrangement rule. Schematic representation of the TCR gene heptamer and nonamer sequences that are adjacent to sites at which recombination takes place. These are separated by 12bp and 23bp spacers. Only those segments that possess recognition sequences containing 23bp spacers can be joined to those with 12bp spacers.

In addition to the combinatorial diversity generated by V(D)J rearrangements another mechanism exists to generate variation within the antigen binding pocket of the TCR (Davis and Bjorkman, 1988). During the formation of the V(D)J junctions, nucleotides are added or excised randomly. In this manner, even if the same two segments are joined by different cells the joining region will be distinct. The V(D)J junctions constitute the third hyper-variable loop (CDR3) that contributes to the antigen binding site of the TCR. Because the complete TCR is made up of TCRα and TCRβ chains that have both undergone rearrangements and have had additional variation generated at the joining regions, the potential diversity of TCR specificities is vast.

1.4 Thymic selection is essential for preventing the generation of T cells that recognise self.

The potential problem of generating T cells with the capability of recognising an almost infinite number of antigens is that a sizable subset of these antigens will be “self”. Clearly an immune response to “self”-antigens would be detrimental. Thus, the thymus has evolved a mechanism to overcome this dilemma; namely, T cell selection. This process assesses each T cell on the ability of its TCR to recognise self proteins presented by MHC. Based on this, thymocytes are either deleted or maintained. The fate of the developing T cell is dependent on the affinity of its TCR for self-antigen-MHC presented by thymic stromal cells (Figure 1.7) (Klein et al., 2009). Developing T cells that express “useless” TCRs that are unable to interact with self-peptide-MHC as a result of low affinity binding do not survive; a process known as “death by neglect” (Huesmann et al., 1991; Kisielow et al., 1988).

By contrast DP cells that recognise and bind self-peptide-MHC with very high affinity undergo apoptosis; a process known as “negative selection”. This is critical for depleting self-reactive TCRs from the T cell repertoire (Kappler et al., 1987).

Figure 1.7

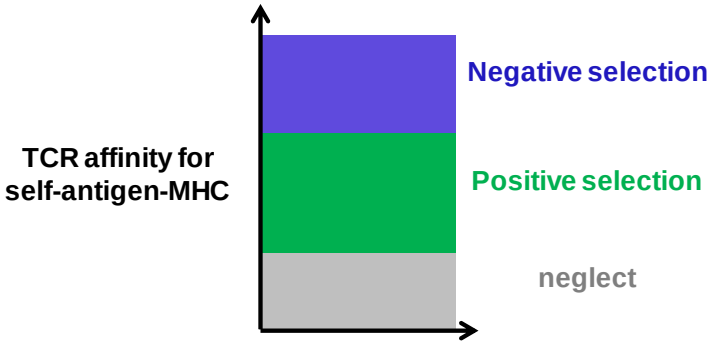

Figure 1.7 TCR affinity for self-antigen-MHC determines developing T cell fate: progenitor T cells in the thymus are “tested” for the self reactivity of their TCRs. Those that express TCRs with high affinity for self-antigen MHC die by apoptosis; those that recognise self-antigen-MHC with little or no affinity die by neglect. Only those T cells that possess intermediate affinity TCRs for self-antigen-MHC are positively selected to survive.

Negative selection thus provides “central tolerance” a term that describes the removal of self-reactive lymphocytes at source. As a result, only the few T cell progenitors that recognise self-peptide-MHC with intermediate affinity are “positively selected” and mature to become effector cells that leave the thymus to populate the periphery (Figure 1.7). As an additional tolerance mechanism the thymus also produces T cells that provide regulatory function. These cells contribute to peripheral tolerance, dampening immune responses to self.

1.5 Autoimmunity: When T cell selection goes wrong.

Self-reactive T cells that escape negative selection have the potential to mount immune responses to self-antigens as if they were a pathogen. Self-reactive T cells mediate tissue damage associated with a number of

autoimmune diseases and immunopathologies. For example, type-1 insulin dependent diabetes mellitus is an organ-specific autoimmune disease characterised by the progressive destruction of pancreatic β-islet insulin-producing cells (Santamaria, 2010). Although the nature of the disease is very complex and not fully understood, it is evident that autoreactive T cells play a central role in the pathogenesis of type-1 diabetes. Autoreactive CD4 and CD8 T cell infiltrates are found in diseased pancreatic islets and β-cell destruction is thought to be a consequence of cytotoxic T cell function. Many different antigen targets of diabetes-specific T cells have been identified, that include insulin, GAD65, as well as islet-specific glucose-6-phosphatase catalytic subunit-related protein IGRP (Santamaria, 2010).

Chapter 2

T cell development in the Thymus

2.1 The Thymus.

The thymus has evolved as the primary lymphoid organ to support T cell development, its appearance, in evolutionary terms corresponding with the appearance of lymphocytes expressing highly diverse antigen receptors (Rodewald, 2008). Consistent with this view, the stromal cells of the thymus, in particular the cortical and medullary epithelial cells (cTECs and mTECs) and thymic dendritic cells have specialised functions that serve particular roles during T cell development (Anderson et al., 2007; Anderson et al., 1996; Klein et al., 2009). cTECs express both MHC-I and MHC-II and are efficient mediators of both positive and negative selection (Anderson et al., 1994b; Goldman et al., 2005). Indeed, expression of the β5t catalytic subunit of the proteosome is exclusive to cTECs in the thymus and is essential for positive selection of CD8 thymocytes (Murata et al., 2007). Moreover, cTECs express a specific acid protease required for MHC-II loading, Cathepsin L, which is necessary for positive selection of CD4 thymocytes (Nakagawa et al., 1998). In the context of immune responses, MHC-II normally presents exogenous antigens to T cells. Thus, in the thymus, thymic epithelial cells have had to evolve a mechanism to present endogenous antigens to T cells, a process known as macroautophagy. This involves engulfment of portions of the cytoplasm by intracellular organelles which then fuse with lysosomes for degradation of their cargo (Klein et al., 2009). Macroautophagy provides a mechanism by which MHC-II molecules

can be loaded with and present endogenous self-antigen to developing $CD4^{(+)}$ cells. Indeed the thymus is a site of unusually high constitutive autophagy activity (Klein et al., 2009).

MHC-I and MHC-II are both also expressed by mTECs (Anderson et al., 2007). Like cTECs, mTECs can also mediate negative selection of thymocytes and possibly positive selection of Regulatory T cells (Aschenbrenner et al., 2007; Ribot et al., 2007). The discovery of the transcription factor AIRE (Autoimmune regulator), which regulates the promiscuous gene expression of hundreds of tissue-restricted antigens in the thymus, has provided insight into how thymocytes are exposed to peripheral self-antigens. AIRE expression is a distinct property of mTECs. However, only a small subset of mTECs express this transcription factor, and the mechanism by which it contributes to central tolerance is still debated (Anderson et al., 2002; Klein et al., 2009). Nonetheless, humans with a mutation in AIRE develop APECED (autoimmune polyendocrinopathy-candidiasis-ectodermal dystrophy), a severe autoimmune disorder (Mathis and Benoist, 2007).

2.2 Conventional T cell development.

2.2.1 Stages of T cell development.

T cell precursors develop in the thymus through distinct stages defined by expression of various surface molecules (Figure 2.1). T cell precursors express neither CD4 nor CD8 co-receptors and are therefore termed double negative (DN). DN cells are further categorised on surface expression of CD25 and CD44; $CD25^{-}CD44^{+}$ (DN1), $CD25^{+}CD44^{+}$ (DN2), $CD25^{+}CD44^{-}$ (DN3) and $CD25^{-}CD44^{-}$ (DN4) (Godfrey et al., 1993).

The DN1 subset is heterogeneous, but consists mainly of early thymic progenitors (Porritt et al., 2004). Single cell analysis has revealed that progenitors that seed the foetal thymus possess T, B and myeloid lineage potential (Benz and Bleul, 2005; Kawamoto et al., 1998). Progression to the DN2 stage is accompanied by a proliferative phase that expands the precursor population in which TCR gene rearrangements occur (Kawamoto et al., 2003).

Figure 2.1

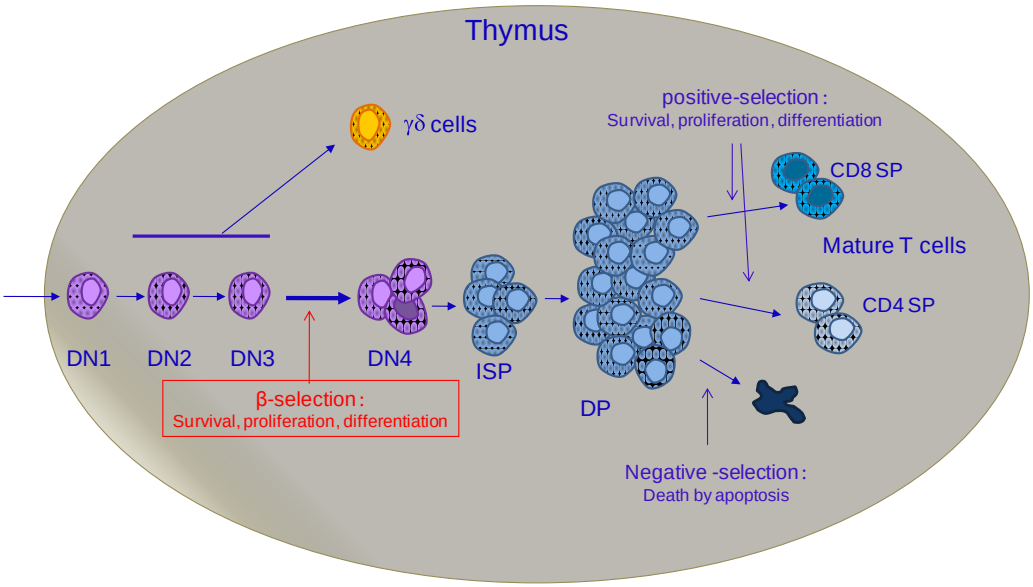

Figure 2.1 Stages of T cell development in the thymus. DN T cell precursors enter the thymus from the bone marrow and progress through a series of stages characterised by expression of various surface molecules. γ, δ and β TCR gene rearrangements occur in DN2 cells; marking commitment to the T lineage. DN cells that rearrange TCR γ and δ genes successfully, commit to the γδ T cell lineage. β-selection, mediated by the preTCR, promotes the survival, proliferation and differentiation of thymocytes that have undergone successful TCRβ gene rearrangements. TCRα rearrangements occur at the DP stage. DP thymocytes are subjected to positive and negative selection determined by the self-reactivity of their TCRs. Positively selected DPs mature to become either CD4 SP or CD8 SP and leave the thymus to populate the periphery. DN, double negative; DP, double positive; SP, single positive and TCR, T cell receptor.

Evidence of T lineage commitment is apparent in DN2 thymocytes which begin to express genes necessary for TCR rearrangement such as RAG1 and RAG2, as well as genes involved in TCR complex formation such as Lck, CD3γ, CD3δ and TCRζ. Importantly, the pre-T cell receptor alpha chain (pTα) is also expressed in DN2 cells (Molina et al., 1992; Mombaerts et al., 1992b; Wilson and MacDonald, 1995). Progression to the DN3 stage establishes T lineage commitment as the cells lose the ability to adopt alternative fates (Masuda et al., 2007). DN3 cells cease proliferating and undergo TCR γ, δ and β gene rearrangements. DN3 cells that have functional γ and δ TCR rearrangements express the γδTCR and are diverted from the αβ lineage to differentiate into γδ T cells (discussed later in this introduction).

DN3 cells that have undergone successful TCRβ gene rearrangements express the pre T cell receptor (preTCR) which mediates an important transition in development known as the "β-selection" checkpoint (Fehling et al., 1995a). The preTCR complex is composed of a rearranged TCRβ chain paired with the invariant pTα chain and various CD3 molecules. Signalling through the preTCR induces downregulation of CD25, cell survival, proliferation and differentiation to the DN4 stage and beyond (Hoffman et al., 1996; Michie and Zuniga-Pflucker, 2002; von Boehmer et al., 1998). DN4 cells subsequently become immature single positive cells (ISPs) by acquiring CD8, before rapidly upregulating CD4 to become "double positive" (DP) cells. The process of β-selection mediated by the preTCR is the focus of this thesis and will be discussed in detail in subsequent chapters of this introduction. The proliferative burst that is associated with the DN3 to DP transition is necessary for expansion of cells that have undergone successful TCRβ rearrangements, providing many progenitors

in which subsequent TCRα rearrangements can then occur. The resulting TCRαβ complexes are then screened for their ability to recognise and interact with MHC-self-antigen expressed by thymic epithelial cells. TCRα rearrangements can continue to an extent in DP thymocytes until the generation of a TCRαβ capable of engaging MHC-peptide complexes and eliciting a productive TCR signal is formed. Signals through the αβTCR induce survival, upregulation of CD5 and CD69, and termination of RAG gene expression, thereby preventing further TCRα gene rearrangements (Bhandoola et al., 1999; Brandle et al., 1992).

2.2.2 Factors regulating T lineage commitment.

Commitment of early thymic progenitors to the T lineage involves the Notch family of signalling proteins (Rothenberg et al., 2008). There are four known Notch receptors in mammals (Notch 1-4) which recognise 5 known ligands; Delta-like 1 (DL1) DL3, DL4, Jagged-1 and Jagged-2. Upon ligation, the Notch receptor is proteolytically cleaved and the intracellular domain migrates to the nucleus where it binds the transcription factor CSL also known as recombination site binding protein J (RBPj). Binding of the Notch intracellular domain converts CSL from a transcriptional repressor to an activator and results in transcription of Notch target genes (Rothenberg et al., 2008). Inactivation of Notch-1 in bone marrow progenitors abrogates commitment to the T cell lineage and as a result, progenitor cells in the thymus adopt a B cell fate (Radtke et al., 1999). Conversely, retroviral transduction of bone marrow hematopoietic stem cells with a constitutively active form of Notch-1, promotes T lineage commitment while preventing B cell development in the bone marrow (Pui et al., 1999). Indeed, expression of DL1 on the bone marrow stromal cell line OP9 generates cells that are able to support T cell development (Schmitt and Zuniga-Pflucker, 2002).

Importantly, continued Notch signalling is required from the DN1-DN3 stages to maintain commitment to the T cell lineage (Schmitt et al., 2004). Moreover, the Notch-CSL complex upregulates the T lineage specific gene expression of Deltex-1, Rag-1, Hes-1 and pTα genes (Reizis and Leder, 2002; Rothenberg et al., 2008).

Acting in concert with Notch signals to promote T cell development are E-proteins, members of the basic-helix-loop-helix family of transcription factors (Rothenberg et al., 2008). E-proteins E2A and HEB are expressed in early thymic progenitors and throughout development until the late DP stage (Engel et al., 2001). E2A knock-out mice display a partial block in T cell development at the DN1 stage and rapidly develop lymphomas, highlighting the role of these proteins in controlling proliferation (Bain et al., 1997). E2A and HEB enforce the DN3 phenotype by arresting their proliferation which allows for initiation of TCR gene rearrangements (Engel and Murre, 2004). Furthermore, E-proteins activate transcription of the pTα gene (Takeuchi et al., 2001). E-protein activity is regulated by inhibitory factors such as Id2 and Id3 which form heterodimers with E2A and HEB and prevent their DNA binding. Id2 is expressed at the DN1 to DN2 transition concurrent with the proliferation observed at this transition. Furthermore, TCRγδ and preTCR signalling both induce expression of Id3 which is necessary for proliferation of thymocytes that have successfully completed TCR gene rearrangements (Bain et al., 2001; Koltsova et al., 2007; Lauritsen et al., 2009).

2.2.3 T cell migration in the thymus.

Interaction of thymocytes with thymic epithelial cells is important for differentiation and maturation of both the T cells and stromal cells that

provide developmental support (Anderson et al., 1996; Takahama, 2006). Various stages of thymocyte development are precisely associated with their migration through specialised compartments of the thymus (Figure 2.2). Chemokines have an important role in guiding the thymocytes as they traffic through the organ (Takahama, 2006).

Figure 2.2

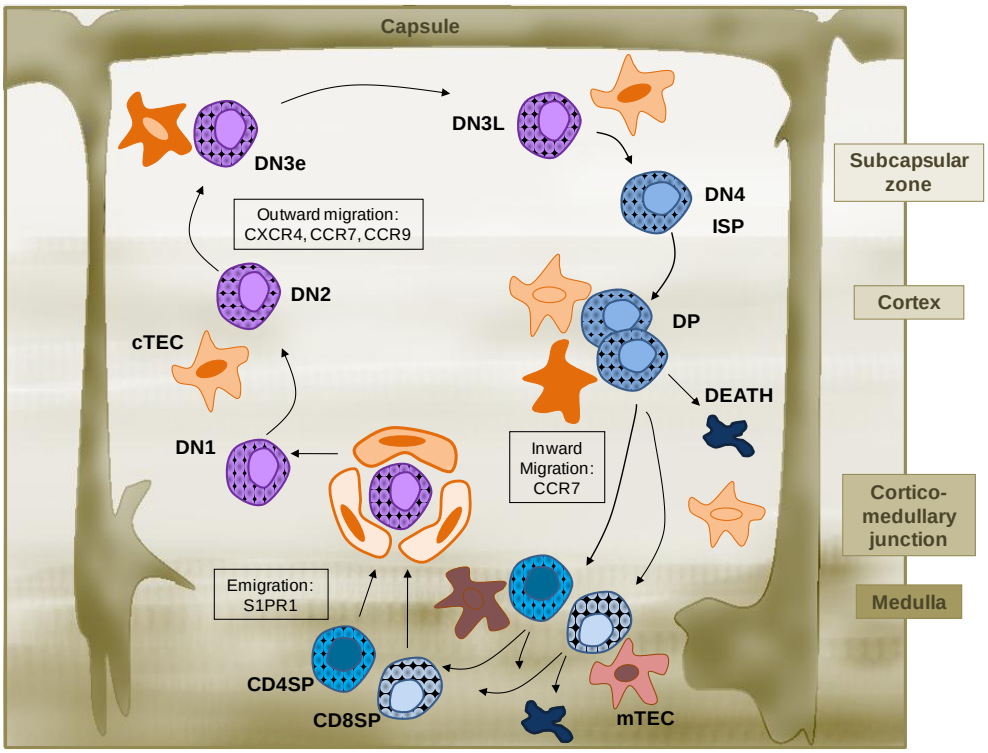

Figure 2.2 Migration of developing thymocytes through the thymus is precisely regulated by chemokines and is closely associated with their differentiation and selection. In the postnatal thymus, early thymic progenitors (DN1) enter the thymus through the vasculature in the cortico-medullary junction. As they differentiate into DN2 and DN3 they migrate outward towards the subcapsular zone (SCZ). CXCR4, CCR7 and CCR9 expression by DN2/DN3 thymocytes mediates their migration and localisation to the SCZ. DP thymocytes, localised within the cortex interact with cTECs for positive and negative selection. Positively selected cells upregulate CCR7 through which they are attracted, inward, towards the medulla. mTECs mediate the deletion of tissue-specific-antigen reactive SP cells. Mature SP cells express sphingosine-1-phosphate receptor 1 ($S1P_1$), through which the cells are attracted back to the circulation that contains a high concentration of sphingosine-1-phosphate. DN, double negative; DP, double positive; SP, single positive; cTEC, cortical thymic epithelial cell; mTEC, medullary thymic epithelial cell.

The seeding of the thymus with lymphoid progenitors occurs as early as embryonic day 11.5 in mice and the eighth month of gestation in humans. During the early stages of embryogenesis colonisation of the foetal thymus by lymphoid progenitor cells is vasculature-independent and requires CCL21 and CCL25 which attract progenitors expressing the receptors CCR7 and CCR9, respectively. In the postnatal thymus, progenitors enter from the blood through the vasculature located close to the cortico-medullary junction. In the adult thymus, this process is regulated by adhesion mediated by P-selectin glycoprotein ligand -1 (PSGL1) and P-selectin which is expressed by the thymic endothelium (Takahama, 2006). Progenitor thymocytes enter the thymus in waves during foetal and adult life (Foss et al., 2001; Jotereau et al., 1987). Experiments with parabiotic adult mice have revealed that colonisation of the thymus is a "gated" process during which the "open gate" period lasts one week followed by a three week "closed gate" period before the gates open again for colonisation with a new wave of progenitor cells (Foss et al., 2001).

Concomitant with early thymic progenitor cell commitment to the T cell lineage, the cells migrate outward from the cortico-medullary junction to the subcapsular zone (SCZ) (Takahama, 2006). Development of immature thymocytes through the DN1 to DN3 stage appears to correlate with the differentiation of keratin-$8^{(+)}$ thymic epithelial cells (TECs) into cortical epithelial cells (cTECs) by downregulation of keratin-5. Localisation of DN2 and DN3 thymocytes to the SCZ is dependent on CXCR4 expression; the ligand (CXCL12) for which is abundantly expressed in this compartment of the thymus (Plotkin et al., 2003; Trampont et al., 2010). Indeed, CXCR4 is essential for DN thymocyte migration to the SCZ and for their differentiation past the β-selection checkpoint (Plotkin et al., 2003; Trampont et al., 2010).

CCR7 and CCR9 expression by DN thymocytes is also required for their localisation to the SCZ (Benz et al., 2004; Misslitz et al., 2004).

Positive and to some extent, negative selection of DP thymocytes occurs in the cortex and involves interactions with peptide-MHC complexes expressed on cTECs and dendritic cells in the cortex. Upon positive selection DP cells in transition to the SP stage are highly motile and migrate rapidly to the medulla, a process mediated by CCR7 that is upregulated following TCR engagement (Ueno et al., 2004). Cortex-medulla migration of positively selected thymocytes plays a crucial role in medulla formation (Ueno et al., 2004). Maturation of SP thymocytes occurs in the medulla resulting in upregulation of CD62L (L-selectin) and downregulation of CD69. Further deletion of self reactive thymocytes also occurs in the medulla to establish central tolerance to tissue specific antigens through interaction of SP thymocytes with AIRE expressing medullary epithelial cells (mTECs). Egress of mature thymocytes from the thymus is regulated by sphingosine-1-phospate receptor-1 ($S1P_1$) mediated chemotaxis towards sphingosine-1-phospate in the circulation (Matloubian et al., 2004).

2.2.4 Duration and strength of TCR signal dictates CD4/CD8 lineage choice.

The αβTCRs expressed by DP thymocytes constitute a hugely diverse pre-selected repertoire. Positive selection not only identifies the relatively few DPs that express TCRs with useful specificity, but also promotes development of SP thymocytes that are committed to either the CD8 lineage, that recognise MHC-I-presented antigens, or the CD4 lineage that recognises MHC-II-presented antigens. CD4 and CD8 function as co-receptors to the TCR through their ability to bind MHC, enhancing the

strength of TCR/MHC binding; CD4 to MHC-II (Doyle and Strominger, 1987) and CD8 to MHC-I (Bosselut et al., 2000; Norment et al., 1988). Furthermore, CD4 and CD8 associate with Lck (Veillette et al., 1988) and linker for activation (LAT) (Bosselut et al., 1999) through their intracellular domains and therefore augment initiation and propagation of TCR signals (Singer et al., 2008).

Figure 2.3

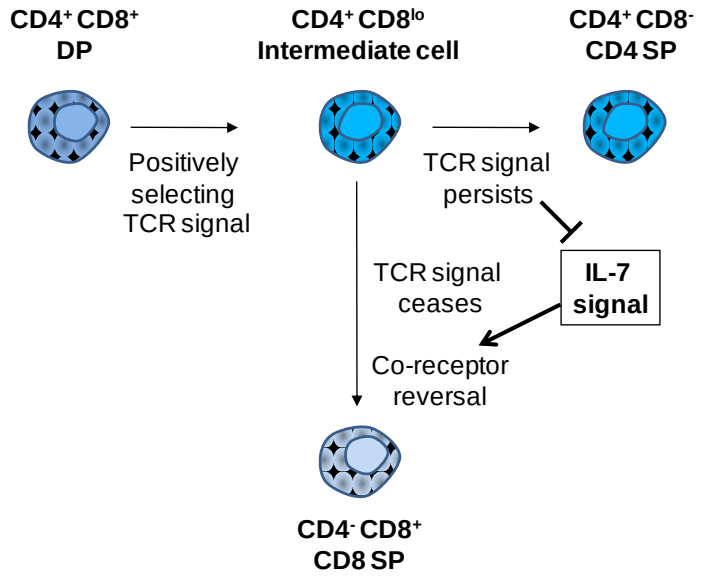

Figure 2.3 The kinetic signalling molecule of CD4/8 lineage commitment: Regardless of the specificity of their T cell receptor (TCR), positively selecting TCR signals induce double-positive (DP) thymocytes to terminate CD8 gene transcription and convert into $CD4^{(+)}CD8^{(lo)}$ intermediate cells. $CD4^{(+)}CD8^{(lo)}$ thymocytes are lineage uncommitted cells that retain the potential to differentiate into either CD4 single-positive (SP) or CD8SP cells. Persistence of TCR signalling in $CD4^{(+)}CD8^{(lo)}$ thymocytes blocks interleukin-7 (IL-7) signalling and induces differentiation into mature CD4SPs. Cessation of TCR signalling in $CD4^{(+)}CD8^{(lo)}$ cells permits IL-7 signalling, which induces $CD4^{(+)}CD8^{(lo)}$ intermediate thymocytes to undergo co-receptor reversal to become CD8SPs.

Alfred Singer has made a significant contribution to our understanding of the events that determine CD4 and CD8 lineage commitment; his kinetic signalling model being a widely accepted concept in the field (Singer, 2002; Singer et al., 2008; Singer and Bosselut, 2004). The kinetic signalling

model of CD4/CD8 T cell lineage commitment (Figure 2.3) suggests that positive selection mediated by TCR signalling does not induce DP thymocytes to undergo lineage commitment but rather induces termination of CD8 expression. This leads to the development of an intermediate ($CD4^{(+)}CD8^{(lo)}$) population that retains the potential to commit to either CD4SP or CD8SP fates. At this stage the developing T cell is in a position to "test" the MHC specificity of its TCR. Thus, if downregulation of CD8 does not interrupt TCR signalling the thymocyte "realizes" that CD8/MHC-I interactions were not contributing to TCR/MHC binding, so the TCR must not recognise MHC-I. However if CD8 downregulation leads to cessation of TCR signalling the cell "realizes" that CD8/MHC was important for signalling, so the TCR must recognise MHC-I. With this information the $CD4^{(+)}CD8^{(lo)}$ DP cell then follows a differentiation pathway appropriate to the TCR specificity for either MHC-I or MHC-II.

Putting the kinetic model in terms of duration of TCR signal, it suggests that extended TCR signals commit DP cells to the CD4SP lineage, while short duration TCR signals commit DPs to the CD8SP lineage. Because high affinity TCR-peptide-MHC interactions are more likely to be prolonged whereas weak affinity interactions are not maintained for long, this model encompasses evidence that shows that high affinity ligands and strong signalling through the TCR promotes CD4 lineage commitment while low affinity or weak signalling promotes CD8 lineage commitment (Singer and Bosselut, 2004).

Interleukin-7 (IL-7) signalling plays an important role in maintaining CD8 progenitor cell viability in the absence of TCR signalling during transition to the SP stage (Brugnera et al., 2000). IL-7Rα is upregulated on DP thymocytes following positively selecting TCR signals (Brugnera et al.,

2000). IL-7 treatment of $CD4^{(+)}8^{(lo)}$ thymocytes in vitro induces upregulation of Bcl-2 (Brugnera et al., 2000; Yu et al., 2003) as well as RUNX3 (Park et al., 2010) promoting their survival and CD8 CTL lineage commitment, respectively. Furthermore, IL-7 signalling in $CD4^{(+)}8^{(lo)}$ thymocytes results in termination of CD4 gene expression through activation of the CD4 silencer element (Brugnera et al., 2000). Importantly, treatment of $CD4^{(+)}8^{(lo)}$ with IL-7 in the presence of PMA and ionomycin, to mimic TCR signals, prevented co-receptor reversal in these cells (Brugnera et al., 2000). Thus $CD4^{(+)}8^{(lo)}$ precursors, committed to the CD4 lineage, avoid the effects of IL-7 through persistent TCR signalling (Brugnera et al., 2000; Singer and Bosselut, 2004).

2.3 Unconventional T cell development.

"Unconventional" T cells are so called because they do not follow conventional mechanisms for their development and function (Hayday, 2009; Pennington et al., 2005). These cells share an unconventional gene expression profile, and are generally found in the tissues rather than the lymph nodes and blood. They are more "innate-like" in their function; showing an "activated-yet-resting" phenotype, and having the capacity for rapid responses that do not require clonal expansion in lymphoid tissue. They have been described as important players in transitional immunity that connects innate and adaptive responses (Hayday, 2009). Unconventional T cells include $\gamma\delta$ T cells and $\alpha\beta$ T cells that express $CD8\alpha\alpha$ in the epithelial layers such as the gut (Pennington et al., 2005). Since their discovery in the 1980s $\gamma\delta$ T cells have been found to mediate stress surveillance responses throughout epithelial layers of the body. In addition, they can function as antigen presenting cells and influence adaptive immune responses. Furthermore, $\gamma\delta$ T cells are important for immunological responses to

cancer and infections such as malaria, TB as well as HIV (Hayday, 2009). CD8αα$^{(+)}$ intraepithelial lymphocytes (IELs) are TCRαβ$^{(+)}$ T cells that line the gut epithelial barrier and possess a regulatory function that is thought to be important in epithelial homeostasis (Poussier et al., 2002).

2.3.1 γδ T cell development

γδ and αβ T cells develop from a common precursor in the thymus (Hayes et al., 2010; Lauritsen et al., 2006; Pennington et al., 2005). Development of γδ T cells requires rearrangement of TCRγ and TCRδ chains and signalling through the γδTCR. However, it is not known at precisely which stage the two lineages diverge, although it is clear that γδ cell commitment occurs at some point between the DN2 stage, in which TCRγ and TCRδ gene rearrangements occur, and before commitment to the DP stage. Indeed DN4 thymocytes are still able to give rise to both αβ and γδ T cells (Petrie et al., 1992).

Figure 2.4

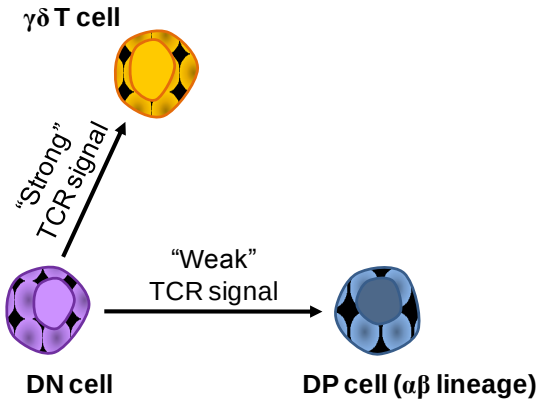

Figure 2.4 The strength of signal model of αβ/γδ T cell lineage commitment. The model suggests that double negative (DN) thymocytes that receive strong signals through their TCR commit to the γδ T cell lineage, while those receiving weak TCR signals commit to a αβ T cell lineage fate. Thus the αβ/γδ lineage decision is not instructed but rather dependent on the strength of signal induced by their TCR.

Rather than αβ/γδ lineage choice being instructed by the preTCR versus the γδ TCR, respectively, it is thought that it is the strength of signal emanating from a TCR complex that determines αβ/γδ lineage commitment; thymocytes receiving strong signals commit to a γδ lineage fate, while those that receive weaker signals commit to an αβ T cell fate. Evidence for this strength-of-signal model was provided by two independent groups (Haks et al., 2005; Hayes et al., 2005). Hayes *et al* used Vγ6/Jγ1Cγ1-Vδ6/Dδ6/Jδ2/Cδ TCR transgenic mice, in which γδTCR transgene expression led to development of both γδ and αβ thymocytes. Crossing the transgenic mice onto a TCRζ$^{(+/-)}$ background resulted in a significant increase in the percentage of DP cells that developed, while the percentage of γδ cells was significantly decreased. Conversely, expression of a TCRζ transgene in γδTCR transgenic TCRζ$^{(+/+)}$ mice significantly increased the level of TCR on the surface of precursor thymocytes resulting in a 7-fold reduction in the percentage of DPs, while favouring γδ T cell development (Hayes et al., 2005). Importantly this showed that high surface expression of the γδ TCR corresponded to γδ T cell lineage commitment while low TCR surface expression favoured αβ lineage commitment.

To determine whether development promoted by differential surface expression of the TCR correlated with signal strength through the γδTCR they generated γδTCR transgenic TCRζ$^{(-/-)}$ mice expressing either the full length TCRζ construct or a truncated version that lacked the 3 immunoreceptor tyrosine-based activation motifs (ITAMs) present within the cytoplasmic domain of the receptor. Despite the equivalent surface expression of TCRγδ on DN thymocytes from these two transgenic mice lines CD5 levels (an indicator of signal strength) were drastically reduced on DNs from mice expressing the tailless TCRζ transgene. Thus, removal

of the ITAMs of TCRζ significantly diminished the strength of signalling through the TCR. As a result, fewer γδ T cells developed in these mice compared to those expressing full length TCRζ. This result resembled that from the γδTCR transgenic TCRζ$^{(+/-)}$ mice which had lower surface expression of the TCR and therefore confirmed that high TCRγδ surface expression correlates with strong signalling and favours γδ T cell development (Hayes et al., 2005). Moreover, analysis of TCRα KO DN thymocytes revealed that those expressing TCRγδ expressed higher levels of phosphorylated ERK1/2 and ZAP-70 compared to those that expressed the preTCR confirming that TCRγδ signals stronger than the preTCR (Hayes et al., 2005).

In the second report, Haks *et al* generated KN6 γδTCR transgenic mice on a RAGKO background (Haks et al., 2005). The KN6 γδTCR recognises the non-classical MHC class Ib molecule T22^{d}, the surface expression of which requires β_2M. Signalling through the receptor was attenuated by backcrossing the mice onto either a p56^{lck}-deficient or β_2M-deficient background. As a result the percentage of mature γδ T cells that developed was drastically reduced whereas the percentage of DPs increased from 0.5% in KN6$^{(+)}$ RAGKO mice to 63% in the absence of p56^{lck} and 94.2% in mice deficient for β_2M (Haks et al., 2005). Moreover, Lck and β_2M deficiency resulted in reduced activation of ERK1/2 and expression of Egr1 and Egr3 in KN6$^{(+)}$ RAG KO DN4 cells consistent with impaired TCR signalling. Furthermore, over-expression of Egr1 in KN6$^{(+)}$ RAGKO thymocytes in FTOC promoted γδ T cell development while reducing the percentage of DP cells (Haks et al., 2005). Together, these reports showed that strong signalling at the DN stage promotes γδ T cell development while weak signalling favours commitment to the αβ lineage.

The signal-strength model of αβ/γδ lineage commitment explains how the γδTCR is able to drive DP development in pTα KO and TCRβKO animals (Fehling et al., 1995a; Mombaerts et al., 1992a). The model suggests that in the absence of the preTCR in these animals, DN cells that have low surface expression of TCRγδ may commit to the αβ lineage. It also explains how early expression of the αβTCR, the surface expression of which is much greater than the preTCR, can promote the development of thymocytes that resemble γδ T cells (Bruno et al., 1996; Terrence et al., 2000).

The nature of the difference in signal strength delivered by either the γδTCR or the preTCR is not well understood. Most likely it is the difference in surface expression of the two receptors that regulates strength of signal; as the γδTCR is expressed on the surface of DN cells at far greater levels than the preTCR (40,000 complexes per cell compared to several hundred of the preTCR) (Hayes et al., 2003). Indeed, the preTCR, but not the γδTCR, is constitutively endocytosed from the surface of thymocytes in a manner that promotes very low surface expression of the receptor (Panigada et al., 2002) (this subject will be covered in more detail in subsequent chapters of the thesis).

2.3.2 IELs; The controversy between extrathymic and intrathymic T cell development.

2.3.2.1 Extrathymic development.

The origin of TCRαβ$^{(+)}$CD8αα$^{(+)}$ gut intraepithelial lymphocytes has been a matter of much controversy. These cells are present to some extent in athymic nude mice (De Geus et al., 1990), prompting the suggestion that T cell development was not solely dependent on the thymus. Certainly, the

development of TCR$\alpha\beta^{(+)}$CD8$\alpha\alpha^{(+)}$ IELs is not conventional. They develop in mice that lack MHC-I (Das and Janeway, 1999), or in F5 transgenic mice that are deficient in Tap-1 and RAG (Levelt et al., 1999). In addition, high-affinity TCR signalling appears to favour IEL development (Levelt et al., 1999) and IELs are enriched for "forbidden" TCRβ chains normally deleted from the conventional T cell repertoire by endogenously expressed MMLV superantigens (Rocha et al., 1991).

The hunt for a site for extrathymic T cell development initially identified small gut-associated lymphoid tissue present in the wall of the large and small intestine (called cryptopatches (CPs)) that contained immature hematopoietic cells (Saito et al., 1998). Transfer of immature CD25$^{(+)}$ IL-7R$^{(+)}$ c-Kit$^{(+)}$ CP cells into severe combined immunodeficient (scid) mice gave rise to TCR$\gamma\delta^{(+)}$ and TCR$\alpha\beta^{(+)}$ IELs (Saito et al., 1998). Consistent with this, the development of TCR$\alpha\beta^{(+)}$CD8$\alpha\alpha^{(+)}$ IELs is significantly abrogated in common cytokine receptor gamma (γ_c) chain KO mice that have no CPs (Oida et al., 2000). Furthermore, transfer of bone marrow (BM) into athymic γ_c KO mice restores CPs and the appearance of TCR$\alpha\beta^{(+)}$CD8$\alpha\alpha^{(+)}$ IELs (Suzuki et al., 2000). Finally, CP precursors of TCR$\alpha\beta^{(+)}$CD8$\alpha\alpha^{(+)}$ IELs appear to express markers of early T cell progenitors such as RAG-1 and pTα (Lambolez et al., 2002).

2.3.2.2 Evidence for thymic origin of TCR$\alpha\beta^{(+)}$CD8$\alpha\alpha^{(+)}$ IELs.

By contrast to the evidence presented in the previous section, a number of studies strongly support a thymic origin for TCR$\alpha\beta^{(+)}$CD8$\alpha\alpha^{(+)}$ IELs. Analysis of HY-TCR transgenic mice on an athymic/nude background revealed that only a small fraction of TCR$\alpha\beta^{(+)}$CD8$\alpha\alpha^{(+)}$ IELs develop extrathymically, whereas the majority originate in the thymus (Guy-Grand et al., 2001).

Further evidence from H-Y, OT-1, AND and 5C.C7-TCR transgenic mice showed that agonist-driven development of TCRαβ$^{(+)}$CD8αα$^{(+)}$ IELs occurs in both an MHC-I and MHC-II-dependent manner (Leishman et al., 2002). Importantly TCRαβ$^{(+)}$CD8αα$^{(+)}$ IEL development was shown to be dependent on expression of cognate self-antigen in the thymus as thymic grafts from adult TCR transgenic mice that did not express the ligand were unable to reconstitute the TCRαβ$^{(+)}$CD8αα$^{(+)}$ IEL compartment of RAG KO mice (Leishman et al., 2002). High affinity self-antigen selection of TCRαβ$^{(+)}$CD8αα$^{(+)}$ IELs was dependent on the connecting peptide domain of TCRα known to be essential for positive but not negative selection of thymocytes (Leishman et al., 2002). Together these data showed that rather than escaping negative selection, TCRαβ$^{(+)}$CD8αα$^{(+)}$ IELs are positively selected in the thymus by agonist self-peptide. This type of selection is consistent with observations in normal mice where TCRαβ$^{(+)}$CD8αα$^{(+)}$ IELs are enriched for cells expressing superantigen-specific “forbidden” Vβ chains that are eliminated from the conventional T cell pool by negative selection (Rocha et al., 1991).

The manner by which TCRαβ$^{(+)}$CD8αα$^{(+)}$ IELs survive high affinity agonist signals in the thymus is not well understood. Circumstantial evidence suggests that CD8αα homodimers raise the threshold of signalling through the TCR; as T cell lines with a greater CD8αβ to CD8αα ratio appeared to be more sensitive to TCR signalling (Cawthon et al., 2001). As CD8αα homodimers are not associated with lipid rafts (Pang et al., 2007) it has been postulated that CD8αα homodimers could bind and sequester signalling components such as Lck and LAT from CD8αβ containing TCR complexes (Cheroutre and Lambolez, 2008; Gangadharan and Cheroutre, 2004). In addition, TCRαβ$^{(+)}$CD8αα$^{(+)}$ IELs have been shown to contain

FcεR1γ chains in place of one or both of the TCRζ chains (Guy-Grand et al., 1994). Because FcεR1γ chains have one rather than three ITAMs the amplitude of signalling through the TCR would be diminished. Furthermore, TCRαβ$^{(+)}$CD8αα$^{(+)}$ IELs express LAT 2 which negatively regulates TCR signalling (Denning et al., 2007; Zhu et al., 2006). Thus, it appears that TCRαβ$^{(+)}$CD8αα$^{(+)}$ IELs are set up to dampen signals received through the TCR which allows them to be positively selected on high affinity self peptide interactions in the thymus.

Evidence against extrathymic development of TCRαβ$^{(+)}$CD8αα$^{(+)}$ IELs was also observed in RAG-GFP transgenic mice that expressed GFP under the control of the RAG-2 promoter. Whether in athymic or euthymic mice, GFP expression was not observed in either IELs or cryptopatch cells suggesting an absence of recombinase activity in these cells (Guy-Grand et al., 2003). However, identification of an intestinal specific isoform of RAG-1 in humans raised the possibility that extrathymic TCR gene rearrangement may be controlled by alternative tissue specific promoters (Bas et al., 2003).

Fate mapping by use of mice expressing GFP under the control of the RORγt gene concluded that all TCRαβ$^{(+)}$CD8αα$^{(+)}$ IELs are progeny of immature DP thymocytes (Eberl and Littman, 2004). During foetal life RORγt is exclusively expressed in lymphoid tissue inducer (LTi) cells, while in the adult RORγt is expressed only in thymic DP cells. In the RORγt-GFP reporter mice all DP thymocytes and TCRαβ$^{(+)}$ thymocytes were GFP positive, whereas TCRγδ$^{(+)}$ T cells were not. Significantly, TCRαβ$^{(+)}$CD8αα$^{(+)}$ IELs of the gut were also GFP positive suggesting that they had arisen from DP thymocytes (Eberl and Littman 2004).

Recently, Hilde Cheroutre and colleagues identified putative precursors of TCR$\alpha\beta^{(+)}$CD8$\alpha\alpha^{(+)}$ IELs within the thymic DP population that express CD4, CD8$\alpha\beta$, and CD8$\alpha\alpha$ and are thus termed “triple positive” (TP) cells (Gangadharan et al., 2006). TP cells were identified using CD8$\alpha\alpha$-specific tetramers that consist of thymic leukaemia (TL) antigen, a non-classical MHC-Ib molecule that binds with high affinity to CD8$\alpha\alpha$ homodimers but not to CD8$\alpha\beta$ heterodimers. $TL^{(+)}$ TP cells constituted 6-9% of the WT DP population. TP cells differ from DPs in their ability to survive and mature in response to agonist antigen. TP cells are more immature than DPs as they are actively dividing and express lower levels of TCRβ and CD5. They are suggested to represent the pre-selection thymic precursors of TCR$\alpha\beta^{(+)}$CD8$\alpha\alpha^{(+)}$ IELs as adoptive transfer of TPs into the thymus of C57BL/6 recipient mice gave rise to TCR$\alpha\beta^{(+)}$CD8$\alpha\alpha^{(+)}$ IELs and $CD5^{(-)}$ TCR$\alpha\beta^{(+)}$ DN T cells in the periphery. The TCR$\alpha\beta^{(+)}$ DN cells were shown to be post-thymic-selection precursors of TCR$\alpha\beta^{(+)}$CD8$\alpha\alpha^{(+)}$ IELs (Gangadharan et al., 2006). However, this study failed to investigate the thymic origin of TP cells; specifically how their differentiation from the earlier DN subset differed from that of DP cells.

2.3.3 Heterogeneity within the DP population; is heterogeneity in preTCR signals a possible explanation?

Identification of TP cells with a different developmental potential to DP cells is strong evidence for heterogeneity within the $CD4^{(+)}$ CD8$\alpha\beta^{(+)}$ subset (Gangadharan et al., 2006). How would this be achieved? $CD4^{(+)}$ CD8$\alpha\beta^{(+)}$ DPs are generated from DNs by signalling through the preTCR (Figure 2.5). Thus heterogeneity within the DP population implies either heterogeneity within the DN subset that is a direct precursor of the DP population, or in the preTCR signal which drives the DN to DP transition.

We propose that the pTα component of the preTCR is central to the provision of differential signalling through the preTCR, and that by analogy to γδ T cell development, which requires a strong signal at the DN stage, a stronger signal through the preTCR is also required for commitment to an unconventional fate (i.e. to TCRαβ$^{(+)}$CD8αα$^{(+)}$ cells) in the αβ T cell lineage.

Figure 2.5

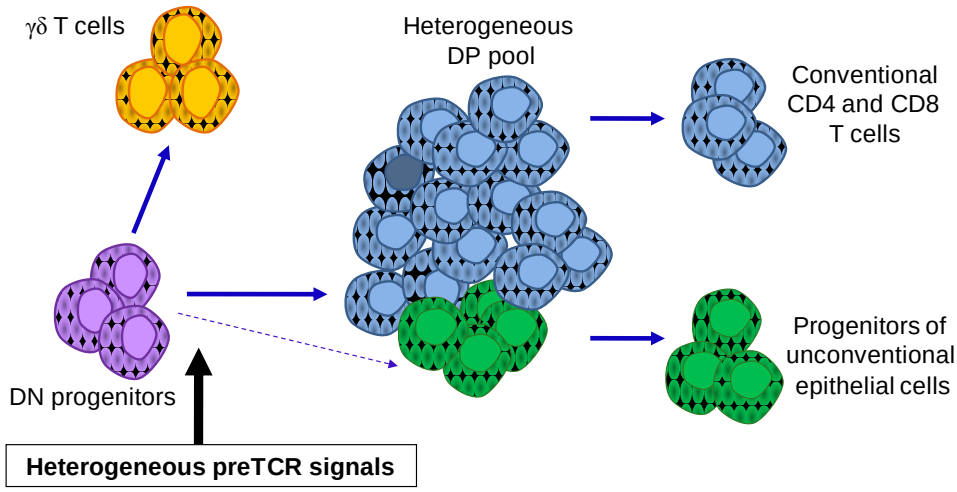

Figure 2.5 Hypothesis: Heterogeneity within the DP subset implicates heterogeneity in the events regulating commitment to the DP stage. We propose that unconventional αβ T cell development requires a different preTCR signal than that received by conventional DP precursors, at the DN to DP transition.

Chapter 3

The pre T cell receptor alpha (pTα).

In the 1980s it was observed that TCRβ chains were rearranged before TCRα chains during T cell development (Raulet et al., 1985; Snodgrass et al., 1985). Expression of TCRβ transgenes in rearrangement-deficient scid and RAG-2 KO mice showed that TCRβ chains were expressed at the surface of thymocytes and resulted in proliferation, upregulation of CD4 and CD8, and transcription of TCRα (Kishi et al., 1991; Shinkai et al., 1993). Analysis of TCRβ KO mice revealed that this chain was critical for the DN to DP transition (Mombaerts et al., 1992a). It was clear from studies in immature T cell lines and TCRα-deficient thymocytes, that TCRβ was forming a complex on the surface of cells with a disulphide linked 33kDa glycoprotein as well as the CD3 signalling molecules CD3ε, CD3δ, CD3γ and very weakly associated TCRζ chains (Groettrup et al., 1993). The gene that encoded this 33kDa glycoprotein was identified as the pre T cell receptor alpha gene or pTα (Saint-Ruf et al., 1994). pTα is a type-1 transmembrane protein of the Ig-superfamily.

The pTα gene is located on chromosome 17 in mice and spans approximately 8.4kb, consisting of four exons (Figure 3.1). The first exon codes for the 5' untranslated region, the leader peptide and the first three amino acids of the protein. Exon-2 encodes the extracellular domain of the protein and includes two cysteine residues which form a disulphide bridge generating an immunoglobulin-like loop. In addition, there are two potential glycosylation sites within this domain. Exon-3 is only 45 base pairs in length

and encodes a connecting peptide which includes the cysteine residue that forms a disulphide bridge with TCRβ. The transmembrane domain, encoded by exon-4, consists of about 20 hydrophobic amino acid residues and includes two basic residues; arginine and lysine that are similar to those found in the transmembrane domain of TCRα. These polar residues are thought to be necessary for interactions with the CD3 signalling cassettes. Exon-4 also encodes the relatively long cytoplasmic tail of pTα, consisting of two tyrosine phosphorlyation sites as well as a proline rich region which could constitute an SH3-domain binding sequence. Exon-4 contains of 540 nucleotides of the 3' untranslated region including the polyadenylation site (Fehling et al., 1995b; Saint-Ruf et al., 1994; von Boehmer and Fehling, 1997).

Figure 3.1

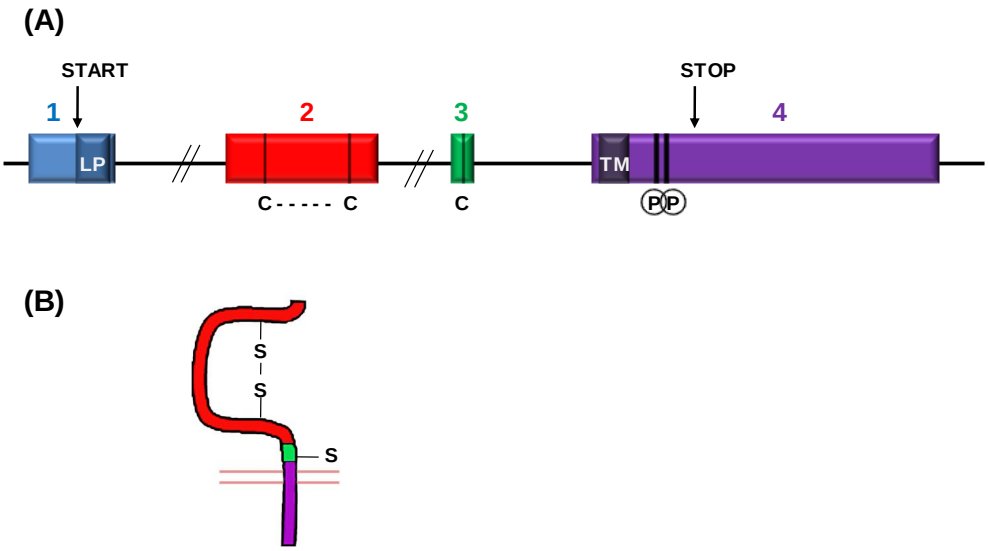

Figure 3.1 pre-T cell receptor alpha (pTα): (A) An illustration of the pTα gene, consisting of four exons; exon-1 (blue), exon-2 (red), exon-3 (green) and exon-4 (purple). The start and stop sites of the amino acid sequence are shown. LP is leader peptide, c----c denotes the cysteine residues in exon 2 which form the disulphide bond in the mature protein (B). TM is transmembrane and (P) denotes the putative phosphorylation sites within the cytoplasmic tail. A cysteine residue encoded within exon-3 forms a disulphide bond with TCRβ in the preTCR complex.

3.1 The function of pTα.

3.1.1 Evidence from pTα-deficient mice.

To investigate the function of pTα in T cell development two different sets of pTα-deficient mice were generated. The first pTα KO was generated by deletion of exons 3 and 4 (Fehling et al., 1995a). These animals have a vastly reduced thymic cellularity to less than 10% of a WT thymus. The majority of pTα KO thymocytes were arrested at the DN3 stage in development, confirming the function of the preTCR in promoting development past this stage. However, the developmental block is not complete as a small number of DP thymocytes are present in the pTα KO thymus. Importantly, pTα was shown to divert cells away from the γδ cell lineage, as a 3 fold increase in the number of γδ thymocytes was observed in the pTα KO thymus. Thus, pTα and the preTCR are necessary for development of αβ but not γδ T cell precursors (Fehling et al., 1995a). Interestingly, only 40% of pTα deficient DP cells express intracellular TCRβ, suggesting that TCRγδ drives development of the majority of DP cells in the pTα KO thymus (Buer et al., 1997a).

A second pTα KO mouse was generated by deletion of Exon-2 and the surrounding introns of the pTα by gene by targeting embryonic stem (ES) cells (Xu et al., 1996). pTα KO ES-cells were injected into RAG-2-deficient blastocysts to generate chimeras. These animals displayed an identical phenotype to the pTα KO mice generated by Fehling *et al*.

3.1.2 Evidence for β-selection in WT mice.

Analysis of pre- and post-β-selection thymocytes in C57BL/6 mice revealed two populations of DN3 cells; those that were of an expected size (DN3e)

and had few in-frame TCRβ rearrangements and those that were large or blasting (DN3L) which had significantly more in-frame TCRβ rearrangements (Hoffman et al., 1996). The majority of DN3e cells were in the G1 phase of the cell cycle with a DNA content of 2n, whereas 66% of the DN3L population had a DNA content greater than 2n. Furthermore, the DN3L population were enriched for cyclin A and CDK2 expression that drive cell cycle entry. These cells also expressed lower levels of RAG-2 in comparison to the DN3e subset (Hoffman et al., 1996), consistent with the observations that RAG proteins are targeted for degradation by cell cycle protein cdc2 kinase (Lin and Desiderio, 1993). These results demonstrate that the preTCR appears to induce proliferation of β-selected thymocytes.

3.2 Signal transduction downstream of the preTCR.

3.2.1 The signalling components of the preTCR.

The signalling components that comprise the preTCR complex are essentially the same as those that form the TCRαβ complex, with the obvious exception of pTα and TCRα (Kruisbeek et al., 2000). However, various gene-deficient mouse models have shown that while CD3ε and CD3γ are essential for the DN to DP transition, CD3δ is not (Berger et al., 1997; Dave et al., 1997; Haks et al., 1998; Malissen et al., 1995). TCRζ is only weakly associated with the preTCR through interactions with the connecting peptide domain of pTα (Kosugi et al., 1997; Trop et al., 1999). Nonetheless, TCRζ is phosphorylated upon preTCR signalling (van Oers et al., 1995) and TCRζ KO mice exhibit a partial block in the DN to DP transition (Love et al., 1993). Because of the similarities between the preTCR and TCRαβ it was assumed that signalling through the two

complexes activated the same signal transduction pathways (Kruisbeek et al., 2000; Michie and Zuniga-Pflucker, 2002; Rothenberg et al., 2008).

3.2.2 TCRαβ signal transduction.

Figure 3.2 summaries the downstream signalling cascade of the αβ T cell receptor (Weiss and Littman, 1994). TCR signals are initiated and propagated by protein tyrosine kinases such as Lck and Fyn (Weiss and Littman, 1994). Lck is associated with the cytoplasmic regions of the co-receptors CD4 and CD8, while both Lck and Fyn are associated with the TCRζ and CD3ε chains (Samelson et al., 1990; Veillette et al., 1988). Upon ligation of TCRαβ through interaction with peptide/MHC, the TCRαβ complexes cluster at the cell surface. As a result Lck and Fyn become activated and phosphorylate the ITAMS of TCRζ and the various CD3 chains.

Phosphorylation of ITAMs on TCRζ and CD3 molecules leads to recruitment and binding of SH2 (Src Homology 2 domain)-containing proteins such as ZAP-70, which in turn phosphorylates the downstream adaptor molecules; LAT and SH2-domain containing leukocyte protein (SLP)-76 (Janssen and Zhang, 2003; Weiss and Littman, 1994). These in turn then activate the three main pathways involved in TCRαβ signal propagation; the MAP kinase, calcium and NFκB pathways. This occurs via activation of phospholipase C-γ (PLC-γ) which catalyses the conversion of phosphatidylinositol bisphosphate (PIP_2) to inositol trisphosphate (IP_3) and Diacylglycerol (DAG). DAG activates RAS-GRP which in turn activates RAS. RAS activates the three major MAP-kinase pathways which include ERK1/2, JNK and p38 that upregulate transcription factors fos, jun and Egr1-3 (Rincon et al., 2001). Concurrent with this, the interaction of IP_3 with

its receptors in the endoplasmic reticulum releases calcium into the cytoplasm, leading to activation of calmodulin, calcineurin and subsequently the transcription factor NFAT (Weiss and Littman, 1994). DAG and calcium also activate various members of the protein kinase C (PKC) family, which activate the transcription factor NFκB (Ruland and Mak, 2003).

Figure 3.2

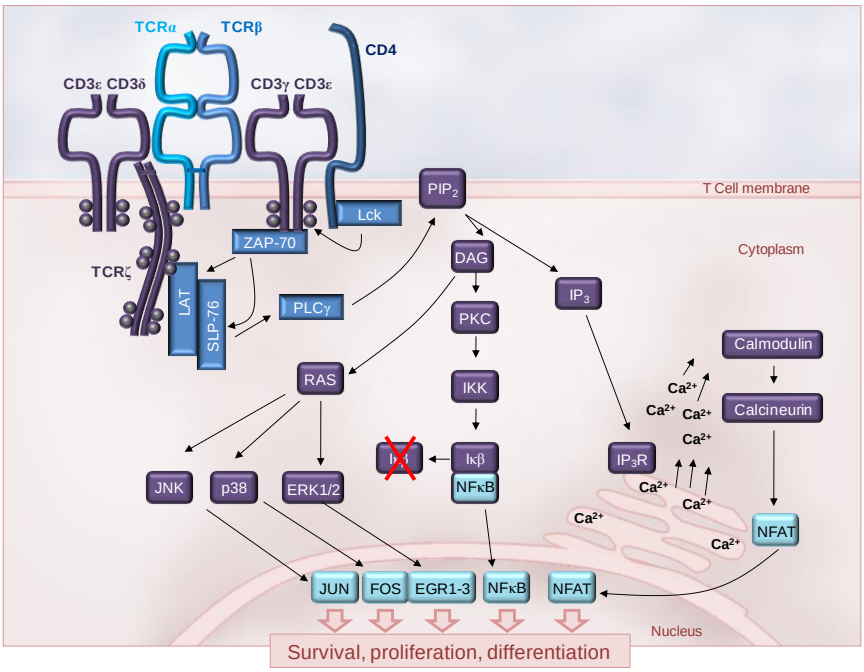

Figure 3.2 Signalling cascades activated downstream of TCRαβ: Interaction of TCRαβ with peptide/MHC induces aggregation of the receptor complexes which leads to activation of protein tyrosine kinases such as Lck that is bound to the intracellular tail of the co-receptor molecules CD4 and CD8. Lck phosphorylates ITAMs present on TCRζ and various CD3 chains, leading to the recruitment of SH2-containing protein ZAP-70. Adaptor molecules LAT and SLP-76 are activated through phosphorylation by ZAP-70 and in turn, activate PLCγ. PLCγ catalyses the conversion of PIP_2 to IP_3 and DAG. DAG activates RAS GRP which in turn activates the three major MAPK pathways; JNK, p38 and ERK which lead to the upregulation of transcription factors fos, jun and Egr1-3. IP_3 interaction with the IP_3R in the ER leads to the release of calcium into the cytoplasm that activates calmodulin, leading to the activation of calcinuerin and the transcription factor NFAT. DAG also activates PKC which phosphorylates IKK which in turn phosphorylates IκB targeting it for degradation. This releases NFκB which migrates to the nucleus. TCRαβ activation of downstream signalling pathways results in the proliferation, survival and differentiation of T cells.

3.2.3 PreTCR signalling activates similar pathways to TCRαβ.

Evidence that preTCR function was mediated by similar signalling pathways to TCRαβ initially arose from mice that lacked Lck or Fyn (Molina et al., 1992; van Oers et al., 1996). Mice that lacked both Lck and Fyn displayed a complete block at the β-selection checkpoint (van Oers et al., 1996). Furthermore, expression of an activated Lck transgene rescued the developmental block in RAG-1 KO and pTα KO mice (Fehling et al., 1997; Mombaerts et al., 1994). A CD4 transgene was also observed to promote development of RAG-deficient thymocytes to the DP stage in the presence, but not in the absence, of MHC-II (Norment et al., 1997). This was proposed to be the result of activation of Lck bound to the cytoplasmic tail of CD4. Importantly Lck did not drive development in the absence of CD3ε (Norment et al., 1997). These experiments demonstrate that Lck activation and subsequent activation of the CD3 signalling cassettes mediates all the functions of the preTCR; proliferation, differentiation of thymocytes to the DP stage and allelic exclusion at the TCRβ locus. Table 1 summarises the gene-targeting experiments that have provided further insight into the proteins involved in preTCR signalling.

The role of MAP kinases in preTCR signalling is apparent from expression of a dominant negative mutant of MEK-1 in E14 TCRα KO thymocytes, as development to the DP stage was blocked (Crompton et al., 1996). In Expression of the preTCR in different T cell lines has also been shown to upregulate JNK and p38 activity as well as phosphorylation of ERK1 and ERK2 (Michie et al., 1999; Murga and Barber, 2002). At this point in the signal transduction cascade, (downstream of SLP-76) the different phenotypes of preTCR signalling segregate with different signalling effectors; activated c-RAF-1 (RAF-CAAX) and RAS-V12 were sufficient to

drive proliferation and differentiation of RAG KO thymocytes, but did not induce allelic exclusion of the TCRβ locus (Gartner et al., 1999; Iritani et al., 1999). However, allelic exclusion was mediated by PKC (Michie et al., 2001).

Table 1

Deficiency	Phenotype	Reference
pTα	Complete block at DN3 stage	(Fehling *et al* 1995a), (Xu *et al* 1996)
TCRβ	Complete block at DN3 stage	(Mombaerts *et al* 1992a)
TCRα	Complete block at DP stage	(Mombaerts *et al* 1992a)
CD3ε	Complete block at DN3 stage	(Malissen *et al* 1995)
CD3γ	Complete block at DN3 stage	(Haks *et al* 1998)
CD3δ	Complete block at DP stage	(Berger *et al* 1997), (Dave et al 1997)
CD3ζ	Partial block at DN3 stage	(Love *et al* 1993)
Lck+Fyn	Severe block at DN3 stage	(van Oers *et al* 1996)
ZAP-70+Syk	Severe block at DN3 stage	(Cheng et al., 1997)
LAT	Complete block at DN3 stage	(Zhang et al., 1999)
SLP-76	Complete block at DN3 stage	(Pivniouk et al., 1998)

Table 1 Mutations that have provided insights into the regulation of preTCR signalling. TCR, T cell receptor; DN, double negative; DP, double positive; LAT, linker for activation of T cells.

3.2.4 PreTCR signalling promotes cell survival by downregulation of p53.

Double-strand DNA breaks produced by V(D)J recombination trigger p53-mediated cell cycle arrest to limit the development of cells with oncogenic potential (Guidos et al., 1996). In normal cells the double-strand DNA breaks are rapidly dealt with by the activity of DNA-dependent protein

kinase (DNA-PK). Mutations in this gene are the underlying cause of the immunodeficiency observed in the naturally-occurring scid mouse (Blunt et al., 1995). In these animals, high levels of p53 expression is detected in DN3 cells, that mediates cell cycle arrest and apoptosis (Guidos et al., 1996). Indeed p53 ablation rescued development of scid DN thymocytes to the DP stage (Guidos et al., 1996). PreTCR-deficiency also results in an increase in cell death at the DN stage; approximately 40% of DN cells from CD3γ or RAG-1 deficient mice stain positive for Annexin V (Haks et al., 1999). This was shown to be p53 dependent as CD3γ/p53 double-deficient mice had restored viability of DN cells and increased development to the DP stage (Haks et al., 1999). Direct evidence that preTCR signalling reduced the activation of p53 came from analysis of T cell lines transfected with preTCR components, which displayed a reduction in phosphorylation of p53 compared to controls (Murga and Barber, 2002). Moreover, gene expression of p53 downstream effectors; death gene BAX and cyclin dependent kinase inhibitor p21, were reduced in preTCR expressing cell lines (Murga and Barber, 2002). Thus, preTCR signalling induces the survival of thymocytes by downregulation of p53.

3.3 Transcription Factors that mediate preTCR function.

3.3.1 NFκB and NFAT.

Numerous transcription factors have been implicated in regulating the DN to DP transition, including NFκB (Kruisbeek et al., 2000; Michie and Zuniga-Pflucker, 2002). All thymocytes express activated NFκB, but the highest levels are seen in DN3L and DN4 subsets that express the preTCR (Voll et al., 2000). Indeed, preTCR expression in a $CD3^{(+)}$ cell line resulted in activation of NFκB, suggesting that NFκB is regulated by preTCR signalling

(Voll et al., 2000). In transgenic mice expressing a dominant active form of IκBα an inhibitor of NFκB, fewer DN cells progressed to the DP stage. Conversely expression of a constitutively active form of IκB kinase (IKK) that leads to the degradation of IκB, rescued the developmental block of RAG KO thymocytes (Voll et al., 2000).

The transcription factor NFAT has been shown to be upregulated in a RAG KO DN cell line after treatment with α-CD3ε suggesting that preTCR signalling induces NFAT expression (Aifantis et al., 2001). The upregulation of NFAT downstream of the preTCR was shown to be dependent on PLCγ and Ca^{2+} (Aifantis et al., 2001). Treatment of E14.5 FTOC lobes with cyclosporine A (CSA) an inhibitor of NFAT dephosphorylation and nuclear transport, resulted in inhibition of DN3 progression, implicating a role of NFAT in preTCR function (Aifantis et al., 2001; Koltsova et al., 2007).

3.3.2 Egr and RORγt.

The early growth response (Egr) transcription factors play an important role in regulating proliferation and differentiation of β-selected cells. Egr1, Egr2 and Egr3 are all upregulated following preTCR signals induced by anti-CD3ε treatment of SCID.adh cell line (Carleton et al., 2002). Expression of Egr genes in preTCR deficient thymocytes, either by retroviral transduction of Egr1, Egr2 or Egr3 in CD3γ-deficient thymocytes in FTOC, or by transgene expression of Egr1 in RAG KO mice, induced proliferation and differentiation past the DN3 stage (Carleton et al., 2002; Miyazaki, 1997). However, Egr-expressing thymocytes developed to the $CD8^{(+)}$ immature single positive (ISP) stage, but not to the DP stage suggesting the requirement for additional factors in the maturation of ISPs to DPs (Carleton et al., 2002). This would be more consistent with Egr

transcription factors inducing proliferation but not differentiation of thymocytes post-β-selection. This is supported by Egr3-deficient mice which do not exhibit a block in the DN to DP transition, but do have reduced thymic cellularity as a result of poor proliferation of β-selected thymocytes (Xi and Kersh, 2004a).

Extensive investigations into the role of Egr transcription factors in β-selection has provided important insight into the interplay of different transcription factors in regulating proliferation and differentiation downstream of the preTCR. DP cells that express Egr3 transgenes under control of the CD2 promoter fail to develop to the CD4 and CD8 SP stages (Xi and Kersh, 2004b). This was due to increased apoptosis of DPs and reduced rearrangement of TCRα genes, and as a result the mice displayed reduced thymic cellularity. Importantly, the lack of survival of DP cells that over-expressed Egr3 was a result of downregulation of Bcl-X_L and the orphan nuclear receptor RORγt (Xi and Kersh, 2004b). These authors performed a time-course experiment in which RAG-1 KO mice were injected with anti-CD3ε antibodies to mimic preTCR stimulation. Total RNA, was extracted from the thymuses of these mice at various time points, after anti-CD3ε showed that while Egr3 expression rapidly increased after preTCR stimulation, by 36 hours expression had returned to basal levels. Expression of RORγt and Bcl-X_L increased at 36 hours and reached a maximum at 4 days after preTCR stimulation (Xi and Kersh, 2004b). Furthermore, RORγt-deficient DP cells displayed a similar phenotype to Egr3 transgenic DP cells, with increased proliferation but poor survival (Sun et al., 2000). This suggested that RORγt negatively regulates proliferation of β-selected thymocytes. Bcl-X_L and RAG-2 were both found to be upregulated in RORγt-expressing cell lines (Xi et al., 2006), and RORγt has

been shown to bind to the TEA promoter that is necessary for TCRα rearrangements (Villey et al., 1999). In summary, it appears that Egr transcription factors, in particular Egr3 promote proliferation of β-selected thymocytes. Egr3 downregulation of RORγt is one possible mechanism for this increased proliferation. However, prolonged proliferation by constitutive activation of Egr3 appears to be deleterious for maturing thymocytes, as very few progress to the DP stage, and those that do have reduced survival and rearrangement of TCRα genes. In normal β-selected thymocytes it appears that Egr3 expression is transient and after 36 hours expression returns to basal levels. This allows for expression of RORγt and further maturation of β-selected DP cells. RORγt expression is therefore necessary for sustaining the resting state of DPs to allow for rearrangement of TCRα genes and to promote survival of cells undergoing active gene rearrangements (Xi et al., 2006).

3.3.3 E-proteins.

To complicate matters further it was found that Egr mediated proliferation of β-selected thymocytes was dependent on induction of the inhibitor of the basic helix-loop-helix (BHLH) E-proteins; Id3 (Koltsova et al., 2007; Xi et al., 2006). Id3 forms heterodimers with E-proteins such as E2A and HEB and prevents their DNA binding activity. E-proteins play a crucial role in regulating T cell development in the thymus (discussed further in other chapters of this introduction). E-proteins are potent inhibitors of proliferation prior to TCR rearrangements (Engel and Murre, 2004). E2A-deficient mice rapidly develop thymic lymphomas, consistent with a role for these factors in regulating lymphocyte proliferation (Bain et al., 1997). Importantly, E47, an isoform of E2A was described to bind E-box sites in the TCRβ promoter and in the enhancer regions regulating TCRβ gene

rearrangement. Analysis of E15 thymocytes from E47 heterozygous and homozygous mutant mice revealed that TCRβ rearrangement was reduced by E47 deficiency in a dose dependent manner (Agata et al., 2007). Moreover E47 was shown to control the accessibility of the TCRβ locus, and histone H3 acetylation, and expression of Vβ germline transcripts were reduced in E47-deficient mice (Agata et al., 2007). Thus E2A expression in pre-β-selected thymocytes arrests proliferation and promotes TCR gene rearrangement. As already mentioned, preTCR signalling induces expression of Id3 through activation of the MAP kinase pathway and Egr transcription factors (Bain et al., 2001; Engel et al., 2001; Koltsova et al., 2007). Id3 upregulation is necessary for inhibition of the E-proteins, promotion of proliferation and differentiation to the DP stage. Indeed, the DN to DP block in LAT-deficient and in Lck/Fyn double-deficient animals is rescued by deletion of E47 (Engel and Murre, 2004). Inhibition of E47 activity is also required for allelic exclusion at the TCRβ locus, over-expression of E47 in DO11.10 TCRαβ transgenic thymocytes induced excessive Vβ-DJβ rearrangements (Agata et al., 2007).

HEB KO mice have a similar phenotype to Egr transgenic mice; few DP thymocytes but an accumulation of ISPs (Barndt et al., 1999). This suggests a delayed role for HEB downstream of the preTCR in establishing the DP phenotype. E47, E12 and HEB bind E-box sites in the RORγt promoter (Xi et al., 2006). Deletion of 2 out of the 4 of these E-box regions drastically reduced the activity of the RORγt promoter. Retroviral expression of E47 in T cell lines induced RORγt and E47-deficient DP cells show reduced RORγt expression (Xi et al., 2006). This suggests that E-proteins positively regulate RORγt in thymocytes.

Figure 3.3

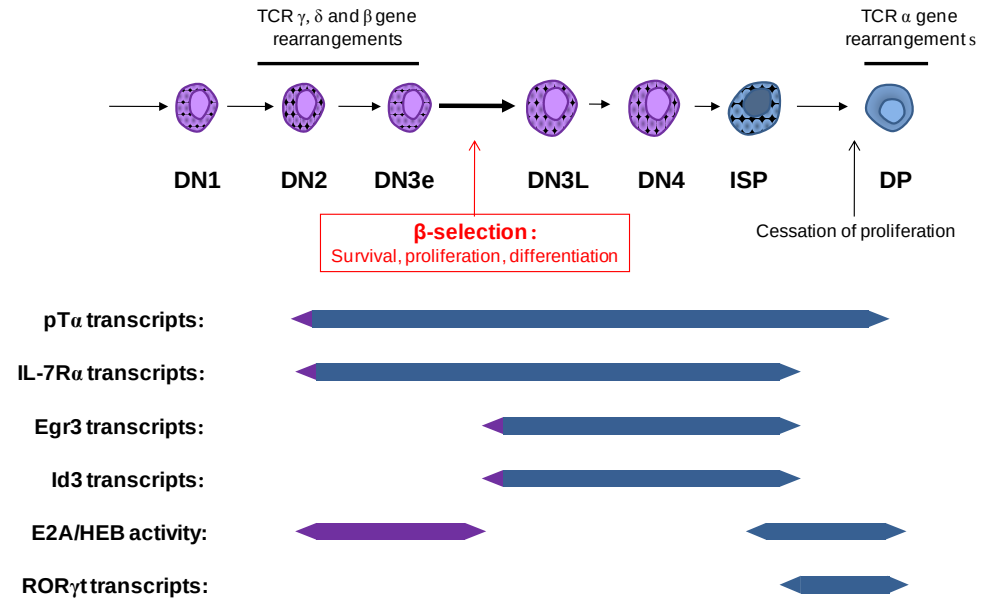

Figure 3.3 Different factors regulate the β-selection checkpoint. E proteins regulate pTα expression, which in turn initiates formation of the preTCR with TCRβ. Signalling through this complex upregulates IL-7Rα, and Egr3 and Id3. These factors induce proliferation and differentiation to the ISP stage. Progression and establishment of the DP stage requires downregulation of IL-7Rα, Egr3 and Id3 and upregulation of E-protein activity which induces RORγt. DN, double negative; ISP, immature single positive; DP, double positive; TCR, T cell receptor.

These reports reveal an important network of transcription factors that controls the DN3 to DP transition (Figure 3.3). To summarise, E-proteins are required at the DN3 stage to arrest proliferation and initiate TCRβ rearrangements and pTα expression (see the next section). Once successful TCRβ rearrangements have been achieved, TCRβ pairs with pTα and forms a preTCR complex with CD3 chains which is expressed on the surface of DN3 cells. Signalling through the preTCR complex induces proliferation through activation of Egr3 and Id3, which inhibits the anti-proliferative activity of the E-proteins. Id3 inhibition of E-proteins also

contributes to allelic exclusion at the TCRβ locus. However, Egr3 expression is transient, and after 36 hours returns to basal levels. This relieves the inhibition of E-protein activity which upregulates RORγt and together these transcription factors arrest proliferation, induce TCRα rearrangements, and ensure survival of DP thymocytes.

3.4 Cytokine signalling: the role of Interleukin-7 (IL-7) at the β-selection checkpoint.

IL-7 signals by binding to the IL-7 receptor which consists of the IL-7Rα chains and the common cytokine receptor γ chain (γ_c) (Sudo et al., 1993). IL-7/IL-7R signalling is crucial for thymocyte survival, proliferation and differentiation throughout T cell development (Peschon et al., 1994; Rothenberg et al., 2008). IL-7/IL-7R signalling is mediated by janus kinase-1 (JAK-1), janus kinase-3 (JAK-3), and signal transducer and activator of transcription-5 (STAT-5). Injection of anti-CD3ε antibodies into RAG-deficient mice resulted in upregulation of IL-7Rα transcripts (Trigueros et al., 2003), suggesting that preTCR signalling induces IL-Rα expression. This was confirmed by retroviral expression of TCRβ in RAG-deficient thymocytes in FTOC, which induced upregulation of IL-7Rα protein on the surface of transduced thymocytes (Trigueros et al., 2003). The expression of IL-7Rα transcripts peaked at 6 hours after preTCR stimulation, preceding CD25 downregulation by DN3s and the increase of cells entering the cell cycle. This implicated IL-7 signalling in the proliferation and differentiation of β-selected thymocytes. Blocking IL-7 signalling, either by IL-7Rα deficiency or through antibody treatment of DN4 cells resulted in reduced proliferation and increased cell death of β-selected thymocytes, confirming the role of IL-7 downstream of the preTCR (Trigueros et al., 2003).

In accordance with these data, retroviral expression of an inhibitor of JAK-STAT signalling, the suppressor of cytokine signalling-1 (SOCS-1) in RAG KO E14 thymocytes in FTOC drastically reduced the proliferation of transduced thymocytes. Furthermore, SOCS-1 expression is transiently suppressed following preTCR signalling in WT thymocytes (Trop et al., 2001).

Importantly, inhibition of signalling through the IL-7R has a more severe effect on DN4 cells and ISP cells, when compared to DP thymocytes (Trigueros et al., 2003). This suggests that IL-7 is more crucial for the proliferation and survival of the DN4 and ISP stages. Also, because IL-7Rα upregulation appears to be transient and is decreased after 12 hours post preTCR stimulation, it appears that the IL-7R may be regulated in a similar manner to Egr3. Indeed, ISP accumulation was promoted by IL-7 treatment of WT E16 FTOCs and the effect was made more profound by expression of an IL-7Rα transgene (Yu et al., 2004). The block in ISP to DP transition induced by IL-7, was accompanied by downregulation of RORγt expression in ISP cells (Yu et al., 2004).

3.5 Chemokine signalling: CXCR4 promotes β-selection.

Chemokines and their receptors regulate thymocyte migration during development (Takahama, 2006). Recently it has emerged that the chemokine receptor CXCR4 and its ligand CXCL12 participate in promoting survival and proliferation of β-selected thymocytes (Janas et al., 2010; Trampont et al., 2010). Evidence for the involvement of CXCR4 in T cell development came from competition assays in mixed chimeras where donor foetal liver cells from CXCR4-deficient mice showed impaired reconstitution compared to WT cells (Ara et al., 2003). Because CXCR4 is

expressed in DN2 thymocytes and upregulated at the DN3 stage before downregulation in the DN4 subset (Ara et al., 2003; Trampont et al., 2010), it seems likely that this receptor functions in and around the β–selection checkpoint. Using a mouse model in which CXCR4 is deleted at the DN2 stage, Trampont and colleagues demonstrate that deletion of CXCR4 hindered development past the DN3 stage and dramatically reduced thymic cellularity (Trampont et al., 2010). Development of CXCR4-deficient DN3 cells cultured on the OP9-DL1 stromal cell line was severely blocked compared to WT and loss of CXCR4 resulted in increased apoptosis of cortical thymocytes (Trampont et al., 2010).

CXCL12 is expressed in the subcapsular zone (SCZ) of the thymus and expression co-localised with DN2 and DN3 thymocytes (Trampont et al., 2010). CXCR4-deficient DN thymocytes exhibited aberrant distribution throughout the thymic cortex, suggesting a role for CXCR4 and CXCL12 in their SCZ localisation (Trampont et al., 2010).

CXCR4 is a G-protein coupled receptor (GPCR) that is dependent on the class 1A and class 1B phosphatidylinositol-3-kinase (PI3K) subunits p110δ, p110γ and p101 for signalling (Janas et al., 2010). Activated PI3K phosphorylates phosphatidylinositol-4,5-trisphosphate (PIP_2) to generate phosphatidylinositol-3,4,5,-trisphosphate (PIP_3) which is bound by pleckstrin-homology domain containing effector molecules such as Akt and PDK1 (Fruman and Bismuth, 2009). p110δ-deficient DN4 thymocytes, unlike WT DN4 cells were unable to phosphorylate Akt after preTCR signalling (Janas et al., 2010). Moreover, T cell development past the DN3 stage was impaired in mice deficient for both p110δ and p110γ and in mice deficient for both p110δ and p101, confirming the role of PI3K in β-selection. CXCL12/CXCR4 signalling was shown to induce phosphorylation

in WT DN3 thymocytes but not in thymocytes lacking both p110δ and p110γ, confirming the role of PI3K in mediating CXCR4 signals (Janas et al., 2010).

3.6. WNT signalling; the role of β-catenin and TCF-1/LEF-1 at the β-selection checkpoint.

IL-7 signalling in β-selected thymocytes downregulates expression of two transcription factors that are components of the canonical WNT signalling pathway, TCF-1 and LEF-1 (Melichar and Kang, 2007; Verbeek et al., 1995; Yu et al., 2004). Although LEF-1 deficient mice do not show any defects in T cell development (van Genderen et al., 1994), TCF-1-deficient mice display a profound block at the ISP stage (Verbeek et al., 1995). A more severe block is seen in LEF-1/TCF-1 double knock-out mice (Okamura et al., 1998). This suggests a redundant role for these two transcription factors in promoting the ISP to DP transition. TCF-1 and LEF-1 both bind to the transcriptional co-activator β-catenin (Melichar and Kang, 2007). β-catenin deletion induced by LCK-promoter-driven Cre resulted in a developmental block at the β-selection check-point (Xu et al., 2003). In the absence of WNT signals β-catenin is targeted for degradation by phosphorylation of sites encoded by exon-3 of the gene (Wodarz and Nusse, 1998). Deletion of exon-3 of β-catenin resulted in a stable form of the protein which was constitutively active (Gounari et al., 2001). Expression of this protein on a RAG-2 KO background rescued development of thymocytes in the absence of the preTCR (Gounari et al., 2001). Analysis of DP thymocytes from transgenic mice expressing the stabilised form of β-catenin under control of the CD4 promoter showed increased survival as a result of upregulation of Bcl-X_L (Xie et al., 2005). However, expression of a truncated form of β-catenin that lacked the tail of

the protein that targets it for degradation, resulted in arrested αβ T cell development at the DN4 and ISP stage (Xu et al., 2009a). The DN4/ISP cells in these mice have abnormally high levels of IL-7Rα and Egr-3 but low levels of RORγt (Xu et al., 2009a). β-catenin is upregulated after preTCR signalling and in turn upregulates IL-7Rα and Egr gene expression through binding TCF-1 (Xu et al., 2009b). Analysis of expression of β-catenin transcripts and protein in WT thymocytes revealed that DN3 cells had much higher levels than DN4 or ISPs (Xu et al., 2009a). This suggests that like Egr-3 and IL-7Rα, β-catenin upregulation may only be transient in post β-selection thymocytes.

3.7 Regulation of expression of pTα.

pTα expression is initiated in DN1 thymocytes and is upregulated in DN2 cells concomitant with commitment to the T cell lineage. Expression reaches its peak in DN3 thymocytes before decreasing in the DN4 and ISP subsets. pTα transcripts are detected in blasting DPs but are absent in mature SPs from both the thymus and lymph nodes, and are absent in γδ T cells. (Saint-Ruf et al., 1994). pTα is also expressed at sites of extrathymic T cell development such as the cryptopatches of the gut (Bruno et al., 1995). Characterisation of the pTα upstream genomic region revealed two specific DNase hypersensitive sites corresponding to a proximal promoter and an upstream enhancer (Reizis and Leder, 1999). The enhancer element is located 4kb upstream of the gene and is essential for pTα expression as deletion of this region abolished expression of a pTα BAC reporter construct in transgenic mice (Reizis and Leder, 2001). The enhancer element of the human pTα gene shares a high degree of homology (60%) with the mouse regulatory element, confirming the central role of the pTα enhancer in regulation of pTα gene expression (Reizis and

Leder, 2001). The pTα enhancer element contains potential binding sites for different transcription factors; c-Myb, ZBP-89, Sp1, CSL, as well as E-box sites recognised by E-protein transcription factors (Reizis and Leder, 2001).

3.7.1 c-Myb.

c-Myb is a member of the tryptophan cluster family of transcription factors and is essential for early T cell development (Allen et al., 1999). c-Myb was shown to bind and activate the c-Myb consensus binding sequence in the pTα enhancer using electrophoretic mobility shift assay (EMSA) and β-galactosidase assays (Reizis and Leder, 2001). Moreover, c-Myb is abundantly expressed in cortical pre-selection thymocytes, but not in post-selection medullary thymocytes or in resting peripheral cells (Ess et al., 1999), consistent with pTα expression.

3.7.2 E-proteins.

E2A and HEB transcription factors recognise and bind the E-box sites (CANNTG) in the pTα upstream enhancer region (Petersson et al., 2002). Expression of luciferase under control of these pTα-specific E-box sites was upregulated upon co-expression with E2A and HEB (Takeuchi et al., 2001). However, upregulation did not occur for mutant E-box constructs (Takeuchi et al., 2001), confirming the ability of E2A and HEB to activate pTα transcription by binding to the E-box sites upstream of the pTα gene. Moreover, E2A and HEB expression follows a very similar pattern to that of pTα throughout T cell development (Tremblay et al., 2003). Importantly E2A- and HEB-deficient DN thymocytes show reduced expression of pTα compared to WT (Tremblay et al., 2003). Thus E-protein transcription factors directly regulate pTα gene expression.

3.7.3 Notch.

The pTα enhancer is activated by Notch signalling and contains binding sites for the Notch nuclear effector CSL (CCTGGGAA) (Reizis and Leder, 2002). Upon ligand binding Notch is protealitically cleaved releasing its intracellular domain which translocates to the nucleus where it binds the transcription factor CSL. Notch binding changes CSL from a transcriptional repressor to an activator inducing transcription of target genes (Rothenberg et al., 2008). CSL was shown to bind to the target site within the pTα enhancer by EMSA (Reizis and Leder, 2002). Use of eGFP under the control of the CSL binding site of the pTα enhancer region, led to GFP expression in DN2 cells and upregulation DN3 cells, consistent with the expression pattern of pTα (Reizis and Leder, 2002). No GFP expression was detected in reporter mice which expressed eGFP under control of the enhancer region containing a mutated CSL binding site (Reizis and Leder, 2002). Furthermore, surface expression of Notch-1 can be detected in DN1 cells and is upregulated at the DN2 stage, peaking in DN3s, followed by downregulation in the DN4 and ISP subsets. Mature CD4 and CD8 SP thymocytes do not express detectable surface levels of Notch1 (Huang et al., 2003; Yashiro-Ohtani et al., 2009). This expression pattern is similar to that of pTα, consistent with regulation of pTα expression by Notch throughout T cell development.

Notch-1 signalling is central for progression through the β-selection checkpoint (Ciofani et al., 2004; Maillard et al., 2006). Inhibition of Notch-1 activation by dominant negative mastermind-like 1, arrests T cell development at the DN3 stage (Maillard et al., 2006). Moreover anti-CD3ε induction of RAG-1 KO thymocytes does not occur in the absence of Notch ligand Delta-like-1 (DL-1) (Ciofani et al., 2004).

Sustained expression of Notch and pTα is associated with ontogenesis in acute lymphoblastic leukaemia (TALL) (Bellavia et al., 2002; Li et al., 2008). Taken together with the observation that constitutive expression of pTα induces apoptosis of DP cells (Lacorazza et al., 2001a) and leads to the development of an abnormal peripheral T cell subset that express CD8αβ and low levels of TCRβ (Ito et al., 2002; Schnell et al., 2006), it suggests that tight control of pTα and Notch is crucial for appropriate T cell development. Expression of pTα and Notch is downregulated post β-selection by negative feedback inhibition controlled by upregulation of the E-protein inhibitor Id3 via preTCR signals (Yashiro-Ohtani et al., 2009). Notch1 regulatory regions also contain E-box elements that bind E47 and HEB (Yashiro-Ohtani et al., 2009). An E47-mediated increase in Notch-1 reporter activity was abrogated by Id3 expression (Yashiro-Ohtani et al., 2009). The binding activity of E2A to the Notch-1 promoter was significantly reduced after PMA/ionomycin treatment of SCID.adh cells, consistent with induction of Id3 downstream of preTCR signals (Yashiro-Ohtani et al., 2009). Furthermore preTCR signalling was shown to disrupt the positive feedback loop of Notch-1 transcription (Yashiro-Ohtani et al., 2009). Thus, preTCR signals induce expression of Id3 which inhibits E-protein transcriptional activation of pTα and Notch-1. Suppression of Notch-1 transcription reduces the amount of Notch-1 protein available to activate pTα transcription, further amplifying the negative feedback loop. In addition, p53 has been shown to activate transcription of Notch-1 in epithelial cells (Sasaki et al., 2002). Therefore preTCR mediated downregulation of p53 could be another mechanism for suppression of Notch and subsequently pTα in β-selected thymocytes.

3.7.4 Regulation of the surface expression of pTα.

PreTCR complexes on the surface of cells are constitutively endocytosed and degraded (Panigada et al., 2002). Endocytosis of the preTCR is dependent on activation of Lck and degradation of the complex is mediated by the c-Cbl ubiquitin ligase (Panigada et al., 2002). In addition, preTCR complex formation in DP cells is thought to be inhibited by expression of the newly rearranged TCRα chain (Trop et al., 2000). Indeed, TCRα chains are thought to out-compete pTα for pairing with TCRβ and CD3 in the endoplasmic reticulum, which leads to reduced levels of the preTCR on the cell surface (Trop et al., 2000).

3.8 Ligand-independent signalling by the preTCR.

Despite considerable knowledge of the downstream signalling events that are initiated from the preTCR, the mechanism by which preTCR signalling is initiated is still not clear. PreTCR surface expression is very low on DN thymocytes compared to that of TCRαβ on mature thymocytes. Thus, it is possible that the preTCR complex does not need to reach the cell surface for productive signalling to occur. However, transgenic mice expressing a TCRβ transgene fused to an ER retention motif from the adenoviral E19 glycoprotein demonstrated that surface expression of the preTCR was necessary for initiation of signalling through the complex (O'Shea et al., 1997). If surface expression of the preTCR was required for signal initiation the issue of whether this was dependent on ligand binding was addressed. For the αβTCR, ligand recognition is mediated by regions within the variable domains of the TCRα and β chains. However, truncated forms of both TCRβ and pTα that lacked any Ig-loops formed receptors on the surface of RAG KO DN thymocytes that were able to signal and promote development to

the DP stage (Irving et al., 1998). Moreover, expression of full length TCRβ and pTα in the Jurkat T cell line induce NFAT activation in the absence of cross-linking by antibodies for CD3ε or TCRβ (Irving et al., 1998). The DN to DP transition is also unaffected in mice lacking MHC-I or MHC-II molecules (Grusby and Glimcher, 1995; Koller et al., 1990). Thus it appears that the preTCR is able to signal independent of ligand binding.

Confocal microscopy of preTCR-expressing DN thymocytes or cell lines revealed a punctate staining pattern for pTα and TCRβ compared to the uniform distribution of CD25 or the γδTCR (Saint-Ruf et al., 2000). The patchy distribution of the preTCR on the surface of the cell was reminiscent of αβTCR after ligand binding and localisation to lipid rafts. Indeed, Cholera toxin B, which binds to the lipid raft constituent ganglioside GM1, was shown to localise to the pTα "patches" on the surface of transfected T cell lines (Saint-Ruf et al., 2000). Importantly, Lck was also shown to co-localise with pTα on the surface of transfected cells (Saint-Ruf et al., 2000). PreTCR localisation to lipid rafts in the presence of Lck results in the phosphorylation of CD3ε, TCRζ and Zap-70, but phosphorylation was not evident after disruption of lipid raft integrity by depletion of membrane cholesterol using methyl-β-cyclodextrin (Saint-Ruf et al., 2000). Targeting of CD3ε to lipid rafts drives preTCR independent development of RAG KO thymocytes (Ferrera et al., 2008). Because palmitoylation of cysteine residue in LAT has been shown to target the protein to lipid rafts (Zhang et al., 1998), it was proposed that palmitoylation of the juxtamembrane cysteine in the cytoplasmic tail of pTα was necessary for lipid raft localisation of the preTCR (Saint-Ruf et al., 2000). However, mutating this residue to alanine did not abolish preTCR signalling (Aifantis et al., 2002; Haks et al., 2003). Indeed, removal of the whole cytoplasmic tail of pTα

does not appear to affect the activity of the preTCR (Gibbons, Douglas et al.2000). Just how much preTCR is localised to lipid rafts is disputed, as analysis of surface CD3 expression on preTCR and αβTCR expressing scid cell lines revealed that only 10% of preTCR complexes localised to lipid rafts, a figure comparable to the number of TCRαβ complexes that associate with lipid rafts (Haks et al., 2003).

It has also been suggested that the nature of DN3 cells themselves is what determines ligand independent signalling at this stage of T cell development (Haks et al., 2003). Using a luciferase reporter system to detect ERK activity, a large proportion of DN3 cells, but not DN4 or DP cells, from TCRα KO mice were shown to have high levels of endogenous activated ERK. Moreover, TCRα-deficient DN4 cells stimulated with anti-TCRβ antibody produced more cytosolic calcium than DP cells. DN cells also have a higher lipid raft content than DP cells (Haks et al., 2003). Together this suggests that DN cells may have a lower threshold for signalling than other thymocytes, this increased sensitivity to TCR signals driving ligand-independent signalling at the β-selection checkpoint.

Further evidence to suggest that ligand-independent signalling of the preTCR is not due to a unique intrinsic property of pTα, is the ability of TCRαβ (and TCRγδ) to drive development past the β-selection checkpoint. TCRα expression in pTα-deficient thymocytes in FTOC was sufficient to promote development to the DP stage (Haks et al., 2003). However, TCRαβ does not appear as efficient as the preTCR at promoting proliferation and differentiation of thymocytes (Borowski et al., 2004; Buer et al., 1997a). Moreover, other reports have suggested that early expression of TCRαβ at the DN stage impairs αβ T cell development (Borowski et al., 2004; Lacorazza et al., 2001b; Steff et al., 2001), instead promoting development

of DN cells to cells which have characteristics of the γδ lineage (Terrence et al., 2000). It is not clear whether αβTCR replacement of the preTCR requires MHC-ligand interaction. TCRα constructs were shown to promote efficient development and proliferation of pTα KO thymocytes in MHC-I/ MHC-II double knockout FTOCs in the additional presence of MHC blocking antibodies (Haks et al., 2003). This suggests that MHC is not required for TCRαβ signal initiation in DN thymocytes and that TCRαβ is able to also signal ligand-independently. Conversely transgenic HY-TCRs expressed in pTα-deficient mice appeared to be most efficient at driving β-selection in the presence, rather than the absence, of their positively selecting MHC molecules (Croxford et al., 2008). Thus the issue remains unresolved.

Despite the evidence listed above, ligand-independent signalling is widely accepted to be an intrinsic property of pTα (Borowski et al., 2004; von Boehmer, 2005). A recent study by Yamasaki and colleagues reported a mechanism of ligand-independent signalling that involved the spontaneous clustering of preTCR complexes at the surface of DN cells (Yamasaki et al., 2006). These clusters form independently of ligand binding and were suggested to explain the punctuate pattern of expression observed for pTα on the surface of preTCR expressing cells (Saint-Ruf et al., 2000). Clustering of the preTCR led to constitutive internalisation of the preTCR complex, in a manner that resembled ligand-mediated endocytosis of the αβTCR (Yamasaki et al., 2006). By fusing the extracellular domain of pTα to the transmembrane and cytoplasmic domains of the human erythropoietin receptor (EPOR) the authors determined that the pTα-EPOR construct formed dimers in the IL-3 dependent BAF3 cell line. They ascribed constitutive dimerization to pTα but not to TCRα, and demonstrated that this

was due to the presence of four charged amino acids in the extracellular domain (aspartic acid at position 22 (D22), arginine at position 24 (R24), arginine at position 102 (R102) and arginine at position 117 (R117)) of pTα that were essential for oligomerization; mutating any of them to alanine abolished the ability of pTα-EPOR to dimerize and induce growth of the BAF3 cell line (Figure 3.4) (Yamasaki et al., 2006).

Figure 3.4

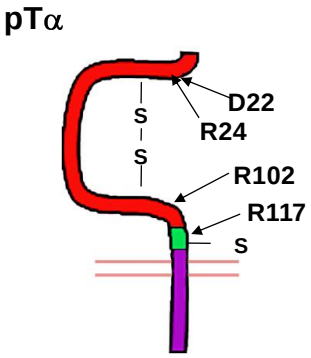

Figure 3.4 Charged residues in pTα extracellular domain mediate oligomerization of the preTCR. An illustration of the positions of the four charged amino acid residues; D22, R24, R102 and R117, located on the extracellular domain of pTα that are implicated in oligomerization of the preTCR. The colours represent the regions of pTα encoded by the different exons; exon-1 is blue; exon-2 is red, exon-3 is green and exon-4 is purple.

Expression of an R102/R117 double mutant of pTα in TCRα-deficient T cells resulted in higher surface expression of the mutant preTCR (Yamasaki et al., 2006), consistent with a role for these residues in promoting oligomerization and internalisation. Importantly, when expressed in pTα-deficient thymocytes in RAG KO mixed bone marrow chimeras, the R102/R117 double mutant pTα chain was unable to promote development to the DP stage (Yamasaki et al., 2006). Thus the authors of this study proposed that ligand-independent signalling of the preTCR is initiated by

cell autonomous oligomerization mediated by charged amino acids in the extracellular domain of pTα (Yamasaki et al., 2006). However, this report did not discuss truncated pTα chains, which lack the extracellular domains of the protein yet are able to signal and drive development past the β-selection checkpoint (Gibbons et al., 2001; Irving et al., 1998).

3.9 The two isoforms of pTα; pTα^{a} and pTα^{b}.

It was demonstrated well over ten years ago that two forms of pTα exist, formed by differential splicing of the pTα transcript; pTα^{a} and pTα^{b}. pTα^{a} is the "full length" version of the gene, using all four exons to construct the protein (Figure 3.5). This protein is the one exclusively referred to as pTα in the vast majority of research articles. By contrast, pTα^{b} lacks exon-2 that codes for the extracellular Ig-loop of the protein (Figure 3.5) (Barber et al., 1998). pTα^{b} was first identified in CD4$^{(+)}$ "β-only" peripheral T cells from TCRα-deficient mice (Barber et al., 1998). The human pTα gene also splices to form both pTα^{a} and pTα^{b} (Saint-Ruf et al., 1998), the conserved splicing across species suggesting an important role for the second isoform of pTα in T cell development.

The pTα^{b} isoform appears functional. In a T cell line, pTα^{b} was shown to form surface complexes with TCRβ (Barber et al., 1998). Expression of a pTα^{b} transgene in pTα KO mice relieved the αβ T cell developmental block and promoted development to the DP stage (Gibbons et al., 2001). In addition, the pTα^{b} transgene reduced the percentage and absolute number of γδ T cells consistent with the preTCRs function of promoting αβ lineage development at the expense of γδ T cells (Gibbons et al., 2001).

Although pTα^{b} appears to have the ability to form a functioning preTCR, the reason for having two different preTCRs, conserved across species, has

not been addressed. Initial characterisation of the two preTCRs *in vitro* revealed that preTCR^{b} exhibits higher surface expression than preTCR^{a} (Barber et al., 1998). Furthermore preTCR^{b} appeared to signal stronger than preTCR^{a} in 4G4 cell lines inducing greater phosphorylation of p38 and JNK (Murga and Barber, 2002).

Figure 3.5

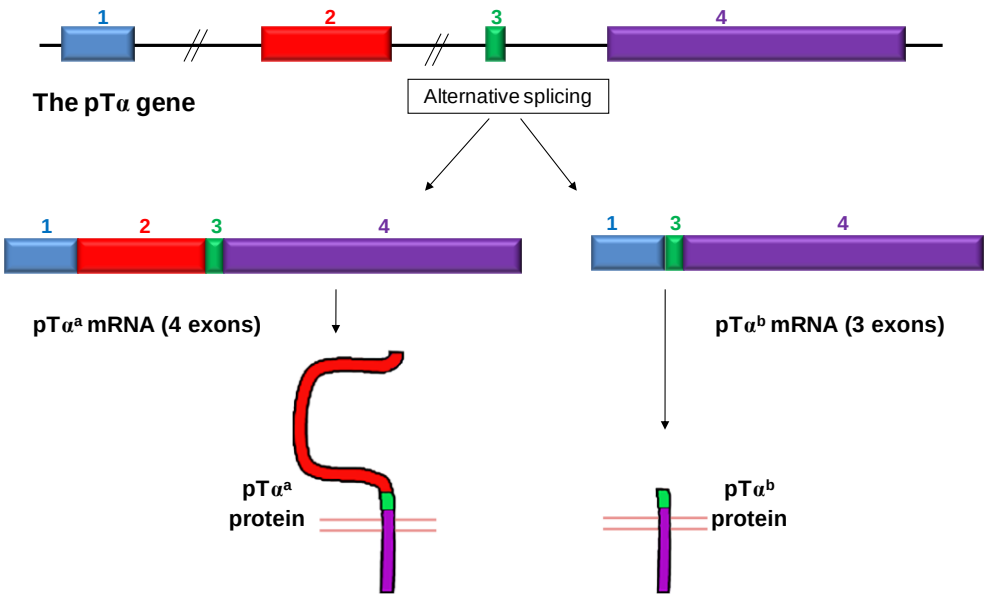

Figure 3.5 pTα codes for two isoforms. Schematic representation of the pTα gene consisting of four exons that undergoes alternative splicing to generate two isoforms; pTα^{a} and pTα^{b}. pTα^{a} is a "full length" version of the gene, while pTα^{b} is a truncated spliced-isoform that lacks exon-2 that codes for the extracellular Ig-loop of the protein. Exons are colour coded; exon-1 is blue, exon-2 is red, exon-3 is green and exon-4 is purple.

The differential surface expression and signalling capabilities described for pTα^{a} and pTα^{b} suggests the two isoforms may have different roles in T cell development. Indeed, a recent report has found that pTα^{b} expression is much greater than that of pTα^{a} in peripheral regulatory T cells and expression was necessary for the normal function of these cells (Campese et al., 2009). Despite the value of pTα^{b} transgenic mice in demonstrating some degree of functionality for preTCR^{b}, the quality of T cell development

was not addressed and a direct comparison with preTCR^{a} was not performed. Moreover, because the transgenes were expressed under control of the Lck proximal promoter, the proteins were not expressed in a physiological manner and would have continued into the later stages of thymocyte development instead of terminating at the DP stage. Thus a comparative analysis of pTα^{a} and pTα^{b} has yet to be carried out, and a definitive function for pTα^{b} has yet to be described. This thesis has attempted to address these two issues.

Hypothesis

We hypothesise that pTα^a and pTα^b have non-redundant roles in T cell development. We hypothesise that pTα^a and pTα^b form preTCR complexes that signal differently to promote differential developmental outcomes. We hypothesise that use of preTCR^a or preTCR^b will differentially determine conventional vs. unconventional T cell development (Figure 4.1).

Figure 4.1

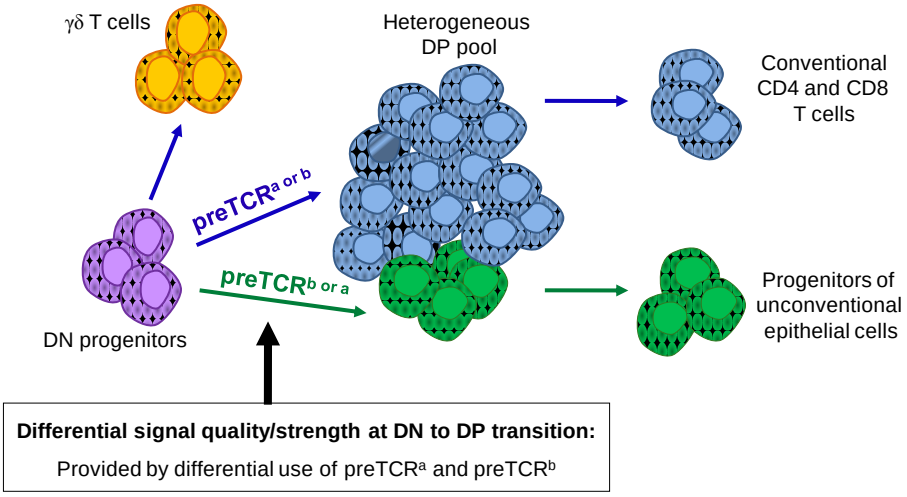

Figure 4.1 A schematic of the hypothesis: Differential use of preTCR^a and preTCR^b promotes differential signal quality/strength driving alternate developmental outcomes.

Aims

- To characterise expression of pTα^a and pTα^b in the thymus.
- To determine whether individual DN progenitors express one or both isoforms of pTα.
- To investigate the function of pTα^a and pTα^b when expressed in isolation in pTα-deficient thymocytes.
- To investigate whether oligomerization is necessary for signal initiation of the preTCR.
- To generate "pTα^a-only" and "pTα^b-only" BAC transgenic mice on a pTα-deficient background where expression of the transgenes will be appropriately controlled through development.

Methods

Chapter 1

Molecular Biology.

1.1 Gel electrophoresis.

Gel electrophoresis was used for separating DNA, either for visualisation of PCR products or restriction digest fragments or for isolation of DNA. Agarose (Melford labs) was dissolved in 1% TAE (see Table 1) with Ethidium Bromide (VWR) the gels were run in 1% TAE buffer.

Table 1

X50 stock TAE	242g Trizma Base (Sigma)
	57.1ml Glacial Acetic Acid (Sigma)
	100ml 0.5M EDTA, pH 8.0 (Gibco, Invitrogen)
	dH_2O to total volume of 1L

Table 1 Recipe for Tris-acetate-EDTA (TAE) stock solution. The stock solution was diluted 1/50 for electrophoresis.

For plasmids and PCR products 1% agarose gels were used and the gels were run at 110V for 45-60 minutes. To separate larger fragments, such as the BAC digests; 0.7% agarose gels were run at 39 volts for 5hours to achieve better resolution of the bands. 6X orange loading dye (Fermentas) was added to samples to facilitate loading of DNA into wells and 1kb DNA ladder (Fermentas) was run along samples to determine the size of the DNA in the samples.

1.2 DNA isolation.

1.2.1 Plasmids.

1.2.1.1 DNA gel extraction.

Plasmid DNA extraction was carried out using QIAquick gel extraction kit (QIAGEN) according to manufacturer's instructions. To summarise, the required DNA fragment was cut from the agarose gel (Melford Labs) using a sterile scalpel (Swann-Morton). The gel fragment was dissolved in 3 volumes buffer QG to 1 volume of gel, at 50^{o}C for approximately 10 minutes, vortexing every 3 minutes. The solution was added to the QIAquick spin columns and centrifuged at 13,000rpm for 1 minute using a Bench-top centrifuge, to bind the DNA. Columns were washed with a 1ml buffer QG to remove any residual agarose, and subsequently with buffer PE (with ethanol) to remove any salts. DNA was eluted in 30μl of sterile water and stored at -20^{o}C.

1.2.1.2 Miniprep.

In order to isolate plasmid DNA; single clones were retrieved from selection LB agar (Invitrogen) plates and left shaking, over night at 37^{o}C in 5ml LB broth (Invitrogen) containing the appropriate antibiotic for selection. Plasmid DNA was isolated from 5ml overnight cultures using QIAGEN miniprep kits (QIAGEN). In summary, the cultures were centrifuged at 7000rpm for 3 minutes and the pellets resuspended in 250μl buffer P1. 250μl lysis buffer (P2) was added and the tubes inverted. 350μl N3 was added for neutralisation and the samples were centrifuged at 13000rpm for 10 minutes. The supernatant was added to the QAIprep spin columns followed

by 1 minute centrifugation. Columns were washed with buffer PE (with ethanol) and DNA was eluted with 50μl sterile water.

1.2.1.3 Maxiprep.

In order to obtain large amounts of plasmid DNA 100ml bacterial cultures in LB broth containing the appropriate antibiotic were inoculated with a 5ml overnight culture. 100ml cultures were left shaking overnight at 37^{o}C before isolation of the DNA using JetStar Maxiprep kits (Genomed). To summarise the protocol, the bacteria were pelleted by centrifugation and all traces of media removed. 10ml buffer E1 was used to resuspend the pellet. 10ml lysis solution E2 was then added and mixed gently by inverting. The mixture was incubated at room temperature for 5min before adding 10ml buffer E3 for neutralization. The tubes were centrifuged at 12000xg for 10 min, and the supernatant was loaded onto an equilibrated column. The lysate was left to run through the column by gravity flow and the column was then washed with 60ml solution E5. Plasmids were eluted with 15ml solution E6 and precipitated by addition of 10.5ml isopropanol (Sigma Aldrich) and centrifugation at 12000xg for 30min at 4^{o}C. Plasmid DNA was washed with 70% ethanol (VWR) and re-centrifuged before air drying the pellet, and re-dissolving the DNA in suitable volume of water.

1.2.2 Bacterial artificial chromosomes (BACs).

1.2.2.1 DNA gel extraction.

BAC DNA fragments ≥ 20kb were isolated from 0.8% Agarose (Melford Laboratories) gels using the QIAEX II kit from QIAGEN. Gel fragments were collected in 1.5ml eppendorf tubes and weighed. 3 volumes of Buffer QX1 and 2 volumes of dH_2O to 1 volume of the gel (1g=1μl) were added to the tubes. QIAEX II silica beads were resuspended by vortexing and 30μl was added to the tubes containing gel fragments. The samples were incubated in a 50°C water-bath for 10 minutes, and mixed by flicking the tubes every 2 minutes. Samples were then centrifuged at 10000xg for 30 seconds and the supernatant removed and discarded. The pellet was washed by resuspending in 500μl Buffer QX1 and then washed twice with buffer PE (with ethanol). DNA pellets were dried for 10 minutes before being resuspended in 20μl dH_2O by incubation at 50°C for 10 minutes. The sample was centrifuged at 10000xg for 30 seconds to remove the silica particles and the DNA was stored at 4°C.

1.2.2.2 Miniprep.

This method of isolation of BAC DNA was used only to isolate small quantities for restriction enzyme analysis of the BAC clones. The DNA produced using this protocol was not clean or pure enough to use for subsequent recombineering steps. SW102 *E.coli* cells (Warming et al., 2005) containing the pTα BAC were grown overnight in 5mL of LB-Luria broth (0.5g/L NaCl – Sigma) with 12.5μg/ml chloramphenicol (Sigma) at 32°C. The bacteria were pelleted by centrifugation and resuspended in 250μL of QIAGEN buffer P1. Then 250μL of QIAGEN buffer P2 and 350μL

of QIAGEN buffer P3 were added to each tube, and the tubes were spun for 4 min. The supernatant fluid was transferred to new 1.5mL eppendorf tubes, which were spun for another 4 min. 750µL of isopropanol (Sigma Aldrich) was added to precipitate the DNA, at room temperature for 10 min, and DNA was collected by spinning the tubes for 10 minutes at the maximal speed. The DNA pellet was washed once with 1mL of 70% ethanol (VWR), dried, and resuspended in 50µL of dH_2O.

1.2.2.3 Maxiprep.

The Phaseprep BAC DNA kit (Sigma Aldrich) was used to isolate large quantities of pTα BAC DNA. The DNA isolated using this kit was of excellent quality and was therefore used for sequencing and subsequent recombineering steps. In summary of the protocol; 150ml LB-Luria broth (0.5g/L NaCl – Sigma) with 12.5µg/ml chloramphenicol was inoculated with a colony from a freshly streaked plate of SW102 cells transformed with the pTα BAC. The cultures were shaken overnight at 32^{o}C and centrifuged at 5000Xg for 10 minutes to harvest the cells. 12ml RNase-A/resuspension solution was added to the bacterial pellet and the cells were resuspended by pipetting up and down. 12ml Lysis-solution was added and the bottles inverted. 12ml chilled Neutralisation-solution was added to the lysate and mixed by inversion. The lysate was centrifuged at 15000xg for 30 minutes at 4^{o}C to pellet the cell debris. The supernatant was transferred to a clean bottle and 22ml of room temperature isopropanol (Sigma) was added and mixed by inversion before centrifugation at 15000xg for 5 minutes at 4^{o}C to pellet the DNA. DNA was air dried for 5 minutes before being dissolved in 5ml Elution solution. Residual RNA was removed by digestion with 5µl RNase cocktail at 60^{o}C for 15 minutes. The solution was then transferred to

a 15ml conical tube and 400μl of 3M sodium acetate buffer solution (pH 7.0) was added to adjust the salt concentration before endotoxin removal. 0.9ml endotoxin removal solution was added to the tube and the tube was inverted for 30 seconds. The samples were chilled on ice for 10 minutes before warming at 37^{o}C in a water-bath for 5 minutes and centrifuged at 4000xg for 5 minutes to separate the phases. The clear aqueous phase was collected into a clean tube. Endotoxin removal was then repeated to ensure complete removal of all impurities. The clear aqueous phase was transferred to a 50ml tube and 5.4ml room-temperature DNA precipitation solution was added before centrifugation at 15000xg for 30 minutes at 4^{o}C to pellet the DNA. The pellet was washed in 5ml 70% ethanol and dried for 5 minutes before dissolving in 1ml dH_2O.

1.2.3 Genomic DNA isolation.

Genomic DNA was isolated from ear pieces of 21-day-old mice for genotyping. The ear pieces were suspended in 1ml of SNET buffer (20mM Tris-Cl (pH 8.0, Sigma Aldrich), 5mM EDTA (pH 8.0, Invitrogen), 400mM NaCl (Sigma Aldrich), 1% SDS and 400μg/ml Proteinase K (QIAGEN)) in 2ml eppendorf tubes. Samples were incubated overnight at 55^{o}C on a rocking platform. 1ml phenol: chloroform: isoamyl alcohol (pH8.0, Sigma) was added to the digested ear samples followed by incubation at room temperature for 30 minutes on a rocking platform. Organic and aqueous phases were separated by centrifugation at 10000xg for 5 minutes at room temperature and the aqueous layer was transferred to a fresh eppendorf tube. DNA was precipitated by addition of 1ml of isopropanol (Sigma) and pelleted by centrifugation at 10000xg for 15 minutes at 4^{o}C. The isopropanol was removed with a pipette and after drying for 5 minutes, the

DNA pellet resuspended in 700µl dH_2O. 10µl of the DNA was removed at this stage and frozen to test by PCR. The rest of the DNA was further cleaned by addition of 1 x volume of phenol: chloroform: isoamyl alcohol, the tubes were shaken and then centrifuged at maximum speed for 5 minutes at room temperature. The aqueous phase was collected into fresh tubes and 10% volume 3M sodium acetate solution pH5.2 was added followed by 2 x volume 100% ethanol (VWR). The samples were incubated on ice for 20 minutes and then centrifuged at maximum speed for 10 minutes at 4^oC. The liquid was removed and the DNA pellet resuspended in 100µl of dH_2O. 1µl of DNA was used for subsequent PCR reactions.

1.3 DNA restriction digests.

1.3.1 Plasmids.

For routine restriction digests 0.5-1μg of plasmid DNA was used per 20μl reaction. For cloning, 2-5μg of plasmid DNA was used. Reaction components were; (x)μl DNA, 2μl 10x buffer (see Table 2 for the appropriate buffer), 1μl enzyme and dH_2O to make the volume 20μl. Reactions were set up in 1.5ml eppendorf tubes and incubated in a 37^oC heat block for 1-2 hours. Table 2 shows the details of all the restriction endonucleases and buffers used for this project. All restriction endonucleases were purchased from New England Biolabs.

Table 2

Enzyme	Restriction site	Buffer
AccII (BstUI)	5'-CG^CG-3' 3'-GC^GC-5'	NEB buffer 4
BamH1	5'-G^GATCC-3' 3'- CCTAG^G-5'	NEB buffer 3
Dpn1	5'-GA(CH_3)^TC-3' 3'-CT^A(CH_3)G-5'	NEB buffer 4
EcoR1	5'-G^AATTC-3' 3'-CTTAA^G-5'	NEB EcoR1
Hha1	5'-GCG^C-3' 3'-C^GCG-5'	NEB buffer 4
Hpa1	5'-GCG^C-3' 3'-C^GCG-5'	NEB buffer 4
Spe1	5'-A^CTAGT-3' 3'-TGATC^A-5'	NEB buffer 4
Xba1	5'-T^CTAGA-3' 3'-AGATC^T-5'	NEB buffer 4
Xho1	5'-C^TCGAG-3' 3'-GAGCT^C-5'	NEB buffer 4

Table 2 List of Restriction endonucleases used in the experiments for this thesis. Restriction enzymes are shown along with the recognition sequence and the corresponding buffer used for DNA digest reactions. All enzymes were obtained from New England Biolabs.

1.3.2 BACs.

3-5μg of BAC DNA was used for restriction digests with a total reaction volume of 50μl. Reaction components were; (x)μl DNA, 5μl 10x buffer (see Table 2 for the appropriate buffer), 2μl enzyme and dH_2O to make the volume 50μl. The reactions were set up in 1.5ml eppendorf tubes and left overnight in a 37^oC heat block before running on a 0.8% agarose gel (Melford Laboratories).

1.4 DNA quantitation.

The concentration of DNA was measured using a Nanodrop ND-100 spectrophotometer (Labtech International) at a wavelength of 260nm.

1.5 RNA isolation.

RNA was isolated from C57BL/6 thymocytes sorted using the Fluorescence activated cell sorter. The cells were lysed in Trizol (Invitrogen) by repetitive pipetting; 1ml of Trizol is used per 5-10x10^6 cells. Trizol is a mono-phasic solution of phenol and guanidine-isothiocyanate that maintains the integrity of the RNA while disrupting cells and dissolving cell components. Homogenised samples were incubated at room temperature for 5 minutes. 50μg RNase-free glycogen (Fermentas) was used as carrier to improve efficiency of recovery and enable the visualisation of the RNA pellet. 200μl of chloroform was added per 1ml of Trizol and the tubes were shaken vigorously. The samples were centrifuged at 13,000xg for 5 minutes to separate the organic and aqueous phases. The aqueous phase containing the RNA was transferred to a fresh eppendorf tube on ice. The RNA was precipitated by addition of 500μl of isopropanol and incubation at room temperature for 15 minutes. The samples were then centrifuged for 8

minutes at 13,000xg. The supernatant was removed carefully so as not to disturb the pellet. The RNA pellet was washed once with 500µl 70% ethanol (VWR) to remove any salt. The pellet was left to air dry, until it acquired a glassy look.

The next step was DNase treatment of the RNA pellet. First the pellet was resuspended in 34µl of dH_2O. 4µl of DNase buffer (Promega), 2µl DNase (Promega) was added and mixed by slow repetitive pipetting at a 40µl final reaction volume. The reaction was left to incubate at 37°C for 20-30 minutes before protein removal. 160µl ddH_2O was added to each sample and 200µl phenol: chloroform: isoamyl alcohol. The tubes were shaken then centrifuged for 5 minutes at maximum speed. The top aqueous phase was collected in a fresh tube and 200µl of chloroform added. The mixture was shaken then centrifuged for 5 minutes at top speed. The top aqueous phase was removed and approximately 10% final volume (20µl) of a 3M sodium acetate solution pH 5.2 was added. 2.5 volumes of 100% ethanol were added and the samples were incubated on ice for 20 min. RNA was pelleted by centrifugation at top speed for 10-12 min. The RNA pellet was resuspended in 11µl dH_2O ready for cDNA synthesis.

1.6 cDNA synthesis.

11µl of ddH_2O was used to resuspend the RNA pellet. 1µl of Oligo dT (500 ng/µl solution, Fermentas) was added to the RNA and the mixture was heated to 70°C for 10 min, followed by immediate cooling on ice before spinning down and adding the rest of the synthesis reaction components; 4µl 5x first-strand buffer (Takara Bio-Clontech), 2µl dNTP mix at a concentration of 10mM of each nucleotide (Takara Bio-Clontech), 2µl DTT (100mM-BD) and 1µl of PowerScript Reverse Transcriptase (RT) (Takara

Bio-Clontech). The cDNA synthesis reaction final volume was 20µl. The reaction was incubated at 42°C for 50-90 minutes and was terminated by heating at 70°C for 15 min. cDNAs were stored at -20^{o}C.

Alternatively SuperScript III Reverse transcriptase (Invitrogen) was used for the first strand cDNA synthesis reactions. The reaction was set up according to the kit protocol. In summary, 0.5µl 100µM oligo dT, 1µl 10mM dNTP mix was mixed with up to 5µg RNA and sterile distilled H_2O, added to a total volume of 13µl. The reaction mix was heated at 65^{o}C for 5 minutes and immediately put on ice for at least 1 minute. The reaction mix was centrifuged briefly and the following reagents were added; 4µl 5X First-strand buffer, 1µl 0.1M DTT 1µl SuperScript III RT (at 200units/µl). The reaction was heated at 50^{o}C for an hour before inactivating by heating at 70^{o}C for 15 minutes. cDNAs were stored at -20^{o}C.

1.7 Polymerase Chain Reaction (PCR).

To prevent contamination of PCR reactions the reactions were set up in a separate room to where the DNA template was added. The basic components of each PCR reaction is summarised in Table 3. Table 4 shows the reaction conditions for a typical PCR reaction. The PCR programmes used followed the same steps; the denaturing temperatures vary depending on the enzymes used and the annealing temperatures also vary depending on the primer pairs.

Table 3

Component:	Volume/reaction:
Template DNA	1µl
10X Buffer	2µl
dNTP mix (25mM)	2µl
Forward primer: (25pmol/µl)	1µl
Reverse primer: (25pmol/µl)	1µl
Enzyme	0.1µl
dH_2O	12.9µl
Total Volume	20µl

Table 3 Reaction components for a typical PCR. The reaction mix was made and aliquoted into PCR tubes before transferring to a separate room to add the DNA.

PCR primers were designed, and ordered from Eurofins MWG Operon, and melting temperatures (TM) were obtained from the oligo-property scan online (www.eurofinsdna.com), or the data-sheet provided. TMs used in each PCR reaction were identified by performing a gradient PCR for each primer pair. The temperature gradient used ranged from ~3^{o}C below the lowest TM to the temperature of the highest TM. For all PCRs, with

exception of the single cell PCRs, DYAD DNA engine thermo-cyclers (MJ Research) were used. Because the PCR conditions varied for each different experiment, they have been further outlined below.

Table 4

Step	Conditions
1	DT for 30-60 seconds
2	DT for 15 seconds
3	TM for 30 seconds
4	72^{o}C 1 minute/kb
5	Cycle to step 2 -37 more times
6	72^{o}C for 5 minutes
7	4^{o}C forever

Table 4 Reaction conditions for a typical PCR: DT is denaturing temperature, which was specific to the enzyme used and TM is melting temperature which specific to the primer pair used.

1.7.1 Semi-quantitative PCR.

Semi-quantitative PCR analysis pTα^{a} and pTα^{b} was performed on cDNAs synthesised from C57BL/6 thymocytes. The cDNA levels were normalised by β-actin PCR. Taq polymerase (New England Biolabs) and the corresponding Taq polymerase buffer were used for the PCR reactions at a denaturing temperature of 94^{o}C. The primers used for these experiments and the corresponding melting temperatures are described in Table 5.

Table 5

Primer	Sequence	TM
pTα F2 (pTα^a forward)	5'-TCTGAAGAGCTGGAAGCCTGGGAGC-3'	67^{o}C
pTα F1-3 (pTα^b Forward)	5'-TCAGGCTCTACCATCAGGGGAATC-3'	63^{o}C
pTα R (Reverse)	5'-GCTATCCTATCAGAGACTGGGCTCT-3'	n/a
β- actin Forward	5'-CAGTTCGCCATGGATGACGATATC-3'	62^{o}C
β- actin Reverse	5'-GTGTTGAAGGTCTCAAACATGATC-3'	62^{o}C

Table 5 Primers for semi-quantitative PCR. The table shows the primers used in semi-quantitative PCR analysis for pTα^a and pTα^b and the β-actin PCR. The same reverse primer (R) was used for pTα^a and pTα^b PCRs.

1.7.2 PCR for cloning pTα^a and pTα^b.

Phusion polymerase (Finnzymes) was used to clone pTα^a and pTα^b from C57BL/6 DN4 thymocyte cDNA. Phusion is a high fidelity polymerase which creates blunt ended PCR products. The denaturing temperature for Phusion was 98^{o}C and the TM for the reaction was 67 ^{o}C. The primers were pTα F4 (forward) 5'-TAGCCCACACCTCAGAGCTGCAG-3' and pTα R2 (Reverse) 5'-GCTATCCTATCAGAGACTGGGCTCT-3'.

1.7.3 Site directed mutagenesis PCR.

*Pfu*Turbo DNA polymerase-AD (Stratagene) was used for the mutagenesis PCRs. The reaction conditions were; denaturing temperature 95^{o}C, extension at 68^{o}C for 4.5 minutes (approximately 4.5kb plasmid template) and 18 cycles. pTα R24A primers were used to generate pTα^a-R24A (Table 6) with pBlunt-pTα^a plasmid as the template. Two mutagenesis steps were carried out generate pTα^a-DRRA; the first using pTα^a-D22R24A primers (Table 6) with pBlunt-pTα^a plasmid as the template (10-20ng), the second using pTα^a-R102A primers (Table 6) with pBlunt-pTα^a-D22R24A mutant plasmid as the template (10-20ng).

Table 6

Primer	Sequence	TM
pTα R24A F	5'-CTGCTGGTAGATGGAGCGCAGCACATGCTGG-3'	72.8^{o}C
pTα R24A R	5'-CCAGCATGTGCTGCGCTCCATCTACCAGCAG-3'	72.8^{o}C
pTα D22R24A F	5'-TCACACTGCTGGTAG CTGGAGCGCAGCACATGCTG-3'	73.2^{o}C
pTα D22R24A R	5'-CAGCATGTGCTGCGCTC CAGCTACCAGCAGTGTGA-3'	73.2^{o}C
pTα R102A F	5'-TGGGGGACAGAACGCGAGCACACACC-3'	69.7^{o}C
pTα R102A R	5'-GGTGTGTGCTCGCGTTCTGTCCCCCA-3'	69.7^{o}C
pTα R117A F	5'-TCTTCGACAGCCGCGAGCTGCTTTCCG-3'	69.9^{o}C
pTα R117A R	5'-CGGAAAGCAGCTCGCGGCTGTCGAAGA-3'	69.9^{o}C

Table 6 Primers used for site directed mutagenesis of pTα^{a} and pTα^{b}. The table shows the sequences of each of the primers (and corresponding TMs) used to generate pTα^{a}-R24A, pTα^{a}-DRRA and pTα^{b}-R117A alleles. Underlined text denotes the desired mutation; F is forward and R is reverse.

To generate pTα^{b}-R117A the pTα^{b}-R117A primers were used (Table 6) with pBlunt-pTα^{b} plasmid as a template. The primers for mutagenesis were designed according to the guidelines provided in the Quick change II XL Site directed mutagenesis kit manual (Stratagene). Both mutagenic primers for each construct contained the desired mutations and annealed to the same sequence on opposite strands of the plasmid. The primers were between 25 and 45 base pairs in length with a melting temperature of ≥78^{o}C.

The following formula was used for estimating the TM

Tm = 81.5 + 0.41(%GC) - 675/*N* - % mismatch

(Where N is the primer length in bases and the percentage of Gs and Cs and mismatch are whole numbers). The desired mutation was located in the middle of each primer with 10-15 bases of correct sequence on both

sides. In addition the primers had a GC content of at least 40% and terminated in one or more G or C bases. The melting temperature used was 5^{o}C lower than that calculated using the formula above. The primers were diluted to 62.5ng/μl and 125ng of each primer was used in each reaction.

1.7.4 Recombineering PCR.

1.7.4.1 PCR amplification of *galK*.

The *galK* sequence to be inserted into the pTα BAC for the first recombineering step (covered in more detail later in the Methods) was amplified by PCR from 2ng of a p*GalK* plasmid obtained from (www.recombineering.ncifcrf.gov). Primers p21 and p22 (Table 7) were used to amplify *galk* generating "homology arms" for homologous recombination into intron-1 of the pTα gene. p21 consisted of 75bp homology to intron-1 of pTα and 24bp homology to the 5'-region of *galK*. p22 consisted of 75bp homology to intron-1 of pTα and 25bp homologous to the 3'-end of *galK*.

Table 7

Primer	Sequence
p21	5'-GACAGGGTTTCTCTGTGTAGCTCCGGCTGTCCTGGAACTCACTCTGTAGA CCAGGCTGGCCTCGAACTCAGAAATCCTGTTGACAATTAATCATCGGCA-3'
p22	5'-TGGGTTGTTGGTGGGTGGGCGGTTGTTAGTTGGTTGCTGTCAGT CTTGGCTTGCTAAGTAGTCGTGGGCAAAGAATCAGCACTGTCCTGCTCCTT-3'

Table 7 primers p21 and p22 for amplifying *galK* and generation of "homology arms" for insertion into the pTα BAC. The primers possess 75bp of homologous sequence to intron-1 of pTα and 25bp homology to the *galK* gene (underlined).

Phusion polymerase (Finnzymes) was used to amplify *galk*. The reaction was heated at; 98°C for 15 seconds, 60°C for 30 seconds, 72°C for 1 min, for 30 cycles.

1.7.4.2 Generating double stranded oligos for *galK* replacement.

The primers used for generating double-stranded DNA oligos to replace the *galK* sequence in the pTα BAC, for generating pTα^{a}-only and pTα^{b}-only BAC constructs are shown in Table 8. P23 and P24 were used to replace galk and fuse exons 1 and 2 of pTα to generate the pTα^{a}-only BAC construct. p23 consisted of 85bp homology to the 3' -end of exon-1 and the 15bp of homology to the 5'-end of exon-2 of pTα. p24 consisted of 15bp of homology to the 3'-end of exon-1 and 85bp homologous to the 5'-end of exon-2.

Table 8

Primer	Sequence
p23	5'-TGGGTCATGCTTCTCCACGAGTGGGCCATGGCTAGGACATGGCTGCTGCT GCTTCTGGGCGTCAGGTGTCAGGCCCTACCATCAGGCATCGCTGGCACCC-3'
p24	5'- AGGCAAACCACCAGCATGTGCTGCCTTCCATCTACCAGCAGTGTGATGGGT GGAGCCAGAGACGGAAAGGGGGTGCCAGCGATGCCTGATGGTAGGGCCT-3'
p31	5'- TGGGTCATGCTTCTCCACGAGTGGGCCATGGCTAGGACATGGCTGCTGCTG CTTCTGGGCGTCAGGTGTCAGGCCCTACCATCAGGGGAATCTTCGACAG-3'
p32	5'-TTCCCAGCCACCGTCCCTCCCTCACCCACTGGTGACTTACCCCCGAGAGG CTCCGGAAAGCAGCTCCTGGCTGTCGAAGATTCCCCTGATGGTAGGGCCT-3

Table 8 Primers for generating double-stranded oligos for the second recombineering step. The table shows primers for generating double-stranded DNA oligos to replace *galk* in the pTα BAC and subsequently generate pTα^{a}–only (with p23 and p24 by fusion of exons 1 and 2 of pTα) and pTα^{b}–only (with p31 and p32 by fusion of exons 1 and 3 of pTα) BAC constructs: The underlined sequence denotes regions of homology to exon-1 of pTα.

p31 and p32 were used to replace *galk* and fuse exons 1 and 3 of pTα to generate the pTα^{b}-only BAC construct. p31 consists of 85bp of homologous sequence to the 3'-end of exon-1 and 15bp homology to the 5'-region of exon 3 of pTα. Because exon 3 of pTα is only 45bp long, p32 was designed to contain 25bp homology to the 3'-end of exon-1, 45bp homology to all of exon-3 and 40bp homology to intron-3 of pTα.

Each primer pair was annealed and extended to generate a double-stranded DNA oligo. 10μg of each primer was used with 2μl dNTPs (25nM) and 5μl 5X PCR buffer (Phusion High Fidelity polymerase kit, Finnzymes) with dH_2O to a total volume of 50μl. The mixture was heated in a thermo-cycler at 98^{o}C for 5 min, and then cooled from 90^{o}C to 80^{o}C at 1^{o}C/ minute. After 2 minute incubation at 80^{o}C, 0.2μl Phusion polymerase was added for extension of the annealed primers. The mixture was further cooled from 80^{o}C to 72^{o}C by 1^{o}C every 2 minutes and then incubated on ice. The double-stranded DNA oligos were gel purified to a final concentration of 200ng/ml in ddH_20. 200ng was used in the recombineering experiments (which will be described later in this chapter).

1.7.5 Single cell Multiplex PCR.

Single cell multiplex PCR was used to determine expression of pTα^{a} and pTα^{b} in single DN3 and DN4 C57BL/6 thymocytes. Because of the sensitivity and accuracy of the assay it was essential that the reagents were kept separate from the template or amplified product. Therefore separate rooms were used for 1) aliquoting reagents and making the master mixes, 2) aliquoting the master mix into the PCR tubes, 3) adding the template DNA and 4) gel electrophoresis of the PCR products. The PCR was performed in 5 steps; 1) Single cell sort, 2) lysis of single cells 3)

Reverse transcription (RT), 4) Multiplex PCR and 5) 2nd round nested-PCR. The DN3 and DN4 single cells used in this experiment were sorted into individual PCR tubes in 5μl PBS (Invitrogen) and stored at -80°C.

1.7.5.1 Primers for Single cell multiplex PCR.

The primers used in this experiment are shown in Table 9. The primers were reconstituted in 1X TE buffer (Promega); 30μl 1000nM aliquots were stored at -80°C for stock solutions. The stocks were further diluted using nuclease-free water (Invitrogen) to 100nM aliquots and frozen at -80°C. The working dilutions were made at 25nM solutions using the nuclease-free water and these were stored at -20°C. The primer aliquots (25nM) were used only 3 times to avoid decreased amplification efficiency due to primer degradation after repeated freeze/thaw cycles.

Table 9

Primer	Sequence	RT	Mltplx	2nd
pTα[a] Fwd_1	5'-TCAGGCTCTACCATCAGGCA-3'	×	✓	×
pTα[a] Fwd_2	5'-TTCTGAAGAGCTGGAAGCCT-3'	×	×	✓
pTα[b] Fwd_1	5'-TCAGGCTCTACCATCAGGGG-3'	×	✓	✓
pTα[a] + pTα[b] Rev_1	5'-TAGGCTCAGCCACAGTACCT-3'	✓	✓	✓
pTα[a] Fwd_3	5'-TTGCCTTCTGAAGAGCTGGA-3'	×	✓	×
pTα[a] Fwd_4	5'-TTCTGAAGAGCTGGAAGCCT-3'	×	×	✓
pTα[a] + pTα[b] Rev_2	5'-CATCGGAGCAGAAGCAGTTTG-3'	✓	✓	✓
EF1a Fwd_1	5'-ACACGTAGATTCCGGCAAGT-3'	×	✓	×
EF1a Fwd_2	5'-TGGTGGAATCGACAAGCGAA-3'	×	×	✓
EF1a Rev_1	5'-ACGCTCACGCTCAGCTTTCA-3'	✓	✓	✓

Table 9 Primers for single cell multiplex PCR. Reverse primers were used in all three reactions; reverse transcription (RT), multiplex PCR (Mltplx) and the nested, 2nd PCR. Forward 1 (Fwd_1) primers for each gene were used in the multiplex reactions only and the Fwd_2 primers for the second PCR, with the exception of pTα[b] Fwd_1.

1.7.5.2 Lysis and reverse transcription.

Cells were removed from the -80^{o}C freezer and thawed on ice before lysis by heating at 65^{o}C in an Applied Biosystems-GeneAmp thermo-cycler for 2 minutes. The cells were kept on ice before adding the reverse transcription (RT) mix to each tube (10μl). Table 10 shows the reaction components for the RT step. The primers for RT were diluted to 12.2μM and the dNTPs (Amersham) were mixed and diluted to 10mM before setting up the reaction. RT was achieved by heating the sample at 37^{o}C for 60 minutes in the thermo cycler and then at 95^{o}C for 3 minutes before cooling at 10^{o}C. The samples were kept on ice until the Multiplex reaction mix was added.

Table 10

Order	Reagents	1x
1	H_2O (nuclease free)	X μl
2	PCR Buffer II (10x)	1.5 μL
3	$MgCl_2$	2 μL
4	dNTPs (10 mM each)	1.5 μL
5	Primer (12.2 μM each)	0.16 μL
6	RNAse Block	1 μL
7	MMLV RT	0.7 μL
	Final Volume	10 μL

Table 10 Reverse transcription reaction components for the single cell multiplex PCR. The PCR buffer and magnesium chloride used for RT were from an AmpliTaqGold kit (Applied Biosystems). MMLV reverse transcriptase was purchased from Applied biosystems and the Rnase Block, ribonuclease inhibitor was purchased from Stratagene.

1.7.5.3 Multiplex PCR.

The Multiplex PCR components are described in table 11. 70μl of the Multiplex PCR mix was added to the RT reaction products and the tubes

were capped, vortexed and centrifuged briefly to ensure that the samples were mixed. The samples were then put through the Multiplex-PCR programme (Table 12).

Table 11

Reagents	1x
H_2O (nuclease free)	X µl
PCR Buffer II (10x)	8.5 µL
$MgCl_2$	7 µL
dNTPs (2.5 mM each)	7 µL
Oligo (25µM each)	0.05 µL
Taq polymerase	0.6 µL
Final Volume	70 µL

Table 11 Multiplex PCR reaction components. The PCR buffer, $MgCl_2$ and Taq polymerase for this reaction were from an AmpliTaqGold PCR kit (Applied Biosystems) and the dNTPs used were TWELVEPAQ-Gene-dNTPs from Applied Biosystems

Table 12

95°C		10 minutes	hold
	94°C	45 seconds	15X
	60°C	1 minute	
	72°C	1.5minutes	
72°C		10 minutes	hold

Table 12 Multiplex PCR programme. Table shows the PCR programme used for the first round, Multiplex PCR.

1.7.5.4 Second-round nested PCR.

The multiplex PCR products were then subjected to second round nested PCR. Table 13 shows the reaction mix for the nested, 2nd PCR. Three

different 2nd PCR reaction mixes were made up, one for each of the three transcripts being amplified; EF1A, pTα[a] and pTα[b].

Table 13

Reagents	1x
H_2O (nuclease free)	X µl
PCR Buffer II (10x)	2 µL
$MgCl_2$	1.6 µL
dNTPs (2.5 mM each)	2 µL
Primer (25µM each)	0.2 µL
Taq polymerase	0.1 µL
Final Volume	18 µL

Table 13 Nested 2nd PCR reaction components. The table shows the components for the 2nd round PCR for the single cell multiplex PCR protocol. This PCR reaction was performed on the products of the multiplex PCR and a separate reaction was set up for each of the three transcripts; EF1a, pTα[a] and pTα[b].

Table 14

95°C		10 minutes	hold
	94°C	30 seconds	2x
	70°C	45 seconds	
	72°C	1 minute	
	94°C	30 seconds	2x
	66°C	45 seconds	
	72°C	1 minute	
	94°C	30 seconds	2x
	62°C	45 seconds	
	72°C	1 minute	
	94°C	30 seconds	48x
	66°C	45 seconds	
	72°C	1 minute	
72°C		10 minutes	hold

Table 14 The 2nd PCR programme.

As with the other reaction mixes, the 2nd PCR reaction mixes were made up in PCR room 1, the cleanest room. The mixes were aliquoted in room 2 and then taken to room 3 where 5μl of the Multiplex PCR product (or 2μl cDNA template) was added to each of the tubes (total volume 20μl). The 2nd PCR programme is shown in table 14.

1.7.5.5 Primer optimization.

To test primer efficiency individual PCR reactions were set up using DN4 cDNA for each of the primer sets, i.e. Fwd_1 with the reverse, and Fwd_2 with the reverse for pTα^a, pTα^b or EF1A. These reactions were performed in triplicate using quantitative real-time PCR. For primer competition a multiplex 1st PCR was set up with pTα^a Fwd_1, pTα^b Fwd_1, EF1A Fwd_1 and the two reverse primers. 1st PCR reactions for each individual sets of primers were run in parallel and 2nd PCRs were then set up using 5μl of each of the 1st PCR products (i.e. from the multiplex or from each of the individual 1st PCRs.) These PCRs were done in triplicate using quantitative real-time PCR. SYBRGreen master mix (Applied Biosystems) was used for the real-time PCRs. The master mix was aliquoted into wells of a MicroAmp optical 96-well reaction plate (Applied biosystems) and 0.2μl of each corresponding primer, at 25μM concentration was added with 4.6μl of water (total volume 5μl). The plate was taken, on ice, to room 3 where 2μl of the cDNA (or 5μl of the 1st PCR product) was added to each of the wells. The plate was sealed using MicroAmp 96 optical adhesive film (Applied Biosystems) and spun down at 1200rpm for 30 seconds in a bench-top centrifuge. The plate was inserted into an Applied Biosystems 7500 real-time machine, the programme is shown in Table 15. The data was collected at 72^{o}C and the Ct values were used for analysis of primer efficiency and competition.

Table 15

95°C		10 minutes	hold
	94°C	30 seconds	40X
	60°C	30 seconds	
	72°C	45 seconds	

Table 15 The real-time PCR programme:

1.7.6 Genotyping pTα^a-transgenic mice by PCR.

To test the quality of the genomic DNA extracted a PCR was performed using primers pTα1s and pTα2 (Table 16) that amplified a 466bp intronic sequence 9.5kb upstream of the pTα gene. Taq polymerase was used for the PCRs (using a TM of 65°C) and 2ng TCRδ KO genomic DNA was used for the positive control. PCR for detection of the pTα^a transgene was performed using primers pTαF4 and pTα^a-transgene-R (Table 16) that amplified a 450bp sequence traversing the exon 1 and 2 boundary of pTα. This sequence is unique to the pTα^a-only BAC transgenic construct. Thus, for the positive control 2ng TCRδ KO genomic DNA was spiked with a single copy of the pTα^a targeted BAC. Taq polymerase was used in the PCR at a TM of 65°C.

Table 16

Primer	Sequence
pTα 1s	5'-CAACTACCAAACTGCCTCTGCTCG-3'
pTα 2	5'-AGTCTGGACACTTGCCACCTGTGG-3'
pTα F4	5'-TAGCCCACACCTCAGAGCTGCAGC-3'
pTα^a Transgene R	5'- CAGGCTTCCAGCTCTTCAGAAGGCA-3'

Table 16 Primers used for genotyping pTα^a transgenic mice genomic DNA. pTα1s and pTα2 were used to test the quality of the genomic DNA and pTαF4 and pTα^a-transgene-R were used to identify the presence of the pTα^a-only transgene.

1.8 Cloning.

1.8.1 Cloning into pCR-Blunt Vectors (Invitrogen).

Zero blunt cloning kit (Invitrogen) was used to clone blunt ended PCR products into the pCR-Blunt (pBlunt) vector (provided with the kit). The pBlunt vector contains a lethal *E.coli ccd*B gene fused to the C-terminus of LacZα. Ligation of a blunt PCR fragment separated the *lacZα-ccd*B gene fusion from the *lac* promoter, disrupting expression of the lethal gene. This allows for negative selection of non-recombinant vectors. In addition, the pBlunt vector contains Zeocin and Kanamycin resistance genes for positive selection of transformants.

Blunt ended PCR products were generated using Phusion polymerase (Finnzymes) and isolated using gel electrophoresis and extraction from the gel. The constructs were then ligated into the pBlunt plasmid at a 10:1 molar ratio of insert: vector for optimal ligation efficiency. Ligation reactions were set up with 5ng of vector; and the formula below was used to estimate the amount of PCR product needed for the ligation:

$$X \text{ ng insert} = \frac{(10)\ (Y \text{bp PCR product})\ (5 \text{ ng linearized pCR-Blunt})}{(3500 \text{ bp pCR-Blunt})}$$

Where X ng is the amount of PCR product of Y base pairs to be ligated. The ligation reaction was set up as follows; 5ng pBlunt, PCR product, 10x Ligation buffer, T4 DNA ligase (4u/μl, Invitrogen) and sterile water to 10μl total reaction volume. The ligation reaction was incubated at 16^{o}C for 1 hour before transforming into One-ShotTOP10 *E.coli* competent cells (Invitrogen). 2μl of ligation reaction was added to 50μl of competent cells on ice and left to incubate on ice for 30 minutes. The cells were then heat-

shocked for 45 seconds at 45^{o}C and then kept on ice for 2mins. 250µl of Luria–Bertani (LB) broth (Invitrogen) with no antibiotic was added to transformed cells and the vials were shaken at 37^{o}C for 1 hour. 100µl of transformed cells were spread at varying concentrations on LB Agar (Invitrogen) plates containing 50ug/ml Kanamycin (Sigma). The plates were incubated over-night at 37^{o}C. Positive transformants were analysed by restriction digest and sent to MWG for sequencing from M13 reverse and the T7 priming sites (see Figure 1).

Figure 1

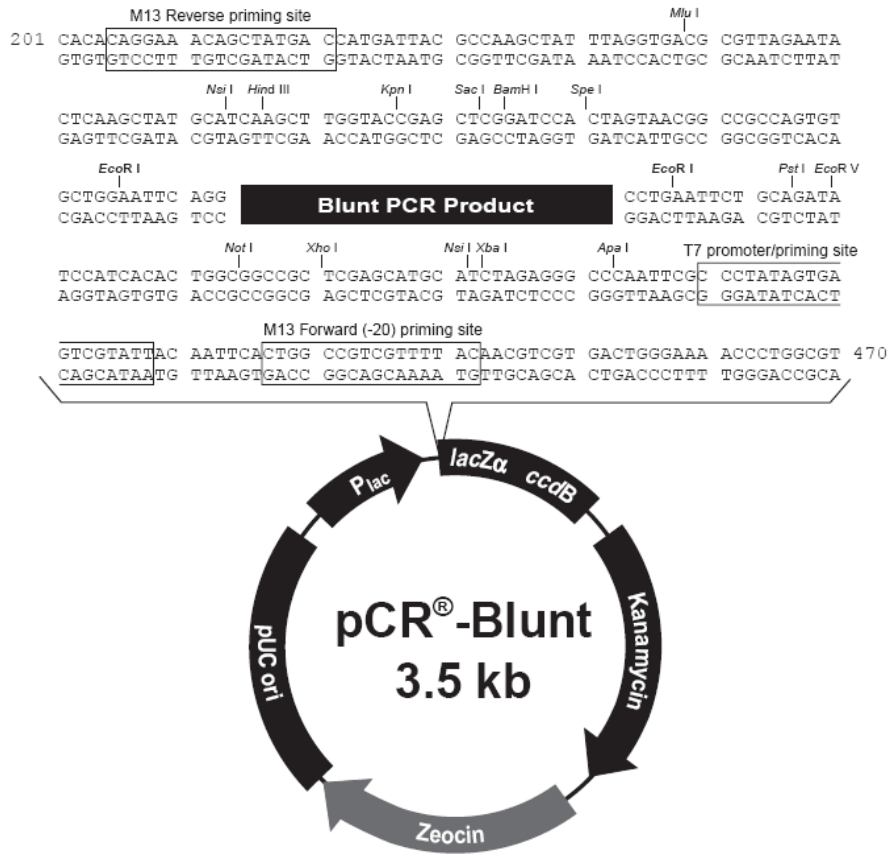

Figure 1 pCR-Blunt vector map and sequence of the multiple cloning site. Plac is the lac promoter which is separated from the lethal lacZ-ccdB gene fusion by the multiple cloning site. Thus pBlunt plasmids that self-ligate are selected against, ensuring high cloning efficiency. pUC ori is the origin of replication of the plasmid. The Kanamycin resistance gene allows for positive selection of transformed bacteria on Kanamycin containing medium. (Figure obtained from the Zero Blunt cloning kit protocol – Invitrogen).

1.8.2 Cloning into pLZRS-IRES-eGFP (pLZ) vectors.

The pLZRS-IRES-eGFP (pLZ) vector (Heemskerk et al., 1997) is a retroviral vector possessing two long terminal repeat (LTR) sequences between which, lies the multiple cloning site (MCS) (Figure 2). Downstream of the cloning site and between the two LTRs there is an internal ribosomal entry site (IRES) followed by the reporter gene, enhanced Green Fluorescent Protein (eGFP) which allows translation of eGFP with the gene of interest in transduced target cells. Upstream of the MCS is a packaging signal (ψ) for packaging of the plasmid into virus particles. pLZ contains Ampicillin and Puromycin resistance genes for selection of positive transformants (bacteria) and transfected phoenix cells respectively.

Figure 2

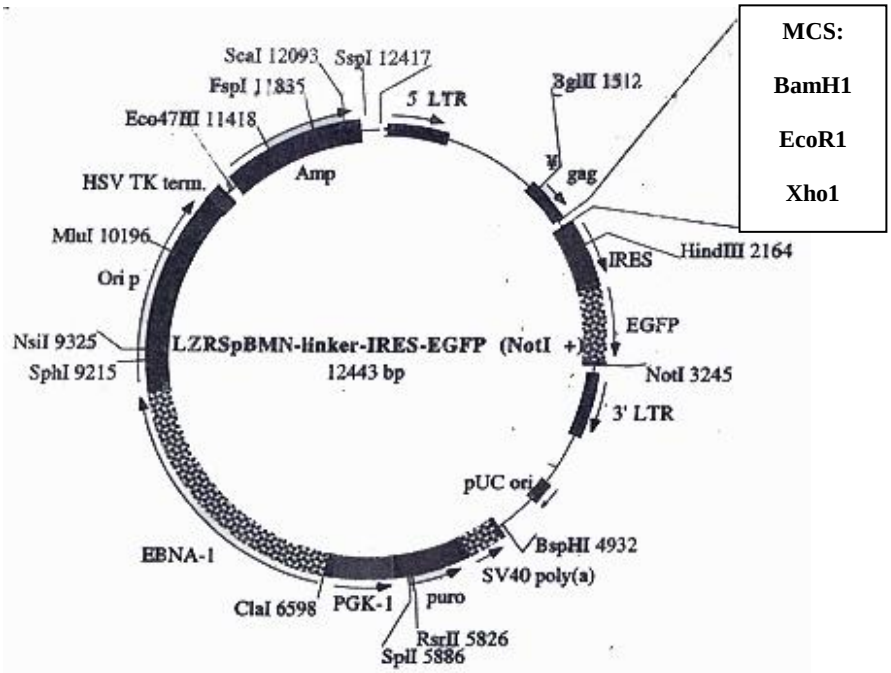

Figure 2 pLZRS-IRES-eGFP (pLZ) vector map. The pLZ retroviral vector multiple cloning site (MCS) lies between two long terminal repeats (LTRs) which allow for constitutive expression of the cloned gene. An internal ribosomal entry site (IRES) upstream of eGFP allows for detection of cells transduced with the retroviral constructs. The Amp gene conveys Ampicillin resistance and puro conveys puromycin resistance for selection of transformed bacteria cells and transfected phoenix cells, respectively.

To clone into pLZ the plasmid was digested, alongside the pBlunt plasmid containing the insert (pTα cDNA) with BamHI (NEB) and XhoI (NEB) enzymes, and the reaction left for 2 hours at 37°C. The digests were run on 0.7% agarose gel for 1 hour 40 minutes at 110v. The linear pLZ vector (12.4kb) and the insert (gene of interest) were extracted from the gel and eluted in sterile water. The water was warmed to 70^{o}C for efficient elution of large fragments; the amount of DNA in each sample was measured using a Nanodrop spectrophotometer.

The isolated digest fragments were ligated into the linearized pLZ vector at a 20:1 insert to vector ratio, using 20ng of pLZ plasmid. The amount of insert to be added was calculated using the below formula:

$$X = \frac{(20)\ (Y \text{ insert bp})\ (20\text{ng linearized pLZ})}{12443 \text{ (pLZ bp)}}$$

To the vector and insert the following was added for the ligation reaction; 1.5μl of 10x T4 Ligase buffer (New England Biolabs), 0.5μl T4 DNA Ligase (New England Biolabs) and sterile water to 15μl reaction volume. The reaction was incubated over night at 16°C. The next day 5μl of ligation reaction was added to 50μl XL GOLD *E.coli* competent cells (Invitrogen). The cells were incubated on ice for 30 minutes then heat shocked for 30 seconds at 42°C. The cells were then placed on ice for 2 minutes before addition of 250μl LB broth medium and incubation at 30^{o}C in a shaking incubator for one hour. The transformed cells were spread on LB Agar (Invitrogen) plates containing 100μg/ml Ampicillin (Sigma) and incubated overnight at 30^{o}C. Single colonies of the positive transformants were cultured overnight in 5ml of LB broth (Invitrogen) and the plasmid DNA was isolated. Restriction enzyme digests were performed on plasmid DNA to characterize the transformant and to confirm the presence of the insert, and

the plasmids were sent to MWG for sequencing using the pLZ-gag primer; 5'-TCTTGTCTGCTGCAGCATCG-3'.

1.9 Recombineering of BAC DNA.

1.9.1 Introduction to recombineering.

pTα^a and pTα^b targeted BAC constructs were be generated using the recombineering technique (Warming et al., 2005). Detailed protocols were obtained from (http://recombineering.ncifcrf.gov). Recombineering stands for genetic engineering by homologous recombination and uses modified E.coli strains to modify the cloned DNA. The E.coli cells (SW102) contain three phage lambda (λ) red recombination genes; *exo*, *bet* and *gam*. *exo* encodes a 5' to 3' exonuclease that creates 3' overhangs from introduced double stranded DNA targeting cassettes. *bet* encodes a protein that binds to the 3' overhang and mediates homologous recombination with the complimentary sequence present in the BAC. *gam* encodes an exonuclease inhibitor that protects the double stranded DNA cassette from being degraded. The three λ-phage genes are regulated by a temperature controlled promoter in SW102 cells. Thus, at 32^{o}C the promoter is inactive but after 15minutes incubation at 42^{o}C the genes are expressed and recombination can take place. The *E.coli* galactose operon consists of four genes; *galE*, *galT galK* and *galM*, in the SW102 strain the *galK* gene has been deleted. *galK* encodes galactokinase; the first enzyme in the galactose degradation pathway, however this enzyme also catalyses the phosphorylation of 2-deoxy-galactose, leading to the toxic build up of 2-deoxy-galactose-1-phosphate which cannot be further metabolised. Therefore the presence of *galK* confers both positive and negative selection

and this enables efficient selection of clones that have undergone homologous recombination.

In the first recombineering step the *galK* PCR product containing homology to the targeted region of the BAC is inserted into the BAC by homologous recombination and *galK*$^{(+)}$ clones are selected for by growing the bacteria on minimal media with galactose as the only carbon source. In the second recombineering step the *galK* sequence is substituted by a double-stranded DNA oligo with homology flanking the *galK* sequence in the BAC. In this case *galK*$^{(+)}$ clones were selected against by growing the bacteria on minimal media with glycerol and 2-deoxy-galactose. This process can be repeated to modify the target gene as many times as necessary.

Table 17

Primer	sequence	For sequencing:
15s	5'-CCTATGAAGTGCTCTTCAGACAGG-3'	Exon 1 (forward)
16s	5'-AACTGGAGAAGGCTGGGAGTGACC-3'	Exon 1 (reverse)
17s	5'-AAACTTCTGGTGGCTGGGCAGTGG-3'	Exon 2 (forward)
18s	5'-TCTTAGCAAACACAGATCAGAGCC-3'	Exon 2 (reverse)
19s	5'-GACTACCATTACCTGTTTGCTTGC-3'	Exon 3 (forward)
20s	5'-GCTGCAGGAACGAGCTTCTGATGC-3'	Exon 3 (reverse)

Table 17 Primers used for sequencing the pTα BAC at the targeting sites.

The pTα BAC (BMQ452P20) was purchased from www.ensemble.org, and consists of 46kb of C57BL/6 mouse chromosomal sequence, which included the pTα gene. The chromosomal DNA had been cloned into the BamH1 site of the BAC vector pBACe3.6. The BAC possesses a chloramphenicol resistance gene for positive selection of transformants.

All recombineering plasmid vectors and *E.coli* strains were purchased from http://recombineering.ncifcrf.gov. Table 17 shows the primers used for sequencing BMQ452P20. The BAC was sequenced to confirm the presence of the pTα gene, but also to identify the sequence of the targeting locus to design the oligonucleotides used for recombineering.

1.9.2 Transforming SW102 cells.

The first step was to transform SW102 cells with the pTα BAC by electroporation. To do this the SW102 cells had to be made electrocompetent. The SW102 agar stab was streaked onto an LB agar plate containing 12.5μg/ml Tetracycline (Sigma). A single colony was picked and cultured overnight in LB broth without tetracycline. 500 μl of the overnight SW102 culture was diluted in 25 ml LB medium with12.5μg/ml Tetracycline in a 50 ml baffled conical flask and grown at 32^{o}C in a shaking water-bath to an OD600 of 0.6 (3-5 hours). The bacteria were cooled in an ice/water-bath slurry and then transferred to pre-cooled 15 ml Falcon tubes (BD Biosciences). The cells were pelleted by centrifugation at 5000 rpm at 0^{o}C for 5 minutes. The supernatant was poured off and the pellet was resuspended in 1ml ice-cold dH_2O by gently swirling the tubes in an ice/water-bath slurry. Subsequently, 10 ml ice-cold dH_2O was added and the samples pelleted again. This step was repeated once more. After the second washing and centrifugation step, the supernatant was removed, and the pellet was resuspended in the residual dH_2O; approximately 50μl. The cells were transferred to ice cold 0.1cm cuvettes (BioRad) and mixed with 5μg BAC DNA. The now electrocompetent bacteria were transformed by electroporation at 25 μF, 1.75 kV and 200Ω. 1ml LB broth was added to the transformed cells and the tubes were shaken at 32^{o}C for 2 hours before

plating the transformants on LB agar plates (Invitrogen) with 12.5μg/ml Chloramphenicol (Sigma).

1.9.3 The recombineering step: *galK* selection.

Insertion of *galK* was performed as follows; to make electrocompetent cells, 500ml of an overnight SW102 (*E.coli*) culture containing the BAC was diluted in 25 ml LB medium with 12.5μg/ml Chloramphenicol in a 50ml baffled conical flask and grown at 32^{o}C in a shaking water-bath to an OD600 of 0.6. 10 ml was transferred to another baffled 50ml conical flask and heat-shocked at 42^{o}C for exactly 15 minutes in a shaking water-bath for activation of the recombineering machinery. The remaining culture was left at 32^{o}C as the uninduced control. After 15 minutes the two samples, induced and uninduced, were briefly cooled in an ice/water-bath slurry and then transferred to two pre-cooled, 15ml Falcon tubes (BD Biosciences) and pelleted by centrifugation at 5000rpm at 0^{o}C for 5 minutes. The supernatant was poured off and the pellet was resuspended in 1 ml ice-cold dH_2O by gently swirling the tubes in an ice/water-bath slurry. Subsequently, 10ml ice-cold dH_2O was added and the samples pelleted again. This step was repeated once more. After the second washing and centrifugation step, the supernatant was removed, and the pellet was resuspended in the residual dH_2O (50μl). The cells were kept on ice until electroporated with the *galK* PCR product.

The *galK* PCR product as generated using p21 and p22 to create a construct with the *galK* gene at the centre and two 75bp homology arms either end (see Section 1.7.4.1 for PCR details). After amplification of *galK*, 2μl DpnI (NEB) was added to the 20 μl reaction and incubated at 37°C for 1 hour. This step serves to remove any plasmid template. The DpnI digested

PCR product was extracted from an agarose gel and eluted in 50μl ddH_20. 30ng of the DNA was used for electroporation.

An aliquot of 25μl of electrocompetent SW102 cells was used for each electroporation in a 0.1 cm cuvette (BioRad) at 25μF, 1.75 kV and 200Ω. After electroporation the bacteria were recovered in 1ml LB broth for 2 hours in a 32^{o}C shaking water-bath. After the recovery period, the bacteria were washed twice in 1xM9 salts as follows: 1 ml culture was pelleted in an eppendorf tube at 13,200 rpm for 15 seconds and the supernatant was removed with a pipette. The pellet was resuspended in 1 ml of 1x M9 salts (Sigma Aldrich) and pelleted again. This washing step was repeated once more. After the second wash, the supernatant was removed and the pellet was resuspended in 1 ml of 1x M9 salts before plating serial dilutions (100 ml, 100 ml each of 1:10, 1:100 and 1:1000 dilutions) on M63 minimal agar (Table 18) with 20% galactose, 10mg/ml L-leucine, 0.2mg/ml d-Biotin and 12.5μg/ml chloramphenicol. Washing in M9 salts is necessary to remove any rich media from the bacteria prior to selection on minimal medium. Plates were left at 30^{o}C for 3 days to allow bacteria to grow on the minimal medium. Recombinant clones were analysed by restriction digest.

Table 18

1L M63 medium:	10g $(NH_4)_2SO_4$
	68g KH_2PO_4
	2.5mg $FeSO_4$-$7H_2O$
	Adjust to pH with KOH
Autoclave and add 200ml to:	Agar Base in 800ml dH_2O (Autoclaved)

Table 18 M63 minimal agar plate components. Components of M63 minimal agar used for recombineering are shown. All chemicals were purchased from Sigma Aldrich, agar base contains no sugars.

Once the recombinant DNA was isolated and sequenced; to confirm homologous recombination had taken place and the *galK* gene was inserted. It was then necessary to re-transform SW102 cells with the recombinant BAC clone in order to remove any DNA that may have been carried through. This was done before each subsequent recombineering step.

1.9.4 The second recombineering step: *galK* counter selection.

The *galK*$^{(+)}$ BAC was transformed into fresh SW102 cells as described above and 200ng of the double-stranded DNA oligo (see Section 1.7.4.2 of Methods) was electroporated into the electrocompetent cells as described for the first targeting step. For the counter selection step, the bacteria were recovered in 10ml LB in a 50ml baffled conical flask and incubated for 4.5 hours in a 32^{o}C shaking water-bath. The cells were pelleted and washed in 1x M9 salts (Sigma Aldrich) as before and dilutions were plated onto M63 minimal agar with 20% glycerol, 10mg/ml L-leucine, 0.2mg/ml d-Biotin, 12.5μg/ml Chloramphenicol and 20% 2-deoxy-galactose. Transformants were analysed by restriction digest and sequenced.

Chapter 2

Cell Biology.

2.1 Flow Cytometry analysis.

2.1.1 Isolation of thymocytes and surface staining for flow cytometry.

Adult mouse thymuses were obtained by dissection and stored on ice in RPMI (Gibco, Invitrogen). The thymuses were transferred to eppendorf tubes containing 0.5ml 1x PBS (Gibco, Invitrogen) with 2% Heat inactivated Foetal Calf Serum (HI-FCS- Gibco, Invitrogen). The lobes were crushed with a pestle and strained using a 40µm cell strainer (BD Falcon) before adding 0.5ml 2% PBS for a total volume of 1ml and kept on ice. The cell suspension was counted using a haemocytometer and approximately $1x10^6$ cells were aliquoted for each single colour control. The samples were stained in 2% PBS at $1x10^6$ cells in 100µl, in glass BD FACS tubes. 1µl of antibody was used to stain 1-2 $X10^6$ cells. Table 1 shows the details of the antibodies used in this project that have not been described elsewhere in the methods section. All antibodies used were anti-mouse and conjugated to fluorochromes (unless specified in the text). The samples were incubated on ice, in the dark for 30-45 minutes. After staining the cells were washed in 2mls 2% PBS and centrifuged in a bench-top centrifuge for 5 minutes at 1100rpm. After centrifugation the medium was removed from tubes by aspiration, leaving approximately 400µl 2% PBS to resuspend the cells. The cells were resuspended by vortexing the tubes and were analysed for surface markers using the LSRII or the CANTOII Flow cytometers (BD).

Thymocytes were isolated from foetal thymic organ cultures (FTOCs) as previously described. The lobes had to be first removed from the filters and this was done by repetitive pipetting 2% PBS over the FTOC filters to dislodge the lobes. Because FTOCs produced very few cells (approximately 200,000) only 0.5μl of each antibody was used.

Table 1

Epitope	Fluorchrome	clone	Supplier
CD4	Pacific Blue	GK 1.5	EBiosciences
CD4	PE cy7	GK 1.5	EBiosciences
CD4	FITC	GK 1.5	EBiosciences
CD8α	FITC	53-6.7	EBiosciences
CD8α	APC cy7	53-6.7	EBiosciences
CD8a	Pacific Blue	53-6.7	EBiosciences
CD8β	FITC	H35 17.2	BD Pharmingen
CD3ε	PEcy 7	145-2C11	BD Pharmingen
CD3ε	PE	145-2C11	Ebioscience
CD5	PE	53-7.3	BD Pharmingen
CD69	PE	H1.2F3	EBiosciences
CD127	PE	SB14	BD Pharmingen
CD25	APC	PC61	EBiosciences
CD44	Pacific Blue	IM7	EBiosciences
CD24	Pacific Blue	M1/69	BioLegend
TCRδ	FITC	GL3	EBiosciences
TCRδ	APC	GL3	EBiosciences
TCRδ	PE	GL3	EBiosciences
TCRβ	Percp cy5	H57-597	EBiosciences
TCRβ	FITC	H57-597	BD Pharmingen
Vα 2	PE	B20.1	EBiosciences
Vα 8	PE	CTVA-8	EBiosciences
Vα 11	PE	RR8-1	BD Pharmingen
Vβ 5	PE	MR9-4	BD Pharmingen
Vβ 6	FITC	RR4-7	BD Pharmingen
Vβ 8	FITC	MR5-2	BD Pharmingen
HNGFR	PE	C40-1547	BD Biosciences
B220	FITC	RA3-6B2	BD Pharmingen
NK1.1	FITC	PK1 36	EBiosciences
DX5	FITC	DX5	EBiosciences
Foxp3	Pacific Blue	FJK-16s	EBiosciences

Table 1 Antibodies used for this thesis. All antibodies used for the experiments in this thesis, that are not mentioned in the methods are shown in this table. All antibodies are anti-mouse and the clone and supplier are shown. APC is Allophycocyanin, FITC is Fluorescein isothiocyanate, PE is phycoerythrin, TCR is T cell receptor and HNGFR is human nerve-growth-factor receptor.

2.1.2 Depletion of $CD4^{(+)}$ and $CD8^{(+)}$ cells for isolation of DN thymocytes.

Adult C57BL/6 mouse thymuses were obtained by dissection and resuspended in plain fresh RPMI (Gibco-Invitrogen). The thymuses were crushed with a pestle and strained using a 40μm cell strainer (BD Falcon) on a Petri dish or in an eppendorf tube. The cell suspension were made up to 7ml with RPMI, 500μl of hybridoma supernatant was added (a mix of anti-CD4 and anti-CD8 antibodies IgM isotype for complement lysis.) The cell suspensions were incubated at 37°C for 10min. 1ml of resuspended complement (Cedar lane Laboratories) was added and mixed by inversion. Cell suspensions were then incubated with complement at 37°C for 30 min.

To separate live thymocytes, including DN cells, from dead complement-lysed thymocytes that were $CD4^{(+)}$ and/or $CD8^{(+)}$, 4mls lymphocyte separation medium (MP Biomedical) was layered underneath each cell suspension. Tubes were centrifuged for 20 minutes at 1,600 rpm at room temperature (22°C) in a bench-top centrifuge with no brake. Live thymocytes were removed from the Ficoll interface by pipetting the interface out using a glass pasteur pipette and transferred to a FACS tube. Lysed dead cells, i.e. cells that expressed CD4 and/or CD8, form a pellet at the bottom of the tube. The cells were washed with 2% PBS before staining for sorting. The Aria-II Cell Sorter (BD) was used to sort the thymocytes.

2.1.3 Intracellular staining.

For all thymocyte intracellular staining the Ebioscience anti-mouse FOXP3 staining kit was used, with exception to the phospho-ERK staining which is

described in the next section. Prior to staining the Fixation/Permeabilization Concentrate was diluted (1 part) into the Fixation/Permeabilization Diluent (3 parts) and kept on ice. The 10x Permeabilization buffer was diluted 1/10 with dH_2O and kept on ice.

$1x10^6$ cells were stained with surface antibodies as described in the previous sections. After staining the cells were washed in 2% PBS. The cells were centrifuged (5 minutes at 1100rpm) and the pellet was resuspended in 1ml Fixation/Permeabilization working solution and vortexed. The samples were then incubated on ice for 1 hour in the dark. The samples were then washed twice with 2ml 1x Permeabilization buffer, followed by centrifugation and removal of the buffer by aspiration. 1μl Fc-Block (Purified anti-mouse CD16/32 clone 93, Ebiosciences) was used to stain the samples in 100μl 1X Permeabilization buffer on ice, in the dark, for 15 minutes. 1μl of the anti-mouse antibody for intracellular staining was then added to the cells and the samples were incubated for a further 30 minutes on ice in the dark. The samples were then washed twice with 2ml 1x Permeabilization buffer, followed by centrifugation and removal of the buffer by aspiration and resuspended in 400μl 2% PBS for analysis on the cytometer.

2.1.4 Assay for intracellular phosphorylated-ERK.

To assay for intracellular phosphorylated-ERK1/2 MAP kinase, thymocytes were isolated as described in previous sections and diluted to $4x10^6$ cells/ml in 2.5ml RPMI without L-glutamine (Invitrogen) and with 10% FCS (Invitrogen) in 50ml falcon tubes (VWR). 23μl of 10 μg/ml anti-CD3ε (2C11, a gift from Patrick Costello, CRUK (Costello et al., 2004)) was added, and

the cells were incubated on ice for 15 minutes. The cells were then washed in 10mls RPMI 10% FCS and pelleted by centrifugation at 1100 RPM for 5 minutes in a bench-top centrifuge. The cells were resuspended in 2.5ml RPMI 10% FCS and rested for 10 minutes in a 37^{o}C water-bath. While the cells were resting, 0.5ml 8% Formaldehyde solution (37-41% from Fisher Scientific, diluted in 1xPBS from Invitrogen) was aliquoted into each of the sample tubes. After 10 minutes 0.5ml of the cells was removed and transferred to a FACS tube containing 0.5ml 8% Formaldehyde. This sample is the zero time point. 125μl (75μg/ml) of the cross-linking anti-Armenian hamster IgG antibody (Jackson Immunoresearch Labs) was added to the remaining 2.0ml cells in water-bath, the tube was swirled to mix the timer was started. 0.5ml aliquots of activated cells was removed at 1, 1.5, 2, 5 and 10 minute time points and transferred to separate tubes containing 0.5ml 8% Formaldehyde for fixing. The cells were then fixed for 10 minutes at room temperature and pelleted by centrifugation. All fixative was removed and the cells were kept on ice. 1ml 100% ice cold methanol (Sigma- stored in -20^{o}C freezer since the morning) was added to the fixed cells drop-wise while vortexing. The samples were incubated on ice for 30 minutes to 2 hours. The cells were then washed three times with 10% PBS and resuspended in 100μl 10% PBS before adding 1μl anti-Phospho-ERK antibody (NEB/Cell Signalling - stored at -20^{o}C). The cells were stained at room temperature for 1hour in the dark. The samples were washed with 2% PBS before staining with conjugated antibodies such as those for CD4 and CD8 as well as the secondary for the phospho-ERK, the anti-rabbit cy5 (Jackson Laboratories) for 30 minutes on ice in the dark. After staining the cells were washed again and resuspended in 2% PBS for analysis on the cytometer.

2.1.5 Staining with thymic leukaemia antigen (TL) tetramer.

The mouse thymic leukaemia antigen (TL) is a non-classical MHC-I molecule that binds the CD8αα homodimer with high affinity (Attinger et al., 2005) . Biotinylated-TL monomers were kindly provided by Dr Hilde Cheroutre La Jolla Institute for Allergy and Immunology. The TL monomers were conjugated by addition streptavidin PE (Molecular Probes) and incubation in the dark for 15 minutes on ice. E16 and E17 thymocytes were obtained from embryos from C57BL/6 timed pregnancies. The thymocytes were stained in 100μl 2% PBS with 1μl Fc Block (Purified anti-mouse CD16/32 clone 93, Ebiosciences) on ice for 20 minutes. Subsequently the conjugated antibodies for surface staining were added (CD4 Pacific Blue and CD8α FITC see Table 1) and the cells incubated on ice for 30 minutes in the dark. The cells were washed in 2ml 2% PBS and centrifuged and the pellet was resuspended in 100μl 2%PBS. 1.5μl of conjugated TL tetramer was added to the cells and the samples were incubated for 30 minutes at room temperature in the dark. The samples were washed twice with 2% PBS before flow cytometry.

2.1.6 Cell cycle analysis: 7-AAD staining.

For analysis of DNA content thymocytes were stained first for surface markers as described above then washed in 2% PBS before resuspending in 2% PBS with 0.3% Saponin. The cells were stained with 7-amino-antinomycin-D (7AAD) solution (Ebioscience) at 0.25μg (5μl)/1 million cells in 0.3% saponin at room temperature for 20 minutes. The cells were then washed in 2mls 2% PBS and analysed by flow cytometry (7-AAD emission is at 650nm).

2.2 Cell culture: the Phoenix Ecotropic Packaging Cell line.

Phoenix Ecotropic (phoenix) cells were kindly provided by the Nolan Laboratory (www.stanford.edu/group/nolan/). The cells were cultured in phoenix media: DMEM with Glutamax (Invitrogen), 10% HI FCS (Gibco-Invitrogen) with 1% Penicillin/Streptomycin (Invitrogen) at 37°C and 5% CO_2. For maximally healthy cells, cultures were split when cells reached 70-80% confluency. Cells were frozen in 10% DMSO (Sigma), and aliquots kept in liquid nitrogen storage.

2.3 Transfection of phoenix cells.

18-24h prior to transfections approx $1x10^6$ phoenix cells were plated per 6cm culture dish in 7ml of culture media, for 60% confluency at the time of transfection. 2μg of plasmid DNA was used for transfection. Fugene-6 reagent (Roche) was used for transfections. A DNA-Fugene complex was prepared with a 3:1 ratio (μl Fugene: μg DNA) in DMEM with a total volume of 200μl. The 200μl transfection complex was added drop wise to cells and left to incubate for 48 hrs at 37^oC and 5% CO_2.

Two days after transfection, Cells were removed from $6cm^2$ plates containing Fugene and plated in T175 flasks (BD-Falcon) in 5ml phoenix media with 2μg/ml of Puromycin (Sigma). Puromycin selection allows for stable transfection of the packaging cell line. Cells were cultured at 37°C, 5%CO_2 until they reached 70-80% confluency, then split or harvested the retroviral supernatants. Cells were visualised under the UV microscope to see green fluorescent protein (GFP) expression from the transfected pLZ vectors.

2.4 Harvesting Retroviruses.

Removal of growth medium containing puromycin, from cells was necessary for harvesting retroviral supernantants. 25 ml of filtered-sterilized DMEM with 20% FCS was added to the cells. This media did not contain antibiotics. Cells were incubated overnight at 32°C**.**

The media on the cells or the supernatant contains the viral particles produced by the cell line. This retroviral supernatant was collected the following day and kept on ice. The supernatants were centrifuged for 3 minutes at 1,000 rpm using a bench top centrifuge to remove any cells; and then filtered using a 0.45 μm filter (Millipore). 1ml of the filtered supernatant was aliquoted into 1.5ml eppendorf tubes. The retroviruses were concentrated by centrifuging the 1ml aliquots at 18,000rpm (13,000g) in a table-top micro centrifuge for 45 minutes at 4°C. The surface liquid was discarded and 100μl of the retroviral "pellet" from 8 aliquots were pooled into one. Concentrated sups were snap frozen in liquid nitrogen and stored at -80^{o}C until used for transduction.

2.5 Retroviral transduction of E14 thymocytes.

Immature E14 thymocytes were transduced with retroviruses in the presence of a surface-bound transduction enhancer Retronectin (RN-Takara Bio Inc). 3.5cm^2 tissue culture dishes were coated with 12 μg/ml of RN in 1 ml PBS (Invitrogen). Dishes were incubated at room temperature for 2 hours then blocked with 2% BSA (Sigma) for half an hour before washing twice with 1xPBS.

E14 embryos were dissected using Dumont forceps and a dissection microscope; their thymic lobes extracted. The lobes were crushed in an

eppendorf containing 250μl FTOC media (RPMI + 10% FCS + 1% Pen/strep, 2mM L-glutamine and 50μM 2-mercaptoethanol - all from Gibco, Invitrogen) using a conical tissue homogenizer and strained to make a single cell suspension. The E14 thymocytes were counted and made up to 1ml in FTOC media. Each 1ml aliquot of cells was then added to 1ml of thawed, concentrated retroviral supernatant in a FACS tube and mixed by gentle repetitive pipetting. The retrovirus/ thymocyte mixture was added to RN coated plates and incubated at 37°C for 5 hours for transduction to take place.

2.6 Foetal thymic organ culture (FTOC).

C57BL/6 E15 embryos were dissected using Dumont forceps under a dissecting microscope and their thymic lobes extracted for organ culture. Lobes were cultured on nucleopore membrane filters (Whatman) in 3ml FTOC media (RPMI + 10% FCS + 1% Pen/strep, 2mM L-glutamine and 50μM 2-mercaptoethanol (all from Gibco, Invitrogen)) in 6 well plates.

For depletion of lymphocytes from FTOCs the lobes were cultured on FTOC medium containing 1.35mM 2-deoxy-guanosine (Sigma) for 5 days. After 5 days the lobes were moved to fresh FTOC media without 2-deoxyguanosine, to rest for 24 hours before reconstitution with E14 thymocytes.

2.7 Reconstitution of Depleted thymic lobes by hanging drop culture.

Following the 5 hour transduction of E14 thymocytes, the cells were removed from the retronectin coated plates by repetitive pipetting. 1ml of cell suspension was pelleted by centrifugation at 2500rpm for 2 minutes in 1.5ml eppendorf tubes. The supernatant was removed and the second 1ml

of cell suspension was added to the pellet and centrifuged again. The retronectin plates were then washed with 1ml FTOC media to ensure that all the cells had been collected. The pelleted cells were resuspended in the appropriate volume of FTOC media considering that 25μl of cell suspension was used for each hanging drop culture. The cell suspension was carefully pipetted into the wells of a 96 well Terasaki plate (Nunc, VWR).

Depleted lobes were removed from filters and added to wells containing 25μl of FTOC media with the transduced thymocytes. The plates were turned upside down with care to ensure all the lobes drift to the bottom of each droplet. Hanging drop cultures were incubated at 37°C for 48 hours until the lobes were reconstituted. After the 48 hour incubation the reconstituted FTOC lobes were transferred onto nucleopore membrane filters on 3ml of FTOC media in a 6 well plate. The FTOCs were cultured for 5-15 days.

Mice.

C57BL/6 and DBA/2 mice were obtained from Harlan Laboratories. pT$\alpha^{-/-}$ (Fehling et al., 1995a), TCR$\delta^{-/-}$ (Itohara et al., 1993), were obtained from Jackson Laboratories. pT$\alpha^{-/-}$ x TCR$\delta^{-/-}$ mice were obtained by breeding. Embryos were obtained by setting up of timed pregnancies. "pTα^{a}-only" and "pTα^{b}-only" transgenic CD1 founders were generated within the Transgenic Core Facility at Queen Mary University of London. Mice were bred and maintained in the specific pathogen–free animal facilities at Queen Mary University of London. All experiments involving animals were done in compliance with relevant laws and institutional guidelines, and were approved by a local ethics committee.

Results

Chapter 1

Expression of pTα^{a} and pTα^{b} during thymic ontogeny.

1.1 Introduction.

Despite pTα^{a} and pTα^{b} being conserved throughout evolution from mice to humans (Fehling et al., 1995b), and the knowledge that both these isoforms can form functional preTCRs (Gibbons et al., 2001), little is known about the function of pTα^{b} and whether it differs to that of pTα^{a}. Thus to begin to determine whether the two isoforms of pTα have non-redundant roles in development, it was first necessary to ascertain the precise expression pattern of pTα^{a} and pTα^{b} throughout thymic ontogeny. Differential expression of the two isoforms would suggest different functions for the two proteins while overlapping expression may be indicative of more redundant functions for pTα^{a} and pTα^{b}. To date, it is not known how the expression of pTα^{a} and pTα^{b} is regulated through development. To this end, we sought to determine expression patterns of pTα^{a} and pTα^{b} in thymocytes from different stages of development.

Developing thymocytes were isolated by Fluorescence activated cell sorting (FACS). Figure 1.1 shows the markers used to isolate the different thymocyte populations; early thymic progenitors are double negative for CD4 and CD8 and are known as DNs. DNs are subdivided on expression of CD44 and CD25; DN2 cells are CD4$^{(-)}$CD8$^{(-)}$CD44$^{(+)}$CD25$^{(+)}$, DN3 cells are CD4$^{(-)}$CD8$^{(-)}$CD44$^{(-)}$CD25$^{(+)}$, and DN4 cells are CD4$^{(-)}$CD8$^{(-)}$CD44$^{(-)}$CD25$^{(-)}$. Immature single positive (ISP) thymocytes in transition to the double positive (DP) stage are marked by expression of CD8 and low levels

of TCRβ. DP cells are $CD4^{(+)}CD8^{(+)}$, and mature thymocytes express high levels of TCRβ. There are several different lineages of mature T cells that develop in the thymus; $CD8^{(+)}$ cytotoxic T cells, $CD4^{(+)}$ T helper cells and $CD4^{(+)}FOXP3^{(+)}$ regulatory T cells, as well as NKT cells which express NK markers such as NK1.1 and DX5.

Figure 1.1

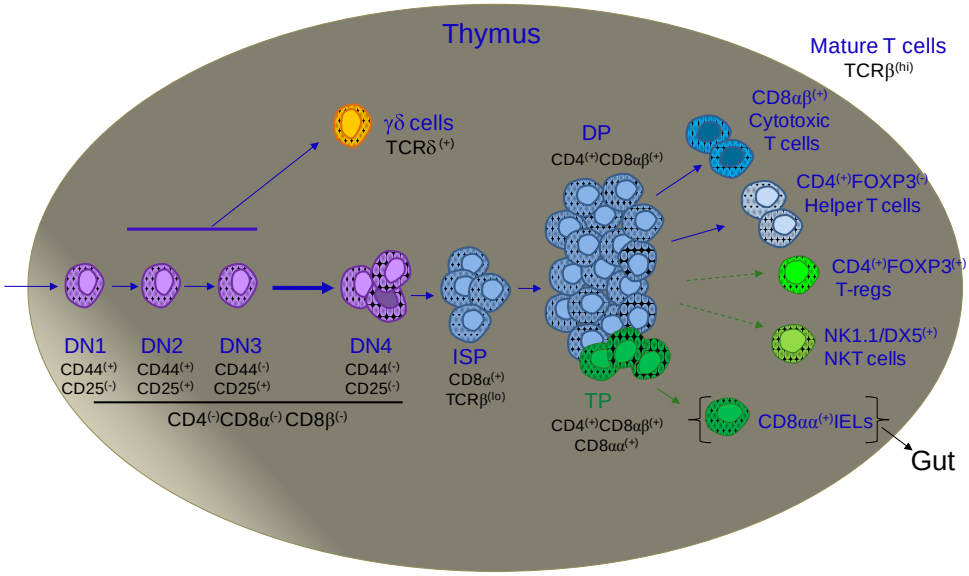

Figure 1.1: Identification of different subsets of thymocytes by their surface marker expression. A schematic of thymic ontogeny; DN is double negative; DP is double positive; TP is triple positive; T regs are regulatory T cells, NKT is natural killer T cells and IEL is intraepithelial lymphocyte. CD8αα was detected with a TL tetramer.

$CD8\alpha\alpha^{(+)}$ intraepithelial lymphocytes of the gut are not found in the thymus but are shown here because a putative thymic precursor of these cells was identified within the DP population (Gangadharan et al., 2006). These unconventional T cell precursors express CD4 and both the heterodimeric form of CD8; CD8αβ, and the homodimer CD8αα. These cells are known as "triple positives" or TPs. γδ T were identified using a TCRδ antibody.

1.2 Semi-quantitative PCR for pTα^{a} and pTα^{b} expression.

Thymocyte populations were obtained from C57BL/6 adult thymus by FACS (Figure 1.2). Live thymocytes are first characterised by using forward scatter (FSC) and side scatter (SSC) which measure the size and granularity of the cells, respectively. For the DN sort, markers for unwanted subsets such as B cells (B220), NK/NKT cells (NK1.1 and DX5) and γδ T cells (δTCR) as well as CD4 and CD8 were used to gate out these cells from the sort. The different DN subsets were then selected according to CD25 and CD44 expression, as described previously. DPs, CD4SPs, CD8SPs and ISPs were selected on expression of CD4 and CD8.The isolated populations were lysed in Trizol, RNA was extracted and cDNA synthesis was performed.

Figure 1.2

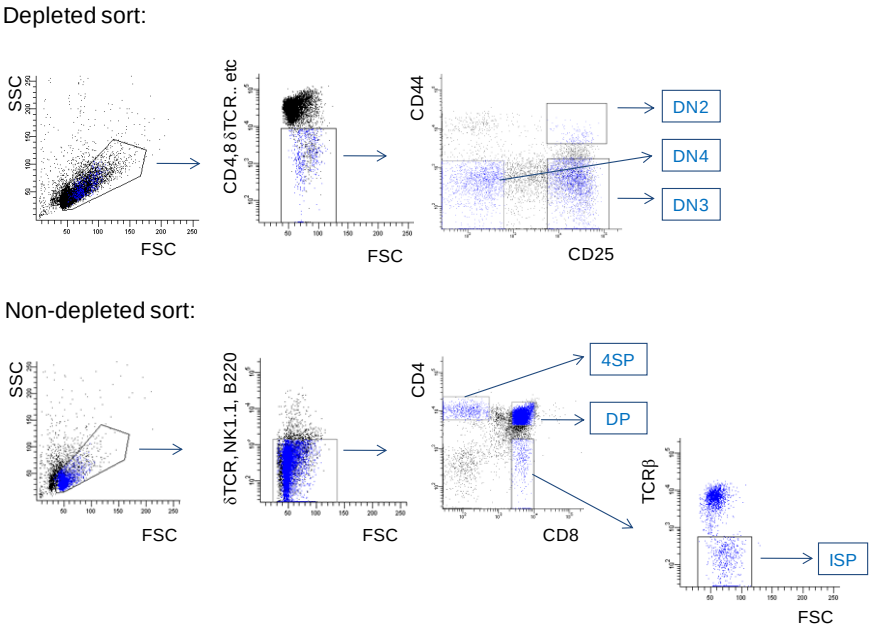

Figure 1.2: Fluorescence activated cell sort to obtain different thymocyte subsets. FACS profiles of adult C57/Bl6 thymocytes. CD4^{+}CD8^{+} thymocytes were depleted using complement for the DN sort. FSC is forward scatter a measure of cell size; SSC is side scatter a measure of cell granularity. DN is double negative; DP is double positive; ISP is immature single positive, SP is single positive. Cells were sorted with 95-98% purity. Depleted sort refers to cells that were subjected to complement lysis to remove CD4$^{(+)}$ and CD8$^{(+)}$ cells.

cDNA levels were normalised using PCR for β-actin. In order to distinguish pTα^a and pTα^b transcripts, PCRs for pTα^a were performed using a forward primer homologous to 25bp of exon-2 and a reverse primer that recognises 25bp within exon-4 of pTα (Figure 1.3A). pTα^b transcripts do not possess exon-2 and therefore only pTα^a transcripts were amplified with these primers. To amplify pTα^b transcripts, a forward primer was used that recognised 16bp of the 3' end of exon-1 and 6bp of the 5' end of exon-3, and therefore was homologous to the exon-1-3 join that is exclusive to pTα^b transcripts. Using these primers, transcripts for both isoforms were detected in DN2 thymocytes and at high levels within the DN3 and DN4 populations undergoing β-selection (Figure 1.3B).

Figure 1.3

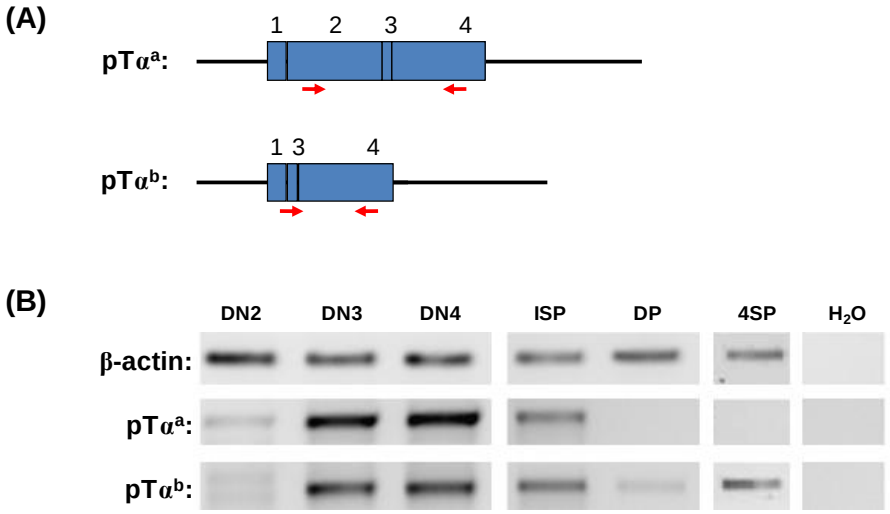

Figure 1.3 pTα^a and pTα^b are differentially expressed throughout thymic ontogeny: (A) pTα^a and pTα^b transcripts with primers specific for pTα^a and pTα^b indicated. (B) Semi-quantitative PCR of thymocyte subsets for pTα^a and pTα^b: cDNA samples extracted from C57BL/6 adult DN2, DN3, DN4, ISP, DP and 4SP subsets were normalised by PCR for β-actin.

Signalling through TCRαβ has been described to regulate expression of the pTα gene (Bruno et al., 1995). Thus we would not expect DP cells and mature cells which possess the αβTCR to express pTα^a and pTα^b. However,

the DP population expressed low levels of both transcripts. pTα^{a} expression appears to be extinguished at this stage but not that of pTα^{b} (Figure 1.3B). pTα^{b} expression continued into mature stages of T cell development (i.e. CD4SPs). pTα^{a} transcripts were not detected in these cells at this level of sensitivity (Figure 1.3B). These data show that expression of pTα^{a} and pTα^{b} are differentially regulated during thymic ontogeny, and suggest a non-redundant role for the two isoforms in T cell development.

1.3 Semi-quantitative PCR for pTα^{a} and pTα^{b} expression in TPs from embryonic day-16-17 C57BL/6 mice.

Low level expression of pTα^{b} but not pTα^{a} in DP thymocytes (at least at this level of detection) may be due to a small population of DPs retaining expression of this isoform within the larger DP population. TP cells, that have been proposed to be the thymic precursors to the CD8αα$^{(+)}$ gut IEL populations express the CD8αα homodimer as well as CD8αβ and CD4 on their surface (Gangadharan et al., 2006). TPs can be identified using TL tetramers which bind CD8αα homodimers with high affinity (Attinger et al., 2005). The TP subset was reported to represent 7-10% of DPs in the adult thymus but are enriched to 60% of DP cells at embryonic day-16-17 (Gangadharan et al., 2006). TL$^{(+)}$ and TL$^{(-)}$ DP thymocytes from E16 and E17 C57BL/6 thymuses were isolated as shown in Figure 1.4. pTα^{a} and pTα^{b} expression were then determined by semi-quantitative PCR.

Similar levels of both pTα^{a} and pTα^{b} were expressed in TL$^{(+)}$ and TL$^{(-)}$ DP cells from both E16 and E17 thymuses (Figure 1.5). Curiously, embryonic DP thymocytes (whether CD8αα$^{(+)}$ or not) express pTα^{a} and pTα^{b} at similar levels, whereas adult DPs did not (levels of pTα^{a} were lower than pTα^{b}) (Figure 1.3). This result suggests that differential expression and use of

pTα^{a} or pTα^{b} is not responsible for the generation of TP cells, and thus is unlikely to underlie the mechanism involved in IEL development.

Figure 1.4

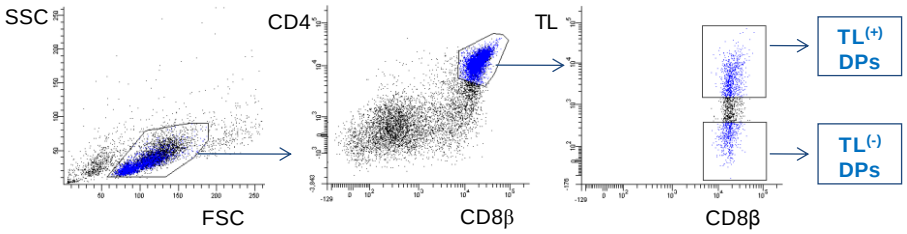

Figure 1.4: Isolation of TP cells by FACS: C57BL/6 E17 thymocytes were stained with the Thymic leukaemia antigen (TL) tetramer for isolation of CD4$^{(+)}$CD8αβ$^{(+)}$ CD8αα$^{(+)}$ cells (that are postulated to be gut IEL progenitors). Cells were sorted to 98% purity.

Figure 1.5

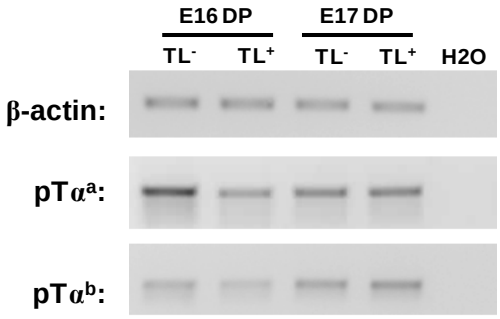

Figure 1.5 E16 and E17 TPs express both pTα^{a} and pTα^{b}: TL$^{(-)}$ and TL$^{(+)}$ DPs were isolated from day 16 and 17 C57BL/6 embryos. Semi-quantitative PCR for pTα^{a} and pTα^{b} was performed on the cDNA extracted from sorted cells. cDNA levels were normalised by β-actin PCR. TL$^{(-)}$ and TL$^{(+)}$ DPs express similar levels of both pTα^{a} and pTα^{b}.

1.4 Single cell multiplex PCR analysis of C57BL/6 adult DN3 and DN4 thymocytes.

Differential regulation of expression of pTα^{a} and pTα^{b} at the population level throughout thymocyte development may be a reflection of differential expression of the two isoforms in individual cells within a given population. Indeed, this scenario would perhaps be indicative of different roles for the two isoforms in T cell development. In order to determine whether individual

cells differentially expressed either pTα^a or pTα^b it was necessary to optimise a single cell quantitative PCR (SCPCR) assay (Figure 1.6).

Figure 1.6

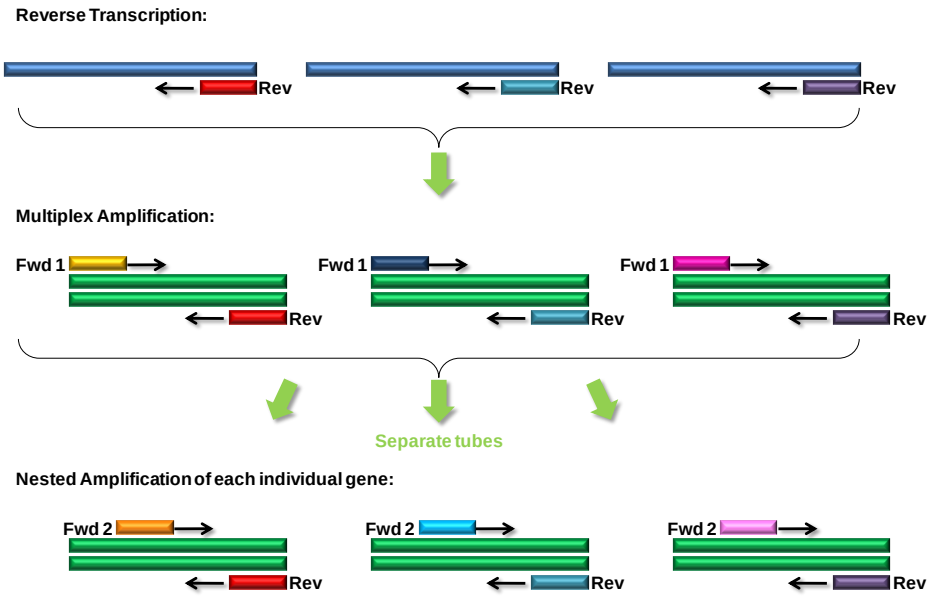

Figure 1.6 Schematic of Single cell Multiplex PCR: RNA is reverse transcribed using specific reverse (Rev) primers. The first PCR reaction uses multiple primer pairs to amplify 3 different genes. These PCR products are then amplified a second time, but this time separately using nested primer sets.

For SCPCR analysis, DN3 and DN4 single cells were sorted by FACS into strips of PCR tubes containing 5µl of PBS. After reverse transcription using specific reverse primers for pTα^a, pTα^b and a house-keeping gene EF1A, the cDNA was amplified a first time by multiplex PCR in the same reaction (Figure 1.6). These PCR products were then amplified a second time separately for EF1A, pTα^a and pTα^b in 3 different reactions. The 2nd PCR reactions are semi-nested in which the forward primer lies within the sequence amplified by the first set of PCR primers (Figure 1.6). To be able to compare PCRs for EF1A, pTα^a and pTα^b from the same cell it was essential that the primers amplified the genes efficiently. This was

assessed by quantitative PCR in the second round. Primer efficiencies for each primer pair were 2 +/- 0.2 (i.e. a doubling of product in each round of PCR) (Figure 1.7). This is sufficient to perform multiplex PCR.

Figure 1.7

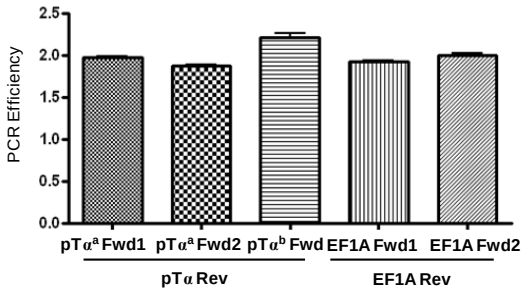

Figure 1.7 SCPCR Primer efficiencies: Primers for the RT, multiplex and 2nd PCR reactions were tested by real-time PCR for efficiency of product amplification. Each primer pair had an efficiency of approximately 100% (2 fold increase in product per cycle). Graph represents three experiments, in which DN4 cDNA was used as the template.

The next stage in optimization was to ensure there was no competition between primer sets used in the first PCR (multiplex). Primer competition leads to inefficient amplification of the target sequence and would produce misleading PCR results. To compare competition between primer sets Ct values were compared for the different PCR reactions in triplicate, using DN4 thymocyte cDNA as a template. No difference was seen between Ct values from reactions in which the first round was performed as a multiplex, to reactions in which the first round was performed with just a single primer set (Figure 1.8). This therefore established that these primers were fit for use in the comparative SCPCR analysis.

Single cell PCR of eight WT DN4 cells were carried out for EF1A, $pT\alpha^a$ and $pT\alpha^b$ (Figure 1.9). EF1A transcripts were detected in six of the eight cells suggesting that only wells 1-6 contained a DN4 cell. Only one of these six cells appeared positive for $pT\alpha^a$ transcripts (cell number 3) and none of the

cells appeared to express pTα^{b}. PCRs for these genes was carried out on a further two strips of DN4 cells and on a strip of DN3 cells. However, on average only 1/8 cells tested positive for pTα^{a} transcripts and only 1/24 were positive for pTα^{b} (data not shown). Because it was not possible to determine whether the lack of pTα transcripts in the single cell PCR was due to lack of expression of pTα transcripts, or limited sensitivity of the protocol it was necessary to determine the sensitivity of the assay. This was done by performing the SCPCR protocol on a series of titrated samples from one hundred DN4 cells down to one cell. These PCRs showed that despite detecting EF1A transcripts in all the samples from one hundred cells down to one cell, it was only possible to detect pTα^{a} transcripts in fifty cells or more, and only possible to detect pTα^{b} in twenty cells or more (Figure 1.10). Thus, the sensitivity of the assay was poor and this could explain why very few DN4 cells appeared to express either pTα^{a} or pTα^{b}. It was therefore necessary to design and optimise new primer sets for pTα^{a} and pTα^{b} for use in this assay. New forward primers for the 1st and 2nd pTα^{a} PCR reaction and a new reverse primer for use at all stages of pTα amplification, were designed.

Figure 1.8

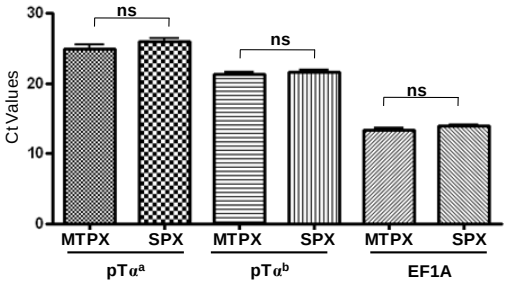

Figure 1.8 No competition between SCPCR primer sets: Similar Ct values are observed for 2nd round PCR on pTα^{a}, pTα^{b} and EF1A, when the template used was from either a multiplex 1st round PCR reaction (MTPX) or from a 1st round PCR that used just a single primer set (SPX). Reactions were performed in triplicate on cDNA from DN4 cells.

Figure 1.9

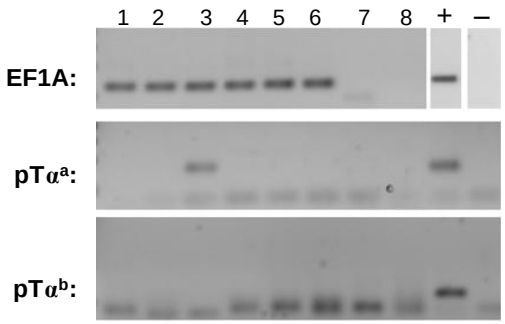

Figure 1.9: SCPCR analysis of 8 DN4 cells: 500 DN4 cells were used for the positive control and PBS was used for the negative control. Adult C57BL/6 DN4 thymocytes were used in this analysis.

Figure 1.10

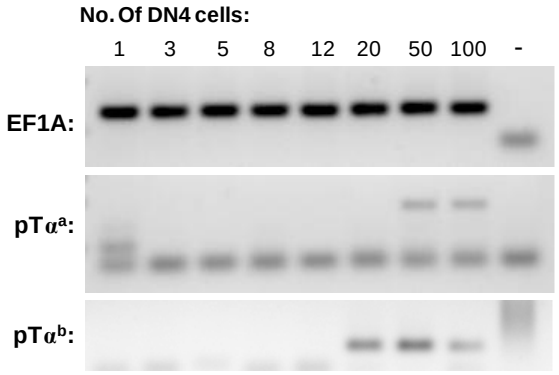

Figure 1.10: Limited sensitivity of pTα^a and pTα^b SCPCR: Unlike EF1A, transcripts for pTα^a and pTα^b were not detected in fewer than 20 cells. PBS was used for the negative control. .

Figure 1.11

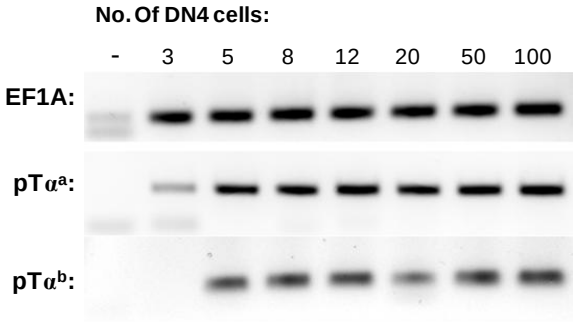

Figure 1.11: Improved sensitivity of pTα^a and pTα^b SCPCR: New PCR primers allowed greater detection of pTα^a and pTα^b transcripts in DN4 cells.

These primers were initially tested for sensitivity, before subsequent efficiency and competition analysis. Figure 1.11 shows EF1A, pTα^{a} and pTα^{b} SCPCRs for DN4 cell titration from one hundred cells down to three cells. The sensitivity of the pTα^{a} PCR was vastly improved with pTα^{a} transcripts being amplified from as few as three DN4 cells. pTα^{b} PCR sensitivity was also improved but pTα^{b} transcripts could not be detected in fewer than five DN4 cells. The optimisation of these new primer sets was only achieved right at the very end of the experimental work that constitutes this thesis. Thus, whether individual DN cells differentially express pTα^{a} and pTα^{b} remains unresolved, but is a focus of ongoing work in the lab. Furthermore, the lessons learned from optimization of SCPCR has provided an important tool that is currently being utilised by other lab members.

Chapter 2

pTα^a and pTα^b expression in FTOC

2.1 Introduction.

To assess the differential effects of pTα^a and pTα^b in T cell development the two proteins were expressed in isolation in pTα KO DN thymocytes in foetal thymic organ culture (FTOC). FTOC is a culture system *in vitro* that supports T cell development that largely resembles that seen *in vivo* (Jenkinson et al., 1992; Mandel and Kennedy, 1978; Owen and Ritter, 1969). The system is easy to manipulate by addition of antibodies or chemicals/drugs to the culture medium. It is also possible to use a retroviral delivery system to express various genes in thymocyte progenitors before culture. This culture system allows the two isoforms of pTα to be expressed alone in pTα-deficient thymocytes. The developmental consequences of this expression is then followed for up to 15 days.

Semi-quantitative PCR had revealed that pTα^a and pTα^b had different expression patterns throughout development, suggesting that the two isoforms of pTα may be regulated differently during T cell development. Thus, we sought to determine whether expression of pTα^a alone or pTα^b alone had different effects in developing thymocytes. To do this, retroviral constructs were generated that permitted delivery of pTα^a or pTα^b (Figure 2.1). The vector used was pLZRS (pLZ) (Heemskerk et al., 1997). This contained two long terminal repeats (LTRs) between which the cloned pTα cDNA was placed. The LTRs allow for integration of the construct into cellular DNA but also serve as promoter elements for transcription of the

cloned gene. An enhanced green fluorescent protein (GFP) gene is present, preceded by an internal ribosomal entry site (IRES). This IRES lies downstream of the cloned gene, which allows for translation of GFP as well as pTα. This feature permits detection of transduced cells.

Figure 2.1

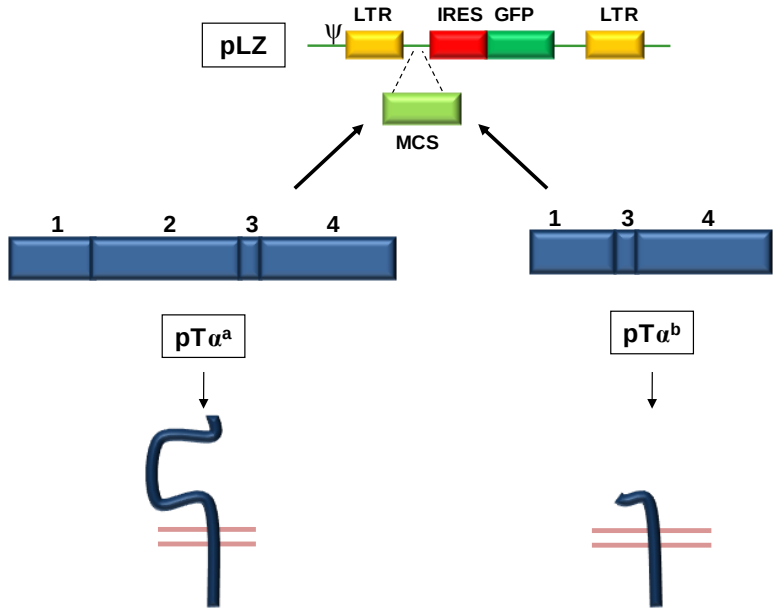

Figure 2.1 pTα^a and pTα^b retroviral constructs: A schematic of the pTα^a and pTα^b cDNAs that were cloned into the multiple cloning site (MCS) of the pLZ retroviral vector. pTα^a is the full length isoform of pTα and consists of four exons. The second isoform of pTα, pTα^b lacks exon-2 that codes for the extracellular Ig-loop of the protein. LTR, long terminal repeat; IRES, internal ribosomal entry site; GFP, green fluorescent protein and ψ denotes the retroviral packaging signal.

Figure 2.2 illustrates the experimental method used in these investigations. The pLZ plasmids containing the pTα cDNAs were transfected into the Phoenix ecotropic packaging cell line (www.stanford.edu/group/nolan/). Phoenix cells are stably transfected with plasmids carrying retroviral genes *env*, *gag* and *pol* for the generation of virus particles. The pLZ plasmid possesses a packaging signal (ψ) that allows full length (i.e. between the two LTRs) pLZ transcripts to be incorporated into the virions. Retroviruses carrying the pTα cDNAs were collected from the supernatant of the phoenix

cells and used to transduce E14 pTα KO thymocytes for 5-15-day culture in FTOC and subsequent analysis by flow cytometry.

Figure 2.2

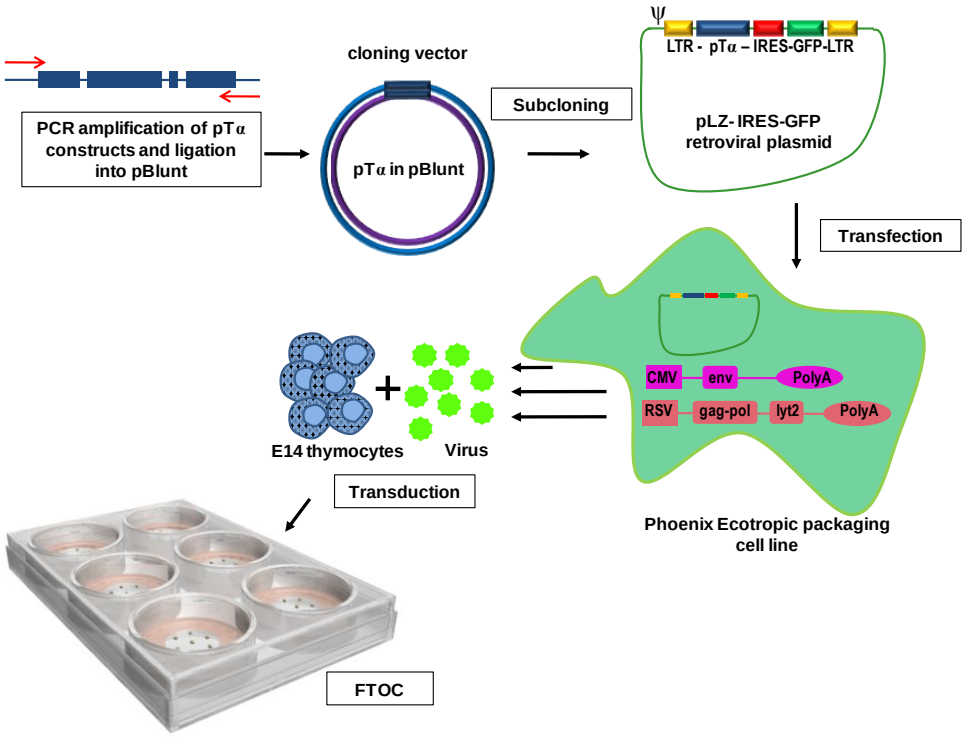

Figure 2.2: A schematic of the experimental method used for cloning pTα cDNAs into pLZ retroviral vectors and retroviral transduction of pTα KO E14s in FTOC. pTα^a and pTα^b were amplified by PCR from DN4 cDNA. The PCR products were cloned into pLZ via the pBlunt cloning plasmid. pLZ plasmids containing the pTα cDNAs were transfected into the phoenix ecotropic packaging cell line. The pTα constructs were packaged into retroviral particles which were used to transduce pTα-deficient E14 thymocytes. Transduced thymocytes were seeded into empty E15 thymic lobes and cultured in FTOC for 5-15-days before subsequent analysis by flow cytometry.

2.2 Generating pTα^a and pTα^b retroviral constructs.

Forward and reverse primers homologous to the first 25bp of exon-1 and a region, 238bp downstream of the stop codon in exon-4, respectively, were used to amplify pTα^a and pTα^b in a single PCR reaction from adult C57BL/6 DN4 thymocytes (Figure 2.3). pTα^a is the longer of the two isoforms at

956bp in length, while pTα^{b} lacks exon-2 (320bp) and is therefore 636bp in length (Figure 2.3).

Figure 2.3

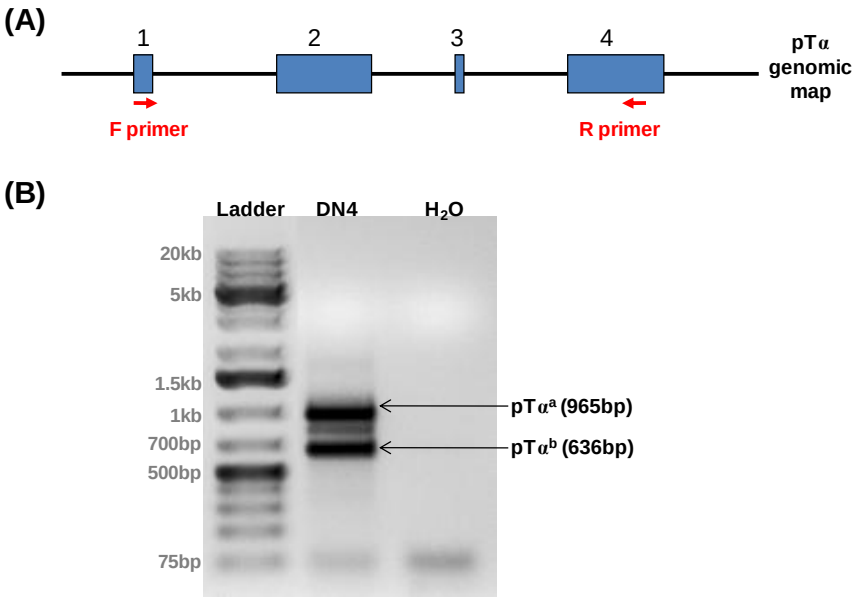

Figure 2.3 PCRs used to sub-clone pTα^{a} and pTα^{b}: (A) schematic displaying the 4 exons of pTα with the primers used to amplify pTα^{a} and pTα^{b}. (B) Agarose gel showing bands corresponding to pTα^{a} (p65bp) and pTα^{b} (636bp). DN4 cDNA from adult C57BL/6 mice was used as a template.

Figure 2.4

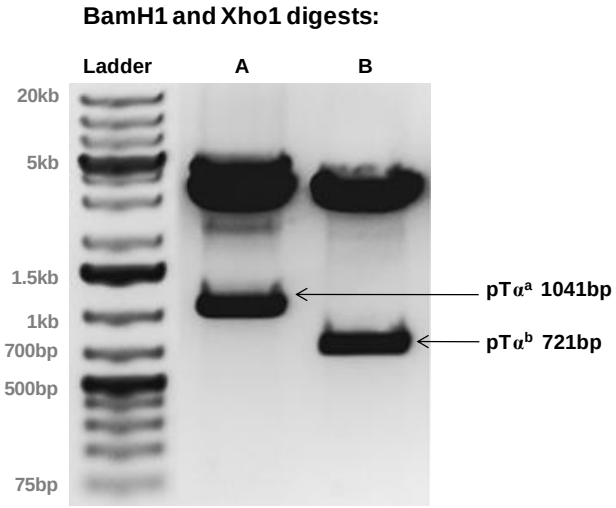

Figure 2.4: pBlunt-pTα^{a} and pBlunt-pTα^{b}: Restriction digest analysis of pBlunt-pTα^{a} (A) and pBlunt-pTα^{b} (B) cut with BamH1/Xho1 to release pTα cDNAs. The digested pBlunt backbone is approximately 3.5kb.

PCR products corresponding to pTα^a and pTα^b were isolated from an agarose gel and ligated into the pBlunt cloning plasmid. Figure 2.4 shows a BamH1/Xho1 digestion for pBlunt-pTα^a and pBlunt-pTα^b. The BamH1 site lies 39bp upstream of the insert, while the Xho1 site lies 37bp downstream of the insert. Digestion with these enzymes releases the pTα cDNAs; pTα^a is 1041bp and pTα^b is 721bp long. The pTα^a and pTα^b cDNAs were then sub-cloned into the retroviral pLZ plasmid. pLZ-pTα^a and pLZ-pTα^b were once again analysed by BamH1 and Xho1 restriction digest, the pTα^a plasmid generating a band of 1041bp in length, while the pTα^b plasmid giving a band of 721bp (Figure 2.5).

Figure 2.5

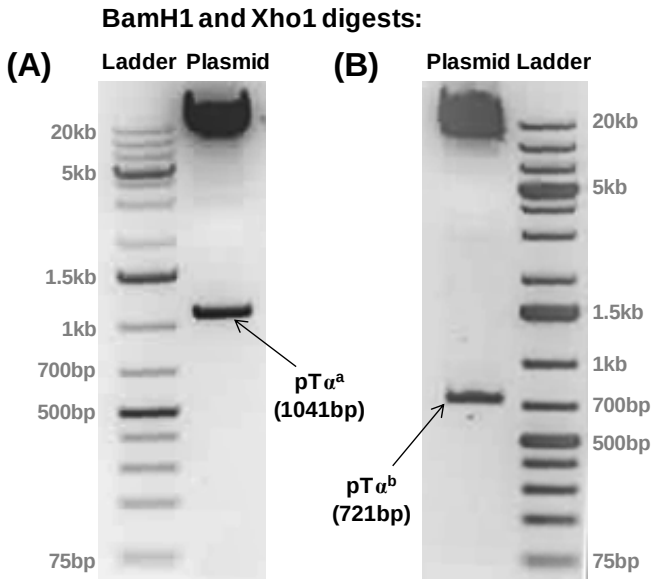

Figure 2.5 pLZ-pTα^a and pLZ-pTα^b: Restriction digest analysis of (A) pLZ-pTα^a and (B) pLZ-pTα^b with BamH1/Xho1 to release the pTα^a and pTα^b cDNAs. The backbone of the pLZ plasmid is approximately 12.4kb.

The plasmids pLZ-pTα^a, pLZ-pTα^b and pLZ alone, were then transfected into the phoenix ecotropic packaging cell line and transfection was confirmed by the presence of GFP detected under a UV microscope (Figure 2.6).

Figure 2.6

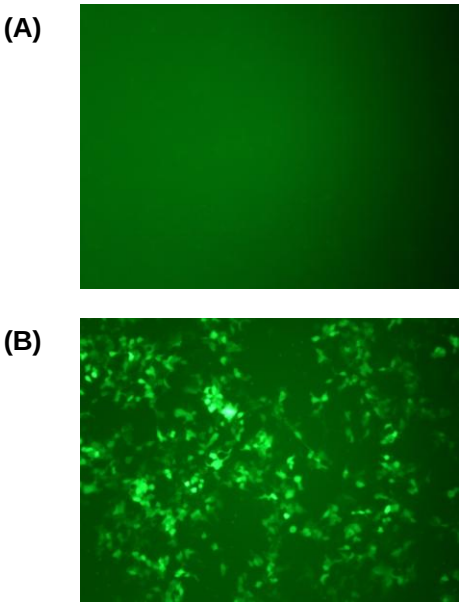

Figure 2.6 Analysis of transfected phoenix cells. Photograph of (A) non-transfected, or (B) transfected (with pLZ) phoenix cells, viewed under a UV light, 24hrs after transfection.

Retrovirus harvested from phoenix cells, transfected with pLZ, pLZ-pTα^a and pLZ-pTα^b were then used to transduce pTα KO E14 thymocytes. The transduced cells were seeded into empty C57BL/6 E15 thymic lobes that had been treated with 2-deoxyguanosine for 5 days to remove endogenous thymocytes. The re-seeded lobes were cultured for 5-15 days to allow for development and maturation of the transduced precursor T cells. Transduced thymocytes could, by GFP expression be detected by flow cytometry. FACS profiles of GFP expression for pLZ, pLZ-pTα^a and pLZ-pTα^b after 11 days in FTOC demonstrate that transduction efficiency was high for each of the constructs (Figure 2.7). Generally, transduction efficiencies were between 25% and 75% for all retrovirus used. GFP positive cells were further analysed to determine the effects of expression of pTα^a and pTα^b on developing thymocytes.

Figure 2.7

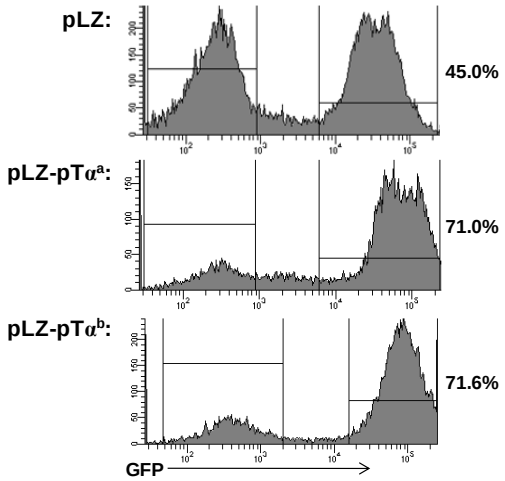

Figure 2.7 Good transduction efficiency for pLZ, pLZ-pTα^a and pLZ-pTα^b. GFP expression as a read-out of transduction efficiency for pTα KO E14 thymocytes transduced with retroviruses generated from the pLZ, pLZ-pTα^a and pLZ-pTα^b retroviral vectors. Percentages are out of cells in the live gate.

2.3 Both pTα^a and pTα^b form signal competent preTCRs able to rescue αβ T cell development in a pTα KO background.

2.3.1 pTα^a and pTα^b form preTCRs on the surface of transduced thymocytes

Cell surface expression of TCRβ is low on most DN cells from pTα-deficient mice as a preTCR cannot form. preTCR surface levels can be estimated by the analysis of mean fluorescence intensity (MFI) of TCRβ staining. The MFI for TCRβ in E14 pTα KO thymocytes transduced with pLZ vector was ~250 units after 8-11 days in FTOC (Figure 2.8). Note that TCRβ$^{(hi)}$ cells were excluded from this analysis, as these cells would likely express TCRαβ. By contrast, pTα-deficient cells transduced with either pTα^a or pTα^b, showed increased surface expression of TCRβ. On average MFI for TCRβ was ~550 units in the presence of pTα^a and ~800 units in the presence of pTα^b (Figure 2.8). These data are consistent with a preTCR being formed with both pTα isoforms. Thus expression of pTα^a and pTα^b in pTα KO thymocytes restores surface expression of a preTCR. Importantly, surface

TCRβ expression is significantly higher with pTα^{b} (MFI of 816 units +/- 111), than with pTα^{a} (544 units +/- 62) (p≤ 0.01).

Figure 2.8

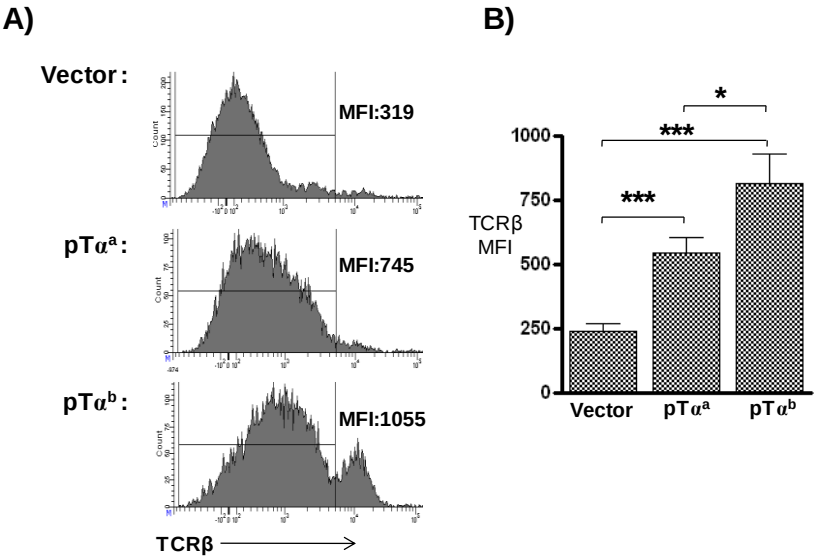

Figure 2.8 pTα^{a} and pTα^{b} both form preTCR complexes in pTα-deficient cells. (A) representative histograms of E14 pTα KO thymocytes transduced with vector alone, pTα^{a} or pTα^{b} and analysed after 11 days in FTOC. Cells are GFP$^{(+)}$ TCRδ$^{(-)}$ and gates shown exclude TCRβ$^{(hi)}$ cells. MFI for TCRβ$^{(lo)}$ cells is shown. (B) Bar chart showing (n=7) experiments of data shown in (A). * p≤0.05, ** p≤0.01, *** p≤0.001.

This suggests that preTCR^{b} is expressed at higher surface levels than preTCR^{a}. If signal strength is proportional to the number of receptor complexes at the surface of the cell, this would suggest that preTCR^{b} signals stronger than preTCR^{a}. Differential preTCR signal strength could have very significant consequences for T cell development as it is described as the mechanism by which different developmental fates are achieved; for example, in γδ/αβ lineage choice (Hayes et al., 2005), as well as for CD4 *vs*. CD8 development (Singer and Bosselut, 2004).

2.3.2 PreTCR^a and preTCR^b are signalling competent TCR complexes.

Although surface expression of the preTCR (as judged by TCRβ) was increased in the presence of pTα^a and pTα^b, it was important to determine whether these preTCR complexes were able to signal. To avoid complicated assays for downstream signal activation a simple method that would determine whether the preTCRs were signalling was required. The pTα KO thymus has a profound developmental block at the DN3 stage of αβ T cell differentiation (Fehling et al., 1995a). As a result, more progenitor cells commit to the γδ lineage (Buer et al., 1997b) resulting in a 5 to 10-fold increase in the percentage of γδ T cells compared to a WT thymus (Figure 2.9).

Figure 2.9

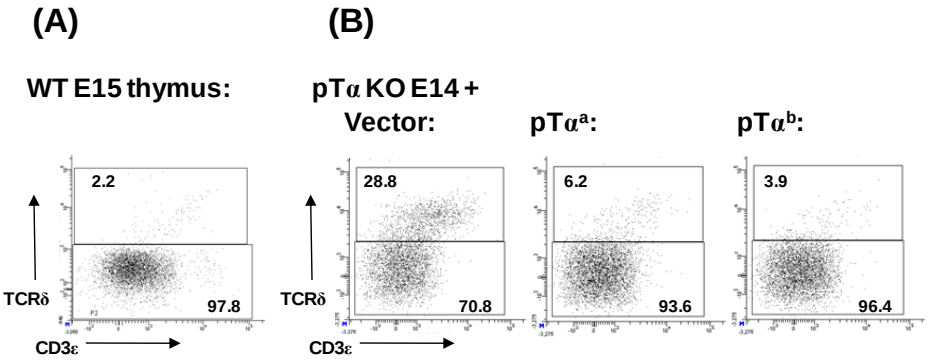

Figure 2.9 preTCR^a and preTCR^b are signal competent receptors. Representative FACS plots (from n = 7 experiments) of (A) a WT E15 thymic lobe, or (B) E14 pTα KO thymocytes transduced with vector only, pTα^a or pTα^b, in depleted thymic lobes, after 8 day FTOC. Plots show live cells analysed for TCRδ and CD3ε expression. Numbers refer to percentage of cells in gates.

The introduction of a functional preTCR into pTα KO thymocytes rescues αβ T cell development and diverts cells away from the γδ lineage restoring the percentage of γδ T cells to ~2-3% of the thymus (Figure 2.9A) (Gibbons et al., 2001). Thus it is possible to utilise the percentage of γδ cells in the

thymus as a clear and simple readout of the functionality of the preTCR. pTα KO thymocytes transduced with vector alone generated ~30% γδ cells over the course of the FTOCs (Figure 2.10). A similar number of γδ cells were also seen in untransduced cells from all infections (Figure 2.10 black bars). However, by contrast, E14 pTα KO thymocytes transduced with $pT\alpha^a$ or $pT\alpha^b$ generated only ~10% γδ cells in the 5-15 day FTOCs (Figure 2.10).

Figure 2.10

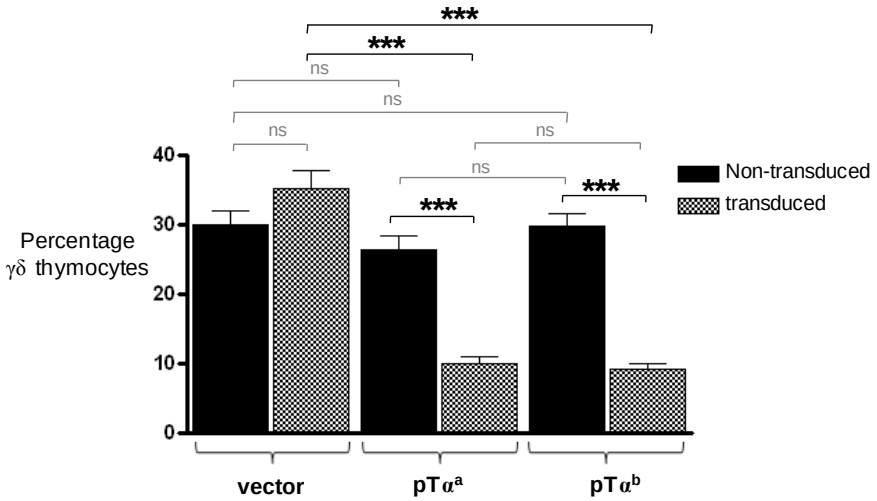

Figure 2.10: $preTCR^a$ and $preTCR^b$ are signal competent receptors. Bar chart (from n=19 experiments) of pTα KO E14 thymocytes transduced with vector alone, $pT\alpha^a$ or $pT\alpha^b$ and cultured for 5-15 days in FTOC. Live cells were analysed for TCRδ and CD3ε. The percentage of $TCR\delta^{(+)}$ $CD3\varepsilon^{(+)}$ cells are shown for untransduced thymocytes (black bars) and transduced thymocytes (hatched bars). ns is not significant, *** p≤0.001.

2.3.3 Analysis of consequences of $preTCR^a$ or $preTCR^b$ expression.

The low surface expression of $preTCR^a$ compared to $preTCR^b$ may indicate that $preTCR^a$ signals with a lower signal strength than $preTCR^b$. To determine whether we could detect differences in the strength of signal produced by $preTCR^a$ and $preTCR^b$, we analysed DN cells transduced with $pT\alpha^a$ and $pT\alpha^b$ for CD5 expression. CD5 is a cell surface glycoprotein, described to be a negative regulator of TCR-mediated signalling (Azzam et al., 2001). CD5 is upregulated on thymocytes as a result of preTCR

signalling (Azzam et al., 1998). Surface levels of CD5 on DPs and SPs are reported to be proportional the affinity of MHC-peptide-TCR interactions (Azzam et al., 1998). Therefore, it was possible that stronger signals through the preTCR would induce higher surface levels of CD5. To investigate, DN3 and DN4 pTα KO thymocytes transduced with vector, pTα^a or pTα^b were analysed for levels of CD5 after 7-8 days in FTOC. DN3 cells transduced with vector, pTα^a or pTα^b had low surface expression of CD5 (~1460, ~1530 and ~1260 MFI units, respectively) (Figure 2.11). CD5 levels significantly increased on DN4 cells transduced with vector, pTα^a or pTα^b (~2830 (p≤0.01), ~3000 (p≤0.01) and ~2760 (p≤0.001) MFI units, respectively), consistent with the induction of CD5 through signalling of a receptor at the β-selection checkpoint (Figure 2.11). However, no significant difference was observed in the surface levels of CD5 on DN4s in the presence of vector only, pTα^a or pTα^b. It is known that TCRγδ can promote the DN3 to DN4 transition in pTα KO mice (albeit inefficiently), that could be responsible for the increase in CD5 expression. Nonetheless, if CD5 is an indicator of signal strength, it suggests little difference between preTCR^a, preTCR^b (and TCRγδ) at the β-selection checkpoint.

Figure 2.11

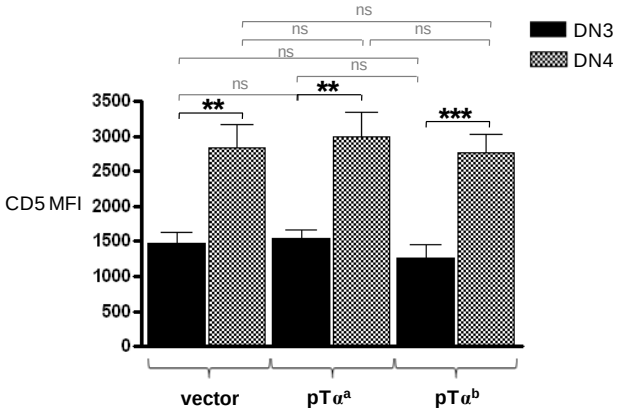

Figure 2.11 CD5 is upregulated on post β-selection thymocytes: Bar chart showing E14 pTα KO cells transduced with vector alone, pTα^a or pTα^b that were analysed for CD5 MFI on DN3 (black bars) and DN4 (hatched bars) cells, after 7-8 days in FTOC. *** p≤0.001, ** p≤0.01, ns is not significant.

PreTCR signalling induces proliferation of β-selected DN4 cells, a mechanism for expansion of the αβ T cell progenitor pool (Hoffman et al., 1996; von Boehmer et al., 1998). To further analyse the function of preTCR^{a} and preTCR^{b}, the cell cycle status of cells transduced with pTα^{a} and pTα^{b} was analysed using 7-Amino-Actinomycin-D (7-AAD) (Rabinovitch et al., 1986). 7-AAD is a fluorescent dye that intercalates into double-stranded DNA allowing the DNA content of a cell to be determined by FACS. Resting cells in G_0 or G_1 have two copies of each chromosome and therefore a DNA content of 2n. Cells undergoing division enter the S-phase and undergo synthesis of new DNA, resulting in an increase in the DNA content and a proportional increase in the fluorescence produced by excitation of 7-AAD. Cells in G_2 have fully replicated their DNA and are about to divide; they have a DNA content of 4n.

Figure 2.12

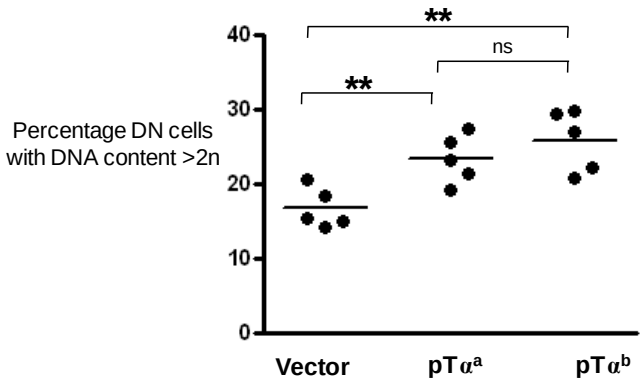

Figure 2.12 preTCR^{a} and preTCR^{b} induce cell cycle entry of DN thymocytes. Graph showing the percentage of pTα KO DN cells transduced with vector alone, pTα^{a}, or pTα^{b}, after 8-day FTOC, with a >2n DNA content as judged by 7-AAD staining. DN cells were GFP$^{(+)}$ TCRδ$^{(-)}$ CD4$^{(-)}$ CD8$^{(-)}$.

At day 8 of FTOC ~17% of vector transduced pTα KO DN thymocytes had a DNA content greater than 2n (Figure 2.12). Transduction of pTα KO cells with either pTα^{a} or pTα^{b} increased the proportion of cycling DN cells to

~23% and ~26%, respectively (Figure 2.12). Therefore, it appears that both preTCR^{a} and preTCR^{b} have a similar capacity to induce proliferation of progenitor thymocytes.

2.4 pTα^{a} and pTα^{b} promote divergent T cell development.

Although preTCR^{a} and preTCR^{b} appeared to have very similar capabilities to divert developing thymocytes away from the $\gamma\delta$ lineage, we next investigated whether these preTCR complexes promoted $\alpha\beta$ T cell development with similar characteristics. To do this we analysed the number and percentage of various $\alpha\beta$-committed thymocyte populations; ISP cells, DP cells and mature CD4SP cells and CD8SP cells.

Figure 2.13 shows representative FACS plots from an experiment analysed at FTOC day-15, which illustrates the development promoted by pTα^{a} and pTα^{b}. After fifteen days in culture the majority (~55%) of pTα KO thymocytes transduced with the vector alone develop as $\gamma\delta$ cells. Only ~39% of the TCR$\delta^{(-)}$ thymocytes have developed to the DP stage and only ~9% of the TCR$\delta^{(-)}$ cells are mature $\alpha\beta$TCR$^{(+)}$ cells. By contrast, pTα KO cells transduced with pTα^{a} or pTα^{b} generate far fewer $\gamma\delta$ cells, as previously discussed. Indeed, the majority of cells are TCR$\delta^{(-)}$ (~85%), emphasising the ability of the two preTCRs to divert thymocytes away from the $\gamma\delta$ lineage. However, a striking difference is observed between cells expressing pTα^{a} and pTα^{b} when comparing the TCR$\delta^{(-)}$ population; whereas the majority of TCR$\delta^{(-)}$ cells expressing pTα^{a} are TCR$\beta^{(lo)}$ (~85%), ~70% of those expressing pTα^{b} are mature T cells that have high surface levels of TCRβ (Figure 2.13). The majority of TCR$\beta^{(lo)}$ thymocytes (~60%) transduced with pTα^{a} are ISPs. This is not the case for pTα^{b} (~35%) or the vector alone (~20%). Indeed, when considering the largest population of

cells represented in each FTOC; ~55% of vector-only transduced cells are γδ cells, ~43% of pTα^{a} transduced cells are ISPs, while ~65% of pTα^{b} transduced cells are TCRβ$^{(hi)}$ (Figure 2.13).

Figure 2.13

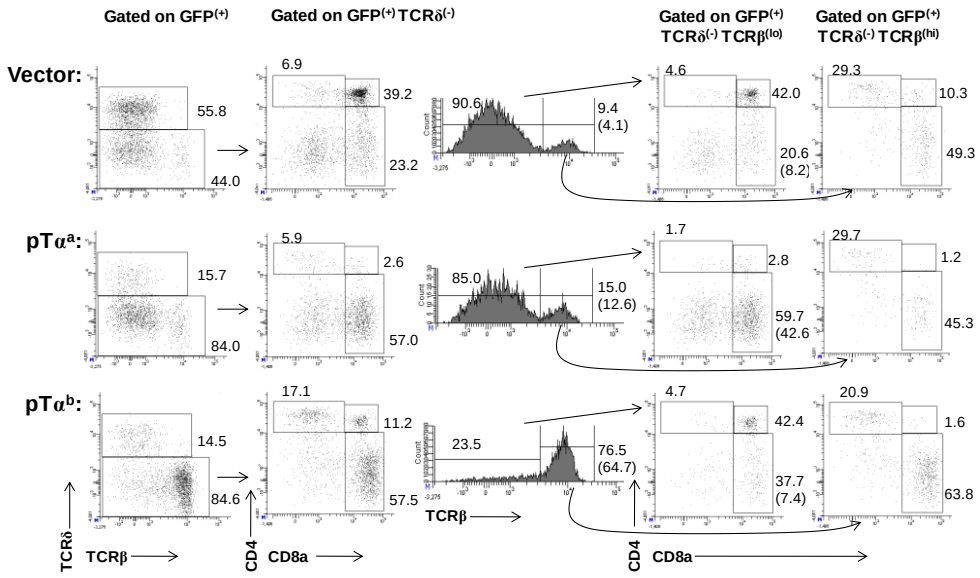

Figure 2.13 Divergent T cell development promoted by preTCR^{a} and preTCR^{b} at FTOC day 15: Representative FACS plots of pTα KO thymocytes transduced with vector alone, pTα^{a}, or pTα^{b} and cultured in FTOC for 15 days. Total live cells were gated for expression of GFP and then analysed as described. Numbers are percentage of cells in indicated gates.

ISPs are a highly proliferative intermediate population in transition from the DN4 to the DP stage. These cells express low levels of TCR but have upregulated CD8. Taking into consideration data from many experiments, it is evident that in 5-11 day FTOCs, ISPs account for ~10% of vector-only transduced pTα KO thymocytes and ~13% of those transduced with pTα^{b}. However, a significantly greater proportion (~23%) of pTα^{a}-transduced cells are ISPs (p≤0.001, Figure 2.14A). This phenotype was significantly more pronounced when FTOCs were run for 12-15 days (Figure 2.14B). Thus, still only ~10% of vector-only-transduced cells and ~11% of pTα^{b}-transduced cells were ISPs, but over ~35% of pTα^{a} transduced cells

displayed this phenotype (p≤0.001). Therefore, the difference in ISP numbers promoted by pTα^{a} and pTα^{b} became greater over time. This is more consistent with distinct functions of the two preTCRs, rather than differential kinetics.

Figure 2.14

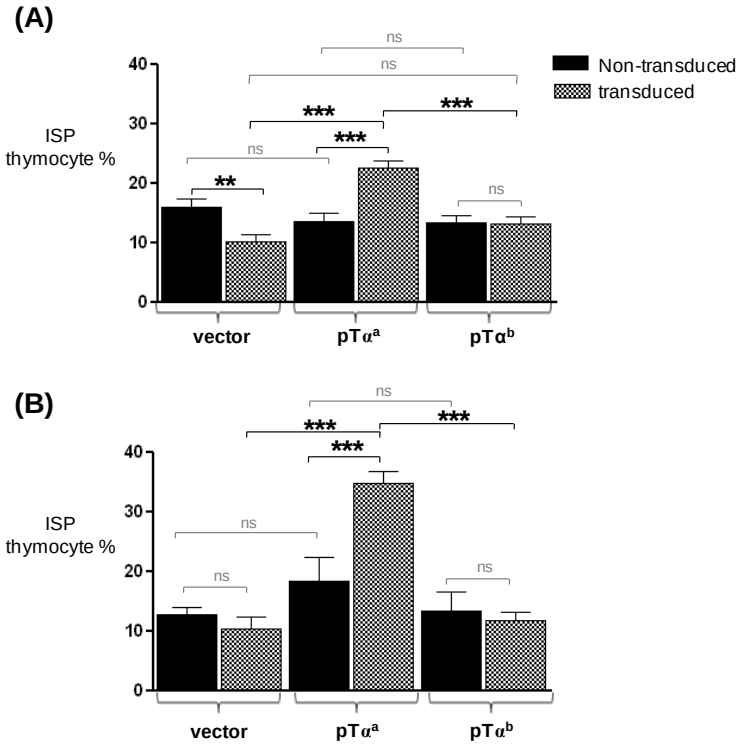

Figure 2.14 preTCR^{a} expression promotes the development and accumulation of ISPs: (A) Bar chart (from n=8 experiments) of pTα KO E14 thymocytes transduced with vector alone, pTα^{a} or pTα^{b} and cultured for 5-11 days in FTOC. (B) Bar chart showing similar cells as (A) but from 12-15 day FTOC cultures (from n=10 experiments). Live cells were analysed for TCRβ and CD8. The percentage of TCRδ$^{(-)}$ TCRβ$^{(+)}$ CD8$^{(+)}$ cells are shown for untransduced thymocytes (black bars) and transduced thymocytes (hatched bars). ns is not significant, *** p≤0.001.

In addition to the analysis of ISPs, we also investigated the generation of mature SP cells; both CD4SP and CD8SP subsets. In FTOC run for 5-11 days only, a very small percentage, ~3%, of vector-only-transduced pTα KO thymocytes develop to a mature αβ stage as detected by high surface levels of the TCRβ chain (Figure 2.15A). In these shorter FTOCs the

transduction of pTα^{a} or pTα^{b} did not significantly promote the development of more mature T cells when compared with non-transduced cells from the same cultures. However, when FTOCs were run longer for 12-15 days, a profound difference in development of TCRβ$^{(hi)}$ cells was observed in cultures expressing pTα^{a} or pTα^{b} (Figure 2.13 and 2.15B). Whereas only ~15% of pTα^{a}-transduced thymocytes expressed high levels of TCRβ, ~45%, of cells transduced with pTα^{b} were TCRβ$^{(hi)}$ (p≤ 0.001) (Figure 2.15B).

Figure 2.15

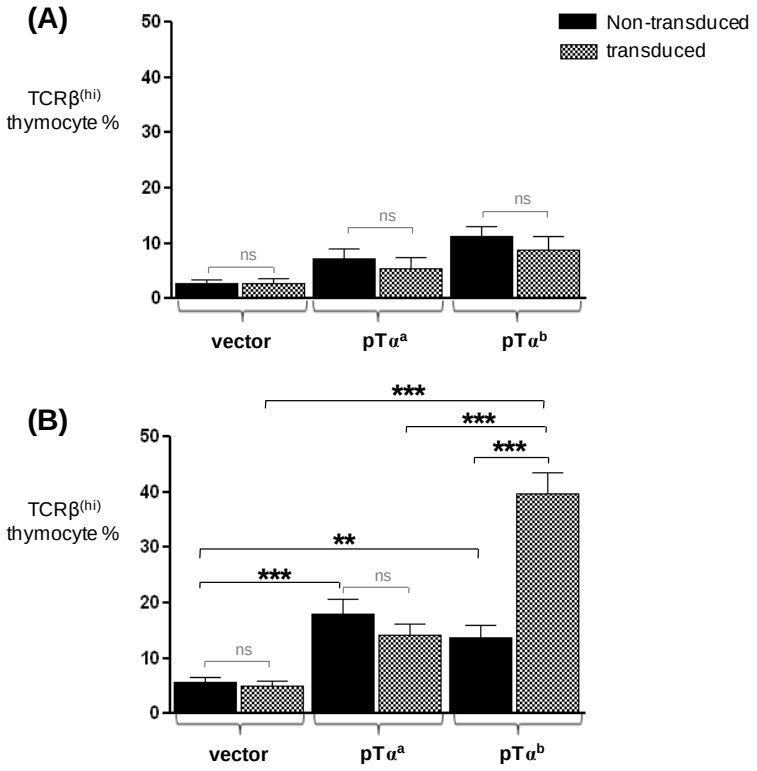

Figure 2.15 **preTCR^{b} expression promotes the development of TCRβ$^{(hi)}$ cells:** (A) Bar chart (from n=8 experiments) of pTα KO E14 thymocytes transduced with vector alone, pTα^{a} or pTα^{b} and cultured for 5-11 days in FTOC. (B) Bar chart showing similar cells as (A) but from 12-15 day FTOC cultures (from n=10 experiments). Live cells were analysed for TCRβ. The percentage of TCRδ$^{(-)}$ TCRβ$^{(hi)}$ cells are shown for untransduced thymocytes (black bars) and transduced thymocytes (hatched bars). ns is not significant, ** p≤0.01 *** p≤0.001.

Taken together these data suggest that the expression of pTα^{a} or pTα^{b} does not result in the same consequences for developing DN thymocytes. pTα^{a}-expressing cells accumulate at the ISP stage, while pTα^{b}-expressing cells preferentially transit to a mature TCRβ$^{(hi)}$ phenotype. Importantly, this does not appear to be a consequence of delayed kinetics as developmental differences became greater the longer the cultures were run.

The results presented above suggest that constitutive expression of pTα^{a} was inhibiting the maturation of ISPs. If this was the case, then perhaps introducing pTα^{b} into pTα^{a}-transduced cells would correct their development and promote their maturation to the DP stage and beyond. To investigate this, a double transduction was performed using both pTα^{a} and pTα^{b} containing retroviruses. To do this pTα^{b} had to be cloned into a retroviral plasmid possessing a different reporter gene; human nerve growth factor receptor (NGFR) that can be detected by a PE conjugated antibody. Thus, pTα^{a} expression was marked by GFP while pTα^{b} expression was marked by NGFR (Figure 2.16). Using these constructs four different populations were evident after 10-day FTOC, which represent non-transduced cells (black), pTα^{a}-expressing cells (green), pTα^{b}-expressing cells (red) and cells expressing both pTα^{a} and pTα^{b} (blue) (Figure 2.16).

Figure 2.16

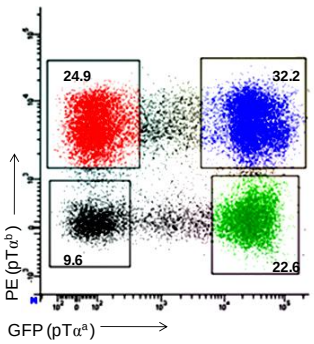

Figure 2.16 FACS profile of pTα^{a} and pTα^{b} double-transduced cells: pTα KO E14 thymocytes transduced with both pTα^{a} and pTα^{b} and cultured for 10 days were analysed for percentage of pTα^{a} (GFP$^{(+)}$) and pTα^{b} (PE-NGFR$^{(+)}$) and double-transduced (GFP$^{(+)}$PE$^{(+)}$) cells. Numbers refer to percentage cells in each gate.

Similar to cells transduced with pTα^{a} or pTα^{b} alone, double-transduced cells exhibited a higher surface expression of TCRβ (MFI of 467) than non-transduced cells (MFI of 248 units): consistent with formation of a preTCR (Figure 2.17A).

Figure 2.17

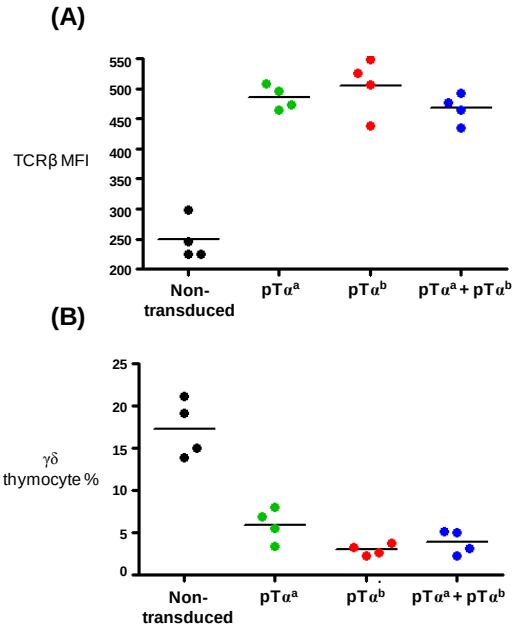

Figure 2.17 TCRβ surface expression and γδ cell development in pTα-deficient thymocytes transduced with both pTα^{a} and pTα^{b}: Dot plots showing E14 pTα KO thymocytes, after day-10 FTOC, that were non-transduced (black dots), transduced with pTα^{a} (green dots), or pTα^{b} (red dots), or both pTα^{a} and pTα^{b} (blue dots). (A) Cells are GFP$^{(+)}$ TCRδ$^{(-)}$ TCRβ$^{(lo)}$ and the MFI for TCRβ is shown. (B) Live cells were analysed for TCRδ expression and the percentage of γδ cells is shown.

A similar reduction in the percentage of γδ cells was also seen for double-transduced cells when compared to those transduced with pTα^{a} or pTα^{b} alone (Figure 2.17B). Whereas ~18% of non-transduced cells were TCRδ$^{(+)}$, only ~4% of double-transduced cells, ~6% of pTα^{a}-transduced cells and ~3% of pTα^{b}-transduced cells had become γδ cells (Figure 2.17B). This suggests that cells expressing both isoforms simultaneously were able to form signal-competent preTCRs resulting in development away from the γδ T cell lineage.

When the developmental characteristics of double-transduced thymocytes were assessed, it was apparent that they developed very similarly to cells expressing pTα^{a} alone, and unlike those that expressed pTα^{b} alone. Figure 2.18 shows the percentages of ISP and TCRβ$^{(hi)}$ cells for two double-transduction experiments after 10 or 13 day FTOC. Compared to cells expressing pTα^{b} alone, a greater percentage of double-transduced cells were ISPs; ~20-25% compared to ~7-8% at day 10 and 13, respectively (Figure 2.18A). This was similar to the percentage of ISPs seen for pTα^{a}-alone which was ~24% at day 10 and ~35% at day 13. When TCRβ$^{(hi)}$ cells were analysed pTα^{b}-alone promoted a 2.1-fold increase in the percentage of TCRβ$^{(hi)}$ cells, relative to that seen for the non-transduced population. However both pTα^{a}-alone and double-transduced cells did not show a similar increase (Figure 2.18B). These data suggest that when pTα^{a} and pTα^{b} are expressed in the same cell, pTα^{a} is dominant.

Figure 2.18

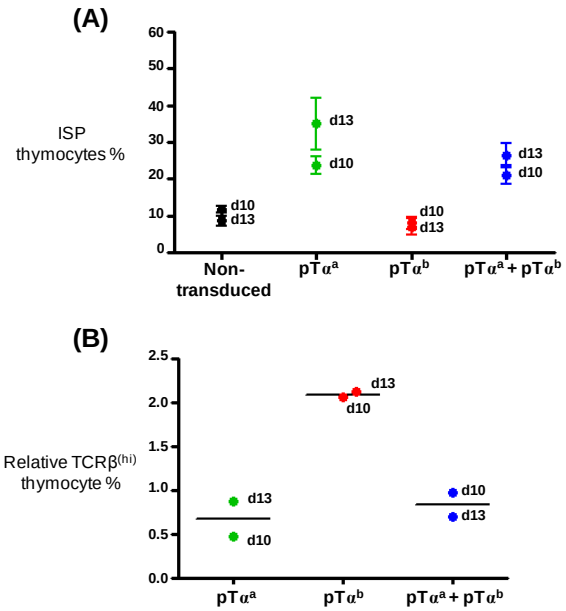

Figure 2.18 Double-transduced cells resemble those transduced with pTα^{a}-alone: Non-transduced, pTα^{a}-only, pTα^{b}-only and double-transduced pTα KO thymocytes were analysed after day-10 or day-13 FTOC for percentage of ISPs (A) and TCRδ$^{(-)}$ TCRβ$^{(hi)}$ cells (B). TCRβ$^{(hi)}$ cells are displayed relative to non-transduced control.

Figure 2.19

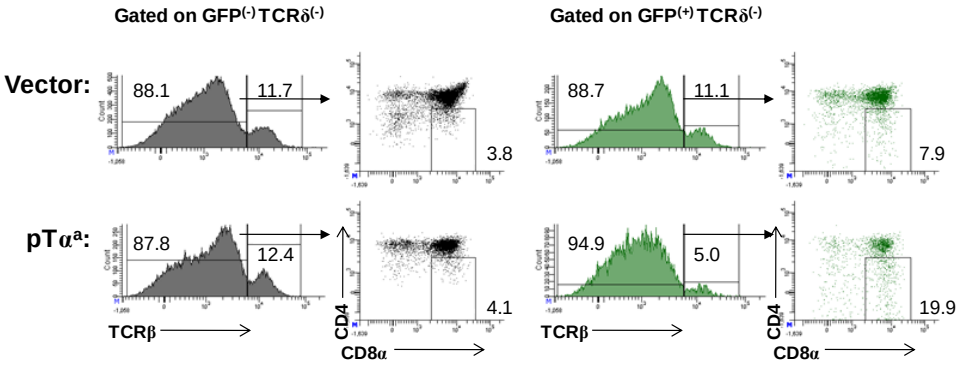

Figure 2.19 WT thymocytes transduced with pTα^a show reduced percentage of TCRβ$^{(hi)}$ cells and a greater proportion of ISPs: C57BL/6 E14 thymocytes transduced with vector-only and pTα^a were analysed for the percentage of ISPs and TCRβ$^{(hi)}$ cells, after 9 days in FTOC. Live cells were gated as shown. Numbers represent the percentage cells in each gate.

To further asses the dominance of preTCR^a, pTα^a was transduced into WT E14 thymocytes that would express normal levels of the preTCR(s), and cultured in FTOC for 9 days (Figure 2.19). Compared to the vector control, expression of pTα^a appears to reduce the percentage of TCRβ$^{(hi)}$ cells from ~11% to ~5%. Furthermore, the percentage of ISPs is increased from ~8% in the vector control to ~20% for cells expressing pTα^a (Figure 2.19). These results suggest that constitutive expression of pTα^a in a WT background leads to pTα^a acting in a dominant-negative manner. This also implies that the correct regulation of pTα^a is necessary for optimal T cell development in the thymus.

Our original hypothesis stated that preTCR^a and preTCR^b would promote the development of different lineages of αβ thymocytes. Thus, to determine whether the ISPs generated by pTα^a expression and the TCRαβ$^{(hi)}$ mature cells that developed as a result of expression of pTα^b, represented different T cell lineages; analysis of different T cell lineages was performed by

FACs. First, the ISPs that accumulated as a result of pTα^{a} expression were characterised to determine whether these were true immature thymocytes *en route* to the DP stage, or indeed, whether they represented a mature CD8$^{(+)}$ population that had been positively selected by preTCR^{a} signalling (Ito et al., 2002). In this report the authors showed that expression of a pTα transgene under control of the lck promoter on a TCRα-deficient background resulted in the development of peripheral CD8 T cells (Ito et al., 2002). These cells had low surface expression of TCRβ but appeared to be "mature" T cells as they expressed low levels of CD24 (heat stable antigen, HSA) and were able to produce IL-2 and upregulate CD69 upon stimulation with PMA and ionomycin (Ito et al., 2002). Therefore, it was possible the ISPs that developed in pTα^{a}-expressing FTOCs were actually mature CD8 T cells with very low levels of TCRαβ. Positive selection induced by pTα^{a} could occur in two ways; either CD8$^{(+)}$TCR$^{(lo)}$ thymocytes had progressed through the DP stage and had been positively selected into the CD8 lineage, or constitutive expression of pTα^{a} promoted development of CD8$^{(+)}$TCR$^{(lo)}$ thymocytes bypassing the DP stage.

CD69 is upregulated upon positive selection of DPs through TCRαβ (Anderson et al., 1994a). Therefore, CD8 T cells that had passed through the DP stage before being positively selected should express CD69 as well as TCRα. On the other hand, if preTCR^{a} signalling positively selects CD8$^{(+)}$ T cells directly, bypassing the DP stage, these cells would be unlikely to upregulate CD69 or express a rearranged TCRα chain. However, both pathways should result in downregulation of HSA (Ito et al., 2002). To this end pTα KO CD8$^{(+)}$ TCRβ$^{(lo)}$ thymocytes transduced with vector, pTα^{a} or pTα^{b} were analysed after 13-15-day FTOC for CD69, HSA and TCRα expression.

A higher surface expression of CD69 (average MFI of 959) was seen for ISPs transduced with vector compared to those expressing pTα^{a} (average MFI of 738) or pTα^{b} (average MFI of 787) (Figure 2.20). Thus, as the CD69 levels on ISPs expressing pTα^{a} were not higher than those expressing vector or pTα^{b}, it was probable that these cells had not undergone positive selection through the TCR and had not passed through the DP stage.

Figure 2.20

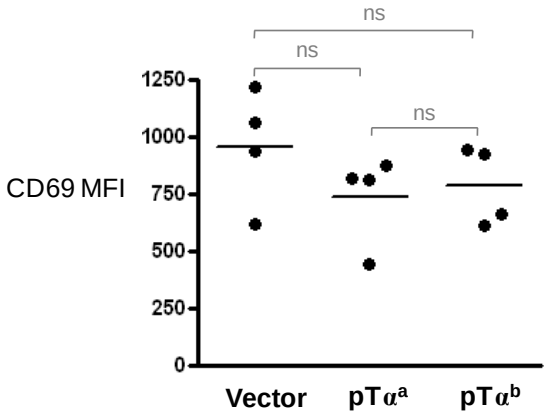

Figure 2.20 Analysis of CD69 MFI in pTα KO ISP cells transduced with pTα^{a} or pTα^{b}: Dot-plot shows ISP pTα KO thymocytes transduced with vector-only, pTα^{a}, or pTα^{b} that were analysed for CD69 expression, after 15-day FTOC. MFI for CD69 is shown. Each dot represents a single FTOC lobe. MFI is mean fluorescence intensity.

HSA is expressed at high levels on immature thymocytes and is downregulated on mature thymocytes (Kishimoto and Sprent, 1997). Three populations of CD8$^{(+)}$ thymocytes were identified by TCRβ/HSA analysis of pTα KO thymocytes transduced with vector-only, pTα^{a} or after 13-day FTOC; TCRβ$^{(lo)}$HSA$^{(hi)}$; TCRβ$^{(lo)}$HSA$^{(lo)}$; and TCRβ$^{(hi)}$HSA$^{(lo)}$ (Figure 2.21). The "true ISP" population expresses low levels of TCRβ but high levels of HSA (TCRβ$^{(lo)}$HSA$^{(hi)}$). The "true CD8$^{(+)}$ SPs" are TCRβ$^{(hi)}$HSA$^{(lo)}$, and the cells described by Ito *et al* are TCRβ$^{(lo)}$HSA$^{(lo)}$ (Ito et al., 2002). For pTα KO cells transduced with vector-only ~37% of CD8$^{(+)}$ thymocytes were TCRβ$^{(lo)}$HSA$^{(hi)}$, ~28% were TCRβ$^{(lo)}$HSA$^{(lo)}$ and 27% were TCRβ$^{(hi)}$HSA$^{(lo)}$

(Figure 2.21). An increased proportion of $CD8^{(+)}$ cells transduced with $pT\alpha^a$ $TCR\beta^{(lo)}HSA^{(hi)}$ (~45%), while ~26% were $TCR\beta^{(lo)}HSA^{(lo)}$ and ~22% were $TCR\beta^{(hi)}HSA^{(lo)}$ (Figure 2.21). Thus, although a readily detectable population of $TCR\beta^{(lo)}HSA^{(lo)}CD8^{(+)}$ cells were present in $pT\alpha^a$-expressing cultures, this was not significantly higher than for vector-only cultures. Instead the presence of $pT\alpha^a$ appears to expand the true ISP subset.

Figure 2.21

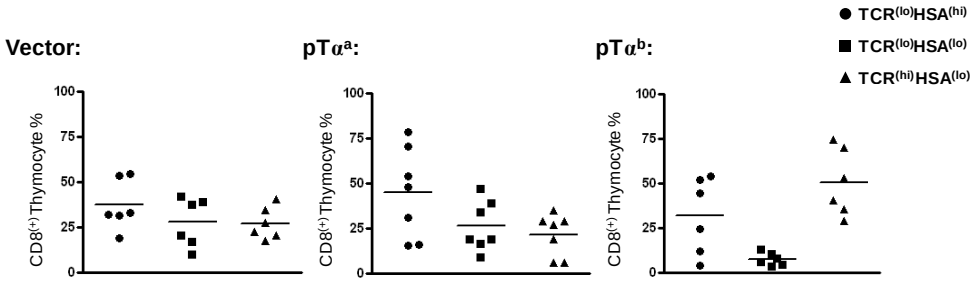

Figure 2.21 HSA and TCRβ analysis of $CD8^{(+)}$ pTα KO cells transduced with $pT\alpha^a$ or $pT\alpha^b$: Dot-plots show $CD8^{(+)}$ pTα KO thymocytes transduced with vector-alone, $pT\alpha^a$ or $pT\alpha^b$ that were analysed for HSA and TCRβ expression, after 13-day FTOC. The percentage of $GFP^{(+)}CD8^{(+)}$ thymocytes that were $TCR\beta^{(lo)}HSA^{(hi)}$ (circles), $TCR\beta^{(lo)}HSA^{(lo)}$ (squares) and $TCR\beta^{(hi)}HSA^{(lo)}$ (triangles) are shown. TCR is T cell receptor, HSA is heat stable antigen.

Figure 2.22

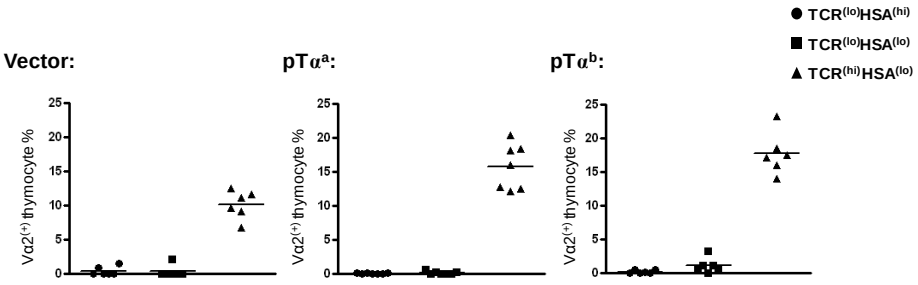

Figure 2.22 Vα2 expression analysis of $CD8^{(+)}$ pTα KO transduced thymocytes: Dot-plots showing $CD8^{(+)}$ pTα KO thymocytes transduced with vector-alone, $pT\alpha^a$ or $pT\alpha^b$ that were analysed for Vα2 expression, after 13-day FTOC. The percentages of $TCR\beta^{(lo)}HSA^{(hi)}$ cells (circles), $TCR\beta^{(lo)}HSA^{(lo)}$ cells (squares) and $TCR\beta^{(hi)}HSA^{(lo)}$ cells (triangles), that were $V\alpha2^{(+)}$ are shown. TCR is T cell receptor, HSA is heat stable antigen.

By contrast to that observed for vector-only, and pTα^{a} cultures, only ~8% of pTα^{b}-transduced CD8$^{(+)}$ T cells were TCRβ$^{(lo)}$HSA$^{(lo)}$, while ~30% were true ISPs (TCRβ$^{(lo)}$HSA$^{(hi)}$) and the majority, ~50% were mature TCRβ$^{(hi)}$HSA$^{(lo)}$ cells. To complete this analysis the three different CD8 populations described above were further assessed for expression of the Vα2 TCRα chain (Figure 2.22).

Figure 2.23

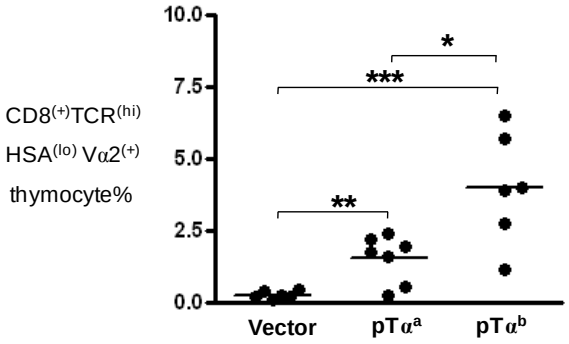

Figure 2.23 pTα^{b} promotes the development of mature CD8SP cells: Dot-plot shows the percentage of CD8SP pTα KO thymocytes transduced with vector-only, pTα^{a} or pTα^{b} from day-13 FTOCs. CD8SP cells are TCRδ$^{(-)}$ CD8$^{(+)}$ TCR$^{(lo)}$ HSA$^{(lo)}$ Vα2$^{(+)}$. * p≥0.05, ** p≥0.01 and *** p≥ .001.

These data show that ≤ 1% of all TCRβ$^{(lo)}$HSA$^{(hi)}$ or TCRβ$^{(lo)}$HSA$^{(lo)}$ CD8$^{(+)}$ cells from FTOCs of pTα KO thymocytes transduced with vector-only, pTα^{a} or pTα^{b} expressed Vα2, suggesting that these populations had not yet undergone TCRα rearrangements (Figure 2.22). This analysis also confirmed that the TCRβ$^{(hi)}$HSA$^{(lo)}$ population of cells were mature CD8$^{(+)}$ T cells that had undergone TCRα rearrangements as well as positive via TCRαβ. Importantly, the proportion of TCRβ$^{(hi)}$HSA$^{(lo)}$CD8$^{(+)}$Vα2$^{(+)}$ thymocytes from pTα^{b} FTOCs was significantly higher at 4% of total GFP$^{(+)}$ cells, compared to 0.2% of vector-only FTOCs (p≤ 0.001) and 1.5% of pTα^{a} FTOCs (p≤ 0.05 Figure 2.23). This confirmed the observation that pTα^{b} has

a superior ability to promote development of mature SP thymocytes in FTOC compared to pTα^{a}.

IL-7Rα is thought to be upregulated on thymocytes downstream of preTCR signalling (Trigueros et al., 2003). Importantly, IL-7Rα expression is extinguished at the ISP stage which is absolutely necessary for the ISP to DP transition (Yu et al., 2004). Indeed, treatment of E15 C57BL/6 thymic lobes with IL-7 arrested thymocyte development at the ISP stage (Yu et al., 2004). We therefore hypothesised that continued expression of pTα^{a} may result in the accumulation of ISP thymocytes due to prolonged expression of IL-7Rα and the IL-7 receptor. To test this we analysed the surface expression of IL-7Rα after pTα-deficient E14 thymocytes transduced with vector-only, pTα^{a} or pTα^{b} were cultured in FTOC for 15 days.

Figure 2.24

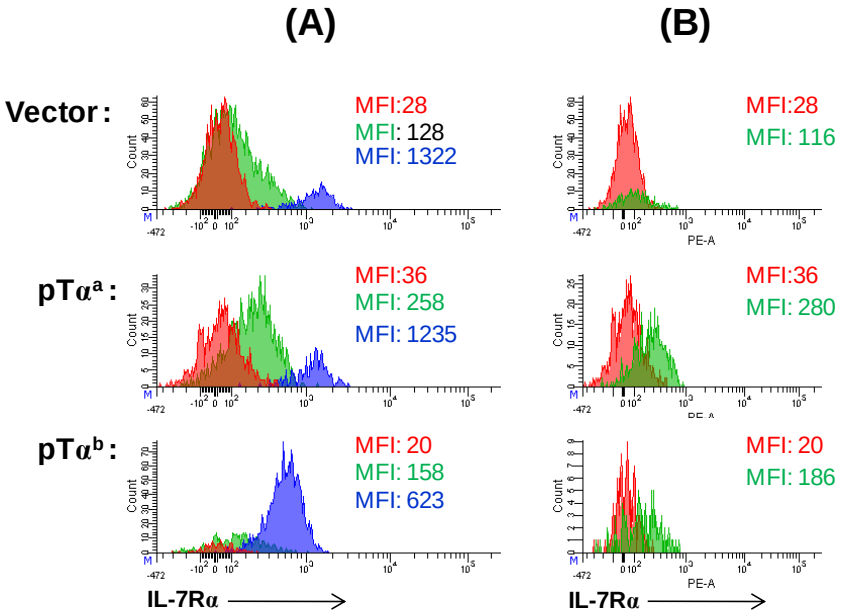

Figure 2.24 thymocytes transduced with pTα^{a} express higher levels of IL-7Rα compared with those transduced with pTα^{b}: Representative FACS plots showing pTα KO E14 thymocytes transduced with vector, pTα^{a} or pTα^{b} that were analysed for IL7-Rα (CD127) expression after 15-day FTOC. (A) Cells are TCRδ$^{(-)}$ TCRβ$^{(lo)}$ (green) or TCRβ$^{(hi)}$ (blue). The green cells represented in (B) are TCRδ$^{(-)}$ TCRβ$^{(lo)}$CD8$^{(+)}$, while the red cells in both (A) and (B) represent GFP$^{(-)}$ TCRβ$^{(lo)}$ DP cells as a negative control.

TCRβ$^{(hi)}$ cells from pTα^{a} and pTα^{b} FTOCs expressed lower levels of IL-7Rα compared with those transduced with vector alone (Figure 2.24). However, the immature thymocytes that developed as a result of preTCR^{a} signalling expressed higher levels of IL-7Rα in comparison to those transduced with pTα^{b} or vector (Figure 2.24A). This higher expression of IL-7Rα was reflected in the ISP population that developed as a result of preTCR^{a} signalling (Figure 2.24B). Therefore, this preliminary result could suggest that IL-7 signalling may regulate the developmental phenotype seen for preTCR^{a}.

2.5 Differential expression of pTα^{a} or pTα^{b} does not influence regulatory T cell development.

To further investigate whether preTCR^{a} and preTCR^{b} promoted the development of different lineages of T cells, development of regulatory T cells (T-regs) was assessed. Recently, thymic T-regs were reported to express high levels of pTα^{b} but not pTα^{a} and expression of pTα^{b} was described to be essential for the regulatory function (Campese et al., 2009). pTα KO E14 thymocytes transduced with vector-only, pTα^{a} or pTα^{b} were analysed for intracellular expression of Foxp3, a gene that marks the T-reg lineage, after 15 days in FTOC (Figure 2.25). When gated on mature CD4SP cells, ~2% of these were Foxp3$^{(+)}$ in vector-only FTOCs. Expression of pTα^{a} appeared to make no difference to the percentage of Foxp3$^{(+)}$ in the 4SP population, being 2% as well (Figure 2.2). Cultures that expressed pTα^{b}-only had a lower representation of Foxp3$^{(+)}$ cells in the CD4SP pool, being ~0.6%. At this stage the significance of this finding is unclear but it suggests that there is not a major effect of pTα^{a} or pTα^{b} on T-reg development, and certainly would not support the observations made by Campese and co-workers for a role for pTα^{b} in T-reg development.

Figure 2.25

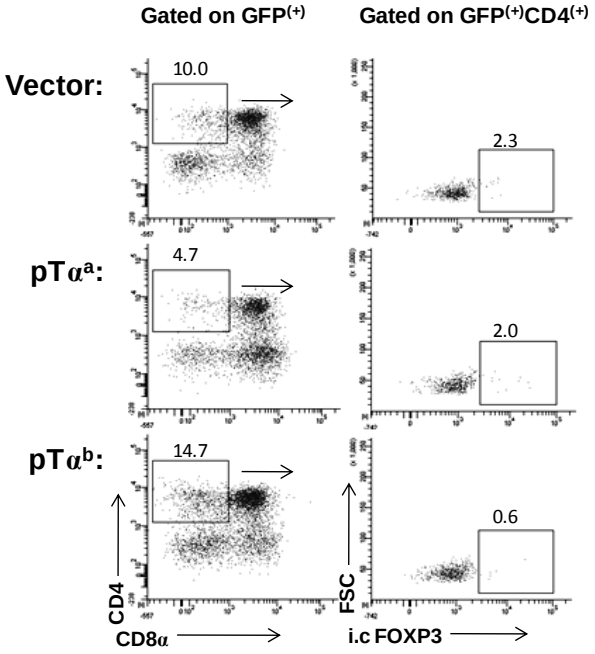

Figure 2.25 Regulatory T cell development is not influenced by expression of either pTα^a or pTα^b: Representative FACS plots (from n=3 experiments) of CD4SP pTα KO thymocytes transduced with vector-alone, pTα^a or pTα^b that were analysed for expression of intracellular (i.c.) Foxp3, after 15-day FTOC. Cells were gated on GFP$^{(+)}$ then analysed as described. Numbers represent percentages in each gate.

2.6 Summary.

In summary, the work presented in this chapter suggests that pTα^a and pTα^b drive qualitatively different T cell development; pTα^a appears to promote development of immature ISP cells, with continued expression of pTα^a detrimental to continued development. By contrast, pTα^b promotes efficient development of mature cells. Evidence suggests that pTα^a may promote sustained expression of the IL-7Rα chain which prevents normal developmental progression. Finally, preliminary experiments do not support the idea that pTα^b is required for T-reg development.

Chapter 3

Investigating oligomerization as a mechanism for signal initiation by the preTCR

3.1 Introduction

Signalling through the preTCR has been shown as weak when compared to the signal delivered by the γδ TCR. Indeed, this difference in signal strength has been proposed to determine αβ versus γδ lineage commitment at the DN stage of thymic ontogeny (Haks et al., 2005; Hayes et al., 2005). The preTCR is thought to signal ligand-independently (Haks et al., 2003; Irving et al., 1998). However, the mechanism by which this occurs is unclear. Among the possibilities are a low signalling threshold in DN thymocytes, which makes the cells very sensitive to signals through TCR complexes when compared to DP and SP cells (Haks et al., 2003). By contrast, a number of groups have suggested that ligand-independent signalling from the preTCR is due to intrinsic properties of the pTα chain (Borowski et al., 2004; Yamasaki et al., 2006). Specifically, the currently accepted idea is that pTα promotes signalling by inducing oligomerization of preTCR complexes (Yamasaki et al., 2006).

3.2 Oligomerization as a mechanism for ligand-independent signalling through the preTCR.

In a recent report by Yamasaki and co-workers (Yamasaki et al., 2006) it was proposed that four charged amino acids in the extracellular Ig-loop of pTα (in this study only $pT\alpha^a$ was considered) were shown to mediate oligomerization of pTα chains, and by extrapolation, preTCR complexes on

the surface of DN cells. This oligomerization was proposed as the mechanism by which signalling from the preTCR was initiated, presumably by clustering of intracellular signalling molecules. The four amino acids involved were identified as aspartic acid at position 22 (from the beginning of the extracellular domain - D22), arginine at position 24 (R24), arginine at position 102 (R102) and arginine at position 117 (R117) (Figure 3.1A). Mutation of any one of these residues to a non-charged amino acid, such as alanine was shown to abolish the oligomerization of the preTCR, as determined by the reduced ability of EPO-receptor-fused mutant pTα chains to drive proliferation of the IL-3-dependent BAF3 cell line.

Figure 3.1

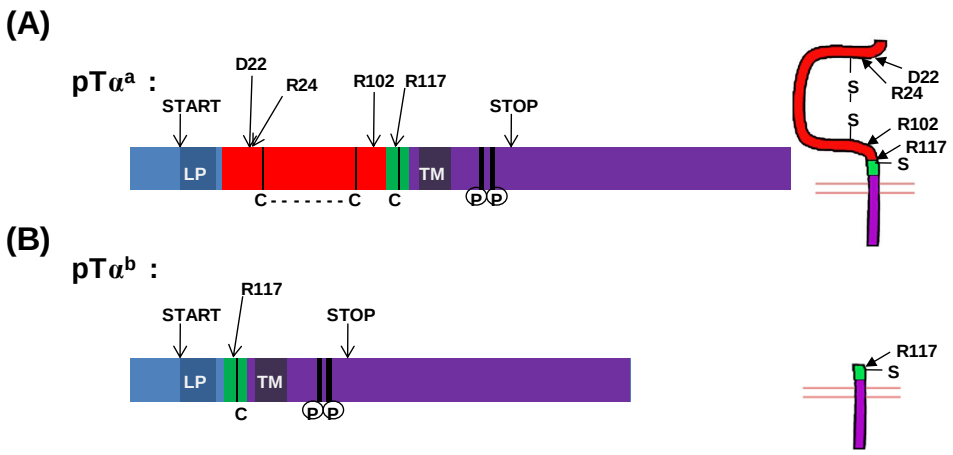

Figure 3.1 Location of the "oligomerization residues" in pTα^a and pTα^b. Schematic representation of pTα^a (A) and pTα^b (B) with exons coloured as blue for exon-1, red for exon-2, green for exon-3 and purple for exon-4. The location of the four amino acids (D22, R24, R102 and R117) implicated in pTα oligomerization are shown. "C" indicates cysteine residues that form disulphide bonds in the mature protein, "LP" indicates leader peptide, "TM" indicates transmembrane domain, and (P) indicates proposed phosphorylation sites. The positions of start and stop codons are shown.

The authors also showed that mutant pTα chains could not drive development when expressed in pTα KO thymocytes in bone-marrow chimeras with RAG-2 KO irradiated recipients. However, in this study the

authors did not consider pTα^{b}. pTα^{b} lacks the extracellular Ig-loop of pTα and therefore three out of the four charged amino acid residues (Figure 1.3B). Nonetheless, this receptor is functional as we have demonstrated in the previous chapter, being signalling-competent and able to rescue αβ T cell development in a pTα KO background.

3.3 Generation of "mutant" pTα constructs that lack specific amino acid residues.

To investigate the role of the charged amino acid residues in the extracellular Ig-loop of pTα, various "mutant" pTα constructs were generated. First, a construct with a single amino acid substitution was generated in which R24 in exon-2 of pTα^{a} was mutated to the non-charged amino acid alanine (R24A Figure 3.2). This mutation, had been described in the Yamasaki report as lacking the capacity to promote oligomerization and to signal to drive β-selection (Yamasaki et al., 2006).

Figure 3.2

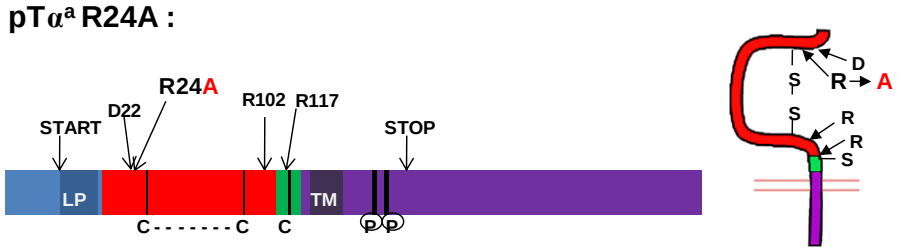

Figure 3.2 pTα^{a} R24A mutant. Schematic representation of pTα^{a}-R24A mutant with exons coloured as blue for exon-1, red for exon-2, green for exon-3 and purple for exon-4. The single amino acid substitution at position 24 within the extracellular domain of pTα^{a} is shown. This mutation replaces arginine (R) with a non-charged amino acid alanine (A) and has been described to abolish the oligomerization capacity of pTα. The location of the other three amino acids (D22, R102 and R117) implicated in pTα oligomerization are shown. "C" indicates cysteine residues that form disulphide bonds in the mature protein, "LP" indicates leader peptide, "TM" indicates transmembrane domain, and (P) indicates proposed phosphorylation sites. The positions of start and stop codons are shown

Site directed mutagenesis (SDM) was employed to generate the R24A mutant. The protocol followed is shown in Figure 3.3; the pBlunt-pTα^{a} plasmid was used as a template for the SDM PCR as it is smaller than pLZ-pTα^{a} and therefore easier to manipulate. Forward and reverse primers were designed that were complimentary to the top and bottom strand of the DNA sequence of pTα. The primers were designed with the mutation at the centre of the sequence, with 10bp of homology either side. The (AGG) codon to be mutated is situated 238bp from the start of the pTα^{a} construct and was replaced by changing two bases; AG to GC, to code for alanine (GCG).

Figure 3.3

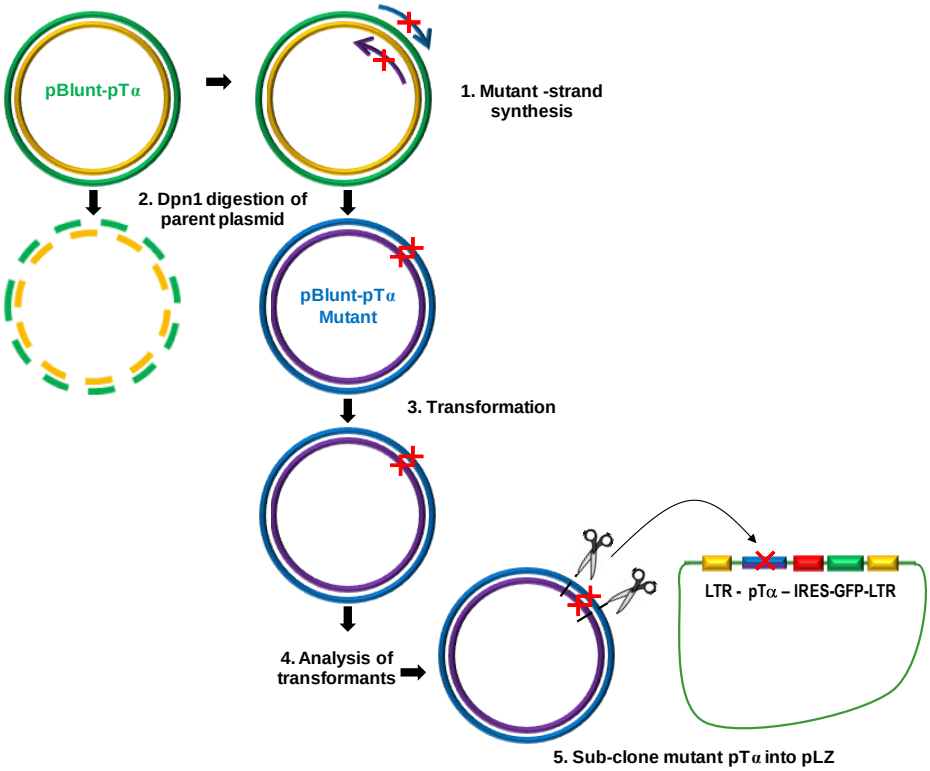

Figure 3.3 Schematic of the method for Site Directed Mutagenesis. Amino acid substitutions were performed on pBlunt-pTα plasmids using homologous primers that contained the desired mutation. Parental plasmid was subsequently removed from the PCR reaction by Dpn1 digestion and the mutant plasmid transformed into *E.coli* for nick repair. Mutant clones were characterised by restriction digest and then sub-cloned into pLZ. The desired mutation is denoted by a red X.

In brief, a thermo-cycler was used to denature the plasmid, anneal the two primers and extend from the primers using a high-fidelity polymerase. The mutations were created in the daughter plasmid and the parent plasmid was digested away using Dpn1. Dpn1 digests methylated DNA specifically and therefore only digests the parent plasmid. Dpn1 digested PCR products for pTα^a R24A are shown in Figure 3.4. Two different concentrations of parent plasmid were used for the PCR reaction; 10ng and 20ng of DNA and a reaction was set up using parent plasmid but no polymerase (no enz) as a control (Figure 3.4). The mutant plasmid was then transformed into competent *E.coli* for nick repair and transformants were selected and characterised (Figure 3.5).

Figure 3.4

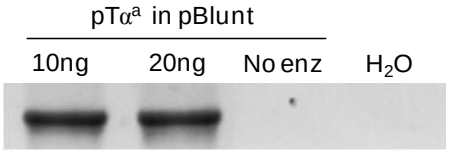

Figure 3.4 pTα^a-R24A PCR: 10ng and 20ng of pBlunt-pTα^a plasmid was used as a template for pTα^a-R24A PCR. PCR products were Dpn1 digested before gel electrophoresis. No enz stands for no enzyme.

Changing the coding sequence from AGG to GCG inserted an Hha1 site at position 238 in the pTα^a sequence. Therefore, mutant plasmids were identified by Hha1 digestion. Hha1 cuts the pBlunt sequence 26 times but only once in the WT pTα^a sequence producing two large fragments of 812bp and 620bp in length (Figure 3.5A). Insertion of the Hha1 site in the pTα^a-R24A mutant construct cleaves the larger of the two fragments producing a 473bp and a 339bp fragment (Figure 3.5B). Figure 3.6 shows a Hha1 digest on six different pTα^a-R24A clones; all six clones have the

mutation inserted resulting in the loss of the 812bp band seen in the parent, and gain of a 473bp and a 339bp band marked in red.

Figure 3.5

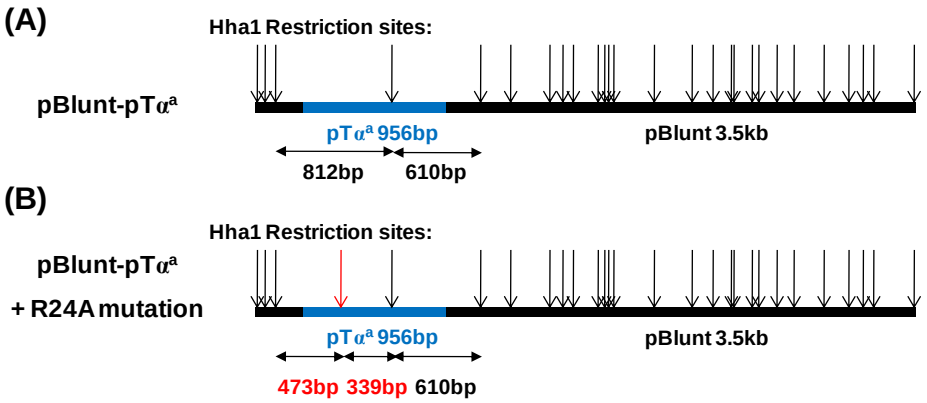

Figure 3.5 Hha1 restriction maps for pBlunt-pTα^a and pBlunt-pTα^a-R24A plasmids. Hha1 restriction maps for (A) pBlunt-pTα^a and (B) pBlunt-pTα^a-R24A plasmids are shown. The R24A mutation generates an Hha1 site within the pTα^a sequence which results in the loss of a 812bp Hha1 fragment present in the parent plasmid. This fragment is replaced by two fragments of 473bp and 339bp in length (shown in red) in pTα^a-R24A.

Figure 3.6

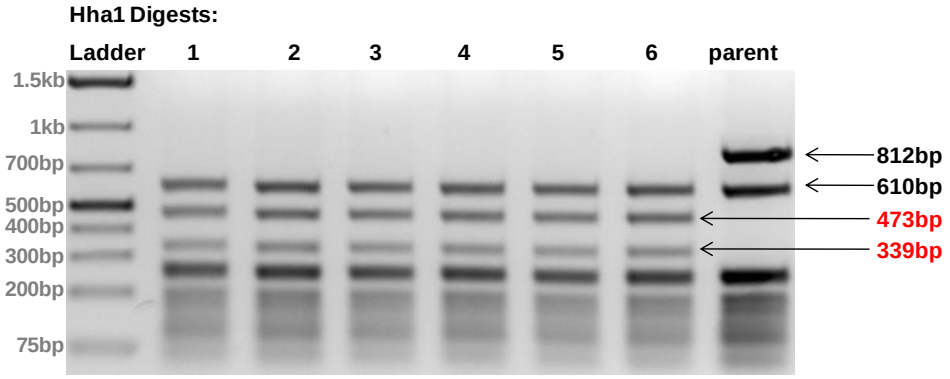

Figure 3.6 Hha1 digests for pBlunt-pTα^a-R24A clones. An agarose gel showing Hha1 restriction digests of six pBlunt-pTα^a-R24A clones (lanes 1-6) and the pBlunt-pTα^a parent plasmid (parent). The R24A mutation generates an Hha1 site within the pTα^a sequence which results in the loss of a 812bp Hha1 fragment present in the parent plasmid. This fragment is replaced by two fragments of 473bp and 339bp in length (shown in red) in pTα^a-R24A.

The pTα^{a} R24A cassette was then sub-cloned out of the pBlunt backbone by BamH1 and Xho1 digestion and ligation into the pLZ plasmid (Figure 3.3). The pLZ-pTα^{a}-R24A transformants were then characterised by digestion with BamH1 and Xho1 for release of the pTα^{a} R24A cassette, generating a 1032bp band (Figure 3.7).

Figure 3.7

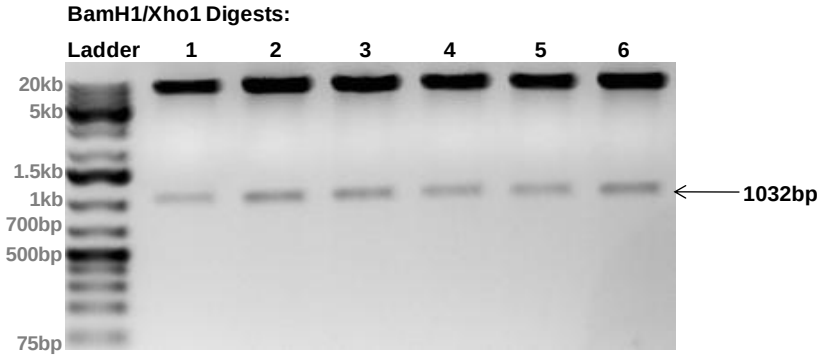

Figure 3.7 BamH1 and Xho1 digests on pLZ-pTα^{a}-R24A transformants. Agarose gel showing BamH1 and Xho1 double-digests on six pLZ-pTα^{a}-R24A transformants (lanes 1-6) which resulted in the release of the pTα^{a}-R24A cassette (1032bp in length).

The pLZ-pTα^{a}-R24A plasmid was transfected into the phoenix ecotropic packaging cell line, and virus harvested. pTα^{a}-R24A virus used in parallel with WT-pTα^{a} and pTα^{b} virus were used to transduce pTα-deficient E14 thymocytes in FTOC, to determine whether the mutation perturbed the function of the preTCR as described by Yamasaki *et al* (Yamasaki et al., 2006). After 8 days in FTOC thymocytes were analysed for preTCR expression by analysis of surface TCRβ on GFP$^{(+)}$TCRδ$^{(-)}$ thymocytes (Figure 3.8). As described in the previous chapter, pTα-deficient thymocytes do not express a preTCR and therefore have low TCRβ surface expression (MFI of ~160). Expression of either pTα^{a} or pTα^{b} in pTα KO thymocytes increases the levels of TCRβ on the surface as a result of the

formation of the preTCR (MFI of 285 and 516 units, respectively). Importantly, pTα^{a}-R24A expression also resulted in increased TCRβ surface levels (MFI of 514 in Figure 3.8). This shows that the R24A mutation does not abolish the ability of the pTα^{a} chain to pair with TCRβ. In fact, pTα^{a}-R24A preTCR surface levels were comparable to those of preTCR^{b} and 1.8 fold higher than those of preTCR^{a}, suggesting that disruption of the ability of the preTCR to oligomerize may lead to higher preTCR surface levels.

Although the pTα^{a}-R24A mutant was able to form a preTCR it may not have been signalling-competent. Thus, to investigate, the percentage of γδ cells generated in pTα^{a}-R24A-expressing FTOCs was determined. As described in chapter 2 of the results, pTα-deficient mice have a large percentage γδ cells in the thymus due to the absence of the preTCR that drives αβ T cell development. Signalling through preTCR^{a} and/or preTCR^{b} promotes αβ T cell development resulting in a huge reduction of the percentage of γδ cells in the thymus. Results from three different experiments, two at FTOC day-8 and one at FTOC day-15 are shown in Figure 3.9. The percentage of γδ cells in transduced (GFP$^{(+)}$) thymocytes (hatched bars) in pTα^{a} or pTα^{b} FTOCs is ~10% which represents a large decrease compared to the vector-only control (~40%) (Figure 3.9). Importantly, FTOCs transduced with pTα^{a}-R24A showed a similar reduction in the percentage of γδ cells to ~12.5%. These results show that the pTα^{a}-R24A mutant was able to form a signal competent preTCR on the surface of pTα KO thymocytes in FTOC; promoting T cell development away from the γδ T cell lineage.

Figure 3.8

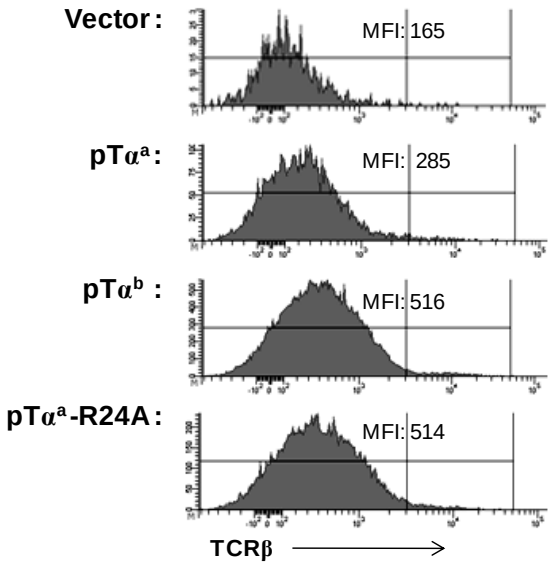

Figure 3.8 pTα^a-R24A appears to form a preTCR with TCRβ. Representative histograms (from n=2 experiments) of E14 pTα KO thymocytes transduced with vector alone, pTα^a, pTα^b or pTα^a-R24A and analysed after 8 days in FTOC. Cells are GFP$^{(+)}$ TCRδ$^{(-)}$ and gates shown exclude TCRβ$^{(hi)}$ cells. MFI for TCRβ$^{(lo)}$ cells is shown.

Figure 3.9

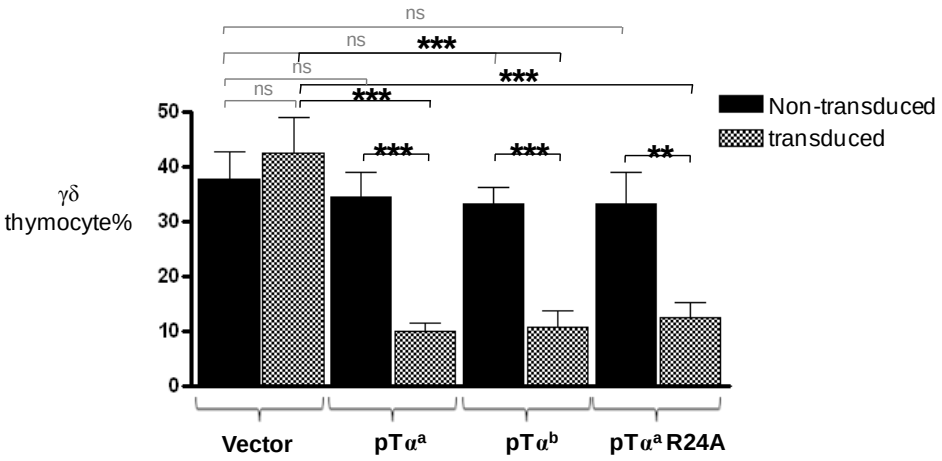

Figure 3.9 pTα^a-R24A mutant forms a signal competent preTCR capable of reducing the percentage of γδ cells in FTOC. Bar graph shows Bar chart (from n=3 experiments) of pTα KO E14 thymocytes transduced with vector alone, pTα^a, pTα^b or pTα^a-R24A and cultured for 8-15 days in FTOC. Live cells were analysed for TCRδ and CD3ε. The percentage of TCRδ$^{(+)}$ CD3ε$^{(+)}$ cells are shown for non-transduced thymocytes (black bars) and transduced thymocytes (hatched bars), ns is not significant, ** p≤ 0.01 *** p≤ 0.001.

3.4 Investigating the oligomerization requirements for signalling through pTα^{b}.

Despite the ability of pTα^{b} to signal in the absence of the extracellular domain of pTα, this isoform does possess one out of the four charged amino acid residues deemed necessary for oligomerization and therefore signalling through the preTCR (R117 Figure 3.10). In order to determine the role of this amino acid in signalling through preTCR^{b}, a pTα^{b} construct was generated in which the charged amino acid residue R117 was mutated to alanine (pTα^{b}-R117A Figure 3.10). SDM to generate pTα^{b}-R117A was performed following the same protocol as that described for pTα^{a}-R24A. The R117 AGG codon at position 197 in the pTα^{b} construct was mutated to alanine; GCG.

Figure 3.10

pTα^{b}-R117A :

Figure 3.10 pTα^{b}-R117A mutant. Schematic representation of pTα^{b}-R117A mutant with exons coloured as blue for exon-1, green for exon-3 and purple for exon-4. The single amino acid substitution at position 197 within the short extracellular domain of pTα^{b} is shown. This mutation replaces arginine (R) with a non-charged amino acid alanine (A) and has been described to abolish the oligomerization capacity of pTα. "C" indicates the cysteine residue that forms a disulphide bond with TCRβ, "LP" indicates leader peptide, "TM" indicates transmembrane domain, and (P) indicates proposed phosphorylation sites. The positions of start and stop codons are shown

Figure 3.11A shows the amplified product from the pTα^{b}-R117A PCR. The mutant plasmids were characterised by AccII digests. The pBlunt plasmid contains fifteen AccII sites but none are found in pTα^{b}. Therefore, digesting the parent plasmid with AccII produces one large fragment of 1219bp

(Figure 3.11B). The pTα^{b}-R117A mutation inserts an AccII site at position 197 of the pTα^{b} construct and therefore reduces the 1219bp fragment to two smaller fragments of 279 and 940bp in size (Figure 3.11C).

Figure 3.11

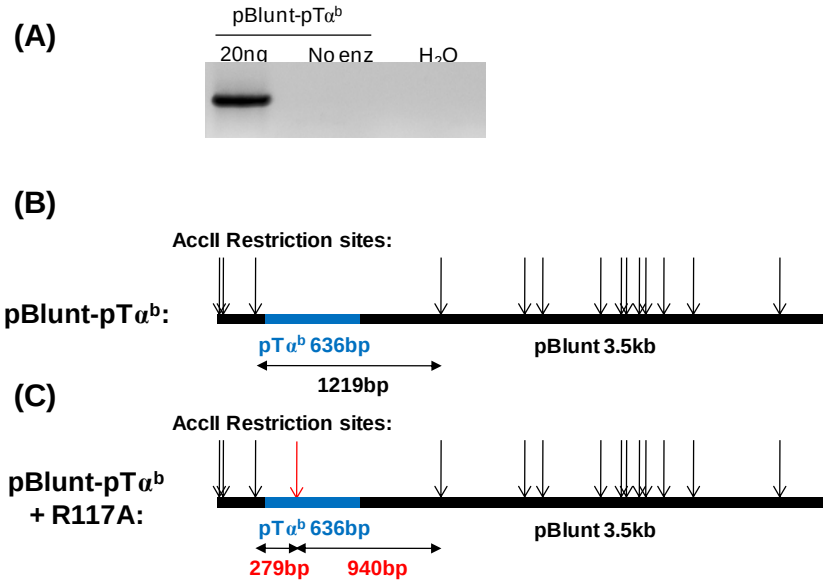

Figure 3.11 pTα^{b}-R117A PCR and AccII restriction maps for pBlunt-pTα^{b} and pBlunt-pTα^{b}-R117A. (A) 20ng of pBlunt-pTα^{b} plasmid was used as a template for pTα^{b}-R117A PCR. PCR products were Dpn1 digested before gel electrophoresis. No enz stands for no enzyme. AccII restriction sites for (B) pBlunt-pTα^{b} and (C) pBlunt-pTα^{b}-R117A are shown. The R117A mutation generates an AccII restriction site within pTα^{b} which results in the loss of a 1219bp AccII fragment present in the parent plasmid. This fragment is replaced by two fragments of 279bp and 940bp (shown in red) in pBlunt-pTα^{b}-R117A.

Figure 3.12 shows the AccII digests of five pTα^{b}-R117A clones; only the first three contain the desired mutation, having lost the 1219bp fragment and replaced it with a 279bp and a 940bp fragment. pTα^{b}-R117A was sub-cloned by BamH1/Xho1 digestion into pLZ. Figure 3.13 shows the BamH1/Xho1 digestion of five pLZ-pTα^{b}-R117A clones each with the correct pTα^{b}-R117A band (712bp band). pLZ-pTα^{b}-R117A pLZ was sequenced and then transfected into the phoenix ecotropic packaging cell line for production or retroviral vectors for expression in FTOC. The results

obtained from this construct will be described after the next section, which describes the generation of the final mutated version of pTα^{a}.

Figure 3.12

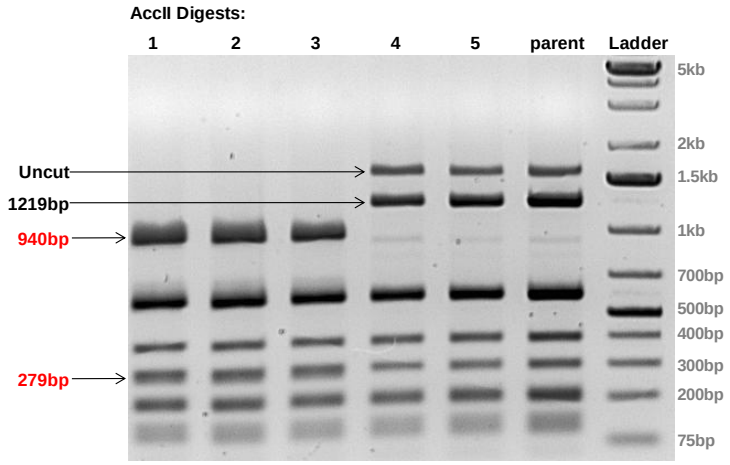

Figure 3.12 AccII restriction digests for pBlunt-pTα^{b}-R117A clones. An agarose gel showing AccII digests for five pBlunt-pTα^{b}-R117A clones (lanes 1-5) and the parent pBlunt-pTα^{b} plasmid (parent). The R117A mutation generates an AccII restriction site within pTα^{b} which results in the loss of a 1219bp AccII fragment present in the parent plasmid. This fragment is replaced by two fragments of 279bp and 940bp (shown in red) in pBlunt-pTα^{b}-R117A. Only clones 1-3 appear to have the desired mutation.

Figure 3.13

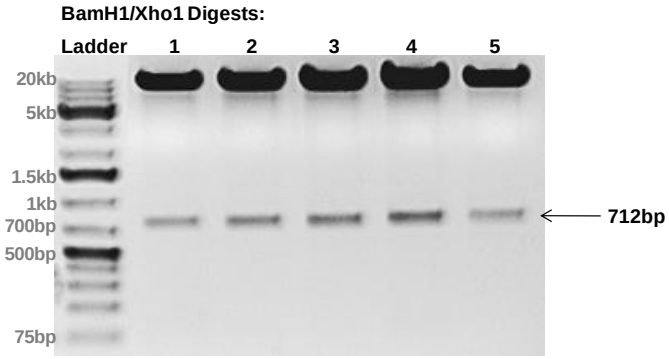

Figure 3.13 BamH1 and Xho1 digests of pLZ-pTα^{b}-R117A clones. An Agarose gel showing the BamH1/Xho1 digests of five pLZ-pTα^{b}-R117A clones (lanes 1-5) which releases the pTα^{b}-R117A cassette (712bp).

3.5 Generation of a mutated pTα^{a} construct that contains only the pTα^{b}-associated R117 oligomerization residue.

pTα^{b} possesses only one of the four "oligomerization" residues present in pTα^{a}. Thus, it could be argued that pTα^{a} would have a superior ability to oligomerize than pTα^{b}. Oligomerization has not only been proposed as a mechanism of preTCR signal initiation, but also has been suggested to induce rapid endocytosis and degradation of the preTCR. Thus the different surface levels of preTCR^{a} and preTCR^{b} that are described in chapter two, may be a result of the degree to which pTα can oligomerize. As surface levels of the preTCR may also influence preTCR signal strength, oligomerization may have a quantitative effect on developmental outcome. Thus, to test this hypothesis a second pTα^{a} mutant was generated where D22, R24 and R102 were mutated to alanine to create a construct that mirrored pTα^{b} in its capacity to oligomerize (Figure 3.14).

Figure 3.14

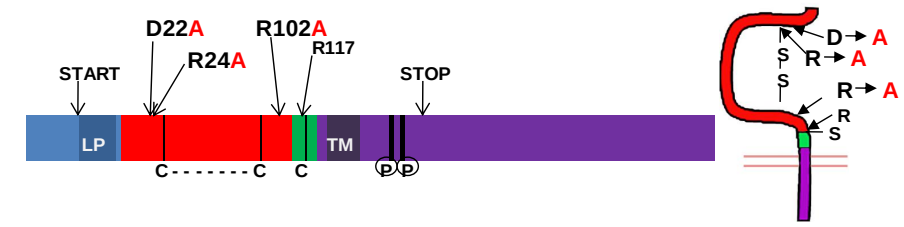

Figure 3.14 pTα^{a} DRRA mutant. Schematic representation of pTα^{a}-DRRA mutant with exons coloured as blue for exon-1, red for exon-2, green for exon-3 and purple for exon-4. The three amino acid substitutions - D to A at position 22, R to A at position 24 and R to A at position 102, within the extracellular domain of pTα^{a} are shown. The location of the fourth amino acids (R117) implicated in pTα oligomerization is also shown. "C" indicates cysteine residues that form disulphide bonds in the mature protein, "LP" indicates leader peptide, "TM" indicates transmembrane domain, and (P) indicates proposed phosphorylation sites. The positions of start and stop codons are shown.

This construct, pTα^a-DRRA, had to be generated by two SDM steps. The first step was to introduce the D22 and R24 mutations into pTα^a by a single mutagenesis. This used primers that contained a single base change from A to C to change the aspartic acid at position 22 (GAT) to GCT (alanine) and two base changes to mutate the arginine at position 24 (AGG) to GCG (alanine). As with the previously described R24A construct pBlunt-pTα^a plasmid was used as a template. Figure 3.15A shows the pTα^a-D22R24A PCR, while Figure 3.15B shows analysis of the pBlunt-pTα^a-D22R24A plasmids by Hha1 digest. As with pTα^a-R24A the desired mutation was identified by loss of an 812bp fragment to give two fragments at 473bp and 339bp. Figure 3.16B shows the Hha1 digests of six different clones each containing the D22R24A mutation. The pTα^a-D22R24A mutant plasmid was then used as a template for the second SDM mutagenesis.

Figure 3.15

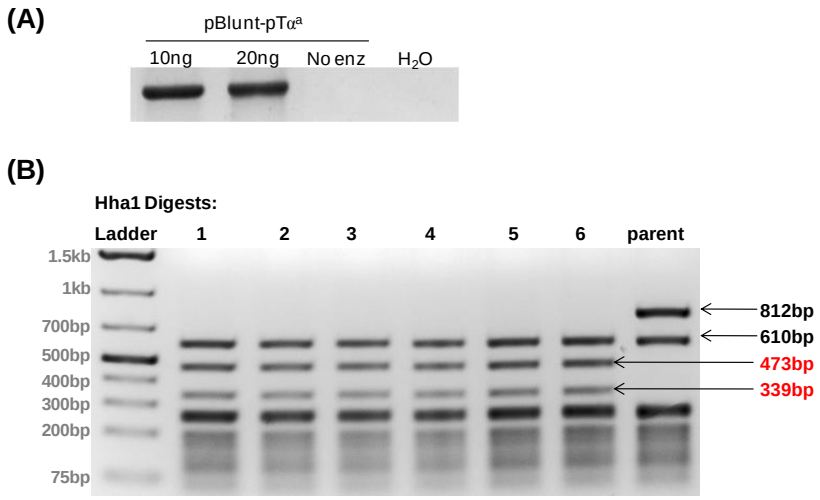

Figure 3.15 pTα^a-D22R24A PCR and Hha1 digests of pBlunt-pTα^a-D22R24A clones. (A) 10ng and 20ng of pTα^a-pBlunt plasmid was used for the pTα^a-D22R24A PCR. PCR products were digested with Dpn1 and "no enz" refers to a control PCR reaction in which there was polymerase. (B) Hha1 digests of six pBlunt-pTα^a-D22R24A clones (lanes 1-6) and pBlunt-pTα^a parent plasmid (parent). The R24A mutation generates an Hha1 site within the pTα^a sequence which results in loss of a 812bp fragment present in the parent plasmid. This fragment is replaced by two fragments of 473bp and 339bp (shown in red) in pTα^a-D22R24A.

The second mutagenesis step used primers that contained a CG to GC base change to mutate the arginine residue (CGG) at position 102 to alanine (GCG). Figure 3.16 shows the R102A PCR while transformants were characterised by AccII restriction digest. Figure 3.17 shows a restriction map of AccII sites in the parent and mutated constructs, showing cleavage of a 1548bp fragment to produce 994bp and 554bp fragments if mutagenesis was successful.

Figure 3.16

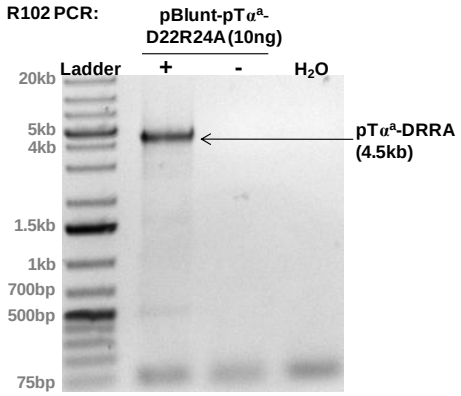

Figure 3.16 pTα^a-R102 PCR. 10ng of pBlunt-pTα^a-D22R24A plasmid was used as a template for the pTα^a-R102 PCR to generate pTα^a-DRRA (4.5kb). PCR products were digested with Dpn1. The (+) refers to the reaction with polymerase, while (-) is without.

The AccII digest of five pTα^a-DRRA clones is shown in Figure 3.18; all five have the desired mutation, having lost a 1548bp fragment present in the parent and gained the smaller 994bp and 554bp fragments. pTα^a-DRRA was then sub-cloned into pLZ and tested by BamH1/Xho1 digests (Figure 3.19). The pLZ-pTα^a-DRRA plasmids were then sequenced and subsequently transfected into phoenix cells to generate virus for retroviral transduction of pTα KO E14 thymocytes in FTOC.

Figure 3.17

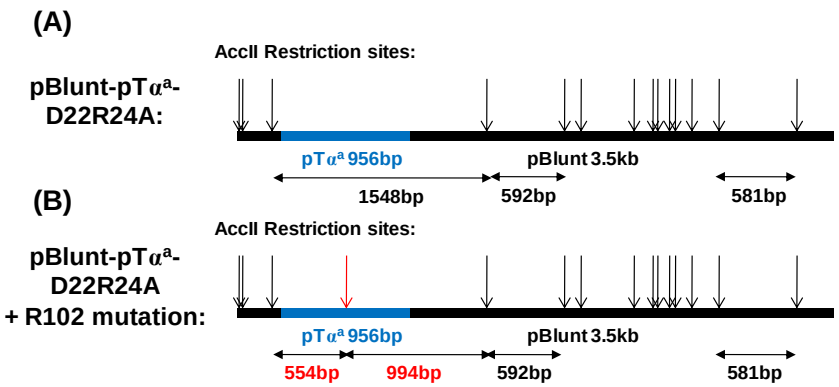

Figure 3.17 AccII restriction map for pBlunt-pTα^a-D22R24A and pBlunt-pTα^a-DRRA plasmids. AccII restriction sites for (A) pBlunt-pTα^a-D22R24A and (B) pBlunt-pTα^a-DRRA are shown. The R102 mutation generates an AccII site which results in loss of a 1548bp fragment present in the parent plasmid (pBlunt-pTα^a-D22R24A). This fragment is replaced by two fragments of 554bp and 994bp in pBlunt-pTα^a-DRRA (shown in red).

Figure 3.18

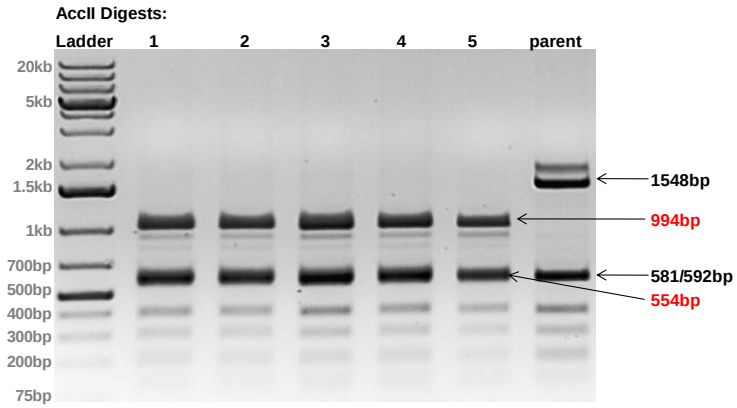

Figure 3.18: AccII digests of pBlunt-pTα^a-DRRA plasmids. An agarose gel showing AccII digests for five pBlunt-pTα^a-DRRA plasmids (lanes 1-5) and the parent plasmid AccII digests of pBlunt-pTα^a-D22R24A (parent). The R102 mutation generates an AccII site which results in loss of a 1548bp fragment present in the parent plasmid. This fragment is replaced by two fragments of 554bp and 994bp in pBlunt-pTα^a-DRRA (shown in red).

Figure 3.19

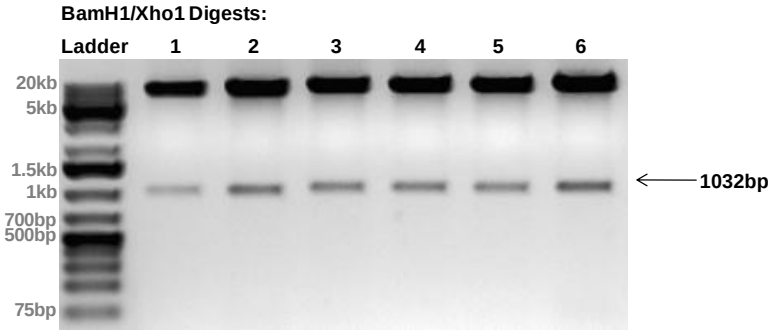

Figure 3.19 BamH1/Xho1 digests of pLZ-pTα^{a}-DRRA clones. An Agarose gel showing the BamH1/Xho1 digests of six pLZ-pTα^{b}-R117A clones (lanes 1-6) which releases the pTα^{a}-DRRA cassette (1032bp).

3.6 pTα^{b}-R117A and pTα^{a}-DRRA form signal competent preTCR complexes.

FTOC experiments were set up with pTα^{b}-R117A and pTα^{a}-DRRA constructs transduced into pTα KO E14 thymocytes to compare the function of these mutant pTα alleles with pTα^{a} and pTα^{b}. First, the ability of the mutant pTα chains to form a preTCR was determined by analysis of surface TCRβ expression. As described previously, pTα KO DN cells have very low TCRβ surface levels. Expression of pTα^{a} and pTα^{b} increases the surface expression of TCRβ from an MFI of ~200 units seen for vector-only, to ~400 units for preTCR^{a} and ~500 units for preTCR^{b} (Figure 3.20).

Importantly, pTα^{b}-R117A and pTα^{a}-DRRA expression also resulted in a significant increase in TCRβ surface levels when compared to vector-only cells; to 590 units and 605 units, respectively ($p \leq 0.001$, Figure 3.20). In addition, these levels of TCRβ were similar to those seen with pTα^{b}, but significantly higher than those of pTα^{a} ($p \leq 0.01$, Figure 3.20). Thus, as seen with the pTα^{a}-R24A allele, mutation of oligomerization residues in pTα^{a}

promotes a higher surface expression of the preTCR (as judged by TCRβ surface expression).

Figure 3.20

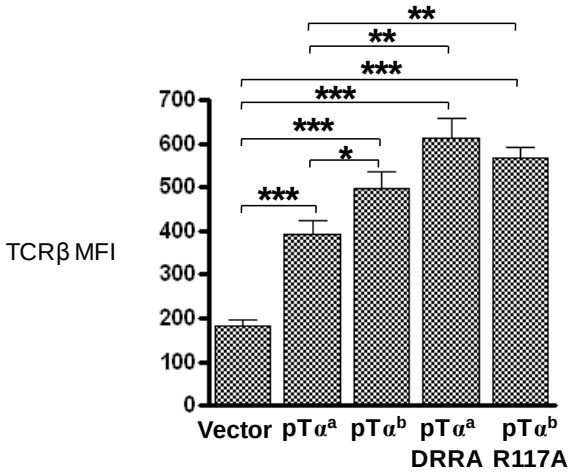

Figure 3.20 pTα^a-DRRA and pTα^b-R117A promote surface expression of TCRβ comparable to that seen with pTα^b. Bar chart showing (from n=5 experiments) E14 pTα KO thymocytes transduced with vector-only, pTα^a, pTα^b, pTα^a-DRRA or pTα^b-R117A that were analysed after 8-10-day FTOC, for TCRβ expression. Cells are GFP$^{(+)}$TCRδ$^{(-)}$TCRβ$^{(lo)}$ and the MFI for TCRβ is shown. MFI is mean fluorescence intensity. * p≤ 0.05 ** p≤ 0.01 *** p≤ 0.001

The signalling capabilities of pTα^b-R117A and pTα^a-DRRA were determined by analysis of the percentage of γδ cells in FTOC. Figure 3.21 shows data from seven different FTOCs analysed from day-8 to day-15 for percentage of γδ cells. On average ~30-35% of pTα KO untransduced cells, shown in black, developed as γδ cells, although this number varied slightly from culture to culture (Figure 3.21). Approximately 40% of GFP$^{(+)}$ pLZ-transduced cells developed as γδ cells. As described previously, expression of preTCR^a or preTCR^b reduced the percentage of γδ cells to ~10-12%. Expression of the mutant alleles of pTα, pTα^{b-}R117A and pTα^a-DRRA, also resulted in a significant reduction in γδ cell percentage to 9-11% (p≤ 0.001-Figure 3.21). Therefore, both pTα^a-DRRA and pTα^b-R117A formed signalling-competent preTCRs capable of rescuing αβ T cell development in

a pTα KO background, as shown by the reduction of γδ cells in FTOC. This provides strong evidence that oligomerization of the preTCR is not required for signal initiation at the β-selection checkpoint.

Figure 3.21

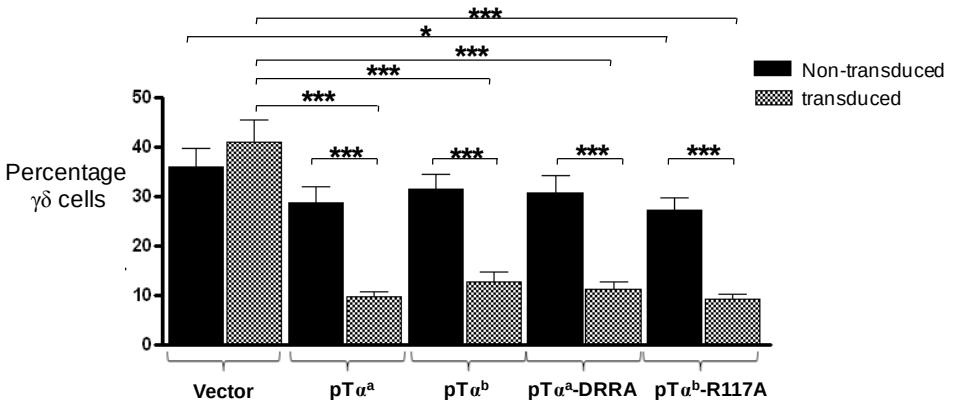

Figure 3.21 pTα^a-DRRA and pTα^b-R117A form signalling-competent preTCRs. Bar chart (from n=7 experiments) of pTα KO E14 thymocytes transduced with vector alone, pTα^a, pTα^b, pTα^a-DRRA or pTα^b-R117A and cultured for 8-15 days in FTOC. Live cells were analysed for TCRδ and CD3ε. The percentage of TCRδ$^{(+)}$ CD3ε$^{(+)}$ cells are shown for untransduced thymocytes (black bars) and transduced thymocytes (hatched bars).* p≤ 0.05 and *** p≤ 0.001.

3.7 pTα^a-DRRA and pTα^b-R117A promote qualitatively similar development to pTα^b.

The previous result clearly indicates that pTα^a-DRRA and pTα^b-R117A can form signalling competent preTCRs. To further investigate, the characteristics of αβ T cell development was assessed. Because the most striking difference between the phenotype of pTα^a and pTα^b was seen in the percentage of mature TCRβ$^{(hi)}$ cells and ISPs that developed in 15-day FTOC, analysis of pTα^a-DRRA and pTα^b-R117A was focused on these populations. As described in chapter two, pTα^a expression in pTα KO thymocytes promoted the accumulation of ISPs resulting in a significantly higher percentage (~37%) to that seen in vector-only or pTα^b-expressing cultures (both ~10% p≤ 0.001) (Figure 3.22). Importantly, the percentage of

ISP thymocytes that developed as a result of pTα^{a}-DRRA expression was only ~16%, significantly lower than pTα^{a} ($p \leq 0.001$) (Figure 3.22). Indeed, this percentage of ISPs was not significantly different to that promoted by pTα^{b} (Figure 3.22). Thus, mutating the three "oligomerization" residues unique to pTα^{a} (i.e. absent in pTα^{b}) generates a pTα allele that behaves similarly to pTα^{b}; it promotes increased surface expression of TCRβ and does not expand the ISP subset.

pTα^{b}-R117A expression also promoted development of few ISPs (~13.5% - Figure 3.23) that was not significantly different to pTα^{b} but much reduced compared to pTα^{a} ($p \leq 0.001$). However, both pTα^{a}-DRRA and pTα^{b}-R117A generated significantly increased numbers of mature TCRβ$^{(hi)}$ cells (Figure 3.23). Expression of pTα^{a} results in only ~15% of these cells (compared to ~5% for vector only). By contrast, pTα^{b} promoted development of ~40% TCRβ$^{(hi)}$ cells, while both pTα^{a}-DRRA and pTα^{b}-R117A generated ~37% TCRβ$^{(hi)}$ cells. Importantly, there was no significant difference between these figures and that seen for pTα^{b}.

Figure 3.22

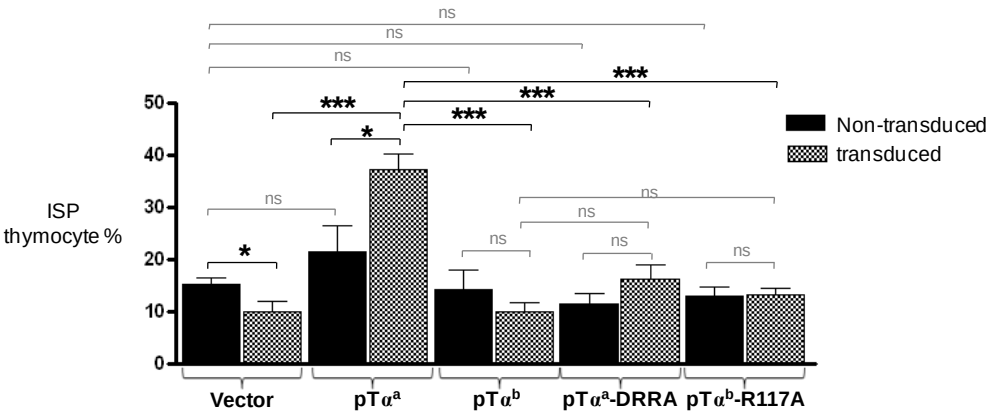

Figure 3.22 pTα^{a}-DRRA and pTα^{b}-R117A do not expand the ISP population. Bar chart (from n=6 experiments) of E14 pTα KO thymocytes transduced with vector alone, pTα^{a}, pTα^{b}, pTα^{a}-DRRA or pTα^{b}-R117A that were analysed for percentage of ISPs after 8-15 days in FTOC. Percentage of ISPs is shown for non-transduced thymocytes (black bars) and transduced thymocytes (hatched bars). Cells are TCRδ$^{(-)}$ TCRβ$^{(lo)}$ CD8$^{(+)}$. ns is not significant, * $p \leq 0.05$ and *** $p \leq 0.001$.

Figure 3.23

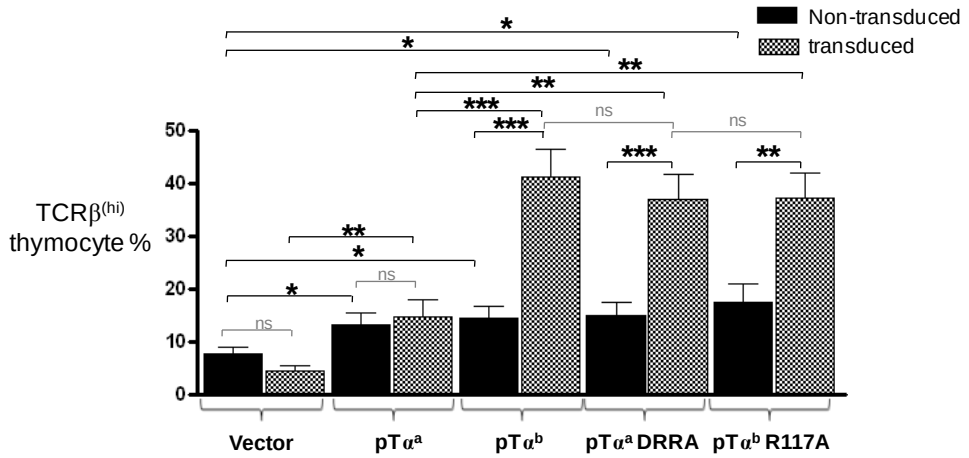

Figure 3.23 pTα^a-DRRA and pTα^b-R117A promote development of mature TCRβ$^{(hi)}$ cells. Bar chart (from n=6 experiments) of E14 pTα KO thymocytes transduced with vector alone, pTα^a, pTα^b, pTα^a-DRRA or pTα^b-R117A that were analysed for percentage of TCRβ$^{(hi)}$ cells after 8-15 days in FTOC. Percentage of TCRβ$^{(hi)}$ cells is shown for non-transduced thymocytes (black bars) and transduced thymocytes (hatched bars). Cells are TCRδ$^{(-)}$ TCRβ$^{(hi)}$, ns is not significant, * p≤ 0.05 ** p≤ 0.01 and *** p≤ 0.001.

3.8 Summary.

To conclude, mutation of oligomerization residues in both pTα^a and pTα^b did not perturb their interaction with TCRβ as all pTα mutant alleles; pTα^a-R24A, pTα^a-DRRA and pTα^b-R117A were able to increase TCRβ on the surface of transduced thymocytes. Importantly, the preTCRs formed by the mutated pTα alleles were also able to signal and rescue αβ T cell development in pTα KO FTOCs as judged by a reduction in the percentage of γδ cells. Although removing the oligomerization residues did not affect preTCR signal initiation, it did affect the characteristics of the preTCRs that were formed from the mutant alleles. The oligomerization-deficient preTCRs were expressed at higher levels on the cell surface, similar to that seen for pTα^b, and promoted very similar T cell development to pTα^b. Thus, the ISP subset was not expanded (as seen for pTα^a) and generation of mature TCRβ$^{(hi)}$ cells was favoured. Therefore, it appears that

oligomerization of the preTCR is not required for signalling *per se*. However, the ability to oligomerize appears to regulate the surface expression of the preTCR which in turn determines the functional outcome of preTCR signalling. Importantly, because pTα^a-DRRA promotes development in a similar manner to pTα^b, the ability to oligomerize is what distinguishes pTα^a from pTα^b.

Chapter 4

Investigating the role of the preTCR in establishment of signalling thresholds in pre-selection DP thymocytes.

4.1 Introduction.

The results described in the previous chapters do not provide strong evidence to support our original hypothesis that pTα^a and pTα^b specified developments of different T cell lineages. Nonetheless, it was clear from the pTα KO FTOCs that sustained expression of pTα^a was deleterious to the maturation of thymocytes beyond the ISP stage. By contrast, pTα^b did not show this developmental restriction, allowing cells to progress through to the mature SP stage apparently unperturbed. Thus, it is possible that pTα^b is required alongside pTα^a for efficient development of αβ T cells. Because pTα^b-expressing thymocytes were not blocked at the ISP to DP transition, signalling through preTCR^b may promote progression to, and establishment of, the DP stage. Evidence from the expression analysis may support this hypothesis as transcripts for pTα^b were found in greater abundance than those for pTα^a within the DP population. Moreover, because a greater percentage of mature thymocytes developed as a result of pTα^b expression, it is possible that this isoform also promotes the DP to SP transition. In this regard, the role of the preTCR and specifically preTCR^b in the establishment of the DP stage and in positive selection was investigated.

Positive selection of DP thymocytes is achieved through weak interactions of TCRαβ with self-peptide/MHC. It has been reported that pre-selected DPs are highly sensitive to signals through the TCR, and that this increased

sensitivity is required in order to select as broad a TCR repertoire as possible (Gallo et al., 2007). These authors identified a pool of “sensitive” pre-selected DPs by cross-linking CD3ε that resulted in rapid phosphorlyation of the ERK1/2 MAP kinases. Calcium signalling via calcineurin was described to be essential for setting up the sensitized state, as “ERK-sensitive” DP cells could not be detected in calcineurin-deficient mice. The mechanisms underlying calcium release and calcineurin activation were not described in this report. However, it was evident that prior prolonged inhibition of calcineurin activation by CSA resulted in abrogation of the DP cell sensitivity, whereas CSA administered alongside TCR stimulation had little effect (Gallo et al., 2007). Thus, it appears that signals prior to the establishment of the DP stage are required for sensitizing DP cells for efficient positive selection.

4.2 The preTCR is required for efficient positive selection of DP cells; ERK sensitivity is absent from pTα-deficient thymocytes.

We hypothesised that preTCR signalling was necessary for setting up the “ERK-sensitive” state of DP cells that allows efficient positive selection through the TCR. To test this hypothesis pTα KO CD69$^{(lo)}$ DP thymocytes were analysed for their ability to phosphorylate ERK1/2 after 1-10 minutes cross-linking by anti-CD3ε antibody. Figure 4.1 shows phosphor-ERK analysis of adult C57BL/6 CD69$^{(lo)}$DP cells, adult pTα KO CD69$^{(lo)}$DP cells and WT CD69$^{(lo)}$DP cells in the presence of an inhibitor of ERK phosphorylation. Phospho-ERK was assessed for each of these conditions, before cross-linking of CD3ε (0 minutes), or after 1, 2, 5 and 10 minutes of activation through the TCR. Cross-linking WT adult thymocytes revealed a population of cells that rapidly phosphorylated ERK1/2; ~21% after 1

minute and ~25% after 2 minutes. These represented the “ERK-sensitive” DP cells described by Gallo and co-workers (Gallo et al., 2007).

Figure 4.1

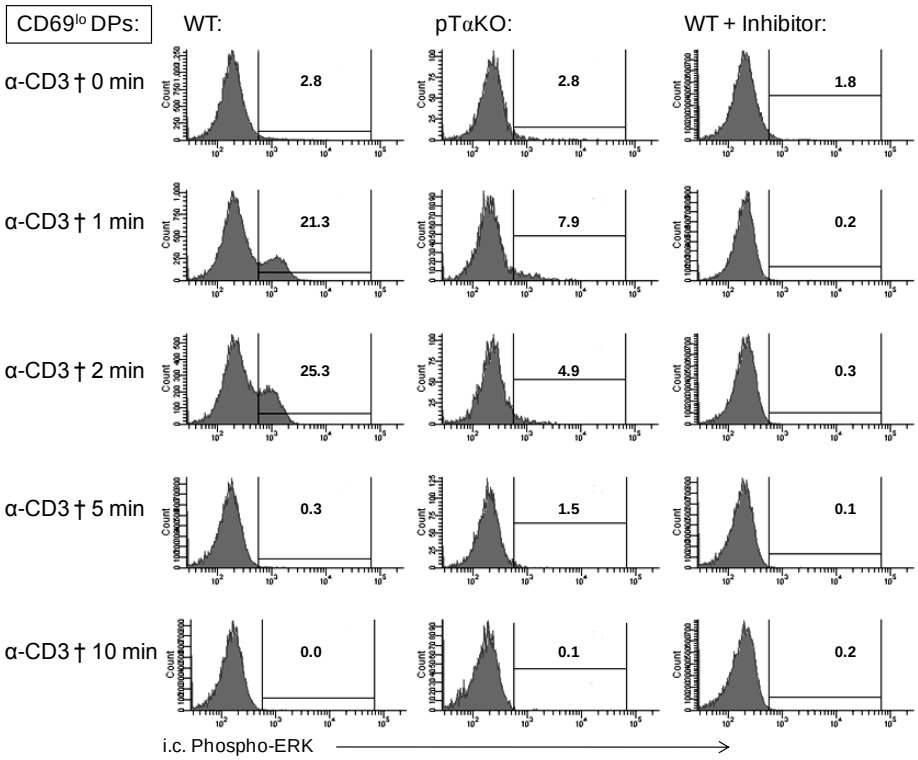

Figure 4.1 The “ERK-sensitive” DP population is absent in pTα KO mice. Representative FACS plots (from n=3 experiments) of CD69$^{(lo)}$DP thymocytes from C57BL/6 (WT) and pTα KO adult mice that were analysed for intracellular ERK1/2 phosphorylation at time-zero (0 min) and after 1, 2, 5 and 10 minutes cross-linking of anti-CD3ε. WT CD69$^{(lo)}$DP cells were activated in the presence of an inhibitor of ERK-phosphorylation (UO126) as a negative control. Numbers represent percentages of cells within the gates.

Phosphorylation of ERK was transient and was lost after 5 minutes of activation. In the presence of the phosphorylation inhibitor no increase in phospho-ERK was seen and the proportion of phospho-ERK$^{(+)}$ cells remained low (≤ 0.2%) at all time points. Importantly, the increase in phospho-ERK in DP cells was not observed for pTα KO CD69$^{(lo)}$DP cells. Only ~8% were phospho-ERK$^{(+)}$ after 1 minute, a figure which decreased at 2 minutes to ~5%. Similar to the WT DP cells the percentage of pTα KO

phospho-ERK$^{(+)}$ DP cells returned to basal levels by 5 minutes. These data suggest that pTα KO DP cells have a markedly reduced "ERK sensitivity" as very few were able to phosphorylate ERK after brief stimulation through the TCR. To ensure that the lack of ERK phosphorylation by pTα KO DP cells was not merely due to a lower level of CD3ε on the surface of the cells, C57BL/6 (WT) and pTα KO DP cells were analysed for surface CD3ε levels. Figure 4.2 demonstrates that if anything there is a higher surface expression of CD3ε (MFI 735) in pTα KO DP cells compared to the equivalent WT population (MFI 535).

Figure 4.2

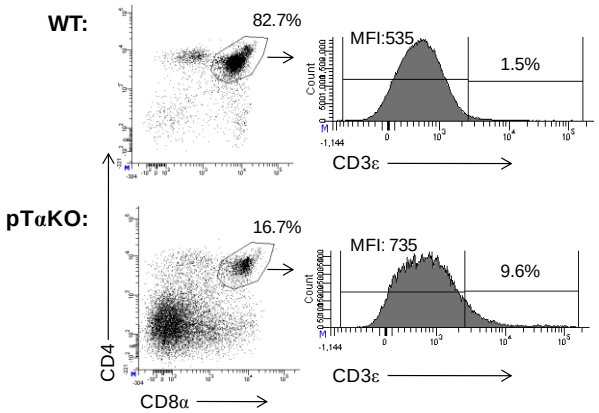

Figure 4.2: pTα KO DP cells express comparable surface levels of CD3ε compared to WT DP cells. Representative FACS plots of total thymocytes from C57BL/6 (WT) and pTα KO adult mice that were analysed for CD3ε expression on DP cells. MFI is mean fluorescence intensity.

The results suggest that the preTCR plays a role in sensitising DP cells to subsequent signals through TCRαβ and that in the absence of the preTCR the "ERK-sensitive" CD69$^{(lo)}$DP population was markedly reduced. Therefore we wanted to determine whether re-introduction of preTCR signalling by expression of either pTα^a or pTα^b in pTα KO thymocytes restored the "ERK-sensitive" DP state. To this end, E14 pTα KO thymocytes were transduced with pTα^a and pTα^b, and after 12-day FTOC were assayed for ERK-sensitivity by cross-linking CD3 and intracellular

analysis of phospho-ERK on DP cells as described above. Figure 4.3 shows the results from this analysis. The first column represents adult WT DP cells after 0, 1, 1.5, 2 and 5 minutes of anti-CD3ε cross-linking; the second column shows adult pTα KO DP cells; the third shows the results for pTα KO DP cells transduced with $pT\alpha^a$ and the fourth pTα KO cells transduced with $pT\alpha^b$. The FTOCs produced limited thymocyte numbers, so only two time points could be performed; time 0 and 1 minute cross-linking.

Figure 4.3

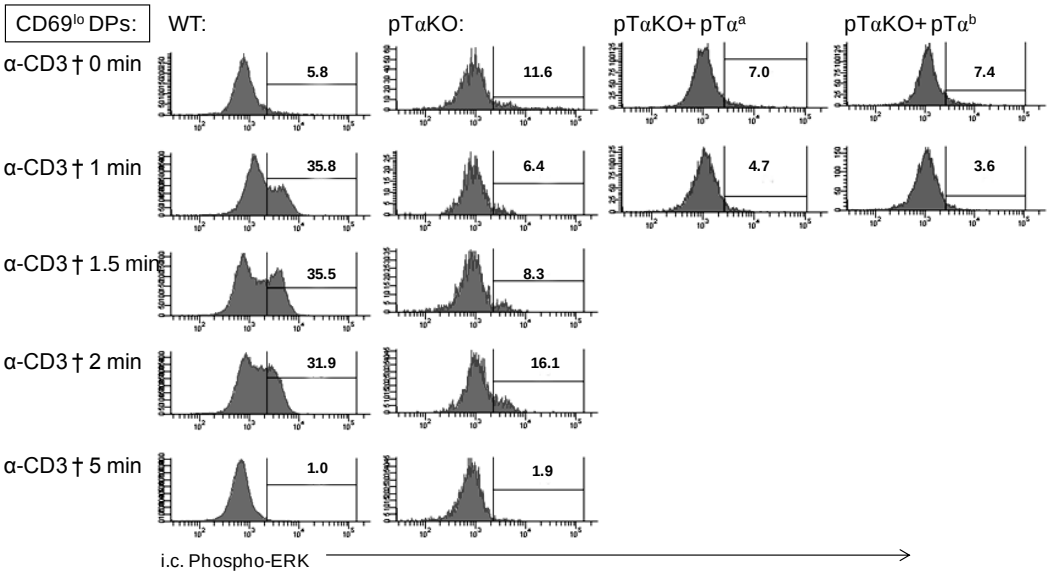

Figure 4.3 Expression of $preTCR^a$ and $preTCR^b$ in pTα KO DP thymocytes did not restore "ERK-sensitivity": FACS plots show $CD69^{(lo)}$DP cells from adult C57BL/6 or pTα KO mice and pTα KO DP thymocytes transduced with either $pT\alpha^a$ or $pT\alpha^b$, after 11-day FTOC. $CD69^{(lo)}$DP cells were analysed for intracellular ERK1/2 phosphorylation after time zero, or 1, 1.5, 2 and 5 minutes activation by cross-linking with anti-CD3ε antibody. The numbers represent the percentage cells in each gate.

Similar to previous results (Figure 4.1) after 1 minute activation a large proportion of WT DP cells have phosphorylated ERK (~36% compared to ~6% at time 0). This percentage remained high after 1.5 and 2 minutes of cross-linking before reducing to basal levels after 5 minutes (Figure 4.3). pTα KO DP cells again displayed a reduced capacity to phosphorylate ERK

compared to WT DP cells. Surprisingly, DP thymocytes transduced with pTα^{a} and pTα^{b} did not show increased phosphorylated ERK, instead behaving in a similar manner to pTα KO thymocytes (Figure 4.3). Therefore, in this experiment it was not possible to restore the ERK-sensitivity of pTα KO thymocytes to that of WT cells by expression of either preTCR^{a} or preTCR^{b}. Despite this result, it appears that preTCR-deficient DP thymocytes lack ERK sensitivity and are therefore unresponsive to weak signalling through the TCR suggesting that these cells will have altered signalling thresholds for positive and negative selection.

4.3 Evidence that pTα KO thymocytes have an altered threshold for selection.

The relative unresponsiveness of pTα KO DP cells to signals through the TCR would suggest that these cells may require strong signals for positive selection. In other words, the threshold for positive selection would be higher for pTα KO thymocytes (Figure 4.4). Therefore, we hypothesised that high-affinity TCR/MHC/peptide interactions which would normally delete WT DP thymocytes would positively select pTα KO DP thymocytes (Figure 4.4).

Superantigens are pathogen products capable of activating subsets of T cells bearing specific TCRβ chains (Kappler et al., 1988; MacDonald et al., 1988). This broad specificity is due to the fact that superantigens do not follow conventional antigen processing pathways in order to bind MHC. On the contrary, these proteins are able to attach to MHC-II alpha chains outside of the peptide binding pocket. Superantigens activate T cells by binding to specific TCRβ chain variable regions (Figure 4.5). Superantigen cross-linking of the TCR in peripheral tissues results in massive production

of cytokines (Figure 4.5a), a mechanism by which the superantigen-producing microbe mediates its pathogenicity.

Figure 4.4

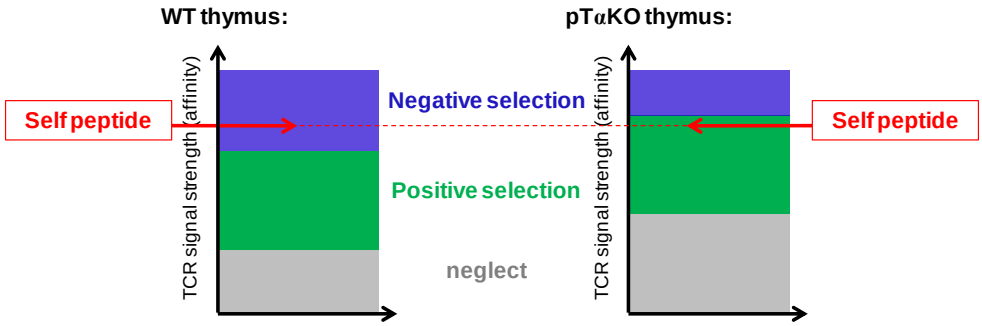

Figure 4.4: A schematic of the hypothesis: pTα KO thymocytes have a higher threshold for positive selection so that a high affinity interaction with MHC-self-peptide which would negatively select WT thymocytes, results in positive selection of pTα KO cells.

Many inbred mouse strains encode endogenous retroviral elements, specifically those of the mouse mammary tumour virus (MMTV) family, which express superantigens (Kappler et al., 1988; MacDonald et al., 1988). When expressed in the thymus the high-affinity TCR-MHC interaction induced by the superantigen leads to the deletion of T cells bearing specific Vβ chains (Woodland et al., 1991) (Figure 4.5b). Therefore, superantigen expression provides a useful tool for analysing negative selection events in the mouse thymus.

Here, we sought to determine whether superantigen-driven negative selection occurred normally in pTα KO thymocytes. However, the pTα KO mouse is bred on a C57BL/6 background that does not express the MHC-II I-Eα chain that presents MMTV superantigens. Therefore, T cells are not deleted by superantigens in C57BL/6 or pTα KO mice. In an attempt to

overcome this limitation mixed FTOCs were set-up using pTα KO mice, C57BL/6 mice and DBA/2 mice, that are Eα positive and encode seven MMTV endogenous proviruses; 1, 6, 7, 8, 11, 14 and 17, capable of deleting nine different TCRβ chains; Vβ3, 5, 6, 7, 8.1, 9, 11 and 12.

Figure 4.5

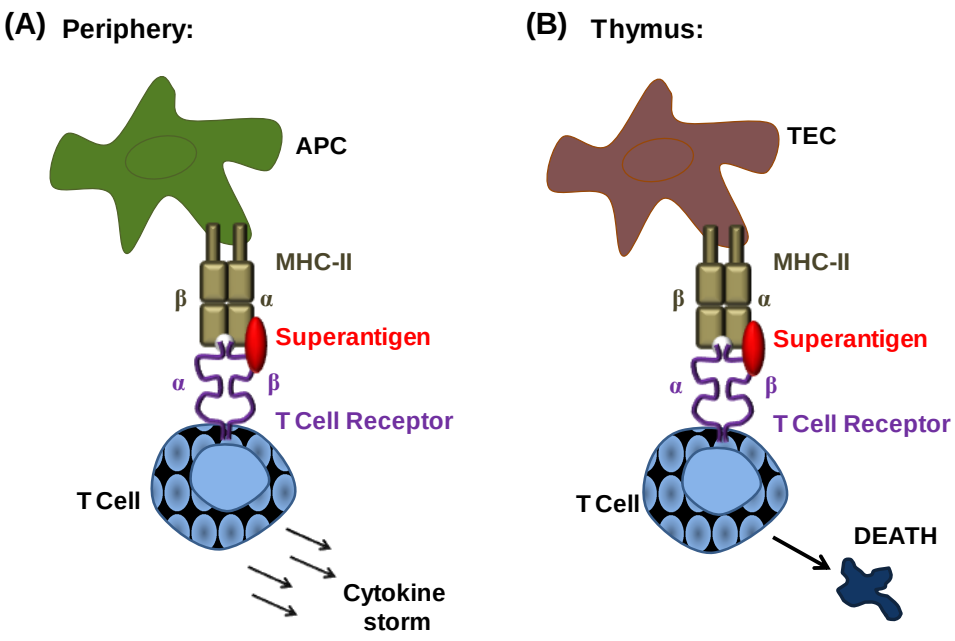

Figure 4.5 Depiction of the action of superantigens in the periphery and thymus. Superantigens bind MHC-II outside of the peptide binding pocket. Superantigens activate T cells by binding to specific TCRβ chain variable regions. In the periphery (A) this results in massive production of cytokines by the activated T cell (cytokine storm). In the thymus (B) superantigen activation of T cells leads to deletion (death) of thymocytes bearing superantigen-specific TCRβ chains. APC is antigen presenting cell and TEC is thymic epithelial cell.

Figure 4.6 illustrates the experimental design; thymic lobes were collected from the DBA/2 E15 mice and depleted by 5-day 2-deoxy-guanosine treatment. C57BL/6 and pTα KO DN2/3 thymocytes were then sorted by FACS and used to repopulate the depleted DBA/2 lobes. After 10-15-day FTOC CD4 thymocytes were analysed for Vβ-specific TCRβ expression (Figure 4.6). C57BL/6 E15 lobes were used as controls as negative

selection of thymocytes is not expected to occur in these lobes as they lack the Eα chain for superantigen presentation.

Figure 4.6

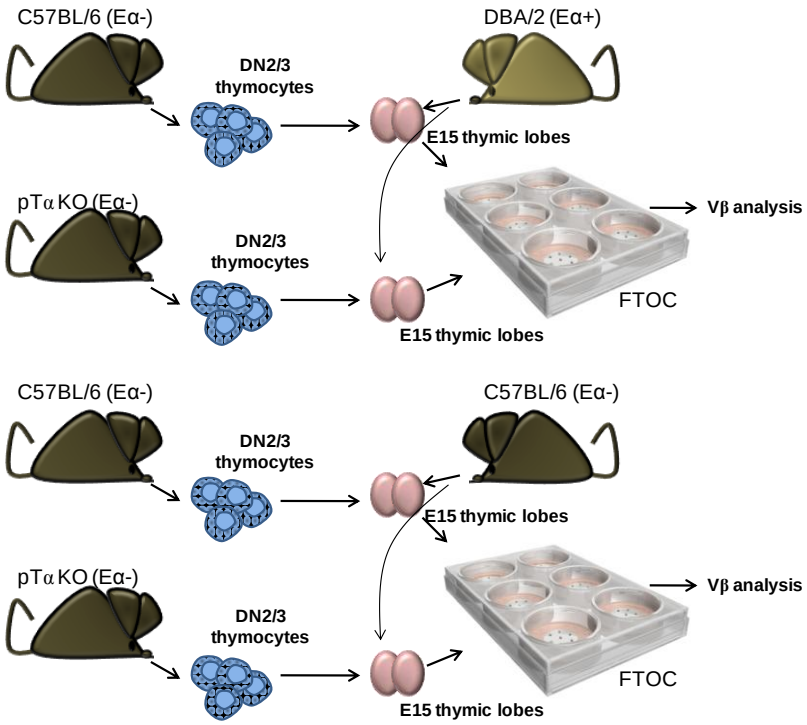

Figure 4.6 Experimental design for investigating the negative selection threshold of pTα KO thymocytes. An illustration of the mixed FTOC method is shown. DN2/3 thymocytes were isolated by FACS from C57BL/6 or pTα KO adult mice and used to repopulate depleted E15 thymic lobes from DBA/2 ($E\alpha^{(+)}$) or C57BL/6 ($E\alpha^{(-)}$) mice. After 10-15-day FTOC CD4 thymocytes were analysed for Vβ-specific TCRβ expression.

The lack of T cells bearing Vβ5 and Vβ6 was evident in adult DBA/2 mouse thymus, as only 0.7% of $TCR\alpha\beta^{(+)}CD4^{(+)}$ T cells were $V\beta6^{(+)}$ and only 0.8% were $V\beta5^{(+)}$. By contrast, in C57BL/6 mice, 6.9% were $V\beta6^{(+)}$ and 2.1% were $V\beta5^{(+)}$ (Figure 4.7).

$TCR\alpha\beta^{(+)}CD4^{(+)}$ thymocytes from C57BL/6 and pTα KO mice were analysed for Vβ5, Vβ6 and Vβ8 after 15 days FTOC in DBA/2 or C57BL/6 stroma. Unfortunately, the staining for Vβ5 and Vβ8 analysis was not of the quality

which allowed definitive conclusions to be drawn. However, the Vβ6 analysis was more robust, although not entirely as expected. WT C57B/L6 T cells were not deleted in C57B/L6 lobes consistent with the lack of superantigen presentation (Figure 4.8). However, they were also not deleted in DBA/2 lobes. We think this may be due to low MHC-II expression in depleted lobes, although direct evidence for this has not yet been obtained.

Figure 4.7

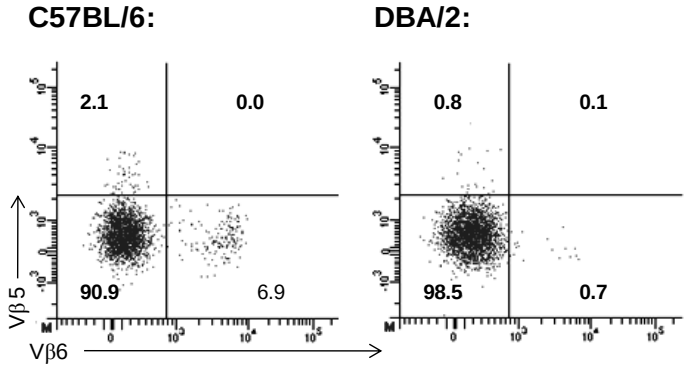

Figure 4.7 Thymocytes bearing Vβ6 and Vβ5 chains are deleted in the DBA/2 thymus: $CD4^{(+)}TCR\beta^{(hi)}$ thymocytes from adult C57BL/6 and DBA/2 mice were analysed for Vβ6 and Vβ5 expression. Numbers represent percentages in relevant quadrants.

Importantly, however, we did see a significant difference in Vβ6 expression when pTα KO thymocytes were cultured in C57BL/6 lobes compared to DBA/2 lobes (Figure 4.9). In C57B/L6 lobes 4.2% of $CD4^{(+)}TCR\beta^{(hi)}$ cells were $V\beta6^{(+)}$ which increased to 13.1% in DBA/2 lobes. Thus, there is preliminary evidence to suggest that pTα KO thymocytes may respond differently to WT thymocytes upon interaction with high-affinity TCR-stimulation.

Figure 4.8

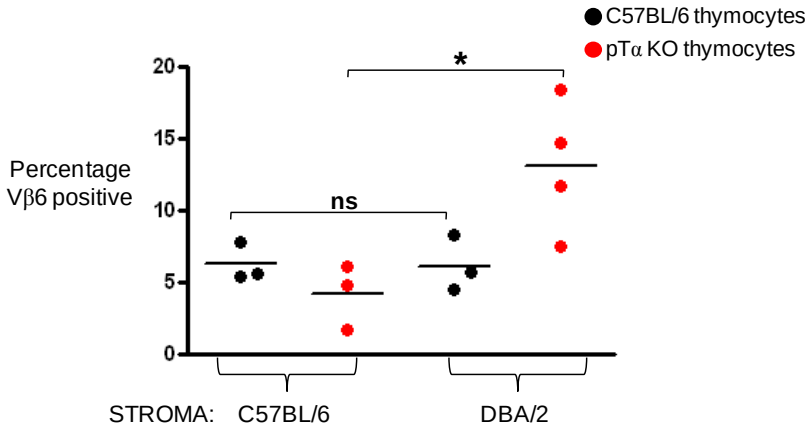

Figure 4.8 pTα KO thymocytes respond differently to WT thymocytes in DBA/2 stroma. Dot plot showing CD4SP thymocytes from C57BL/6 (black dots) and pTα KO (red dots) mice that were cultured for 15 days in C57BL/6 or DBA/2 depleted E15 thymic lobes. $CD4^{(+)}TCR\beta^{(hi)}$ cells were analysed for Vβ6 expression. The percentage of $V\beta6^{(+)}$ cells is shown, * p≤ 0.05, ns is not significant.

Collectively the results begin to suggest a role for the preTCR regulating the threshold for positive selection at the DP stage in thymic ontogeny. Admittedly, the project would benefit from a more extensive investigation into the negative selection thresholds of pTα KO thymocytes, but preliminary data would suggest that the T cell repertoire of the pTα KO mouse could be enriched for auto-reactive T cells. If proved correct, these results would implicate the preTCR in regulating the appropriate selection of a broad non-self-reactive TCR repertoire, with important consequences for autoimmune disease.

Chapter 5

pTα^a and pTα^b BAC transgenic mice

5.1 Introduction

The FTOC data of the previous chapter clearly demonstrate the differential effects of expression of pTα^a and pTα^b on T cell development. However, despite the usefulness of the FTOC system there are limitations. Perhaps the most important of these for this work is that the regulation of expression of pTα^a and pTα^b is under the control of a retroviral promoter (LTR) and thus not regulated by its own regulatory sequences. This is important, especially when considering pTα^a as constitutive expression of pTα^a into the DP stage, where, as the PCR data suggests, pTα^a expression should be normally terminated, appears to be detrimental for continued T cell development. Thus, physiological regulation of pTα^a expression at the DN-ISP stage, is critical for the appropriate developmental outcome of developing thymocytes. A further limitation of FTOC is that only a relatively small number of thymocytes can be obtained from each thymic lobe. Unlike an adult mouse thymus which contains approximately 200 million thymocytes, FTOC produces nearer 200,000 cells. Rigorous analyses such as intracellular stains are much more difficult to perform on low numbers of cells. For example, when staining the pTα^b-transduced thymocytes for Foxp3, very few T-regs were recovered, making the results less reliable. In order to overcome these limitations bacterial artificial chromosome (BAC) transgenic mice for pTα^a and pTα^b were generated.

pTα-deficient mice that express either pTα^a or pTα^b under the Lck promoter have been made (Gibbons et al., 2001). In this report, it was shown that both isoforms of pTα were able to function and rescued the αβ developmental block in the pTα KO mouse. However, the rescued mice did not have completely normal development and the different developmental capabilities of the two isoforms were not thoroughly analysed in this study. In addition, the pTα^a and pTα^b transgenes were expressed under the Lck promoter, so like our FTOC system, were not physiologically regulated. BAC transgenic mice are advantageous in this respect because a large section of genomic DNA containing the pTα gene can be used. Thus, pTα will be incorporated into the host genome along with its regulatory elements and so physiological timing of expression of pTα^a and pTα^b at the DN stage should be achieved. A further advantage of making BAC transgenics is that it makes it possible to perform analyses that are otherwise not possible when using the FTOC system. These include the analysis of the migration of T cells once they leave the thymus, and the identification of their function and location in the periphery.

5.2 Recombineering to generate pTα^a and pTα^b BAC constructs.

5.2.1 The pTα^a and pTα^b BAC constructs.

BACs are large vector plasmids that carry up to 70kb of inserted DNA. Figure 5.1 shows the BAC constructs used for generating "pTα^a-only" and "pTα^b-only" transgenic mice. The "pTα^a-only" construct consists of the complete coding sequence for pTα but with exons 1 and 2 fused to prevent any splicing events taking place that would remove exon-2 and produce pTα^b. Thus, mice expressing this construct will only be able to express pTα^a. The "pTα^b-only" construct lacks exon-2, intron-1 and intron-2,

effectively fusing exons 1 and 3 so that only pTα^{b} can be generated by mice expressing this construct.

Figure 5.1

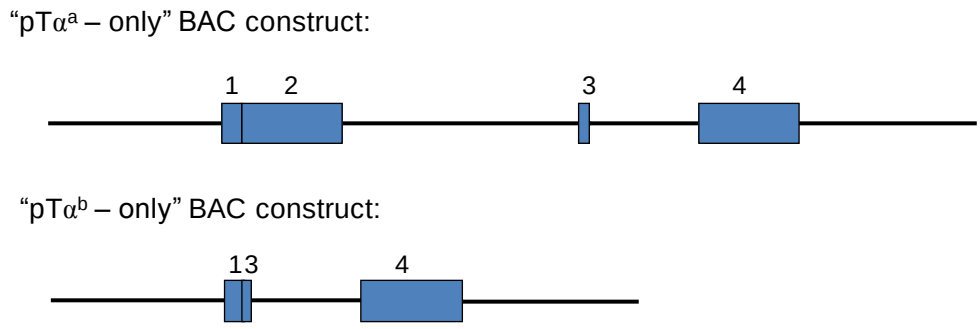

Figure 5.1 Constructs for "pTα^{a}- only" and "pTα^{b}- only" BAC transgenic mice: Exon 1 and 2 are fused in the "pTα^{a}- only" construct preventing removal of exon-2 by differential splicing. Exon-2, intron-1 and intron-2 have been knocked out of the "pTα^{b}- only" construct and exons 1 and 3 fused, so that pTα^{b} is exclusively expressed by this construct.

The BMQ452P20 BAC, used for generating the constructs, was purchased from Ensembl organisation and consisted of 46KB of chromosomal DNA from chromosome 17 of C57BL/6 mice. This region included an 8.5kb region in the centre of the BAC that contained the pTα gene. The constructs were generated by a method called recombineering, which is a method of genetic engineering by use of bacterial homologous recombination (Warming et al., 2005).

5.2.2 An overview of the Recombineering system.

The BMQ452P20 BAC was electroporated into SW102 *E.coli* cells for recombineering (Warming et al., 2005). SW102 contain a defective λ prophage inserted into the bacterial genome. The phage genes, *exo*, *bet*, and *gam*, are transcribed from a temperature regulated promoter. The

promoter is inactive at 32°C but can be activated after 15 minutes heat shock at 42°C. This activation generates the recombination proteins; *exo* codes for a 5'-3' exonuclease that creates single-stranded overhangs on linear DNA that is introduced into the SW102 cells that is homologous to the site that is to be targeted; *bet* protects these overhangs and aids in the subsequent recombination process; and *gam* prevents degradation of the linear DNA (Warming et al., 2005). The linear DNA that is to be used to target the BAC (for example a PCR product or oligo) is introduced into heat-shocked electrocompetent SW102 bacteria using electroporation. The introduced DNA then undergoes homologous recombination with the BAC changing its sequence (Figure 5.2).

Figure 5.2

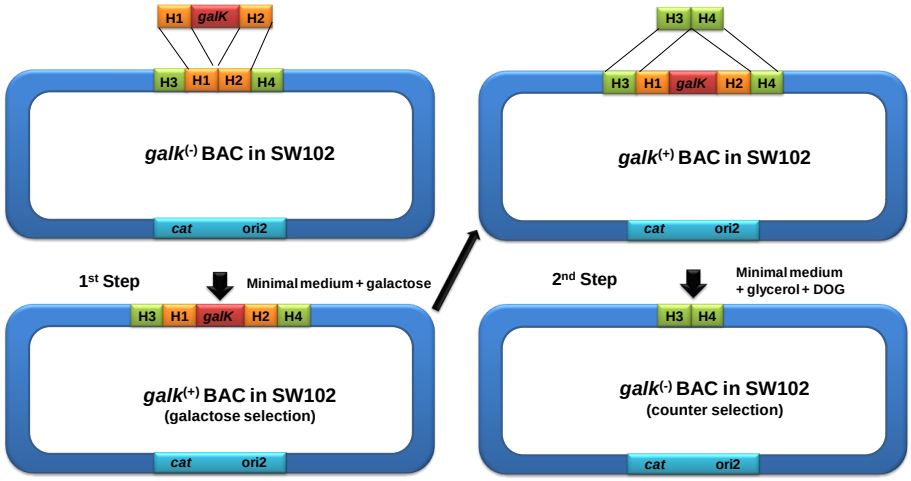

Figure 5.2 An illustration of the *galk* selection and counter-selection recombineering method. In the first step *galk* is introduced to the BAC, via linear DNA (a *galk* PCR product), by homologous recombination between homology regions (H1 and H2) in the BAC and *galk* cassette. *galk*$^{(+)}$ SW102 bacteria are then selected for by culture on galactose containing medium. *galk* is then replaced with a double-stranded DNA oligo that contains regions of homology (H3 and H4) with the BAC. This is achieved by counter selection using minimal medium containing 2-deoxy-galactose (DOG) with glycerol as the sole carbon source. Thus the *galk*$^{(+)}$ SW102 bacteria are selected against in this 2nd step.

In addition to the phage genes, SW102 cells also contain a fully functional *gal* operon, except the *galk* gene is missing. The ability to grow on galactose minimal medium can be restored by adding *galk* in *trans* (i.e. by inserting a *galk* expression cassette into the BAC). Therefore, SW102 clones that have undergone a recombination event to insert the *galk* cassette can be selected on galactose-containing medium. Next, the *galk* cassette can be replaced by any DNA of choice by selection against *galk* using 2-deoxy-galactose. Thus, BAC sequences can be manipulated using homologous recombination with the galactose selection and counter-selection process (Figure 5.2).

5.3 Insertion of *galk* into the pTα-containing BAC.

Figure 5.3 shows the recombineering strategy for generating the $pT\alpha^a$ BAC constructs (see figure 5.8 for $pT\alpha^b$ BAC strategy). The first targeting step was common for generation of both the $pT\alpha^a$ and $pT\alpha^b$ constructs. Two primers; P21 and P22, were used to amplify *galk* from a p*Galk* containing plasmid. P21 and P22 also contain 50bp homology to the intron sequence of pTα between exon-1 and exon-2 as well as 25bp homology to the 5' and 3' end of the *galk* cassette. The resulting PCR product consists of the *galk* gene flanked by 50bp homology arms to the targeted site in the pTα gene. The *galk* PCR product was electroporated into SW102 cells containing the pTα BAC that had been heat-shocked to activate the recombineering machinery. The cells were grown on galactose-containing medium to select for those bacteria containing the BAC that had incorporated the *galk* sequence by homologous recombination. Transformants were analysed by restriction digest to confirm the presence of the *galk* sequence. The enzymes used for restriction digest characterisation were Hpa1, Xho1 and Xba1. Each of these enzymes was chosen because they cut in and around

the target site and because they cut the pTα BAC in fewer than 15 places (Figure 5.4).

Figure 5.3

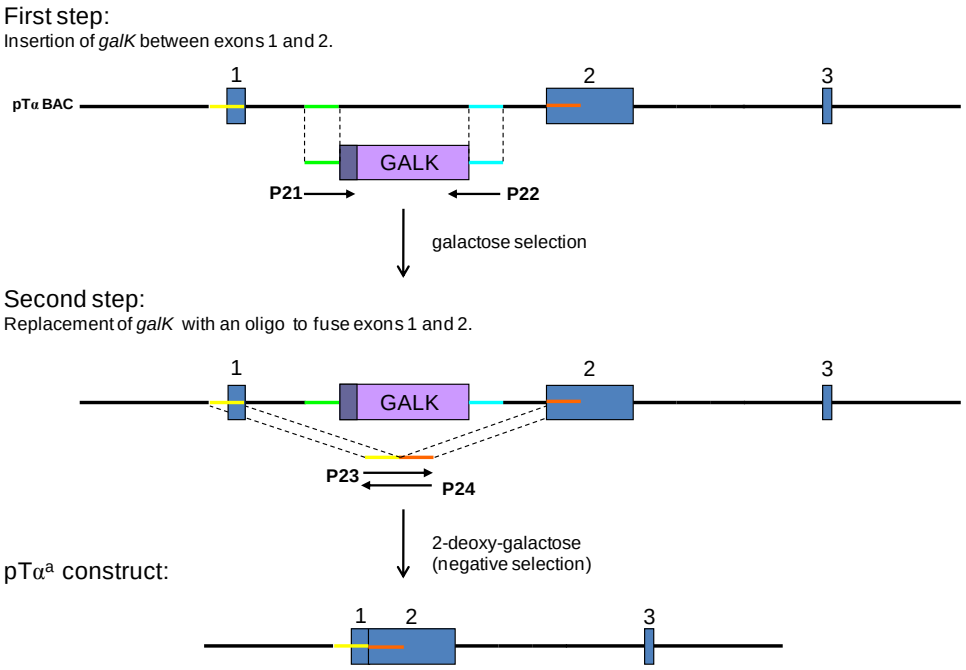

Figure 5.3 Diagram of the recombineering method to generate the "pTα^a-only" BAC construct: In the first step *galk* is inserted into a BAC containing the pTα gene, via a *galk* PCR product, by homologous recombination. The *galk* PCR product was generated using primers p21 and p22 that possess 50bp homology to the intron sequence between exons 1 and 2 of pTα (green and turquoise). The *galk*$^{(+)}$ pTα BAC is selected for by the presence of galactose in the medium. *galk* is then replaced by a double stranded DNA oligo (p23+p24) that is homologous to 75bp regions at the 3' end of exon-1 (yellow) and the 5' end of exon-2 (orange) of pTα. Thus, replacement of *galk* results in fusion of exons 1 and 2 to generate the pTα^a construct. The *galk*$^{(-)}$ pTα BAC was selected for on 2-deoxy-galactose containing medium with glycerol as the only carbon source.

A successful integration of *galk* could be readily detected by changes in the sizes of DNA fragments produced by these enzymes. Figure 5.4A shows the restriction maps for Hpa1, Xho1 and Xba1 for the pTα BAC sequence. Insertion of the *galk* cassette between exon-1 and 2 of pTα removes two Hpa1 sites generating one large fragment across the target site (19kb) in place of two smaller fragments present in the parent BAC (Figure 5.4B).

For the Xho1 and Xba1 digests, insertion of the *galk* cassette results in a decrease in size of about 2.8kb for each of the fragments traversing the target site; so that the 14.8kb Xho1 fragment is reduced to 11.9kb and the 11.8kb Xba1 fragment is reduced to 9kb (Figure 5.4B).

Figure 5.4

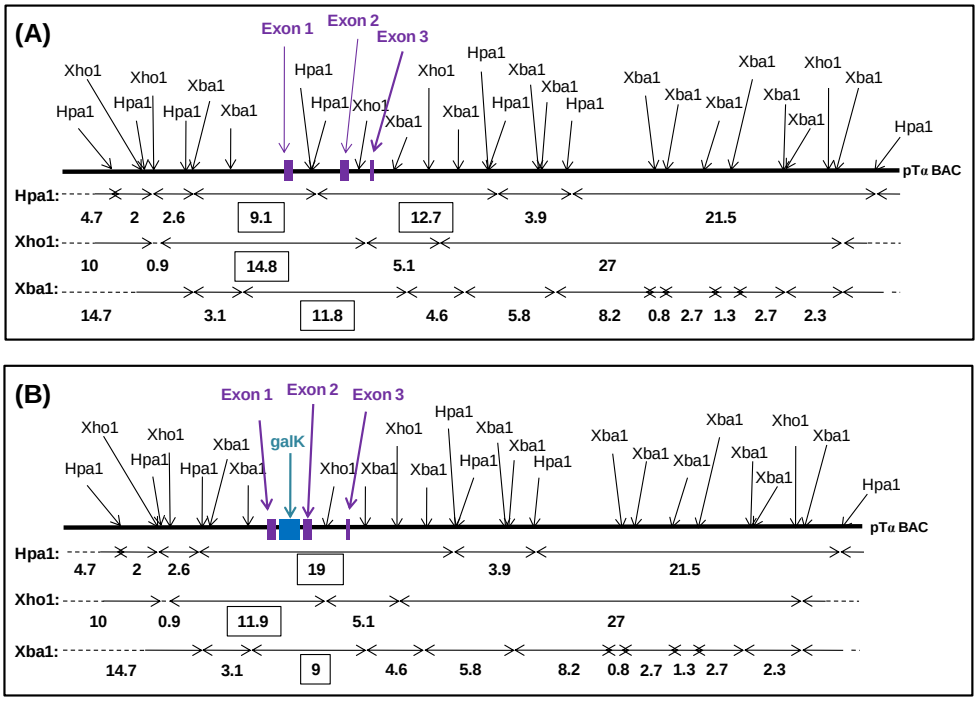

Figure 5.4 Hpa1, Xho1 and Xba1 restriction digest maps for the pTα BAC and the *galk*$^{(+)}$ pTα BAC. Restriction maps for Hpa1, Xho1 and Xba1 for the parent pTα BAC (A) and the *galk*$^{(+)}$ pTα BAC (B) in which *galk* was inserted between exons 1 and 2 of pTα. Insertion of *galk* results in the loss of two Hpa1 sites resulting in the formation of a 19kb fragment in the *galk*(+) pTα BAC in place of two fragments of 9.1kb and 12.7kb present in the parent BAC. *galk* insertion results in the loss of ~2.8kb from the target region thus, reducing the size of an Xho1 fragment from 14.8kb to 11.9kb, and a Xba1 fragment from 11.8kb to 9kb in the *galk*(+) pTα BAC. Boxes are drawn around the fragment sizes that are altered as a result of *galk* insertion.

Figure 5.5 shows that *galk*$^{(+)}$ clones could be detected by Hpa1, Xho1 and Xba1 digests. The Xho1 digest revealed four potential *galk*$^{(+)}$ clones that had gained a ~11.9kb fragment in place of the 14.8kb fragment seen in the parent BAC (clones 1,3,8 and 11 Figure 5.5A). Three of the four potential *galk*$^{(+)}$ clones, when digested with Xba1, appeared to have gained a 9kb

fragment in place of the 11.8kb fragment present in the parent BAC (clones 3, 8 and 11) (Figure 5.5B). From the Hpa1 digest it appears that all four clones had lost the 9.1kb and 12.7kb fragments, present in the parent BAC and gained a 19kb fragment in their place. The *galk*$^{(+)}$ BAC clones were sequenced and clone 11 was transformed into fresh SW102 cells for use in subsequent recombineering steps.

Figure 5.5

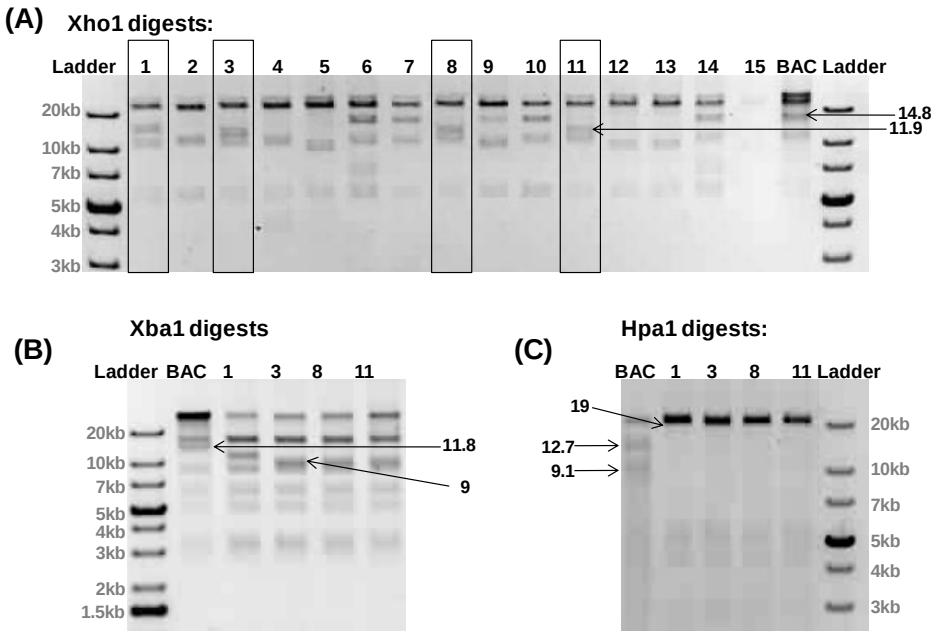

Figure 5.5: Restriction digest analysis of *galk*$^{(+)}$ pTα BAC clones. (A) 15 *galk*$^{(+)}$ pTα BAC clones that had been positively selected on galactose containing medium were subjected to Xho1 digestion which revealed four potential *galk*$^{(+)}$ pTα BAC clones that had lost a 14.8kb fragment present in the parent (BAC) and gained an 11.9kb fragment. (B) the four *galk*$^{(+)}$ pTα BAC clones identified in (A) were digested with Xba1. Clones 3,8 and 11 appear to have gained a 9kb fragment in place of an 11.8kb fragment present in the parent BAC. (C) the four *galk*$^{(+)}$ pTα BAC clones identified in (A) were digested with Hpa1 and all appeared to have gained a 19kb fragment in place of the 12.7kb and 9.1kb fragments present in the parent BAC. Clone 11 was used for subsequent targeting steps. Sizes of fragments are in kilobases (kb).

5.4. Generation of the pTα^{a} BAC construct.

The second recombineering step (see Figure 5.3) involved the deletion of intron-1 and fusion of exons 1 and 2. This was achieved by "replacement" of the *galk* sequence with a double-stranded oligonucleotide. For the pTα^{a} BAC a double-stranded oligonucleotide was generated by annealing two 100bp complimentary primers consisting of 50bp of homology to the 3' end of exon-1 and 50bp of homology from the 5' end of exon-2 (P23 and P24). The annealed P23 and P24 primers was electroporated into SW102 cells containing the *galk*$^{(+)}$ BAC. Homologous recombination by the bacteria resulted in the removal of the *galk* cassette and fusion of exon-1 with exon-2, with the *galk*$^{(-)}$ transformants being selected on deoxy-galactose containing medium.

Figure 5.6

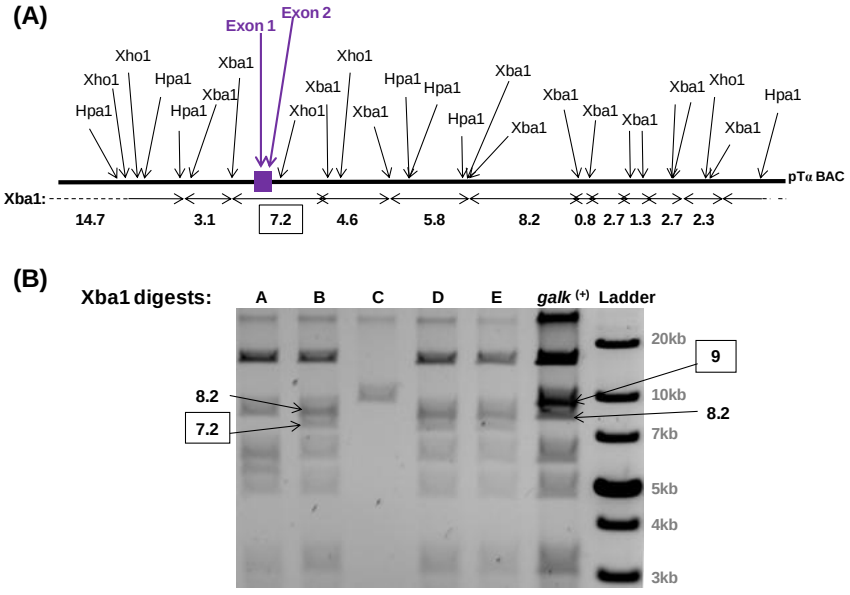

Figure 5.6 Generation of the pTα^{a}-only BAC; Xba1 digests of *galk*$^{(-)}$ clones. (A) A restriction map for Xba1 for the pTα^{a}-only BAC in which exons 1 and 2 have been fused and intron-1 and *galk* removed. The loss of intron-1/*galk* results in a reduction in size of a Xba1 fragment from 9kb to 7.1kb. (B) Xba1 digests for 5 *galk*$^{(-)}$ clones (selected on media containing deoxy-galactose) and the *galk*$^{(+)}$ parent BAC (from the first recombineering step). Three clones appear to have lost the 9kb fragment present in the parent and gained a 7.2kb fragment in its place (B, D and E). Boxes are drawn around the fragment sizes that characterise the recombination event (sizes are in kilobases).

The transformants were analysed by Xba1 digest. Figure 5.6A is an Xba1 restriction map for the pTα^{a}-only BAC. The fusion of exons 1 and 2 reduces the size of a 9kb fragment seen in the parent BAC (*galk*$^{(+)}$ pTα BAC, Figure 5.4B) to 7kb in length. Figure 5.6B shows an Xba1 digest of five *galk*$^{(-)}$ transformants, three of which appear to have lost the 9kb fragment present in the parent BAC and gained a 7kb band (clones B, D and E in Figure 5.6B).

Figure 5.7

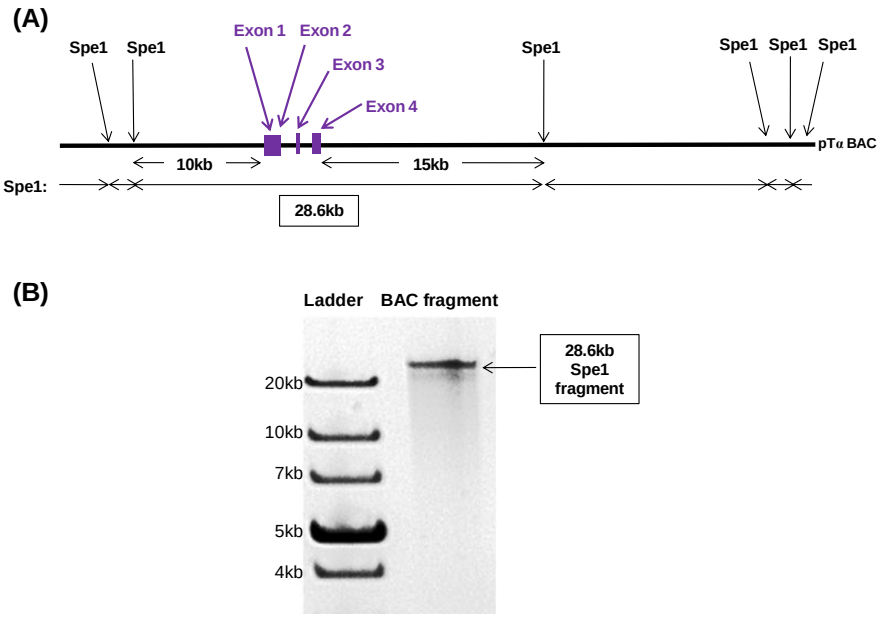

Figure 5.7 Isolation of the pTα^{a}-only fragment for generation of transgenic mice. (A) Spe1 restriction map for the pTα^{a}-only BAC. Spe1 digestion produces a 28.6kb fragment that includes the pTα^{a}-only gene encompassed by 10kb and 15kb of sequence either side. (B) Gel electrophoresis of the pTα^{a}-only gene Spe1 fragment (26.8kb) that was isolated for pro-injection.

Once putative pTα^{a} BACs were identified by restriction digest they were sent for sequencing in the area of the mutated DNA. The pTα^{a} BAC was then digested using Spe1 to generate a 28.6kb fragment with the pTα^{a}-only gene in the centre. Spe1 was used because it cut 10kb upstream of the start site and 15kb downstream of exon-4 therefore ensuring that the regulatory elements for pTα transcription were included in the transgene

(Reizis and Leder, 1999) (Figure 5.7A). Following gel extraction and purification the fragment was resuspended in pro-injection buffer and used for pronuclear injection for generation of a pTα^{a}-only transgenic mouse line (Figure 5.7).

5.5 Generation of the pTα^{b} BAC construct.

The pTα^{b} BAC construct was generated from the same *galk*$^{(+)}$ parent BAC as the pTα^{a} construct (Figure 5.8). Deletion of exon-2, intron-1 and intron-2, and fusion of exons 1 and 3 was achieved by removal of the *galk* sequence using a double-stranded oligo generated by annealing complimentary 100bp primers p31 and p32 (yellow and orange lines in Figure 5.8).

Figure 5.8

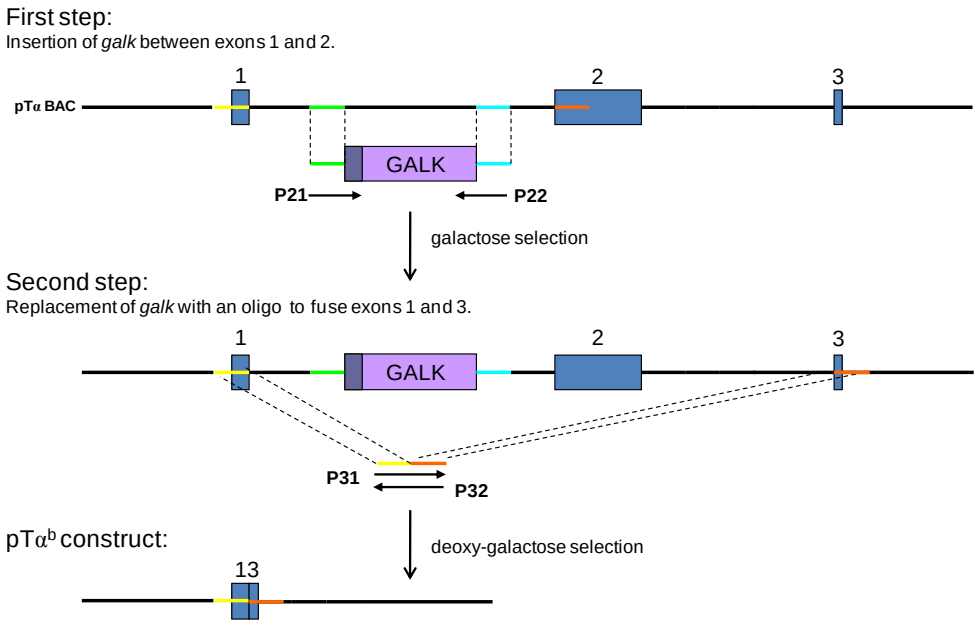

Figure 5.8 A diagram of the recombineering method to generate the "pTα^{b}-only" BAC construct: In the first step *galk* is inserted into a BAC containing the pTα gene, via a *galk* PCR product, by homologous recombination. The *galk* PCR product was generated using primers p21 and p22 that possess 50bp homology to the intron sequence between exons 1 and 2 of pTα (green and turquoise). The *galk*$^{(+)}$ pTα BAC is selected for by the presence of galactose in the medium. *galk* is then replaced by a double stranded DNA oligo (p31+p32) that is homologous to 85bp regions at the 3' end of exon-1 (yellow) and exon-3/intron-3 (orange) of pTα. Thus replacement of *galk* results in fusion of exons 1 and 3 to generate the pTα^{b} construct. The *galk*$^{(-)}$ pTα BAC was selected for on 2-deoxy-galactose containing medium with glycerol as the only carbon source.

P31 consisted of 85bp homology to the 3' region of exon-1 and 15bp homology to the 5' end of exon-3. P32 consisted of 15bp homology to the 3' end of exon-1, all 45bp of exon-3 and 40bp of the 5' end of intron-3. Once the primers were annealed and extended the oligo was then electroprated into SW102 cells containing the *galk*$^{(+)}$ BAC and homologous recombination removed the *galk* cassette by replacing the sequence with that of the oligo resulting in the fusion of exons 1 and 3. Once again *galk*$^{(-)}$ transformants were analysed for identification of the fusion event by Xba1 restriction digest (Figure 5.9A). Figure 5.9B shows Xba1 digests for six *galk*$^{(-)}$ transformants; two putative pTα^{b}-only BAC clones were identified by the loss of the 9kb fragment present in the parent BAC and acquisition of a 5.4kb band (clones A and B in figure 5.9B).

Figure 5.9

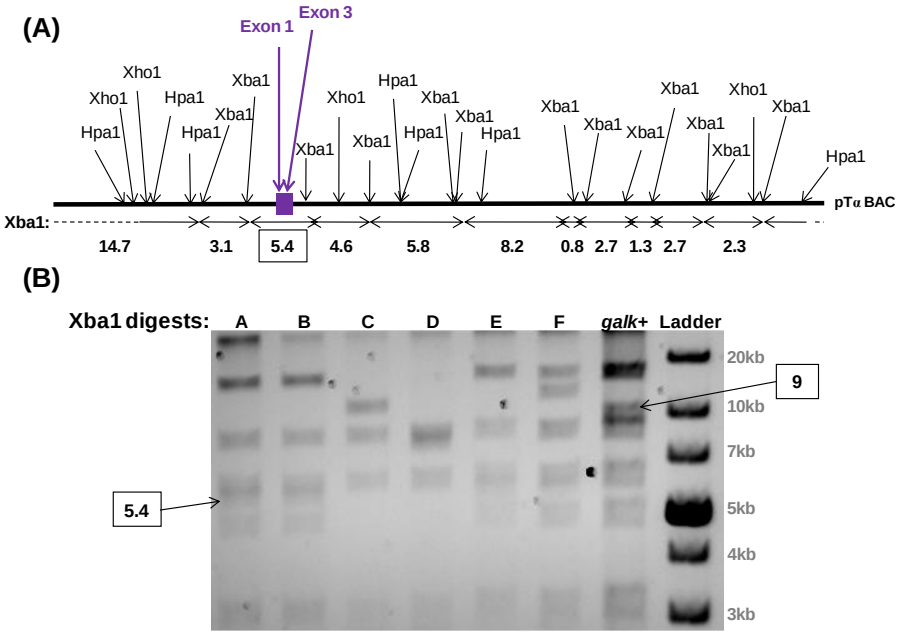

Figure 5.9 Generation of the pTα^{b}-only BAC; Xba1 digests of *galk*$^{(-)}$ clones. (A) A restriction map for Xba1 for the pTα^{b}-only BAC in which exons 1 and 3 have been fused. Fusion of exons 1 and 3 results in a reduction in size of a Xba1 fragment from 9kb to 5.4kb. (B) Xba1 digests for six *galk*$^{(-)}$ clones (selected on media containing deoxy-galactose) and the *galk*$^{(+)}$ parent BAC (from the first recombineering step). Two clones appear to have lost the 9kb fragment present in the parent and gained a 5.4kb fragment in its place (A and B). Boxes are drawn around the fragment sizes that characterise the recombination event (sizes are in kilobases).

The identified pTα^{b}-only BAC was then sent for sequencing before being digested with Spe1 to produce a 25.4kb fragment for proinjection (Figure 5.10A). The quality of the DNA was tested by running it out on an agarose gel (Figure 5.10B).

Figure 5.10

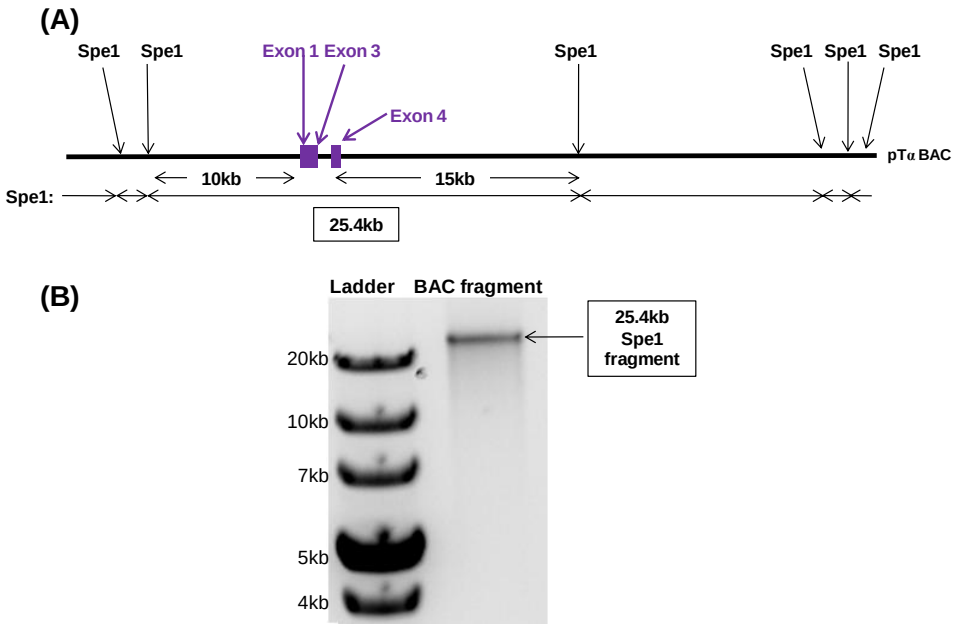

Figure 5.10 Isolation of the pTα^{b}-only fragment for generation of transgenic mice. (A) Spe1 restriction map for the pTα^{b}-only BAC. Spe1 digestion produces a 25.4kb fragment that includes the pTα^{b}-only gene encompassed by 10kb and 15kb of sequence either side. (B) Gel electrophoresis of the pTα^{b}-only gene Spe1 fragment (25.4kb) that was isolated for pro-injection.

5.6 Analysis of pTα^{a}-only BAC transgenic founders.

The pTα^{a}-only transgenic construct was passed to the transgenic core facility at our institute for pronuclear injection into the male pronucleus of CD1 mouse fertilised eggs, as illustrated in Figure 5.11.

Figure 5.11

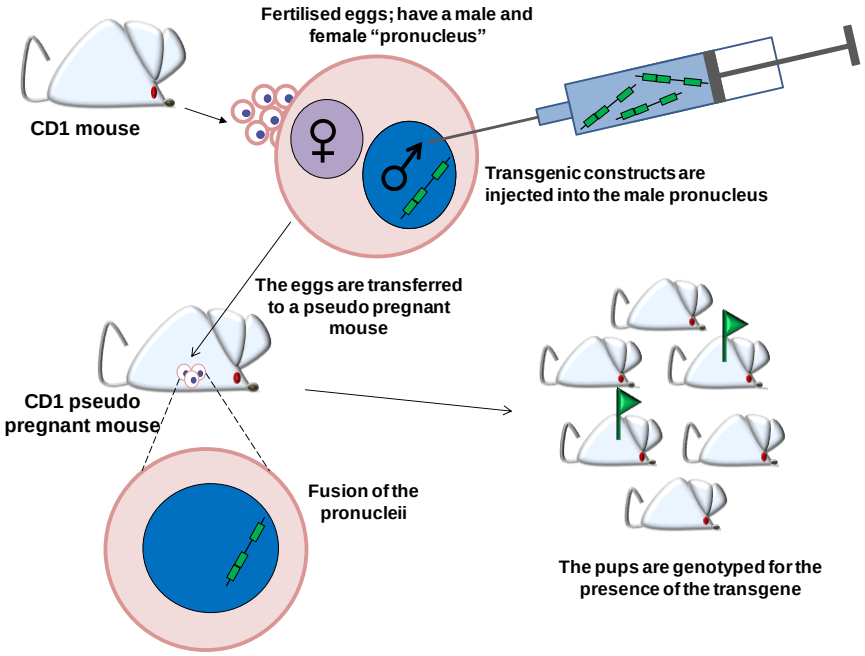

Figure 5.11 Generating a BAC transgenic mouse line: A schematic of the steps involved in generating the BAC transgenic founders. The BAC transgenic constructs were injected into the male pronucleus of CD1 mouse fertilised eggs. Once transferred to a pseudo-pregnant female the pronuclei fuse and the fertilised eggs begin to divide. The litter were genotyped for the presence of the transgene by PCR on genomic DNA.

Once transferred into a pseudo-pregnant female the male pronucleus fuses with the female pronucleus and the fertilised eggs begin to divide. At weaning age the litter was ear-marked and the ear tissue used to extract genomic DNA for genotyping. The samples were genotyped using PCR on genomic DNA. Primers that amplified a 466bp non-coding sequence of the genome 9.5kb upstream of the pTα gene were used for a control PCR to confirm the presence and quality of the DNA (Figure 5.12A). PCR primers

that amplified a 450bp sequence traversing the exon-1 and 2 boundary were used to identify the pTα^{a} transgene as this sequence would not be present in non-transgenic animals.

Figure 5.12

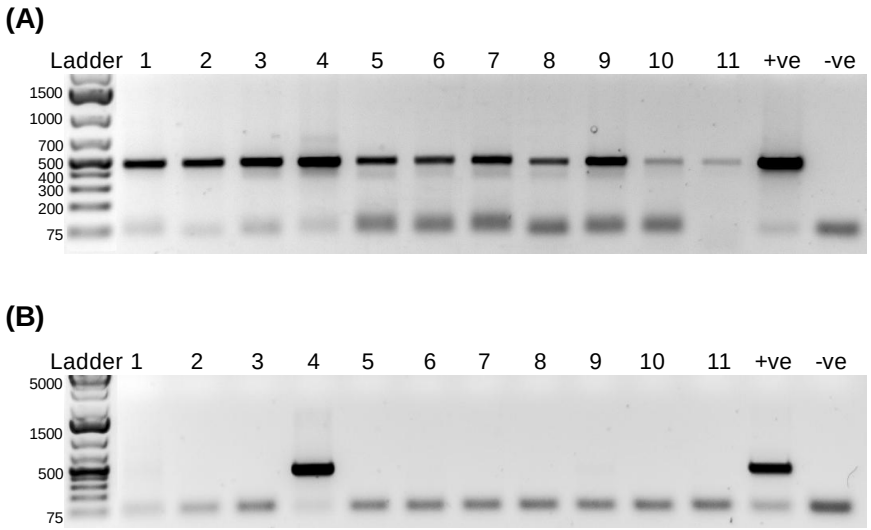

Figure 5.12 Genotyping pTα^{a}-only BAC transgenic founders: 11 pTα^{a}-only BAC transgenic founders were genotyped by PCR. (A) control PCR to confirm the presence and quality of the DNA using primers that amplified a 466bp non-coding sequence 9.5kb upstream of the pTα gene. 2ng of TCRδ KO genomic DNA was used for the positive control. (B) pTα^{a} transgene PCR using primers that amplify a 450bp sequence traversing the exon-1 and 2 boundary unique to the transgene. For the positive control 2ng of TCRδ KO genomic DNA was spiked with the pTα^{a}-only Spe1 fragment.

PCR on genomic DNA from eleven founder pups from the first pTα^{a} transgene pro-injection identified only one transgene positive animal (sample number 4 in Figure 5.12B). This was the first pTα^{a} transgenic founder. This animal was then paired with a pTα$^{-/-}$ x TCRδ$^{-/-}$ double knockout mouse (bred in our lab) in order to generate a "pTα^{a}-only" transgenic mouse on a pTα$^{-/-}$ x TCRδ$^{-/-}$ background.

Figure 5.13 shows the PCR analysis of a litter from a ("pTα^{a}-only" transgenic founder x pTα$^{-/-}$.TCRδ$^{-/-}$) pairing. There were 13 pups in this litter

and despite the fact that not all of the samples came up positive for the genomic DNA test, five of the animals (numbers 4, 6, 8, 9 and 10) were transgene positive.

Figure 5.13

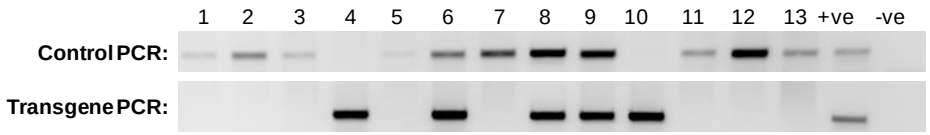

Figure 5.13 Genotyping a "pTα^{a}-only" transgenic founder X pTα$^{-/-}$.TCRδ$^{-/-}$ litter. PCRs for 13 mice from a "pTα^{a}-only" transgenic founder X pTα$^{-/-}$.TCRδ$^{-/-}$ pairing are shown. A control PCR was performed to confirm the presence and quality of the DNA using primers that amplified a 466bp non-coding sequence 9.5kb upstream of the pTα gene. 2ng of TCRδ KO genomic DNA was used as a positive control (+ve). The pTα^{a} transgene PCR was performed using primers that amplified a 450bp sequence traversing the exon-1 and 2 boundary unique to the transgene. For the positive control 2ng of TCRδ KO genomic DNA was spiked with a single copy of pTα^{a}-only Spe1 fragment DNA.

5.7 Initial analysis of pTα^{a}-only mice on a "WT" background.

To initially characterise the "pTα^{a}-only" transgenic mice on a normal "WT" background, two transgene positive and two transgene negative animals were analysed. Figure 5.14 shows FACS analysis on thymocytes for two transgenic positive animals (8 and 9) compared to two transgene negative littermates (1 and 11). Effectively, these transgenic animals (on a WT background) are over expressing pTα^{a}, so a dramatic phenotype was not expected. However, there did appear to be a subtle effect on mature TCRαβ$^{(+)}$ mature thymocytes in transgene positive animals. Thus, whereas normal littermates had 24.0% and 23.7% TCRαβ$^{(hi)}$ cells, this was reduced to 19.3% and 18.7% in transgene positive mice. This result is consistent with pTα^{a} expression reducing the percentage of mature cells. However, the

transgenic mice did not appear to have an overt increase in the ISP population.

Figure 5.14

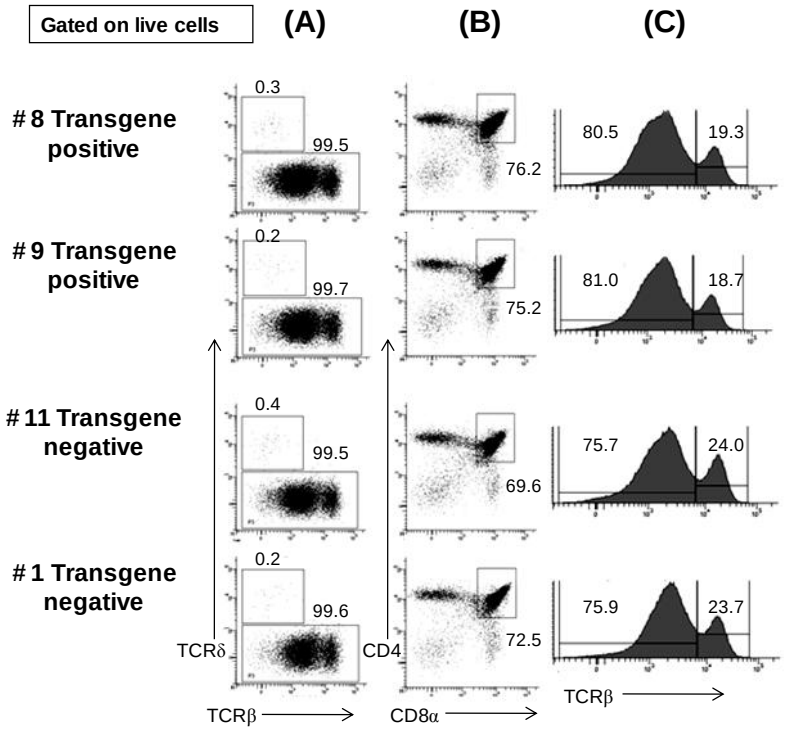

Figure 5.14 FACS analysis of pTα^{a}-only transgenic mice on a "WT" pTα$^{+/-}$ TCRδ$^{+/-}$ background: FACS plots show thymocytes from two pTα^{a}-transgene positive (8 and 9) and two pTα^{a}-transgene negative littermates on a pTα$^{+/-}$ TCRδ$^{+/-}$ background that were analysed for expression of TCRδ, CD4, CD8α and TCRβ. (A) shows the percentage of TCRδ$^{(+)}$ cells, (B) shows the percentage of DP cells, and (C) shows the TCRβ expression profile for each of the mice that were analysed. Live cells are shown and the numbers represent percentages in each of the gates.

5.8 Preliminary analysis of "pTα^{a}-only" BAC transgenic mice on a pTα$^{-/-}$TCRδ$^{-/-}$ background.

After two generations of crossing pTα^{a}-transgene-positive animals with pTα$^{-/-}$ x TCRδ$^{-/-}$ mice, four mice were identified by PCR (as in Figure 5.13) and blood typing as being pTα^{a}-transgene$^{(+)}$ pTα$^{-/-}$. In addition to these, two littermates were identified as pTα^{a}-transgene$^{(+)}$ pTα$^{+/-}$ and two as pTα^{a}-transgene$^{(-)}$ pTα$^{(-/-)}$. Flow cytometric analysis of the blood of these animals showed that γδ T cells were found in all of the mice that were analysed

(data not shown), suggesting that each of these mice had at least one intact TCRδ allele. Comparison of the ratio of $CD4^{(+)}$ and $CD8^{(+)}$ T cells in blood was helpful in determining the pTα gene status of the mice. $pT\alpha^{+/+}$ or $pT\alpha^{+/-}$ (i.e. WT for pTα) mice appear to have a greater proportion of $CD4^{(+)}$ T cells in the blood compared with mice that lack the pTα gene (Figure 5.15). For example the CD4/CD8 ratio in the blood of $pT\alpha^{+/+}$ mice is higher at 4.2 compared with that of the $pT\alpha^{-/-}$ mice at 1.4 (Figure 5.15). Interestingly, the presence of the $pT\alpha^{a}$-transgene did not appear to significantly increase the CD4/CD8 ratio of a $pT\alpha^{-/-}$ background (Figure 5.15).

Figure 5.15

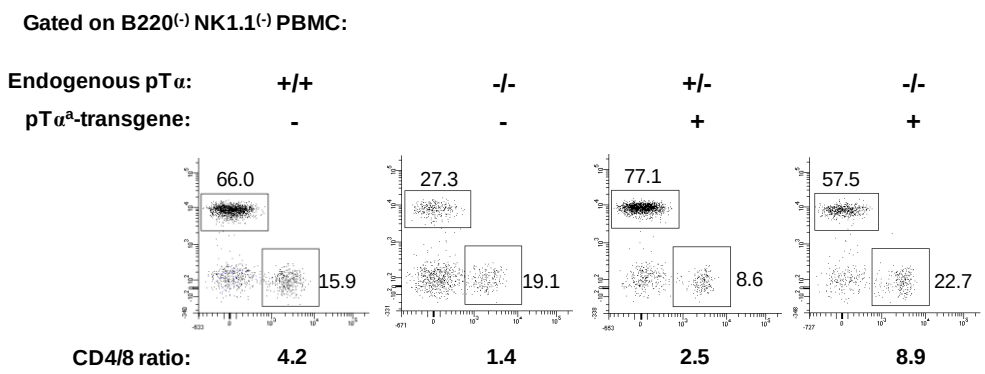

Figure 5.15 Analysis of PBMC from $pT\alpha^{a}$-transgenic mice on different pTα backgrounds: Analysis of CD4 and CD8 T cell populations in the blood of $pT\alpha^{+/+}$, $pT\alpha^{-/-}$, $pT\alpha^{a}$-$transgene^{(+)}pT\alpha^{+/-}$ and $pT\alpha^{a}$-$transgene^{(+)}pT\alpha^{-/-}$ mice. Cells shown are $B220^{(-)}NK1.1^{(-)}$. Numbers indicate the percentages of cells in each gate.

Analysis of the thymus of $pT\alpha^{a}$-$transgene^{(+)}$ $pT\alpha^{-/-}$ mice revealed that $pT\alpha^{a}$ transgene expression was able to largely rescue thymus size, as these mice (on average) had approximately $8.5x10^{7}$ cells compared with $2x10^{7}$ cells observed for pTα-deficient animals (Figure 5.16). However, the rescue does not appear to be complete as the size of the $pT\alpha^{a}$-$transgene^{(+)}$ $pT\alpha^{-/-}$ thymus was 2.3 fold less than the $pT\alpha^{+/+}$ thymus which consisted of approximately $2x10^{8}$ cells (Figure 5.16). The size of the $pT\alpha^{a}$-$transgene^{(+)}$ $pT\alpha^{+/-}$ thymus, however, did resemble that of the WT at $1.9x10^{8}$ cells.

Figure 5.16

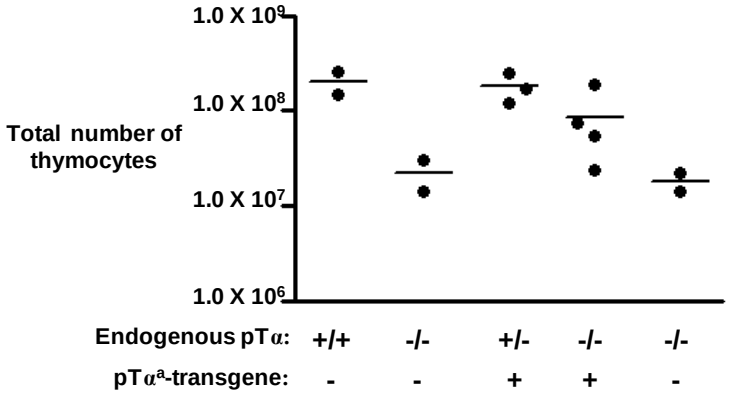

Figure 5.16 pTα^a expression partially restores the thymus size of pTα$^{-/-}$ mice. Total cell counts from thymuses from pTα$^{+/+}$, pTα$^{-/-}$,pTα^a-transgene$^{(+)}$pTα$^{+/-}$, pTα^a-transgene$^{(+)}$pTα$^{-/-}$ and pTα^a-transgene$^{(-)}$pTα$^{-/-}$ (littermates). Each dot represents an individual animal.

5.9 The pTα^a-transgene partially rescues αβ T cell development in a pTα$^{-/-}$ background.

Consistent with the FTOC results and the increase in thymus size, pTα^a expression largely rescued αβ T cell development in pTα-deficient animals, resulting in the reduction in the percentage of γδ cells in the thymus (Figure 5.17A). Whereas, the percentage of γδ cells in the pTα$^{-/-}$ thymus was found to be ~13% (~7% for pTα$^{-/-}$ littermate), only ~1.2% of the pTα^a-transgene$^{(+)}$ pTα$^{-/-}$ thymocytes were TCRδ$^{(+)}$. However, the percentage of γδ cells in the pTα^a-transgene$^{(+)}$ pTα$^{-/-}$ thymus was approximately 5 fold greater than that observed for pTα$^{+/+}$ and pTα$^{+/-}$ animals (Figure 5.17A), perhaps indicating that the rescue was not complete.

The expression of the pTα^a-transgene restored the proportion of DPs to approximately 60% in comparison with ~20% in pTα-deficient mice (Figure 5.17B). Once again however, the restoration of αβ T cell development promoted by pTα^a expression in pTα-deficient thymocytes does not appear to be complete, as the percentage of DPs in these mice was not equivalent

to that observed for pTα$^{+/+}$ or pTα$^{+/-}$ animals, which had a larger proportion of DPs (79.4% and 73.6%, respectively) (Figure 5.17B). These results suggest that either the transgene is not expressed appropriately in these mice (despite expressing all the necessary pTα regulatory elements) or that pTα^{a} alone is not sufficient to completely rescue T cell development in a pTα-deficient background.

Figure 5.17

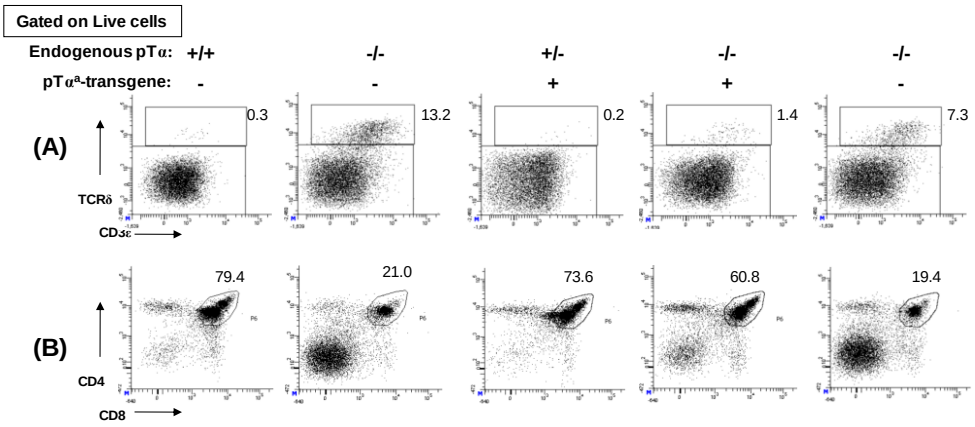

Figure 5.17 pTα^{a}-transgene expression partially rescues αβ T cell development in pTα$^{-/-}$ mice. Representative FACS plots showing thymocytes from pTα$^{+/+}$, pTα$^{-/-}$,pTα^{a}-transgene$^{(+)}$pTα$^{+/-}$, pTα^{a}-transgene$^{(+)}$pTα$^{-/-}$ and pTα^{a}-transgene$^{(-)}$ pTα$^{-/-}$ (littermates) were analysed for expression of TCRδ, CD3ε (A) and CD4 and CD8 (B). Numbers indicate percentages in each gate.

5.10 Analysis of the DN compartment in pTα^{a}-transgenic mice.

To further investigate the nature of the incomplete rescue of αβ T cell development in these pTα^{a}-transgenic mice, DN thymocytes, specifically DN3 and DN4, were analysed in more detail. In the thymus of pTα$^{+/+}$ mice ~37% of DN thymocytes were DN3 with ~40% being DN4 (Figure 5.18). In the absence of a preTCR, the majority of thymocytes are arrested at the DN3 stage. This can be seen in the pTα-deficient thymuses in which ~90% of DN thymocytes were DN3, with only ~5% DN4. In the presence of the pTα^{a}-transgene in a pTα-deficient background the percentage of DN3s was

reduced to ~73% and the proportion of DN4s was increased slightly to ~12% (Figure 5.18). This appears to be consistent with evidence from the percentages of both γδ and DP thymocytes, suggesting only a partial rescue of the pTα$^{-/-}$ phenotype. Progression of DN3 cells to the DN4 stage was not inhibited by the pTα^{a}-transgene in pTα$^{+/-}$ thymocytes (Figure 5.18).

Figure 5.18

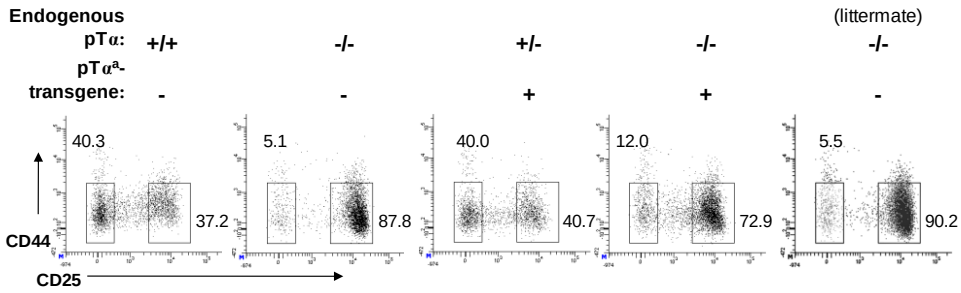

Figure 5.18 Analysis of DN thymocytes from pTα^{a}-transgenic mice. Representative FACS plots showing the percentages of DN3 and DN4 thymocytes from pTα$^{+/+}$, pTα$^{-/-}$, pTα^{a}-transgene$^{(+)}$pTα$^{+/-}$, pTα^{a}-transgene$^{(+)}$pTα$^{-/-}$ and pTα^{a}-transgene$^{(-)}$pTα$^{(-/-)}$ (littermates) mice. Cells are TCRδ$^{(-)}$B220$^{(-)}$NK1.1$^{(-)}$CD4$^{(-)}$CD8$^{(-)}$ that were analysed for CD25 and CD44 expression. DN3 cells are CD44$^{(-)}$CD25$^{(+)}$ and DN4 are CD44$^{(-)}$CD25$^{(-)}$. Numbers indicate percentages in each gate.

5.11 pTα^{a}-transgenic mice do not accumulate ISP cells.

Expression of the pTα^{a}-transgene restored development of a normal proportion of mature TCRβ$^{(hi)}$ cells in a pTα-deficient background. pTα$^{-/-}$ mice have only ~3.5% TCRβ$^{(hi)}$ cells, but this jumped to ~15% in the presence of the pTα^{a}-transgene (Figure 5.19A).

Importantly, when TCRβ$^{(lo)}$CD8$^{(+)}$CD4$^{(-)}$ ISP cells were assessed, there was no apparent accumulation of ISP cells in the thymuses of pTα^{a}-transgene$^{(+)}$ pTα$^{-/-}$ animals (in comparison with pTα$^{+/+}$ and pTα$^{-/-}$ mice) (Figure 5.19B). Indeed, a low percentage (~2.4%) was observed in all the mice analysed. These results suggest that the increased proportion of ISPs and fewer

TCRβ$^{(hi)}$ cells, observed for pTα^{a} expression in FTOC may have been a direct result of prolonged constitutive expression of pTα^{a} from the retroviral promoter. Thus, in the pTα^{a}-transgenic mouse, in which the expression of pTα^{a} is under control of endogenous regulatory elements, this phenotype is not observed.

Figure 5.19

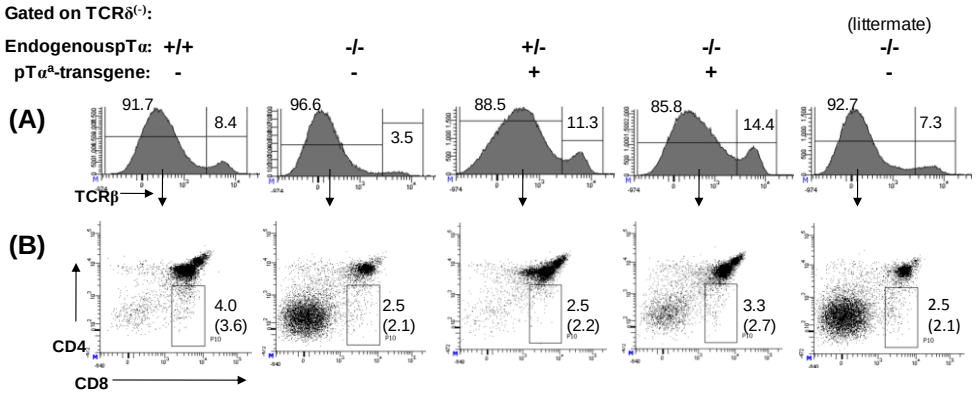

Figure 5.19 ISP thymocyte development is not promoted by pTα^{a} transgene expression: Representative FACS plots showing thymocytes from pTα$^{+/+}$, pTα$^{-/-}$, pTα^{a}-transgene$^{(+)}$pTα$^{+/-}$, pTα^{a}-transgene$^{(+)}$pTα$^{-/-}$ and pTα^{a}-transgene$^{(-)}$pTα$^{(-/-)}$ (littermates) mice that were analysed for TCRβ, CD4 and CD8. (A) TCRβ surface expression of TCRδ$^{(-)}$ cells is shown. (B) TCRβ$^{(lo)}$ thymocytes from (A) were analysed for expression of CD4 and CD8 to determine the percentage of ISPs. Numbers indicate percentages in each gate numbers in brackets represent percentages from the live gate.

5.12 Analysis of phosphor-ERK levels in DP cells from pTα^{a}-transgenic mice.

The restoration of a normal TCRβ$^{(hi)}$ population by expression of the pTα^{a}-transgene suggests that positive selection of DP cells is rescued in pTα^{a}-transgenic animals. To investigate further, DP thymocytes from pTα^{a}-transgene$^{(+)}$pTα$^{-/-}$ mice were analysed for “ERK-sensitivity”. As described in the previous chapter, the preTCR may be required for regulating signalling thresholds for TCRαβ during positive selection. Cross-linking of WT DP

thymocytes with anti-CD3ε antibody resulted in rapid and transient phosphorylation of ERK1/2, while ERK1/2 phosphorylation was drastically reduced in pTα-deficient DPs (Figure 5.20). Cross-linking of TCRαβ in $pT\alpha^{-/-}$ DP thymocytes expressing the $pT\alpha^{a}$-transgene resulted in ~30% phosphor-$ERK^{(+)}$ cells after 1 minute. This was greater than that observed for WT controls (only 15-20% phosphor-ERK).

Figure 5.20

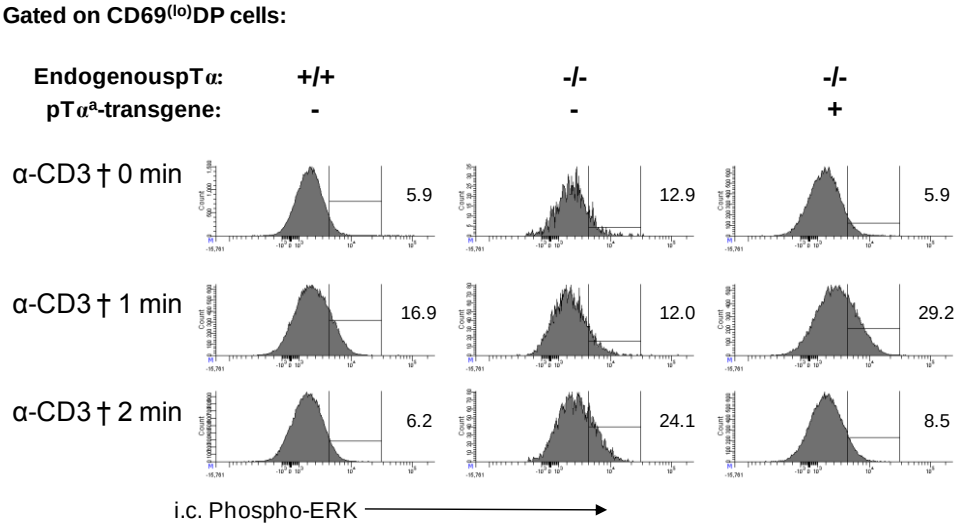

Figure 5.20 $pT\alpha^{a}$–transgene expression restores the "ERK-sensitivity" of $pT\alpha^{(-/-)}$ DP thymocytes: Representative FACS plots of $CD69^{(lo)}$DP thymocytes from $pT\alpha^{+/+}$, $pT\alpha^{-/-}$, $pT\alpha^{a}$-$transgene^{(+)}pT\alpha^{-/-}$ mice that were analysed for intracellular ERK1/2 phosphorylation at time-zero (0 min) and after 1, and 2 minutes cross-linking of anti-CD3ε. Numbers represent percentages of cells within the gates.

Interestingly, the kinetics for WT cells, and $pT\alpha^{-/-}$ cells expressing $pT\alpha^{a}$ were very different to the phosphor-ERK kinetics of pTα-deficient DP cells. The latter display a more gradual and sustained increase in phosphor-ERK rather than a rapid transient burst. This may have important implications for both positive and negative selection in these cells, as will be discussed later. It should also be noted that this result is in contrast to the FTOC result in which retroviral expression of $pT\alpha^{a}$ was not able to rescue the ERK-sensitive state of $CD69^{(lo)}$ pTα-deficient DPs. Thus the precise timing and

regulation of pTα^{a} may be very important in setting appropriate selection thresholds for TCRαβ signalling in pre-selection DP thymocytes.

5.13 Summary.

In summary, BAC-transgenic mice that express pTα^{a} under pTα regulatory elements in the absence of pTα^{b} have been generated. T cell development is largely rescued when these mice are crossed onto a pTα$^{-/-}$ background as the proportion of γδ cells is reduced and the percentage of DP cells increased. Furthermore, expression of pTα^{a} restores development of mature TCRβ$^{(hi)}$ cells in the thymus, possibly as a result of restoration of positive selection thresholds for TCRαβ signalling in DP cells. Despite the apparent functionality of preTCR^{a}, T cell development in the pTα^{a}-transgenic pTα$^{-/-}$ mice is not absolutely comparable to that of pTα$^{+/+}$ mice. The size of the thymus is distinctly smaller and the percentage of DP cells marginally less than WT. Interestingly, a large percentage of pTα^{a}-transgenic pTα$^{-/-}$ thymocytes remain DN3 and do not appear to downregulate CD25, possibly explaining the differences in T cell development observed at later stages. However, very importantly, an accumulation of ISP cells is not observed in pTα^{a}-transgenic pTα$^{-/-}$ mice. This suggests that termination of pTα^{a} expression is vital for appropriate T cell development, and continued expression, as observed when pTα^{a} is expressed from a retroviral promoter in FTOC, leads to a developmental block at the highly proliferative ISP stage. As proliferation is one of the pre-requisites for oncogenesis, this conclusion has important implications for T cell leukaemia.

Conclusions and Discussion

Conclusions and Discussions

A functional *ptcra* gene is essential for adaptive immunity, as αβ T cell development is severely compromised in the absence of a preTCR (Fehling et al., 1995a). This and other observations initially suggested that the preTCR possessed unique qualities that "instructed" an αβ T cell fate in uncommitted DN progenitors (Borowski et al., 2004; Saint-Ruf et al., 2000). Nonetheless, both TCRγδ (Buer et al., 1997a) and a prematurely expressed transgenic TCRαβ (Lacorazza et al., 2001b), were later shown to partly drive αβ T cell development in a preTCR-deficient background. By way of explanation, it emerged that a key component of fate determination was the strength of signal delivered by a TCR complex at the DN stage (Haks et al., 2005; Hayes et al., 2005). Thus, the preTCR, that provides a weak signal due to its low surface expression, drives αβ T cell development, while TCRγδ, that generally signals more strongly, drives commitment to a γδ cell fate (Pennington et al., 2005). Although providing a compelling model for αβ lineage commitment at the DN stage, these studies did not focus on the DP products of preTCR-driven differentiation. Indeed, it was assumed that αβ -committed DP cells were a homogenous pool of progenitors for subsequent selection events mediated through the αβTCR. More recently, this view has changed, with several studies suggesting heterogeneity in the DP population that may subsequently influence the type of T cell generated, be it conventional αβ T cells, regulatory T cells (Pennington et al., 2006; van Santen et al., 2004), or T cells destined for the epithelial layers of the gut (Gangadharan et al., 2006).

The mechanism for generation of heterogeneity in the DP pool has been a principle focus of this thesis. We hypothesised that heterogeneity in post-β-selection thymocytes arose from differential use of a preTCR formed with either pTα^{a}, or the splice variant of pTα that lacks the extracellular Ig-loop, pTα^{b}. We hypothesised that preTCR^{a} and preTCR^{b} signal differently to promote differential T cell developmental outcomes.

To directly address our hypotheses we aimed to characterise expression of pTα^{a} and pTα^{b} in the thymus, on the population level and at the single cell level. In addition, our aim was to investigate the function of pTα^{a} and pTα^{b} when expressed in isolation in pTα-deficient thymocytes, and to generate BAC-transgenic mice where expression of pTα^{a} and pTα^{b} is controlled by endogenous regulatory elements.

1.1 pTα^{a} and pTα^{b} expression in the thymus

Semi-quantitative PCR for pTα^{a} and pTα^{b} revealed that both isoforms are expressed as early as DN2 cells, with expression appearing to peak in the DN3 and DN4 subsets, correlating with β-selection. Relative expression of pTα^{a} and pTα^{b} appears to decrease after the DN4 stage, as ISPs and DPs expressed lower levels of pTα^{a} and pTα^{b} RNA. Thus, pTα^{b} appears to share the same expression pattern as pTα^{a} in DN2, DN3, DN4 and ISP subsets, being similar to that already described for pTα (pTα^{a}) (Saint-Ruf et al., 1994). However, DP thymocytes appeared to express more pTα^{b} than pTα^{a}. This suggests that the regulation of splicing of the primary pTα transcript is biased in DP thymocytes to favour production of pTα^{b}.

Transcripts for pTα^{b} were also found in greater abundance than those for pTα^{a} in CD4 SP thymocytes, consistent with observations in TCRα KO mice from which pTα^{b} was first identified (Barber et al., 1998). In this report it was

shown that TCRβ$^{(+)}$ CD4 peripheral T cells ("β"-only cells) from TCRα KO mice expressed pTα^{b} but not pTα^{a} (Barber et al., 1998). In a recent report peripheral Foxp3$^{(+)}$ T-regs were shown to express pTα, predominantly in the form of pTα^{b} (Campese et al., 2009). Thus, the expression observed for pTα^{b} in CD4 SPs may be a representation of pTα^{b} expression in T-regulatory cells, or perhaps "β-only" cells, in the thymus. It would be interesting to investigate this further, perhaps by analysing CD25$^{(+)}$ CD4SP cells, or looking in Foxp3-GFP transgenic mice (Fontenot et al., 2005).

Thymic precursors of CD8αα$^{(+)}$TCRαβ$^{(+)}$ intraepithelial lymphocytes of the gut have been identified within the DP subset. In addition to CD4 and CD8αβ, these cells express the CD8αα homodimer and are termed "triple positive" (TP). In an adult thymus TPs constitute approximately 7% of the DP subset (Gangadharan et al., 2006). At embryonic day 17, however, 60% of DPs were found to express CD8αα. TP thymocytes can be distinguished from DPs by staining with fluorochrome-conjugated, thymic leukaemia (TL) tetramers. PCR analysis of CD4$^{(+)}$CD8β$^{(+)}$TL$^{(+)}$ (TP) and TL$^{(-)}$ (DP) thymocytes from E17 C57BL/6 mice, revealed that both TL$^{(+)}$ and TL$^{(-)}$ thymocytes appeared to express similar levels of pTα^{a} and pTα^{b}. This would suggest that unconventional and conventional T cell precursors in the thymus do not differentially use pTα^{a} and pTα^{b}. Thus, the heterogeneity observed in the TP population is not explained by the use of either preTCR^{a} or preTCR^{b}. This might suggest that TCRβ has a more prominent role at the β-selection checkpoint than is currently believed.

Our initial hypothesis stated that differential use of a preTCR formed with either pTα^{a} or pTα^{b} by progenitor thymocytes would promote different T cell developmental outcomes. Thus, single cell PCR for pTα^{a} and pTα^{b} was set up to directly test whether individual DN3 and DN4 cells expressed either

pTα^{a} or pTα^{b} or both pTα^{a} and pTα^{b}. The assay has been optimised. However, due to time constraints, these experiments have not been completed, and therefore this question remains to be answered. Nevertheless, single cell PCR is a very useful tool and now that the technique has been established, will prove to be very beneficial for future research in the lab.

1.2 preTCR^{a} and preTCR^{b} promote different T cell development.

The alternatively-spliced isoform of pTα, pTα^{b}, was initially identified as forming a signalling-competent preTCR complex *in vitro* (Barber et al., 1998). Subsequently, pTα^{b} was shown to largely rescue T cell development when expressed as a transgene from the p56^{lck} promoter in pTα-deficient mice (Gibbons et al., 2001). However, only steady-state conditions were assessed in these animals, and variation in transgene copy number and integration site meant a direct comparison between preTCR^{b}-driven and preTCR^{a}-driven T cell development was unfeasible. Here, by using FTOC to carefully track T cell development over time, we reveal that early steps of thymocyte development mediated by preTCR^{a} and preTCR^{b} are not equivalent; preTCR^{a} drives sustained expansion of the immature ISP subset, while preTCR^{b} promotes the rapid development of TCRαβ$^{(hi)}$ SP cells.

The observed difference in development promoted by preTCR^{a} and preTCR^{b} suggests that the two receptors produce qualitatively different signals. Both pTα^{a} and pTα^{b}, however, share an identical intracellular domain. Consistent with observations *in vitro* (Barber et al., 1998), our data demonstrate that surface expression of preTCR^{b} is significantly greater than preTCR^{a} in γδ$^{(-)}$, immature thymocytes. Surface expression of TCRs

on DN thymocytes has been shown to positively correlate with signal strength (Hayes et al., 2005). As signal strength has profound effects on DN cell development (Haks et al., 2005; Hayes et al., 2005), it is possible that differential surface expression of preTCR^{a} and preTCR^{b}, and hence signalling capacity, underpins the differential developmental potential of pTα^{a}- and pTα^{b}-expressing DN cells.

1.3 Differential surface expression distinguishes the function of preTCR^{a} and preTCR^{b}.

Surface expression of the preTCR is known to be regulated by pTα (Carrasco et al., 2003; Panigada et al., 2002). Indeed, it was recently shown that four charged amino acids in the extracellular domain of full-length pTα (i.e. pTα^{a}) were necessary for pTα oligomerization and subsequent internalisation of the receptor (Yamasaki et al., 2006). Moreover, this study claimed that pTα oligomerization was essential for ligand-independent signalling from the preTCR and hence its function.

Here, our data confirm that pTα^{b}, which lacks three of these four "essential" amino acids (D22, R24, and R102), forms a preTCR in DN thymocytes that can signal to drive thymocyte development beyond the β-selection checkpoint. A pTα^{b} R117A mutant, that lacks the remaining charged residue, can also drive thymocyte development in a manner indistinguishable to that of pTα^{b}. Furthermore, a pTα^{a} DRR mutant, in which the three charged amino acids unique to pTα^{a} were mutated to alanine, induced increased TCRβ surface expression and a pattern of thymocyte development comparable to that seen for preTCR^{b}.

Thus, our results demonstrate that pTα oligomerization is not essential for preTCR signalling *per se*. Instead, oligomerization of pTα^{a} limits preTCR^{a}

surface expression in DN cells, driving prolonged expansion of the ISP subset toward the DP stage. By contrast, pTα^{b}, which lacks three of the four amino acids required for pTα^{a} oligomerization, permits preTCR^{b} to be expressed at higher surface levels than preTCR^{a}. This drives rapid development of DN cells through to mature TCRαβ$^{(hi)}$ SP cells.

1.4 Ligand-independent signalling at the β-selection checkpoint.

Our data demonstrate that regions of the pTα chain that mediate preTCR oligomerization are not required for signal initiation in DN thymocytes. These results have led us to consider alternative hypotheses for the mechanism of signal initiation at the β-selection checkpoint. Thus, we propose that ligand independent signalling is a property conferred to DN cells by the presence of unbound, readily available, "free" Lck at the cell surface. Lck is the most upstream signalling molecule in the TCR signal transduction pathway (Molina et al., 1992). Lck molecules are trafficked to the cell membrane soon after their synthesis (Bijlmakers et al., 1997; Bijlmakers and Marsh, 1999). In DP or SP cells, the majority of Lck molecules at the cell surface are bound to the cytoplasmic tails of the co-receptor molecules CD4 and CD8 (Figure 1.1) (Van Laethem et al., 2007; Veillette et al., 1988). In order to signal, TCR complexes expressed at the surface of DP cells must interact with peptide/MHC in order to aggregate and recruit either CD4 or CD8 into the TCR complex, thus bringing Lck into close proximity of the intracellular domains of the various CD3 chains. Co-receptor molecules, therefore, enforce MHC-specificity in the developing T cell repertoire (Van Laethem et al., 2007).

DN cells by definition lack both CD4 and CD8. Thus a pool of "free" Lck is readily accessible to TCR complexes expressed at the cell membrane (Van

Laethem et al., 2007). Because of this ligand-independent TCR signalling in DN thymocytes may simply be a consequence of the pairing of appropriately matched TCR chains, which has the result of bringing together CD3ε containing cassettes in the presence of readily accessible "free" Lck. Indeed, early expression of a CD8 transgene effectively sequesters "free" Lck in DN thymocytes, limiting the availability of Lck for ligand-independent signalling and inhibiting their development to DP stage (Wack et al., 2000).

Figure 1.1

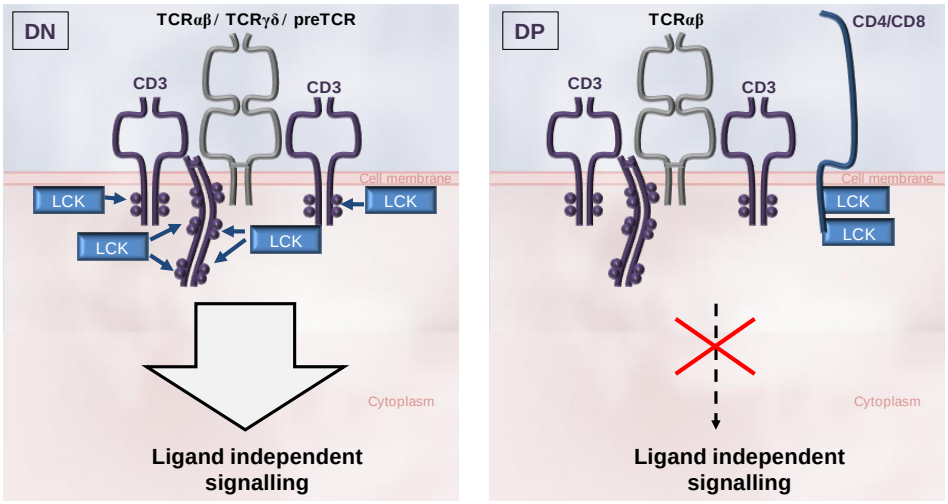

Figure 1.1 Availability of "free" Lck determines ligand independent signalling in thymocytes: DN thymocytes do not express co-receptors CD4 and CD8 therefore all of the Lck expressed by these cells is available at the cell membrane to activate TCR complexes and initiate ligand independent signalling. The nature of the TCR is not important; αβ , γδ or preTCR, as long as 2 CD3 dimers are associated in the proximity of the "free" Lck. In DP thymocytes CD4 and CD8 co-receptors bind with high affinity Lck; limiting the amount of "free" Lck available to interact with TCR complexes and prohibiting ligand independent signals.

This view on the mechanism that underpins ligand-independent signalling allows us to suggest that the acquisition of CD4 and CD8 during DN-DP development marks the transition from a cell that is able to support ligand-independent signalling to one that cannot. Thus in DP cells the association of two CD3ε containing molecules (i.e. CD3εγ or CD3εδ), mediated by

pairing of two TCR chains is not sufficient to induce TCR signalling as “free” Lck has been sequestered by CD4 and CD8 (Figure 1.1).

This proposed mechanism would also neatly explain why cross-linking of CD3ε by monoclonal antibodies on RAG-deficient (DN) thymocytes (Shinkai and Alt, 1994), or dimerization of a huCD8-CD3ε fusion protein in RAG-deficient thymocytes (Yamasaki et al., 2006), both efficiently promote progression past the β-selection checkpoint. Furthermore, it helps to explain the observation that ligand-independent signalling does not appear to be intrinsic to the receptor expressed at the surface of DN thymocytes; as the αβ TCR, γδTCR as well as several mutant forms of the preTCR are all able to drive β-selection (Gibbons et al., 2001; Haks et al., 2003; Haks et al., 2005; Irving et al., 1998).

1.5 Sustained expression of preTCR^{a} but not preTCR^{b} is detrimental to normal T cell development.

Towards the end of this work, preliminary, characterisation of transduced thymocytes in FTOC suggested that preTCR^{a} induced greater IL-7Rα expression on γδ$^{(-)}$ TCRβ$^{(lo)}$, immature thymocytes than preTCR^{b}. This observation may help to explain the developmental phenotype promoted by preTCR^{a}. IL-7 signalling promotes survival and proliferation of β-selected thymocytes (Trigueros et al., 2003). However, this preTCR-induced IL-7Rα upregulation appears to be transient as IL-7Rα expression is terminated at the ISP stage (Yu et al., 2004). IL-7 signalling inhibits expression of transcription factors TCF-1, LEF-1 and RORγt that are required for the ISP to DP transition in the thymus (Yu et al., 2004). Indeed, treatment of E15.5 thymocytes with IL-7 interfered with DP and SP cell development resulting in an increase in the DN and ISP thymocyte populations (Yu et al., 2004). Thus, the effect of sustained IL-7 signalling around the β-selection

checkpoint resembles the phenotype observed for pTα^a expression in FTOC, with accumulation of the ISP subset.

Egr3 is also transiently upregulated following preTCR signalling and induces proliferation of post-β-selected thymocytes (Xi et al., 2006). Importantly, sustained Egr3 transgene expression in RAG KO mice also promotes the development and accumulation of ISP thymocytes (Carleton et al., 2002). A similar phenotype was observed in mice that are deficient for the E-protein, HEB (Barndt et al., 1999). preTCR signalling is known to upregulate the inhibitor of E-proteins, Id3, that allows subsequent thymocyte proliferation (Koltsova et al., 2007). Thus, it is possible that preTCR^a promotes the inhibition of E-proteins via Egr3 and Id3 that, if pTα^a expression is prolonged, promotes the continued proliferation of ISPs and prevents their differentiation to the DP stage. Importantly, the accumulation of the ISP subset is not observed in BAC transgenic pTα^a-only mice that express pTα^a under the pTα regulatory elements. Presumably this is because unlike in FTOC, pTα^a is shut-off at an appropriate stage in these animals. These results emphasise the importance of transcriptional control of pTα^a around the β-selection checkpoint, and suggests that a negative feedback mechanism, by which preTCR signals downregulate pTα transcription may be in operation (Saint-Ruf et al., 1994; Yashiro-Ohtani et al., 2009). Alternatively, splicing of the pTα transcript away from pTα^a toward predominantly pTα^b transcripts may attenuate the effects of preTCR^a (see later). This would be an important area of further investigation along with the transcriptional relationship between pTα and TCF-1, LEF-1, Egr3, Id3, HEB and RORγt.

pTα expression is regulated by Notch and transgenic mice expressing intracellular Notch3 under the control of the proximal Lck promoter develop

T cell lymphomas that express pTα (Bellavia et al., 2000). Deletion of pTα in Notch3 transgenic mice abrogates tumour development, indicating a role for pTα in T cell leukemogenesis (Bellavia et al., 2002). Furthermore, human T-acute lymphoblastic leukaemias (T-ALL) have been shown to express pTα (Bellavia et al., 2002). Thus, the ISPs that accumulate as a result of sustained preTCR^{a} signalling could represent a subset of cells that are prone to oncogenesis, because of their continued proliferation and inhibited differentiation. These results suggest that constitutive expression of pTα^{a} is detrimental to normal T cell development and may underlie a possible mechanism of tumourogenesis. Clearly these are areas that warrant further investigation.

1.6 The function of pTα^{b}.

One of the major initial aims of this thesis was to ascribe a definitive role to the second isoform of pTα; pTα^{b}. Unfortunately, this is one area of the work where questions remain unanswered. Nonetheless, much important information regarding pTα^{b} has been discovered (see pervious discussion points), both for the protein itself, and for its relationship with pTα^{a}. pTα^{a} appears to be dominant to pTα^{b} when expressed in the same cell. Dominance of pTα^{a} over pTα^{b} may be a direct result of the superior ability of pTα^{a} to bind TCRβ and therefore promote low surface expression of the preTCR through receptor oligomerization and internalisation. This would imply that the function of preTCR^{b} would only be effective in cells in which pTα^{b} is expressed more abundantly than pTα^{a}. Our expression data suggests that DP cells express more pTα^{b} than pTα^{a} and preTCR^{b} signalling appears to promote the DP to SP transition very efficiently in FTOC. This would perhaps suggest a role for pTα^{b} in either the establishment of the DP stage, or in the efficient transition of DP

thymocytes to the SP stage. Although a definitive answer is not presently at hand, the section below discusses this in more detail.

1.7 The preTCR may particitpate in the establishment of TCR signalling thresholds in DP thymocytes.

DP thymocytes undergo important selection events based on the strength and duration of signalling through their TCRs that determine their fate. High-affinity self-antigen-MHC interactions induce strong TCR signals in DP thymocytes, resulting in death by apoptosis (negative selection), while low-affinity interactions between TCR and self-peptide-MHC direct differentiation to the SP stage (positive selection). It has been reported that prolonged signalling via calcineurin and NFAT induces an "ERK-sensitized" state in pre-selected DPs that allow them to differentiate in response to "weak" positively selecting signals (Gallo et al., 2007). However, the origin of the signals that result in calcineurin and NFAT activation in pre-selected DPs was not addressed in this report. Our results show that this "ERK-sensitized" population is absent in DP cells from pTα-deficient mice, implicating a role for the preTCR in regulating this sensitized threshold for TCR signalling in DPs. To our surprise, the "ERK-sensitized" state was not restored upon re-introduction of pTα^a or pTα^b into pTα-deficient thymocytes in FTOC. This is difficult to reconcile, especially considering the rapid development of TCR$\alpha\beta^{(hi)}$ SPs as a result of preTCR^b expression. Nevertheless, "ERK-sensitized" DPs were evident in pTα-deficient mice that expressed the pTα^a-BAC-transgene. Thus it appears that precise regulation of preTCR signalling is required for the establishment of this population of pre-selected DPs and again, is clearly an area that deserves further investigation.

Preliminary data from our initial attempts to delve deeper into the relationship between preTCR signalling and appropriate selection of TCRαβ-expressing DP cells, suggested that selection events in pTα-deficient mice were not proceeding as normal. Indeed, Vβ6-expressing cells were over-represented in thymuses that displayed a Vβ-6 superantigen. Although difficult to interpret, at the very least it suggests that pTα-deficient DP cells perceive strong TCR signals differently than WT DP cells. This could imply that the threshold for positive selection is higher in pTα-deficient thymocytes and allows them to escape negative selection. Thus, the preTCR could be necessary for establishing low positive selection thresholds in DP thymocytes that allow their differentiation in response to "weak" TCR signals but not in response to "strong", negatively selecting signals. In this regard, preTCR signalling may contribute to mechanisms that directly prevent the generation of self-reactive T cells in the thymus that would otherwise lead to potentially fatal autoimmune disease.

1.8 Further observations on pTα^{a}-only BAC transgenic mice.

T cell development in pTα^{a}-only BAC transgenic mice is not entirely as expected. Despite expressing pTα^{a} from the pTα regulatory elements and promoter, the majority of DN thymocytes in pTα^{a}-only BAC transgenic mice are at the DN3 stage. Furthermore, the size of the pTα^{a}-only BAC transgenic thymus is substantially smaller than that of WT. This could suggest that the pTα BAC is not completely re-capitulating pTα expression in these animals. Alternatively, it could suggest that in the absence of pTα^{b} T cell development across the β-selection checkpoint is not normal. This is an area for future investigation, as is the observation that the CD4/CD8 ratio in the periphery of these transgenic animals is partially inverted towards CD8SPs. This may have roots in the problems with positive

selection as discussed earlier. Clearly these mice must be further characterised, with analysis of gut IELs being of particular interest. It would also be fascinating to compare the pTα^a-only BAC transgenic mice with pTα^b-only BAC transgenic mice that are presently being generated. It is hoped that the combination of data from these animals will help to shed insight into what appears to be a specific but subtle role for pTα^b during T cell development.

1.9 Summary.

To summarise, the results presented in this thesis shed new insight on T cell development at the β-selection checkpoint. They reveal for the first time that distinct preTCRs, formed in DN cells when TCRβ pairs with either pTα^a or pTα^b, drive divergent T cell development. These results demonstrate that pTα oligomerization is not essential for initiation of preTCR signalling, demanding re-assessment of the mechanisms that underpin this ligand-independent process. Instead, we propose that pTα^a oligomerization establishes a lower set-point for preTCR^a surface expression that regulates subsequent development. By contrast, pTα^b, that lacks the ability to oligomerize, allows higher surface expression of preTCR^b, driving distinct T cell development. Finally, these data strongly implicate the preTCR in a hitherto unrecognised role in setting sensitive ERK-mediated selection thresholds in pre-selected DP thymocytes that prevents the development of auto-reactive T cells and, therefore, autoimmune disease.

References

Agata, Y., Tamaki, N., Sakamoto, S., Ikawa, T., Masuda, K., Kawamoto, H., and Murre, C. (2007). Regulation of T cell receptor beta gene rearrangements and allelic exclusion by the helix-loop-helix protein, E47. Immunity *27*, 871-884.

Aifantis, I., Borowski, C., Gounari, F., Lacorazza, H.D., Nikolich-Zugich, J., and von Boehmer, H. (2002). A critical role for the cytoplasmic tail of pTalpha in T lymphocyte development. Nat Immunol *3*, 483-488.

Aifantis, I., Gounari, F., Scorrano, L., Borowski, C., and von Boehmer, H. (2001). Constitutive pre-TCR signaling promotes differentiation through Ca2+ mobilization and activation of NF-kappaB and NFAT. Nat Immunol *2*, 403-409.

Allen, R.D., 3rd, Bender, T.P., and Siu, G. (1999). c-Myb is essential for early T cell development. Genes Dev *13*, 1073-1078.

Anderson, G., Lane, P.J., and Jenkinson, E.J. (2007). Generating intrathymic microenvironments to establish T-cell tolerance. Nat Rev Immunol *7*, 954-963.

Anderson, G., Moore, N.C., Owen, J.J., and Jenkinson, E.J. (1996). Cellular interactions in thymocyte development. Annu Rev Immunol *14*, 73-99.

Anderson, G., Owen, J.J., Moore, N.C., and Jenkinson, E.J. (1994a). Characteristics of an in vitro system of thymocyte positive selection. J Immunol *153*, 1915-1920.

Anderson, G., Owen, J.J., Moore, N.C., and Jenkinson, E.J. (1994b). Thymic epithelial cells provide unique signals for positive selection of CD4+CD8+ thymocytes in vitro. J Exp Med *179*, 2027-2031.

Anderson, M.S., Venanzi, E.S., Klein, L., Chen, Z., Berzins, S.P., Turley, S.J., von Boehmer, H., Bronson, R., Dierich, A., Benoist, C., and Mathis, D. (2002). Projection of an immunological self shadow within the thymus by the aire protein. Science *298*, 1395-1401.

Ara, T., Itoi, M., Kawabata, K., Egawa, T., Tokoyoda, K., Sugiyama, T., Fujii, N., Amagai, T., and Nagasawa, T. (2003). A role of CXC chemokine ligand 12/stromal cell-derived factor-1/pre-B cell growth stimulating factor and its receptor CXCR4 in fetal and adult T cell development in vivo. J Immunol *170*, 4649-4655.

Aschenbrenner, K., D'Cruz, L.M., Vollmann, E.H., Hinterberger, M., Emmerich, J., Swee, L.K., Rolink, A., and Klein, L. (2007). Selection of Foxp3+ regulatory T cells specific for self antigen expressed and presented by Aire+ medullary thymic epithelial cells. Nat Immunol *8*, 351-358.

Attinger, A., Devine, L., Wang-Zhu, Y., Martin, D., Wang, J.H., Reinherz, E.L., Kronenberg, M., Cheroutre, H., and Kavathas, P. (2005). Molecular basis for the high affinity interaction between the thymic leukemia antigen and the CD8alphaalpha molecule. J Immunol *174*, 3501-3507.

Azzam, H.S., DeJarnette, J.B., Huang, K., Emmons, R., Park, C.S., Sommers, C.L., El-Khoury, D., Shores, E.W., and Love, P.E. (2001). Fine tuning of TCR signaling by CD5. J Immunol *166*, 5464-5472.

Azzam, H.S., Grinberg, A., Lui, K., Shen, H., Shores, E.W., and Love, P.E. (1998). CD5 expression is developmentally regulated by T cell receptor (TCR) signals and TCR avidity. J Exp Med *188*, 2301-2311.

Bain, G., Cravatt, C.B., Loomans, C., Alberola-Ila, J., Hedrick, S.M., and Murre, C. (2001). Regulation of the helix-loop-helix proteins, E2A and Id3, by the Ras-ERK MAPK cascade. Nat Immunol *2*, 165-171.

Bain, G., Engel, I., Robanus Maandag, E.C., te Riele, H.P., Voland, J.R., Sharp, L.L., Chun, J., Huey, B., Pinkel, D., and Murre, C. (1997). E2A deficiency leads to abnormalities in alphabeta T-cell development and to rapid development of T-cell lymphomas. Mol Cell Biol *17*, 4782-4791.

Barber, D.F., Passoni, L., Wen, L., Geng, L., and Hayday, A.C. (1998). The expression in vivo of a second isoform of pT alpha: implications for the mechanism of pT alpha action. J Immunol *161*, 11-16.

Barndt, R., Dai, M.F., and Zhuang, Y. (1999). A novel role for HEB downstream or parallel to the pre-TCR signaling pathway during alpha beta thymopoiesis. J Immunol *163*, 3331-3343.

Bas, A., Hammarstrom, S.G., and Hammarstrom, M.L. (2003). Extrathymic TCR gene rearrangement in human small intestine: identification of new splice forms of recombination activating gene-1 mRNA with selective tissue expression. J Immunol *171*, 3359-3371.

Bellavia, D., Campese, A.F., Alesse, E., Vacca, A., Felli, M.P., Balestri, A., Stoppacciaro, A., Tiveron, C., Tatangelo, L., Giovarelli, M.*, et al.* (2000). Constitutive activation of NF-kappaB and T-cell leukemia/lymphoma in Notch3 transgenic mice. EMBO J *19*, 3337-3348.

Bellavia, D., Campese, A.F., Checquolo, S., Balestri, A., Biondi, A., Cazzaniga, G., Lendahl, U., Fehling, H.J., Hayday, A.C., Frati, L.*, et al.* (2002). Combined expression of pTalpha and Notch3 in T cell leukemia identifies the requirement of preTCR for leukemogenesis. Proc Natl Acad Sci U S A *99*, 3788-3793.

Benz, C., and Bleul, C.C. (2005). A multipotent precursor in the thymus maps to the branching point of the T versus B lineage decision. J Exp Med *202*, 21-31.

Benz, C., Heinzel, K., and Bleul, C.C. (2004). Homing of immature thymocytes to the subcapsular microenvironment within the thymus is not an absolute requirement for T cell development. Eur J Immunol *34*, 3652-3663.

Berger, M.A., Dave, V., Rhodes, M.R., Bosma, G.C., Bosma, M.J., Kappes, D.J., and Wiest, D.L. (1997). Subunit composition of pre-T cell receptor complexes expressed by primary thymocytes: CD3 delta is physically associated but not functionally required. J Exp Med *186*, 1461-1467.

Bhandoola, A., Cibotti, R., Punt, J.A., Granger, L., Adams, A.J., Sharrow, S.O., and Singer, A. (1999). Positive selection as a developmental progression initiated by alpha beta TCR signals that fix TCR specificity prior to lineage commitment. Immunity *10*, 301-311.

Bijlmakers, M.J., Isobe-Nakamura, M., Ruddock, L.J., and Marsh, M. (1997). Intrinsic signals in the unique domain target p56(lck) to the plasma membrane independently of CD4. J Cell Biol *137*, 1029-1040.

Bijlmakers, M.J., and Marsh, M. (1999). Trafficking of an acylated cytosolic protein: newly synthesized p56(lck) travels to the plasma membrane via the exocytic pathway. J Cell Biol *145*, 457-468.

Blunt, T., Finnie, N.J., Taccioli, G.E., Smith, G.C., Demengeot, J., Gottlieb, T.M., Mizuta, R., Varghese, A.J., Alt, F.W., Jeggo, P.A., and et al. (1995). Defective DNA-dependent protein kinase activity is linked to V(D)J recombination and DNA repair defects associated with the murine scid mutation. Cell *80*, 813-823.

Borowski, C., Li, X., Aifantis, I., Gounari, F., and von Boehmer, H. (2004). Pre-TCRalpha and TCRalpha are not interchangeable partners of TCRbeta during T lymphocyte development. J Exp Med *199*, 607-615.

Bosselut, R., Kubo, S., Guinter, T., Kopacz, J.L., Altman, J.D., Feigenbaum, L., and Singer, A. (2000). Role of CD8beta domains in CD8 coreceptor function: importance for MHC I binding, signaling, and positive selection of CD8+ T cells in the thymus. Immunity *12*, 409-418.

Bosselut, R., Zhang, W., Ashe, J.M., Kopacz, J.L., Samelson, L.E., and Singer, A. (1999). Association of the adaptor molecule LAT with CD4 and CD8 coreceptors identifies a new coreceptor function in T cell receptor signal transduction. J Exp Med *190*, 1517-1526.

Brandle, D., Muller, C., Rulicke, T., Hengartner, H., and Pircher, H. (1992). Engagement of the T-cell receptor during positive selection in the thymus down-regulates RAG-1 expression. Proc Natl Acad Sci U S A *89*, 9529-9533.

Brugnera, E., Bhandoola, A., Cibotti, R., Yu, Q., Guinter, T.I., Yamashita, Y., Sharrow, S.O., and Singer, A. (2000). Coreceptor reversal in the thymus: signaled CD4+8+ thymocytes initially terminate CD8 transcription even when differentiating into CD8+ T cells. Immunity *13*, 59-71.

Bruno, L., Fehling, H.J., and von Boehmer, H. (1996). The alpha beta T cell receptor can replace the gamma delta receptor in the development of gamma delta lineage cells. Immunity *5*, 343-352.

Bruno, L., Rocha, B., Rolink, A., von Boehmer, H., and Rodewald, H.R. (1995). Intra- and extra-thymic expression of the pre-T cell receptor alpha gene. Eur J Immunol *25*, 1877-1882.

Buer, J., Aifantis, I., DiSanto, J.P., Fehling, H.J., and von Boehmer, H. (1997a). Role of different T cell receptors in the development of pre-T cells. J Exp Med *185*, 1541-1547.

Buer, J., Aifantis, I., DiSanto, J.P., Fehling, H.J., and von Boehmer, H. (1997b). T-cell development in the absence of the pre-T-cell receptor. Immunol Lett *57*, 5-8.

Campese, A.F., Grazioli, P., Colantoni, S., Anastasi, E., Mecarozzi, M., Checquolo, S., De Luca, G., Bellavia, D., Frati, L., Gulino, A., and Screpanti, I. (2009). Notch3 and pTalpha/pre-TCR sustain the in vivo function of naturally occurring regulatory T cells. Int Immunol *21*, 727-743.

Carleton, M., Haks, M.C., Smeele, S.A., Jones, A., Belkowski, S.M., Berger, M.A., Linsley, P., Kruisbeek, A.M., and Wiest, D.L. (2002). Early growth response transcription factors are required for development of CD4(-)CD8(-) thymocytes to the CD4(+)CD8(+) stage. J Immunol *168*, 1649-1658.

Carrasco, Y.R., Navarro, M.N., and Toribio, M.L. (2003). A role for the cytoplasmic tail of the pre-T cell receptor (TCR) alpha chain in promoting constitutive internalization and degradation of the pre-TCR. J Biol Chem *278*, 14507-14513.

Cawthon, A.G., Lu, H., and Alexander-Miller, M.A. (2001). Peptide requirement for CTL activation reflects the sensitivity to CD3 engagement: correlation with CD8alphabeta versus CD8alphaalpha expression. J Immunol *167*, 2577-2584.

Cheng, A.M., Negishi, I., Anderson, S.J., Chan, A.C., Bolen, J., Loh, D.Y., and Pawson, T. (1997). The Syk and ZAP-70 SH2-containing tyrosine kinases are implicated in pre-T cell receptor signaling. Proc Natl Acad Sci U S A *94*, 9797-9801.

Cheroutre, H., and Lambolez, F. (2008). Doubting the TCR coreceptor function of CD8alphaalpha. Immunity *28*, 149-159.

Ciofani, M., Schmitt, T.M., Ciofani, A., Michie, A.M., Cuburu, N., Aublin, A., Maryanski, J.L., and Zuniga-Pflucker, J.C. (2004). Obligatory role for cooperative signaling by pre-TCR and Notch during thymocyte differentiation. J Immunol *172*, 5230-5239.

Costello, P.S., Nicolas, R.H., Watanabe, Y., Rosewell, I., and Treisman, R. (2004). Ternary complex factor SAP-1 is required for Erk-mediated thymocyte positive selection. Nat Immunol *5*, 289-298.

Crompton, T., Gilmour, K.C., and Owen, M.J. (1996). The MAP kinase pathway controls differentiation from double-negative to double-positive thymocyte. Cell *86*, 243-251.

Croxford, A.L., Akilli-Ozturk, O., Rieux-Laucat, F., Forster, I., Waisman, A., and Buch, T. (2008). MHC-restricted T cell receptor signaling is required for alpha beta TCR replacement of the pre T cell receptor. Eur J Immunol *38*, 391-399.

Das, G., and Janeway, C.A., Jr. (1999). Development of CD8alpha/alpha and CD8alpha/beta T cells in major histocompatibility complex class I-deficient mice. J Exp Med *190*, 881-884.

Dave, V.P., Cao, Z., Browne, C., Alarcon, B., Fernandez-Miguel, G., Lafaille, J., de la Hera, A., Tonegawa, S., and Kappes, D.J. (1997). CD3 delta deficiency arrests development of the alpha beta but not the gamma delta T cell lineage. EMBO J *16*, 1360-1370.

Davis, M.M., and Bjorkman, P.J. (1988). T-cell antigen receptor genes and T-cell recognition. Nature *334*, 395-402.

De Geus, B., Van den Enden, M., Coolen, C., Nagelkerken, L., Van der Heijden, P., and Rozing, J. (1990). Phenotype of intraepithelial lymphocytes in euthymic and athymic mice: implications for differentiation of cells bearing a CD3-associated gamma delta T cell receptor. Eur J Immunol *20*, 291-298.

Denning, T.L., Granger, S.W., Mucida, D., Graddy, R., Leclercq, G., Zhang, W., Honey, K., Rasmussen, J.P., Cheroutre, H., Rudensky, A.Y., and Kronenberg, M. (2007). Mouse TCRalphabeta+CD8alphaalpha intraepithelial lymphocytes express genes that down-regulate their antigen reactivity and suppress immune responses. J Immunol *178*, 4230-4239.

Doyle, C., and Strominger, J.L. (1987). Interaction between CD4 and class II MHC molecules mediates cell adhesion. Nature *330*, 256-259.

Eberl, G., and Littman, D.R. (2004). Thymic origin of intestinal alphabeta T cells revealed by fate mapping of RORgammat+ cells. Science *305*, 248-251.

Engel, I., Johns, C., Bain, G., Rivera, R.R., and Murre, C. (2001). Early thymocyte development is regulated by modulation of E2A protein activity. J Exp Med *194*, 733-745.

Engel, I., and Murre, C. (2004). E2A proteins enforce a proliferation checkpoint in developing thymocytes. EMBO J *23*, 202-211.

Ess, K.C., Witte, D.P., Bascomb, C.P., and Aronow, B.J. (1999). Diverse developing mouse lineages exhibit high-level c-Myb expression in immature cells and loss of expression upon differentiation. Oncogene *18*, 1103-1111.

Fehling, H.J., Iritani, B.M., Krotkova, A., Forbush, K.A., Laplace, C., Perlmutter, R.M., and von Boehmer, H. (1997). Restoration of thymopoiesis in pT alpha-/- mice by anti-CD3epsilon antibody treatment or with transgenes encoding activated Lck or tailless pT alpha. Immunity *6*, 703-714.

Fehling, H.J., Krotkova, A., Saint-Ruf, C., and von Boehmer, H. (1995a). Crucial role of the pre-T-cell receptor alpha gene in development of alpha beta but not gamma delta T cells. Nature *375*, 795-798.

Fehling, H.J., Laplace, C., Mattei, M.G., Saint-Ruf, C., and von Boehmer, H. (1995b). Genomic structure and chromosomal location of the mouse pre-T-cell receptor alpha gene. Immunogenetics *42*, 275-281.

Ferrera, D., Panigada, M., Porcellini, S., and Grassi, F. (2008). Recombinase-deficient T cell development by selective accumulation of CD3 into lipid rafts. Eur J Immunol *38*, 1148-1156.

Fontenot, J.D., Rasmussen, J.P., Williams, L.M., Dooley, J.L., Farr, A.G., and Rudensky, A.Y. (2005). Regulatory T cell lineage specification by the forkhead transcription factor foxp3. Immunity *22*, 329-341.

Foss, D.L., Donskoy, E., and Goldschneider, I. (2001). The importation of hematogenous precursors by the thymus is a gated phenomenon in normal adult mice. J Exp Med *193*, 365-374.

Fruman, D.A., and Bismuth, G. (2009). Fine tuning the immune response with PI3K. Immunol Rev *228*, 253-272.

Gallo, E.M., Winslow, M.M., Cante-Barrett, K., Radermacher, A.N., Ho, L., McGinnis, L., Iritani, B., Neilson, J.R., and Crabtree, G.R. (2007). Calcineurin sets the bandwidth for discrimination of signals during thymocyte development. Nature *450*, 731-735.

Gangadharan, D., and Cheroutre, H. (2004). The CD8 isoform CD8alphaalpha is not a functional homologue of the TCR co-receptor CD8alphabeta. Curr Opin Immunol *16*, 264-270.

Gangadharan, D., Lambolez, F., Attinger, A., Wang-Zhu, Y., Sullivan, B.A., and Cheroutre, H. (2006). Identification of pre- and postselection TCRalphabeta+ intraepithelial lymphocyte precursors in the thymus. Immunity *25*, 631-641.

Gartner, F., Alt, F.W., Monroe, R., Chu, M., Sleckman, B.P., Davidson, L., and Swat, W. (1999). Immature thymocytes employ distinct signaling pathways for allelic exclusion versus differentiation and expansion. Immunity *10*, 537-546.

Germain, R.N. (1994). MHC-dependent antigen processing and peptide presentation: providing ligands for T lymphocyte activation. Cell *76*, 287-299.

Gibbons, D., Douglas, N.C., Barber, D.F., Liu, Q., Sullo, R., Geng, L., Fehling, H.J., von Boehmer, H., and Hayday, A.C. (2001). The biological activity of natural and mutant pTalpha alleles. J Exp Med *194*, 695-703.

Godfrey, D.I., Kennedy, J., Suda, T., and Zlotnik, A. (1993). A developmental pathway involving four phenotypically and functionally distinct subsets of CD3-CD4-CD8- triple-negative adult mouse thymocytes defined by CD44 and CD25 expression. J Immunol *150*, 4244-4252.

Goldman, K.P., Park, C.S., Kim, M., Matzinger, P., and Anderson, C.C. (2005). Thymic cortical epithelium induces self tolerance. Eur J Immunol *35*, 709-717.

Gounari, F., Aifantis, I., Khazaie, K., Hoeflinger, S., Harada, N., Taketo, M.M., and von Boehmer, H. (2001). Somatic activation of beta-catenin bypasses pre-TCR signaling and TCR selection in thymocyte development. Nat Immunol *2*, 863-869.

Groettrup, M., Ungewiss, K., Azogui, O., Palacios, R., Owen, M.J., Hayday, A.C., and von Boehmer, H. (1993). A novel disulfide-linked heterodimer on pre-T cells consists of the T cell receptor beta chain and a 33 kd glycoprotein. Cell *75*, 283-294.

Grusby, M.J., and Glimcher, L.H. (1995). Immune responses in MHC class II-deficient mice. Annu Rev Immunol *13*, 417-435.

Guidos, C.J., Williams, C.J., Grandal, I., Knowles, G., Huang, M.T., and Danska, J.S. (1996). V(D)J recombination activates a p53-dependent DNA damage checkpoint in scid lymphocyte precursors. Genes Dev *10*, 2038-2054.

Guy-Grand, D., Azogui, O., Celli, S., Darche, S., Nussenzweig, M.C., Kourilsky, P., and Vassalli, P. (2003). Extrathymic T cell lymphopoiesis: ontogeny and contribution to gut intraepithelial lymphocytes in athymic and euthymic mice. J Exp Med *197*, 333-341.

Guy-Grand, D., Pardigon, N., Darche, S., Lantz, O., Kourilsky, P., and Vassalli, P. (2001). Contribution of double-negative thymic precursors to CD8alpha alpha (+) intraepithelial lymphocytes of the gut in mice bearing TCR transgenes. Eur J Immunol *31*, 2593-2602.

Guy-Grand, D., Rocha, B., Mintz, P., Malassis-Seris, M., Selz, F., Malissen, B., and Vassalli, P. (1994). Different use of T cell receptor transducing modules in two populations of gut intraepithelial lymphocytes are related to distinct pathways of T cell differentiation. J Exp Med *180*, 673-679.

Haks, M.C., Belkowski, S.M., Ciofani, M., Rhodes, M., Lefebvre, J.M., Trop, S., Hugo, P., Zuniga-Pflucker, J.C., and Wiest, D.L. (2003). Low activation threshold as a mechanism for ligand-independent signaling in pre-T cells. J Immunol *170*, 2853-2861.

Haks, M.C., Krimpenfort, P., Borst, J., and Kruisbeek, A.M. (1998). The CD3gamma chain is essential for development of both the TCRalphabeta and TCRgammadelta lineages. EMBO J *17*, 1871-1882.

Haks, M.C., Krimpenfort, P., van den Brakel, J.H., and Kruisbeek, A.M. (1999). Pre-TCR signaling and inactivation of p53 induces crucial cell survival pathways in pre-T cells. Immunity *11*, 91-101.

Haks, M.C., Lefebvre, J.M., Lauritsen, J.P., Carleton, M., Rhodes, M., Miyazaki, T., Kappes, D.J., and Wiest, D.L. (2005). Attenuation of gammadeltaTCR signaling efficiently diverts thymocytes to the alphabeta lineage. Immunity *22*, 595-606.

Hayday, A.C. (2009). Gammadelta T cells and the lymphoid stress-surveillance response. Immunity *31*, 184-196.

Hayes, S.M., Laird, R.M., and Love, P.E. (2010). Beyond alphabeta/gammadelta lineage commitment: TCR signal strength regulates gammadelta T cell maturation and effector fate. Semin Immunol.

Hayes, S.M., Li, L., and Love, P.E. (2005). TCR signal strength influences alphabeta/gammadelta lineage fate. Immunity *22*, 583-593.

Hayes, S.M., Shores, E.W., and Love, P.E. (2003). An architectural perspective on signaling by the pre-, alphabeta and gammadelta T cell receptors. Immunol Rev *191*, 28-37.

Heemskerk, M.H., Blom, B., Nolan, G., Stegmann, A.P., Bakker, A.Q., Weijer, K., Res, P.C., and Spits, H. (1997). Inhibition of T cell and promotion of natural killer

cell development by the dominant negative helix loop helix factor Id3. J Exp Med *186*, 1597-1602.

Hoffman, E.S., Passoni, L., Crompton, T., Leu, T.M., Schatz, D.G., Koff, A., Owen, M.J., and Hayday, A.C. (1996). Productive T-cell receptor beta-chain gene rearrangement: coincident regulation of cell cycle and clonality during development in vivo. Genes Dev *10*, 948-962.

Huang, E.Y., Gallegos, A.M., Richards, S.M., Lehar, S.M., and Bevan, M.J. (2003). Surface expression of Notch1 on thymocytes: correlation with the double-negative to double-positive transition. J Immunol *171*, 2296-2304.

Huesmann, M., Scott, B., Kisielow, P., and von Boehmer, H. (1991). Kinetics and efficacy of positive selection in the thymus of normal and T cell receptor transgenic mice. Cell *66*, 533-540.

Iritani, B.M., Alberola-Ila, J., Forbush, K.A., and Perimutter, R.M. (1999). Distinct signals mediate maturation and allelic exclusion in lymphocyte progenitors. Immunity *10*, 713-722.

Irving, B.A., Alt, F.W., and Killeen, N. (1998). Thymocyte development in the absence of pre-T cell receptor extracellular immunoglobulin domains. Science *280*, 905-908.

Ito, Y., Arai, S., van Oers, N.S., Aifantis, I., von Boehmer, H., and Miyazaki, T. (2002). Positive selection by the pre-TCR yields mature CD8+ T cells. J Immunol *169*, 4913-4919.

Itohara, S., Mombaerts, P., Lafaille, J., Iacomini, J., Nelson, A., Clarke, A.R., Hooper, M.L., Farr, A., and Tonegawa, S. (1993). T cell receptor delta gene mutant mice: independent generation of alpha beta T cells and programmed rearrangements of gamma delta TCR genes. Cell *72*, 337-348.

Janas, M.L., Varano, G., Gudmundsson, K., Noda, M., Nagasawa, T., and Turner, M. (2010). Thymic development beyond beta-selection requires phosphatidylinositol 3-kinase activation by CXCR4. J Exp Med *207*, 247-261.

Janssen, E., and Zhang, W. (2003). Adaptor proteins in lymphocyte activation. Curr Opin Immunol *15*, 269-276.

Jenkinson, E.J., Anderson, G., and Owen, J.J. (1992). Studies on T cell maturation on defined thymic stromal cell populations in vitro. J Exp Med *176*, 845-853.

Jotereau, F., Heuze, F., Salomon-Vie, V., and Gascan, H. (1987). Cell kinetics in the fetal mouse thymus: precursor cell input, proliferation, and emigration. J Immunol *138*, 1026-1030.

Kappler, J.W., Roehm, N., and Marrack, P. (1987). T cell tolerance by clonal elimination in the thymus. Cell *49*, 273-280.

Kappler, J.W., Staerz, U., White, J., and Marrack, P.C. (1988). Self-tolerance eliminates T cells specific for Mls-modified products of the major histocompatibility complex. Nature *332*, 35-40.

Kawamoto, H., Ohmura, K., Fujimoto, S., Lu, M., Ikawa, T., and Katsura, Y. (2003). Extensive proliferation of T cell lineage-restricted progenitors in the thymus: an essential process for clonal expression of diverse T cell receptor beta chains. Eur J Immunol *33*, 606-615.

Kawamoto, H., Ohmura, K., and Katsura, Y. (1998). Presence of progenitors restricted to T, B, or myeloid lineage, but absence of multipotent stem cells, in the murine fetal thymus. J Immunol *161*, 3799-3802.

Kishi, H., Borgulya, P., Scott, B., Karjalainen, K., Traunecker, A., Kaufman, J., and von Boehmer, H. (1991). Surface expression of the beta T cell receptor (TCR) chain in the absence of other TCR or CD3 proteins on immature T cells. EMBO J *10*, 93-100.

Kishimoto, H., and Sprent, J. (1997). Negative selection in the thymus includes semimature T cells. J Exp Med *185*, 263-271.

Kisielow, P., Teh, H.S., Bluthmann, H., and von Boehmer, H. (1988). Positive selection of antigen-specific T cells in thymus by restricting MHC molecules. Nature *335*, 730-733.

Klein, L., Hinterberger, M., Wirnsberger, G., and Kyewski, B. (2009). Antigen presentation in the thymus for positive selection and central tolerance induction. Nat Rev Immunol *9*, 833-844.

Koller, B.H., Marrack, P., Kappler, J.W., and Smithies, O. (1990). Normal development of mice deficient in beta 2M, MHC class I proteins, and CD8+ T cells. Science *248*, 1227-1230.

Koltsova, E.K., Ciofani, M., Benezra, R., Miyazaki, T., Clipstone, N., Zuniga-Pflucker, J.C., and Wiest, D.L. (2007). Early growth response 1 and NF-ATc1 act in concert to promote thymocyte development beyond the beta-selection checkpoint. J Immunol *179*, 4694-4703.

Kosugi, A., Noda, S., Saitoh, S., Narumiya, S., Ogata, M., Hashimoto, Y., Takase, K., Saito, T., and Hamaoka, T. (1997). Subunit composition of the pre-T-cell receptor complex analysed by monoclonal antibody against the pre-T-cell receptor alpha chain. Immunology *91*, 618-622.

Kruisbeek, A.M., Haks, M.C., Carleton, M., Michie, A.M., Zuniga-Pflucker, J.C., and Wiest, D.L. (2000). Branching out to gain control: how the pre-TCR is linked to multiple functions. Immunol Today *21*, 637-644.

Lacorazza, H.D., Porritt, H.E., and Nikolich-Zugich, J. (2001a). Dysregulated expression of pre-Talpha reveals the opposite effects of pre-TCR at successive stages of T cell development. J Immunol *167*, 5689-5696.

Lacorazza, H.D., Tucek-Szabo, C., Vasovic, L.V., Remus, K., and Nikolich-Zugich, J. (2001b). Premature TCR alpha beta expression and signaling in early thymocytes impair thymocyte expansion and partially block their development. J Immunol *166*, 3184-3193.

Lambolez, F., Azogui, O., Joret, A.M., Garcia, C., von Boehmer, H., Di Santo, J., Ezine, S., and Rocha, B. (2002). Characterization of T cell differentiation in the murine gut. J Exp Med *195*, 437-449.

Lauritsen, J.P., Haks, M.C., Lefebvre, J.M., Kappes, D.J., and Wiest, D.L. (2006). Recent insights into the signals that control alphabeta/gammadelta-lineage fate. Immunol Rev *209*, 176-190.

Lauritsen, J.P., Wong, G.W., Lee, S.Y., Lefebvre, J.M., Ciofani, M., Rhodes, M., Kappes, D.J., Zuniga-Pflucker, J.C., and Wiest, D.L. (2009). Marked induction of the helix-loop-helix protein Id3 promotes the gammadelta T cell fate and renders their functional maturation Notch independent. Immunity *31*, 565-575.

Leishman, A.J., Gapin, L., Capone, M., Palmer, E., MacDonald, H.R., Kronenberg, M., and Cheroutre, H. (2002). Precursors of functional MHC class I- or class II-restricted CD8alphaalpha(+) T cells are positively selected in the thymus by agonist self-peptides. Immunity *16*, 355-364.

Levelt, C.N., de Jong, Y.P., Mizoguchi, E., O'Farrelly, C., Bhan, A.K., Tonegawa, S., Terhorst, C., and Simpson, S.J. (1999). High- and low-affinity single-peptide/MHC ligands have distinct effects on the development of mucosal CD8alphaalpha and CD8alphabeta T lymphocytes. Proc Natl Acad Sci U S A *96*, 5628-5633.

Li, X., Gounari, F., Protopopov, A., Khazaie, K., and von Boehmer, H. (2008). Oncogenesis of T-ALL and nonmalignant consequences of overexpressing intracellular NOTCH1. J Exp Med *205*, 2851-2861.

Lin, W.C., and Desiderio, S. (1993). Regulation of V(D)J recombination activator protein RAG-2 by phosphorylation. Science *260*, 953-959.

Love, P.E., Shores, E.W., Johnson, M.D., Tremblay, M.L., Lee, E.J., Grinberg, A., Huang, S.P., Singer, A., and Westphal, H. (1993). T cell development in mice that lack the zeta chain of the T cell antigen receptor complex. Science *261*, 918-921.

MacDonald, H.R., Schneider, R., Lees, R.K., Howe, R.C., Acha-Orbea, H., Festenstein, H., Zinkernagel, R.M., and Hengartner, H. (1988). T-cell receptor V beta use predicts reactivity and tolerance to Mlsa-encoded antigens. Nature *332*, 40-45.

Maillard, I., Tu, L., Sambandam, A., Yashiro-Ohtani, Y., Millholland, J., Keeshan, K., Shestova, O., Xu, L., Bhandoola, A., and Pear, W.S. (2006). The requirement for Notch signaling at the beta-selection checkpoint in vivo is absolute and independent of the pre-T cell receptor. J Exp Med *203*, 2239-2245.

Malissen, M., Gillet, A., Ardouin, L., Bouvier, G., Trucy, J., Ferrier, P., Vivier, E., and Malissen, B. (1995). Altered T cell development in mice with a targeted mutation of the CD3-epsilon gene. EMBO J *14*, 4641-4653.

Mandel, T.E., and Kennedy, M.M. (1978). The differentiation of murine thymocytes in vivo and in vitro. Immunology *35*, 317-331.

Masuda, K., Kakugawa, K., Nakayama, T., Minato, N., Katsura, Y., and Kawamoto, H. (2007). T cell lineage determination precedes the initiation of TCR beta gene rearrangement. J Immunol *179*, 3699-3706.

Mathis, D., and Benoist, C. (2007). A decade of AIRE. Nat Rev Immunol *7*, 645-650.

Matloubian, M., Lo, C.G., Cinamon, G., Lesneski, M.J., Xu, Y., Brinkmann, V., Allende, M.L., Proia, R.L., and Cyster, J.G. (2004). Lymphocyte egress from thymus and peripheral lymphoid organs is dependent on S1P receptor 1. Nature *427*, 355-360.

Melichar, H., and Kang, J. (2007). Integrated morphogen signal inputs in gammadelta versus alphabeta T-cell differentiation. Immunol Rev *215*, 32-45.

Michie, A.M., Soh, J.W., Hawley, R.G., Weinstein, I.B., and Zuniga-Pflucker, J.C. (2001). Allelic exclusion and differentiation by protein kinase C-mediated signals in immature thymocytes. Proc Natl Acad Sci U S A *98*, 609-614.

Michie, A.M., Trop, S., Wiest, D.L., and Zuniga-Pflucker, J.C. (1999). Extracellular signal-regulated kinase (ERK) activation by the pre-T cell receptor in developing thymocytes in vivo. J Exp Med *190*, 1647-1656.

Michie, A.M., and Zuniga-Pflucker, J.C. (2002). Regulation of thymocyte differentiation: pre-TCR signals and beta-selection. Semin Immunol *14*, 311-323.

Misslitz, A., Pabst, O., Hintzen, G., Ohl, L., Kremmer, E., Petrie, H.T., and Forster, R. (2004). Thymic T cell development and progenitor localization depend on CCR7. J Exp Med *200*, 481-491.

Miyazaki, T. (1997). Two distinct steps during thymocyte maturation from CD4-CD8- to CD4+CD8+ distinguished in the early growth response (Egr)-1 transgenic mice with a recombinase-activating gene-deficient background. J Exp Med *186*, 877-885.

Molina, T.J., Kishihara, K., Siderovski, D.P., van Ewijk, W., Narendran, A., Timms, E., Wakeham, A., Paige, C.J., Hartmann, K.U., Veillette, A., and et al. (1992). Profound block in thymocyte development in mice lacking p56lck. Nature *357*, 161-164.

Mombaerts, P., Anderson, S.J., Perlmutter, R.M., Mak, T.W., and Tonegawa, S. (1994). An activated lck transgene promotes thymocyte development in RAG-1 mutant mice. Immunity *1*, 261-267.

Mombaerts, P., Clarke, A.R., Rudnicki, M.A., Iacomini, J., Itohara, S., Lafaille, J.J., Wang, L., Ichikawa, Y., Jaenisch, R., Hooper, M.L., and et al. (1992a). Mutations in T-cell antigen receptor genes alpha and beta block thymocyte development at different stages. Nature *360*, 225-231.

Mombaerts, P., Iacomini, J., Johnson, R.S., Herrup, K., Tonegawa, S., and Papaioannou, V.E. (1992b). RAG-1-deficient mice have no mature B and T lymphocytes. Cell *68*, 869-877.

Murata, S., Sasaki, K., Kishimoto, T., Niwa, S., Hayashi, H., Takahama, Y., and Tanaka, K. (2007). Regulation of CD8+ T cell development by thymus-specific proteasomes. Science *316*, 1349-1353.

Murga, C., and Barber, D.F. (2002). Molecular mechanisms of pre-T cell receptor-induced survival. J Biol Chem *277*, 39156-39162.

Nakagawa, T., Roth, W., Wong, P., Nelson, A., Farr, A., Deussing, J., Villadangos, J.A., Ploegh, H., Peters, C., and Rudensky, A.Y. (1998). Cathepsin L: critical role in Ii degradation and CD4 T cell selection in the thymus. Science *280*, 450-453.

Norment, A.M., Forbush, K.A., Nguyen, N., Malissen, M., and Perlmutter, R.M. (1997). Replacement of pre-T cell receptor signaling functions by the CD4 coreceptor. J Exp Med *185*, 121-130.

Norment, A.M., Salter, R.D., Parham, P., Engelhard, V.H., and Littman, D.R. (1988). Cell-cell adhesion mediated by CD8 and MHC class I molecules. Nature *336*, 79-81.

O'Shea, C.C., Thornell, A.P., Rosewell, I.R., Hayes, B., and Owen, M.J. (1997). Exit of the pre-TCR from the ER/cis-Golgi is necessary for signaling differentiation, proliferation, and allelic exclusion in immature thymocytes. Immunity *7*, 591-599.

Oida, T., Suzuki, K., Nanno, M., Kanamori, Y., Saito, H., Kubota, E., Kato, S., Itoh, M., Kaminogawa, S., and Ishikawa, H. (2000). Role of gut cryptopatches in early extrathymic maturation of intestinal intraepithelial T cells. J Immunol *164*, 3616-3626.

Okamura, R.M., Sigvardsson, M., Galceran, J., Verbeek, S., Clevers, H., and Grosschedl, R. (1998). Redundant regulation of T cell differentiation and TCRalpha gene expression by the transcription factors LEF-1 and TCF-1. Immunity *8*, 11-20.

Owen, J.J., and Ritter, M.A. (1969). Tissue interaction in the development of thymus lymphocytes. J Exp Med *129*, 431-442.

Pang, D.J., Hayday, A.C., and Bijlmakers, M.J. (2007). CD8 Raft localization is induced by its assembly into CD8alpha beta heterodimers, Not CD8alpha alpha homodimers. J Biol Chem *282*, 13884-13894.

Panigada, M., Porcellini, S., Barbier, E., Hoeflinger, S., Cazenave, P.A., Gu, H., Band, H., von Boehmer, H., and Grassi, F. (2002). Constitutive endocytosis and degradation of the pre-T cell receptor. J Exp Med *195*, 1585-1597.

Park, J.H., Adoro, S., Guinter, T., Erman, B., Alag, A.S., Catalfamo, M., Kimura, M.Y., Cui, Y., Lucas, P.J., Gress, R.E*., et al.* (2010). Signaling by intrathymic cytokines, not T cell antigen receptors, specifies CD8 lineage choice and promotes the differentiation of cytotoxic-lineage T cells. Nat Immunol *11*, 257-264.

Pennington, D.J., Silva-Santos, B., and Hayday, A.C. (2005). Gammadelta T cell development--having the strength to get there. Curr Opin Immunol *17*, 108-115.

Pennington, D.J., Silva-Santos, B., Silberzahn, T., Escorcio-Correia, M., Woodward, M.J., Roberts, S.J., Smith, A.L., Dyson, P.J., and Hayday, A.C. (2006). Early events in

the thymus affect the balance of effector and regulatory T cells. Nature *444*, 1073-1077.

Peschon, J.J., Morrissey, P.J., Grabstein, K.H., Ramsdell, F.J., Maraskovsky, E., Gliniak, B.C., Park, L.S., Ziegler, S.F., Williams, D.E., Ware, C.B*., et al.* (1994). Early lymphocyte expansion is severely impaired in interleukin 7 receptor-deficient mice. J Exp Med *180*, 1955-1960.

Petersson, K., Ivars, F., and Sigvardsson, M. (2002). The pT alpha promoter and enhancer are direct targets for transactivation by E box-binding proteins. Eur J Immunol *32*, 911-920.

Petrie, H.T., Scollay, R., and Shortman, K. (1992). Commitment to the T cell receptor-alpha beta or -gamma delta lineages can occur just prior to the onset of CD4 and CD8 expression among immature thymocytes. Eur J Immunol *22*, 2185-2188.

Pivniouk, V., Tsitsikov, E., Swinton, P., Rathbun, G., Alt, F.W., and Geha, R.S. (1998). Impaired viability and profound block in thymocyte development in mice lacking the adaptor protein SLP-76. Cell *94*, 229-238.

Plotkin, J., Prockop, S.E., Lepique, A., and Petrie, H.T. (2003). Critical role for CXCR4 signaling in progenitor localization and T cell differentiation in the postnatal thymus. J Immunol *171*, 4521-4527.

Porritt, H.E., Rumfelt, L.L., Tabrizifard, S., Schmitt, T.M., Zuniga-Pflucker, J.C., and Petrie, H.T. (2004). Heterogeneity among DN1 prothymocytes reveals multiple progenitors with different capacities to generate T cell and non-T cell lineages. Immunity *20*, 735-745.

Poussier, P., Ning, T., Banerjee, D., and Julius, M. (2002). A unique subset of self-specific intraintestinal T cells maintains gut integrity. J Exp Med *195*, 1491-1497.

Pui, J.C., Allman, D., Xu, L., DeRocco, S., Karnell, F.G., Bakkour, S., Lee, J.Y., Kadesch, T., Hardy, R.R., Aster, J.C., and Pear, W.S. (1999). Notch1 expression in early lymphopoiesis influences B versus T lineage determination. Immunity *11*, 299-308.

Rabinovitch, P.S., Torres, R.M., and Engel, D. (1986). Simultaneous cell cycle analysis and two-color surface immunofluorescence using 7-amino-actinomycin D and single laser excitation: applications to study of cell activation and the cell cycle of murine Ly-1 B cells. J Immunol *136*, 2769-2775.

Radtke, F., Wilson, A., Stark, G., Bauer, M., van Meerwijk, J., MacDonald, H.R., and Aguet, M. (1999). Deficient T cell fate specification in mice with an induced inactivation of Notch1. Immunity *10*, 547-558.

Raulet, D.H., Garman, R.D., Saito, H., and Tonegawa, S. (1985). Developmental regulation of T-cell receptor gene expression. Nature *314*, 103-107.

Reizis, B., and Leder, P. (1999). Expression of the mouse pre-T cell receptor alpha gene is controlled by an upstream region containing a transcriptional enhancer. J Exp Med *189*, 1669-1678.

Reizis, B., and Leder, P. (2001). The upstream enhancer is necessary and sufficient for the expression of the pre-T cell receptor alpha gene in immature T lymphocytes. J Exp Med *194*, 979-990.

Reizis, B., and Leder, P. (2002). Direct induction of T lymphocyte-specific gene expression by the mammalian Notch signaling pathway. Genes Dev *16*, 295-300.

Ribot, J., Enault, G., Pilipenko, S., Huchenq, A., Calise, M., Hudrisier, D., Romagnoli, P., and van Meerwijk, J.P. (2007). Shaping of the autoreactive regulatory T cell repertoire by thymic cortical positive selection. J Immunol *179*, 6741-6748.

Rincon, M., Flavell, R.A., and Davis, R.J. (2001). Signal transduction by MAP kinases in T lymphocytes. Oncogene *20*, 2490-2497.

Rocha, B., Vassalli, P., and Guy-Grand, D. (1991). The V beta repertoire of mouse gut homodimeric alpha CD8+ intraepithelial T cell receptor alpha/beta + lymphocytes reveals a major extrathymic pathway of T cell differentiation. J Exp Med *173*, 483-486.

Rodewald, H.R. (2008). Thymus organogenesis. Annu Rev Immunol *26*, 355-388.

Rothenberg, E.V., Moore, J.E., and Yui, M.A. (2008). Launching the T-cell-lineage developmental programme. Nat Rev Immunol *8*, 9-21.

Ruland, J., and Mak, T.W. (2003). Transducing signals from antigen receptors to nuclear factor kappaB. Immunol Rev *193*, 93-100.

Saint-Ruf, C., Lechner, O., Feinberg, J., and von Boehmer, H. (1998). Genomic structure of the human pre-T cell receptor alpha chain and expression of two mRNA isoforms. Eur J Immunol *28*, 3824-3831.

Saint-Ruf, C., Panigada, M., Azogui, O., Debey, P., von Boehmer, H., and Grassi, F. (2000). Different initiation of pre-TCR and gammadeltaTCR signalling. Nature *406*, 524-527.

Saint-Ruf, C., Ungewiss, K., Groettrup, M., Bruno, L., Fehling, H.J., and von Boehmer, H. (1994). Analysis and expression of a cloned pre-T cell receptor gene. Science *266*, 1208-1212.

Saito, H., Kanamori, Y., Takemori, T., Nariuchi, H., Kubota, E., Takahashi-Iwanaga, H., Iwanaga, T., and Ishikawa, H. (1998). Generation of intestinal T cells from progenitors residing in gut cryptopatches. Science *280*, 275-278.

Samelson, L.E., Phillips, A.F., Luong, E.T., and Klausner, R.D. (1990). Association of the fyn protein-tyrosine kinase with the T-cell antigen receptor. Proc Natl Acad Sci U S A *87*, 4358-4362.

Santamaria, P. (2010). The long and winding road to understanding and conquering type 1 diabetes. Immunity *32*, 437-445.

Sasaki, Y., Ishida, S., Morimoto, I., Yamashita, T., Kojima, T., Kihara, C., Tanaka, T., Imai, K., Nakamura, Y., and Tokino, T. (2002). The p53 family member genes are involved in the Notch signal pathway. J Biol Chem *277*, 719-724.

Schmitt, T.M., Ciofani, M., Petrie, H.T., and Zuniga-Pflucker, J.C. (2004). Maintenance of T cell specification and differentiation requires recurrent notch receptor-ligand interactions. J Exp Med *200*, 469-479.

Schmitt, T.M., and Zuniga-Pflucker, J.C. (2002). Induction of T cell development from hematopoietic progenitor cells by delta-like-1 in vitro. Immunity *17*, 749-756.

Schnell, S., Demolliere, C., van den Berk, P., Kirberg, J., and Jacobs, H. (2006). Constitutive expression of the pre-TCR enables development of mature T cells. Int Immunol *18*, 911-920.

Shinkai, Y., and Alt, F.W. (1994). CD3 epsilon-mediated signals rescue the development of CD4+CD8+ thymocytes in RAG-2-/- mice in the absence of TCR beta chain expression. Int Immunol *6*, 995-1001.

Shinkai, Y., Koyasu, S., Nakayama, K., Murphy, K.M., Loh, D.Y., Reinherz, E.L., and Alt, F.W. (1993). Restoration of T cell development in RAG-2-deficient mice by functional TCR transgenes. Science *259*, 822-825.

Shinkai, Y., Rathbun, G., Lam, K.P., Oltz, E.M., Stewart, V., Mendelsohn, M., Charron, J., Datta, M., Young, F., Stall, A.M., and et al. (1992). RAG-2-deficient mice lack mature lymphocytes owing to inability to initiate V(D)J rearrangement. Cell *68*, 855-867.

Singer, A. (2002). New perspectives on a developmental dilemma: the kinetic signaling model and the importance of signal duration for the CD4/CD8 lineage decision. Curr Opin Immunol *14*, 207-215.

Singer, A., Adoro, S., and Park, J.H. (2008). Lineage fate and intense debate: myths, models and mechanisms of CD4- versus CD8-lineage choice. Nat Rev Immunol *8*, 788-801.

Singer, A., and Bosselut, R. (2004). CD4/CD8 coreceptors in thymocyte development, selection, and lineage commitment: analysis of the CD4/CD8 lineage decision. Adv Immunol *83*, 91-131.

Snodgrass, H.R., Dembic, Z., Steinmetz, M., and von Boehmer, H. (1985). Expression of T-cell antigen receptor genes during fetal development in the thymus. Nature *315*, 232-233.

Steff, A.M., Trop, S., Maira, M., Drouin, J., and Hugo, P. (2001). Opposite ability of pre-TCR and alpha beta TCR to induce apoptosis. J Immunol *166*, 5044-5050.

Sudo, T., Nishikawa, S., Ohno, N., Akiyama, N., Tamakoshi, M., and Yoshida, H. (1993). Expression and function of the interleukin 7 receptor in murine lymphocytes. Proc Natl Acad Sci U S A *90*, 9125-9129.

Sun, Z., Unutmaz, D., Zou, Y.R., Sunshine, M.J., Pierani, A., Brenner-Morton, S., Mebius, R.E., and Littman, D.R. (2000). Requirement for RORgamma in thymocyte survival and lymphoid organ development. Science *288*, 2369-2373.

Suzuki, K., Oida, T., Hamada, H., Hitotsumatsu, O., Watanabe, M., Hibi, T., Yamamoto, H., Kubota, E., Kaminogawa, S., and Ishikawa, H. (2000). Gut cryptopatches: direct evidence of extrathymic anatomical sites for intestinal T lymphopoiesis. Immunity *13*, 691-702.

Takahama, Y. (2006). Journey through the thymus: stromal guides for T-cell development and selection. Nat Rev Immunol *6*, 127-135.

Takeuchi, A., Yamasaki, S., Takase, K., Nakatsu, F., Arase, H., Onodera, M., and Saito, T. (2001). E2A and HEB activate the pre-TCR alpha promoter during immature T cell development. J Immunol *167*, 2157-2163.

Terrence, K., Pavlovich, C.P., Matechak, E.O., and Fowlkes, B.J. (2000). Premature expression of T cell receptor (TCR)alphabeta suppresses TCRgammadelta gene rearrangement but permits development of gammadelta lineage T cells. J Exp Med *192*, 537-548.

Tonegawa, S. (1983). Somatic generation of antibody diversity. Nature *302*, 575-581.

Trampont, P.C., Tosello-Trampont, A.C., Shen, Y., Duley, A.K., Sutherland, A.E., Bender, T.P., Littman, D.R., and Ravichandran, K.S. (2010). CXCR4 acts as a costimulator during thymic beta-selection. Nat Immunol *11*, 162-170.

Tremblay, M., Herblot, S., Lecuyer, E., and Hoang, T. (2003). Regulation of pT alpha gene expression by a dosage of E2A, HEB, and SCL. J Biol Chem *278*, 12680-12687.

Trigueros, C., Hozumi, K., Silva-Santos, B., Bruno, L., Hayday, A.C., Owen, M.J., and Pennington, D.J. (2003). Pre-TCR signaling regulates IL-7 receptor alpha expression promoting thymocyte survival at the transition from the double-negative to double-positive stage. Eur J Immunol *33*, 1968-1977.

Trop, S., De Sepulveda, P., Zuniga-Pflucker, J.C., and Rottapel, R. (2001). Overexpression of suppressor of cytokine signaling-1 impairs pre-T-cell receptor-induced proliferation but not differentiation of immature thymocytes. Blood *97*, 2269-2277.

Trop, S., Rhodes, M., Wiest, D.L., Hugo, P., and Zuniga-Pflucker, J.C. (2000). Competitive displacement of pT alpha by TCR-alpha during TCR assembly prevents surface coexpression of pre-TCR and alpha beta TCR. J Immunol *165*, 5566-5572.

Trop, S., Steff, A.M., Denis, F., Wiest, D.L., and Hugo, P. (1999). The connecting peptide domain of pT alpha dictates weak association of the pre-T cell receptor with the TCR zeta subunit. Eur J Immunol *29*, 2187-2196.

Ueno, T., Saito, F., Gray, D.H., Kuse, S., Hieshima, K., Nakano, H., Kakiuchi, T., Lipp, M., Boyd, R.L., and Takahama, Y. (2004). CCR7 signals are essential for cortex-medulla migration of developing thymocytes. J Exp Med *200*, 493-505.

van Genderen, C., Okamura, R.M., Farinas, I., Quo, R.G., Parslow, T.G., Bruhn, L., and Grosschedl, R. (1994). Development of several organs that require inductive

epithelial-mesenchymal interactions is impaired in LEF-1-deficient mice. Genes Dev *8*, 2691-2703.

Van Laethem, F., Sarafova, S.D., Park, J.H., Tai, X., Pobezinsky, L., Guinter, T.I., Adoro, S., Adams, A., Sharrow, S.O., Feigenbaum, L., and Singer, A. (2007). Deletion of CD4 and CD8 coreceptors permits generation of alphabetaT cells that recognize antigens independently of the MHC. Immunity *27*, 735-750.

van Oers, N.S., Lowin-Kropf, B., Finlay, D., Connolly, K., and Weiss, A. (1996). alpha beta T cell development is abolished in mice lacking both Lck and Fyn protein tyrosine kinases. Immunity *5*, 429-436.

van Oers, N.S., von Boehmer, H., and Weiss, A. (1995). The pre-T cell receptor (TCR) complex is functionally coupled to the TCR-zeta subunit. J Exp Med *182*, 1585-1590.

van Santen, H.M., Benoist, C., and Mathis, D. (2004). Number of T reg cells that differentiate does not increase upon encounter of agonist ligand on thymic epithelial cells. J Exp Med *200*, 1221-1230.

Veillette, A., Bookman, M.A., Horak, E.M., and Bolen, J.B. (1988). The CD4 and CD8 T cell surface antigens are associated with the internal membrane tyrosine-protein kinase p56lck. Cell *55*, 301-308.

Verbeek, S., Izon, D., Hofhuis, F., Robanus-Maandag, E., te Riele, H., van de Wetering, M., Oosterwegel, M., Wilson, A., MacDonald, H.R., and Clevers, H. (1995). An HMG-box-containing T-cell factor required for thymocyte differentiation. Nature *374*, 70-74.

Villadangos, J.A. (2001). Presentation of antigens by MHC class II molecules: getting the most out of them. Mol Immunol *38*, 329-346.

Villey, I., de Chasseval, R., and de Villartay, J.P. (1999). RORgammaT, a thymus-specific isoform of the orphan nuclear receptor RORgamma / TOR, is up-regulated by signaling through the pre-T cell receptor and binds to the TEA promoter. Eur J Immunol *29*, 4072-4080.

Voll, R.E., Jimi, E., Phillips, R.J., Barber, D.F., Rincon, M., Hayday, A.C., Flavell, R.A., and Ghosh, S. (2000). NF-kappa B activation by the pre-T cell receptor serves as a selective survival signal in T lymphocyte development. Immunity *13*, 677-689.

von Boehmer, H. (2005). Unique features of the pre-T-cell receptor alpha-chain: not just a surrogate. Nat Rev Immunol *5*, 571-577.

von Boehmer, H., Aifantis, I., Azogui, O., Feinberg, J., Saint-Ruf, C., Zober, C., Garcia, C., and Buer, J. (1998). Crucial function of the pre-T-cell receptor (TCR) in TCR beta selection, TCR beta allelic exclusion and alpha beta versus gamma delta lineage commitment. Immunol Rev *165*, 111-119.

von Boehmer, H., and Fehling, H.J. (1997). Structure and function of the pre-T cell receptor. Annu Rev Immunol *15*, 433-452.

Wack, A., Coles, M., Norton, T., Hostert, A., and Kioussis, D. (2000). Early onset of CD8 transgene expression inhibits the transition from DN3 to DP thymocytes. J Immunol *165*, 1236-1242.

Warming, S., Costantino, N., Court, D.L., Jenkins, N.A., and Copeland, N.G. (2005). Simple and highly efficient BAC recombineering using galK selection. Nucleic Acids Res *33*, e36.

Watts, C. (1997). Capture and processing of exogenous antigens for presentation on MHC molecules. Annu Rev Immunol *15*, 821-850.

Weiss, A., and Littman, D.R. (1994). Signal transduction by lymphocyte antigen receptors. Cell *76*, 263-274.

Williams, A., Peh, C.A., and Elliott, T. (2002). The cell biology of MHC class I antigen presentation. Tissue Antigens *59*, 3-17.

Wilson, A., and MacDonald, H.R. (1995). Expression of genes encoding the pre-TCR and CD3 complex during thymus development. Int Immunol *7*, 1659-1664.

Wodarz, A., and Nusse, R. (1998). Mechanisms of Wnt signaling in development. Annu Rev Cell Dev Biol *14*, 59-88.

Woodland, D.L., Happ, M.P., Gollob, K.J., and Palmer, E. (1991). An endogenous retrovirus mediating deletion of alpha beta T cells? Nature *349*, 529-530.

Xi, H., and Kersh, G.J. (2004a). Early growth response gene 3 regulates thymocyte proliferation during the transition from CD4-CD8- to CD4+CD8+. J Immunol *172*, 964-971.

Xi, H., and Kersh, G.J. (2004b). Sustained early growth response gene 3 expression inhibits the survival of CD4/CD8 double-positive thymocytes. J Immunol *173*, 340-348.

Xi, H., Schwartz, R., Engel, I., Murre, C., and Kersh, G.J. (2006). Interplay between RORgammat, Egr3, and E proteins controls proliferation in response to pre-TCR signals. Immunity *24*, 813-826.

Xie, H., Huang, Z., Sadim, M.S., and Sun, Z. (2005). Stabilized beta-catenin extends thymocyte survival by up-regulating Bcl-xL. J Immunol *175*, 7981-7988.

Xu, M., Sharma, A., Hossain, M.Z., Wiest, D.L., and Sen, J.M. (2009a). Sustained expression of pre-TCR induced beta-catenin in post-beta-selection thymocytes blocks T cell development. J Immunol *182*, 759-765.

Xu, M., Sharma, A., Wiest, D.L., and Sen, J.M. (2009b). Pre-TCR-induced beta-catenin facilitates traversal through beta-selection. J Immunol *182*, 751-758.

Xu, Y., Banerjee, D., Huelsken, J., Birchmeier, W., and Sen, J.M. (2003). Deletion of beta-catenin impairs T cell development. Nat Immunol *4*, 1177-1182.

Xu, Y., Davidson, L., Alt, F.W., and Baltimore, D. (1996). Function of the pre-T-cell receptor alpha chain in T-cell development and allelic exclusion at the T-cell receptor beta locus. Proc Natl Acad Sci U S A *93*, 2169-2173.

Yamasaki, S., Ishikawa, E., Sakuma, M., Ogata, K., Sakata-Sogawa, K., Hiroshima, M., Wiest, D.L., Tokunaga, M., and Saito, T. (2006). Mechanistic basis of pre-T cell receptor-mediated autonomous signaling critical for thymocyte development. Nat Immunol *7*, 67-75.

Yashiro-Ohtani, Y., He, Y., Ohtani, T., Jones, M.E., Shestova, O., Xu, L., Fang, T.C., Chiang, M.Y., Intlekofer, A.M., Blacklow, S.C*., et al.* (2009). Pre-TCR signaling inactivates Notch1 transcription by antagonizing E2A. Genes Dev *23*, 1665-1676.

Yu, Q., Erman, B., Bhandoola, A., Sharrow, S.O., and Singer, A. (2003). In vitro evidence that cytokine receptor signals are required for differentiation of double positive thymocytes into functionally mature CD8+ T cells. J Exp Med *197*, 475-487.

Yu, Q., Erman, B., Park, J.H., Feigenbaum, L., and Singer, A. (2004). IL-7 receptor signals inhibit expression of transcription factors TCF-1, LEF-1, and RORgammat: impact on thymocyte development. J Exp Med *200*, 797-803.

Zhang, W., Sommers, C.L., Burshtyn, D.N., Stebbins, C.C., DeJarnette, J.B., Trible, R.P., Grinberg, A., Tsay, H.C., Jacobs, H.M., Kessler, C.M*., et al.* (1999). Essential role of LAT in T cell development. Immunity *10*, 323-332.

Zhang, W., Trible, R.P., and Samelson, L.E. (1998). LAT palmitoylation: its essential role in membrane microdomain targeting and tyrosine phosphorylation during T cell activation. Immunity *9*, 239-246.

Zhu, M., Koonpaew, S., Liu, Y., Shen, S., Denning, T., Dzhagalov, I., Rhee, I., and Zhang, W. (2006). Negative regulation of T cell activation and autoimmunity by the transmembrane adaptor protein LAB. Immunity *25*, 757-768.